Path integral Modelling of Interest Rates, Options and Commodities

XIN DU
(B.Sc., Soochow University)

A thesis submitted for the
Degree of Doctor of Philosophy

Supervisor
Professor Belal E Baaquie

DEPARTMENT OF PHYSICS
NATIONAL UNIVERSITY OF SINGAPORE

2015

Declaration

I hereby declare that the thesis is my original work and it has been written by me in its entirety. I have duly acknowledged all the sources which have been used in the thesis.

This thesis has also not been submitted for any degree in any university previously.

DU XIN

January 2015

Acknowledgements

There are many people who have helped and inspired me for the completion of this thesis.

First of all, I am particularly indebt to my supervisor, Professor Belal E. Baaquie, who has supported me with his patient guidance, invaluable encouragement and persistent help. It is a great opportunity to be his student, and he has influenced me in many ways of life.

I am also grateful to Pan Tang, Yang Cao, Jitendra Bhanap and Winson Tanputramana for their useful discussions and collaborations. I thank National University of Singapore and Department of Physics for the financial support.

Lastly, I would like to thank my family for their nurture and education with unconditional support and love.

Contents

Summary

Finance is the discipline that studies science of fund management like borrowing, lending and investing capital. In financial markets, people purchase and sale of stocks, bonds, commodities, futures and options, and other derivatives. Unlike traditional economies, the financial market nowadays is the potential force for the expansion and growth of world economics. However, due to factors of uncertainties and randomness of the money capital, it is hard to control and predict the financial markets which may cause personal bankruptcies and even world crisis like 2008. The capital markets need new and fresh theoretical and mathematical methods to design and price financial instruments.

The modern mathematical finance is a benchmark of studying method that refers to the use of applied mathematics in analyzing and studying financial markets where people and entities can trade financial instruments. The future is uncertain and this leads to the random evolution of financial instruments. The randomness in finance is entirely classical, arising from ignorance of all the micro-details of the market. The bedrock of mathematical finance is the stochastic calculus studying random evolution. In recent years, the concepts from physics especially statistical mechanics and quantum field theory have been applied to both economics and finance by physicists and economists.

Quantum Finance is firstly proposed by Baaquie(2004). The term 'quantum' in *Quantum Finance* refers to the use of *quantum mathematics*, which contains the mathematics and theoretical methods of quantum mechanics and quantum field theory, applied to finance problems. Quantum mathematics provides a vast range of powerful mathematical tools for the study of stochastic systems. This new theoretical framework provides an efficient and useful framework for modeling and pricing the financial instruments.

In Quantum finance, a random system is represented by elements of a state space, and the time evolution of states is determined by the Hamiltonian (functional) differential operator [1]. The space-time evolution of the system is determined by the Lagrangian and the conditional probabilities are represented by the Feynman path integral [2], which is an infinite dimensional

functional integration over all possibilities of the random system. Existing Models built in quantum finance are interest rate models, pricing of the interest rate derivatives, computing the correlations of interest rates and equities. These models show that quantum field theory has a great potential in the theory of finance that improves the accuracy by capturing more information from data. However, we still needs to investigate more complicated instruments.

This dissertation consists of three major themes.

A major subject matter is focused on studying the Hamiltonian of Libor Market Model (LMM) and pricing the Range accrual swaps based on LMM in Quantum Finance. We study the range accrual swap in the framework of Quantum Finance [3]. It is shown that the quantum finance formulation can exactly model the instrument. An approximate price is obtained as an expansion in the Libor volatility. The price of accrual swap is numerically analysed by generating daily sample values of a two dimension Gaussian quantum field. The Monte Carlo simulation method is used to study the nonlinear domain of the model and determine the range of validity of the approximate formula. we generalize the drift of Libor market model when applying in the real market data.

The linearized Hamiltonian model is proposed to extend the LIBOR Market Model (LMM) [4]. Firstly, we study the Hamiltonian of LIBOR Market Model in the framework of quantum finance, and the nontrivial upper triangle form of LIBOR drift is derived. The linearized Hamiltonian is derived to improve the explanatory capability of the model for market data. Our approach uses one more parameter to explain the initial condition and the model can be used to calibrate LIBORs with extremely high accuracy.

In the second part, the option pricing using acceleration Lagrangian is studied in Quantum Finance [5]. The acceleration Lagrangian model generates a pricing formula of the option that depends on both the security and the velocity, which is the instantaneous rate of return. The comparison of this pricing model with market prices shows that the velocity of the security in the option price seems to compensate for the shortfall of information in the Black-Scholes pricing formula, which is currently compensated by the concept of implied volatility.

In the third part, the dynamics of commodity market prices is modeled by an action functional within the framework of statistical microeconomics [6]. The correlation functions are investigated using a perturbation expansion in Feynman path integrals and fitted to nine main commodities. The calibration results establishes the existence of the action for commodity prices that was postulated to exit in Statistical microeconomics.

Publication List

[1] B.E. Baaquie, Xin Du*, Tang Pan and Cao Yang. Pricing of range accrual swap in the quantum finance Libor Market Model.*Physica A: Statistical Mechanics and its Applications*, 401(2), 182-200, 2014.[3]

[2] Tang Pan*, B.E. Baaquie, Xin Du and Ying Zhang. Linearized Hamiltonian of the LIBOR Market Model: Analytical and Empirical Results. Submitted in *Quantitative Finance*.

[3] B.E. Baaquie and Xin Du* and Jitendra Bhanap. Option Pricing: Stock Price, Stock Velocity and the Acceleration Lagrangian. *Physica A: Statistical Mechanics and its Applications*, 416, 564-581, 2014.[5]

[4] B.E. Baaquie, Xin Du* and Winson Tanputramana. Empirical Microeconomics Action Functionals. *Physica A: Statistical Mechanics and its Applications*, 428, 19-37, 2015. [6]

* Corresponding author

List of Tables

List of Figures

Symbol

Symbol	Definition
r	spot rate
$B(t,T)$	zero coupon bond
$f(t;T_1,T_2)$	forward interest rate, at calendar time t, for a deposit from future time T_1 to T_2
$f(t,x)$	forward interest rate, at calendar time t, for an instantaneous deposit at future time x
$f_L(t,x)$	Libor forward interest rate
$F(t,T_1,T_2)$	forward price, at calendar time $t < T_1$, of a zero coupon bond $B(T_1,T_2)$
ℓ	Libor tenor, taken to be 90 days in this thesis
$L(t,T_n)$	Libor rate, at calendar time t, for a deposit from future time T_n to $T_n + \ell$
$\Theta(t)$	Heaviside function
$M(t,t_*)$	money market numeraire
$\mathcal{P}_*$	option payoff function
$\alpha_*(t,x)$	drift for forward bond numeraire $B(t,t_*)$
$\sigma(t,x)$	forward interest rate's volatility
$\chi_n(t)$	martingale instruments for Libor Market Model
$\xi(t,x)$	Libor Market Model drift
$\gamma(t,x)$	Libor Market Model deterministic volatility
$R(t)$	Gaussian white noise
$A(t,x)$	Gaussian quantum field
$f_{m,n}, A_{m,n}$	lattice of forward interest rates and $A(t,x)$
$\delta_{mn}(t,x)$	Libor Market Model correlator
$\mathcal{L}[A], S[A]$	Lagrangian and action for $A(t,x)$
$Z[h]$	generating function for $A(t,x)$
$D(t;x,x')$	forward interest rate propagator
$E[...]$	expectation value of interest rate instruments

Symbol	Definition
$\phi(t,x)$	logarithmic Libor rate
$\rho(t,x)$	drift of logarithmic Libor rate
$\mathcal{L}[\phi], S[\phi]$	Lagrangian and action for $\phi(t,x)$
$u(0,1)$	uniform distribution
$N(0,1)$	normal distribution
ϵ	updating step size in calendar time, taken to be 1 day
$\sigma_M(t,x), \gamma_M(t,x)$	market volatility for forward interest rates and Libor
$N(x)$	cumulative normal distribution function
$C(t_0,t_*,T,K)$	call price of instruments, at present time t_0, issued at t_* and matures at future time T with strike price K
S_t	stock price at time t
$x=\ln S$	logarithmic stock price
$dW(t)$	Wiener process
$\mathcal{H}_\phi$	Libor Hamiltonian
$\phi(t,x)$	log-Libor field
τ	market time
v	logarithmic rate of return
$P_{BS}(x,\tau;x')$	pricing kernel for Black-Scholes model
$P_D(x,\tau;x')$	normalized Black-Scholes pricing kernel
Π	portfolio
$X_I(t)$	rate of return of single stock $S_I(t)$
d_I	deterministic drift of $X_I(t)$
$\varphi_I(t)$	Gaussian field for rate of return
$G_{IJ}(t,t')$	non-equal time propagator of rate of return
$\mathcal{L}[\varphi], S[\varphi]$	Lagrangian and action for $\varphi(t)$
p	cumulative n-year default probability
$\mathcal{K}(x,x';v,v';t)$	transition amplitude
$\mathcal{P}(x,x';v,v';t)$	conditional probability
$\mathcal{D}(p)$	demand function
$\mathcal{S}(p)$	supply function
$\mathcal{V}(p)$	potential

Chapter 1

Introduction of Interest rate Derivatives

§ 1.1 Concepts in Interest rate and Rational pricing

§ 1.1.1 Interest rate and Libor

Interest rates are used to define the amount of money paid by the borrower for borrowing money from the lender. Interest rates are the key tool in the valuation of all financial derivatives. There are three different ways to define interest rates.

Simple interest rates: Propose a principal is M at present time t (today), and a simple interest rate r earned per year. r remains constant for each year. The amount of capital will increase to $M[1+r(T-t)]$ at future time T. Conversely, if one will receive a prefixed amount B at future T, the value at earlier time t is given by $B/[1+(T-t)r]$.

Discrete compounding and discounting: If the interest earned for one year is compounded to the principal, the amount will be $M[1+r]$ at the end of one year. This new principal is reinvested at the beginning of second year, the amount will increase to $M[1+r]^2$ at the end of second year. Thus, the amount of capital at future time T will be $M[1+r]^{T-t}$. Also if one will receive a prefixed amount B at future T, the value at earlier time t is given by $B/[1+r]^{(T-t)}$.

Continuous compounding and discounting: continuous compounding is the extreme case of the discrete compounding where the discrete time interval is taken to be infinitesimal. In discrete compounding, the interest rate r is constant for one year. If an infinitesimal period ϵ is used instead of one year, the principal M will increase to $M(1+\epsilon r)$ at time $t+\epsilon$. Following

the same procedure of discrete compounding for infinitesimal interval ϵ, the total amount of capital at future time T will be

$$\lim_{\epsilon \to 0} M(1+\epsilon r)^{(T-t)/\epsilon} = Me^{r(T-t)}. \quad (\S\, 1.1.1)$$

And same for future discounting B at present time t is $Be^{-r(T-t)}$. These three definitions of interest rates are consistent and widely used in the financial markets The forward rate is the future yield on a bond, and is calculated using the interest yield curve. The continuous compounding and discounting is used for studying the interest rates through all Chapters, and the forward rates is discussed in the way of continuous compounding in the following.

Consider a fixed deposit that has a value of \$1 at time t, the deposit will increase to $\{\exp(T-t)r\}$ at time T in the future, where r is the spot rate. Therefore, the present value of zero coupon bond, which yields a value of \$1 at future time T, is given by

$$B(t,T) = e^{-(T-t)r}. \quad (\S\, 1.1.2)$$

In practice, the interest rate is not always constant from time t to T. Instead, the continuous interest rate $r(t,T)$ should be used to describe the term structure of interest rates, which is well known as the *interest yield curve*. The interest rate $r(t,T)$ can be calculated from the zero coupon bond by using

$$B(t,T) = e^{-(T-t)r(t,T)} \quad (\S\, 1.1.3)$$

$$\Rightarrow r(t,T) = -\frac{1}{T-t}\ln B(t,T). \quad (\S\, 1.1.4)$$

Forward interest rates are similar with the continuous interest rate $r(t,T)$, except that the forward interest rates $f(t;T_1,T_2)$, at present time t , are defined on the period of future time from T_1 to T_2. The forward interest rates $f(t;T_1,T_2)$ can be calculated from two bonds with different maturity times T_1 and T_2.

$$B(t,T_2) = e^{-(T_2-T_1)f(t;T_1,T_2)}B(t,T_1) \quad (\S\, 1.1.5)$$

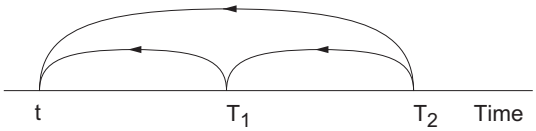

Figure 1.1: The discounting of bond from T_2 to t or first from T_2 to T_1, and then from T_1 to t.

As shown in Figure 1.1, the interest rate, which is discounted from T_2 to present time t directly, should be equivalent to being discounted from T_2 to T_1 and then from T_1 to t. Thus, the forward rates $f(t; T_1, T_2)$ is given by

$$f(t; T_1, T_2) = -\frac{1}{T_2 - T_1} \ln[\frac{B(t, T_2)}{B(t, T_1)}]. \qquad (\S\, 1.1.6)$$

More precisely, the *instantaneous forward interest rates* can be obtained by taking $T_2 = T_1 + \epsilon$, which is the following

$$B(t, T + \epsilon) = B(t, T) \times e^{-\epsilon f(t,T,T+\epsilon)}. \qquad (\S\, 1.1.7)$$

If the bond price is \$1 when the bond matures at future time T, the value of bond at present time t can be obtained by taking infinitesimal backward time step ϵ from future time T to present time t, which is

$$B(t, T) = e^{-\epsilon f(t,t+\epsilon)} e^{-\epsilon f(t,t+2\epsilon)} \cdots e^{-\epsilon f(t,x)} \cdots e^{-\epsilon f(t,T)}. \qquad (\S\, 1.1.8)$$

Simply, $B(t, T)$ is given by

$$B(t, T) = \exp\{-\int_t^T dx f(t, x)\}, \qquad (\S\, 1.1.9)$$

$$\frac{\partial B(t, T)}{\partial T} = -f(t, T) B(t, T) \qquad (\S\, 1.1.10)$$

where $f(t, x)$ is defined as forward interest rates. At every instant calendar t, $f(t, x)$ constitutes an entire curve as a function of future time x. $f(t, x)$ is defined on a two dimensional semi-infinite plane with $t \geq t_0$ and $x \geq t$, shown as the shaded domain in Figure 1.2.

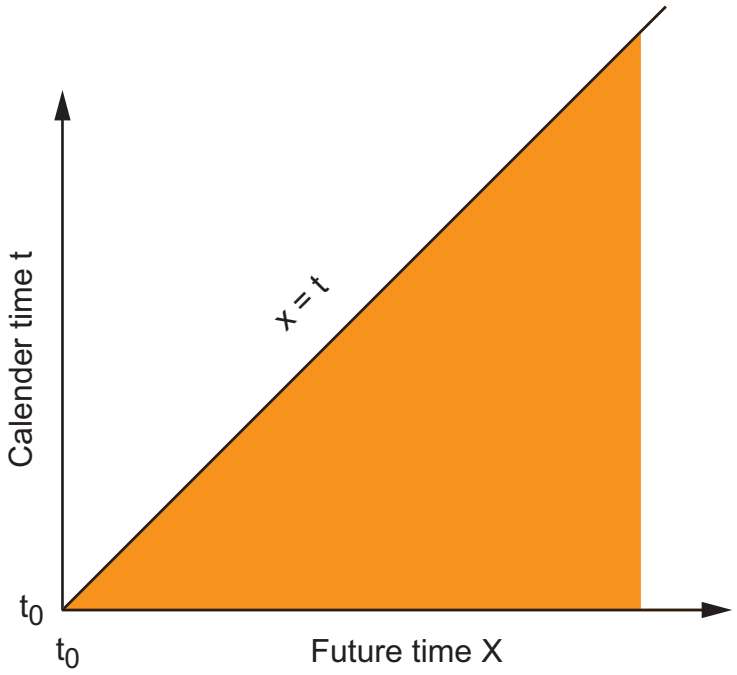

Figure 1.2: Two dimensional forward interest rates $f(t,x)$ which is shown in shaded domain.

Suppose the zero coupon bond $B(t_*,T)$ will be issued at a future time t_* ($t_* > t_0$,) and expire at time T; the forward price of $B(t_*,T)$, at earlier time t_0 denoted by $F(t_0,t_*,T)$, is given by

$$F(t_0,t_*,T) \;=\; \exp\Big\{-\int_{t_*}^{T} dx f(t_0,x)\Big\} = \frac{B(t_0,T)}{B(t_0,t_*)}. \qquad (\S\,1.1.11)$$

Figure 1.3 shows the plot of bond price $B(t_*,T)$ and forward bond price $F(t_0,t_*,T)$. The difference between $B(t_*,T)$ and $F(t_0,t_*,T)$ is that $F(t_0,t_*,T)$ is defined on present time t_0 while $B(t_*,T)$ is issued at future t_*.

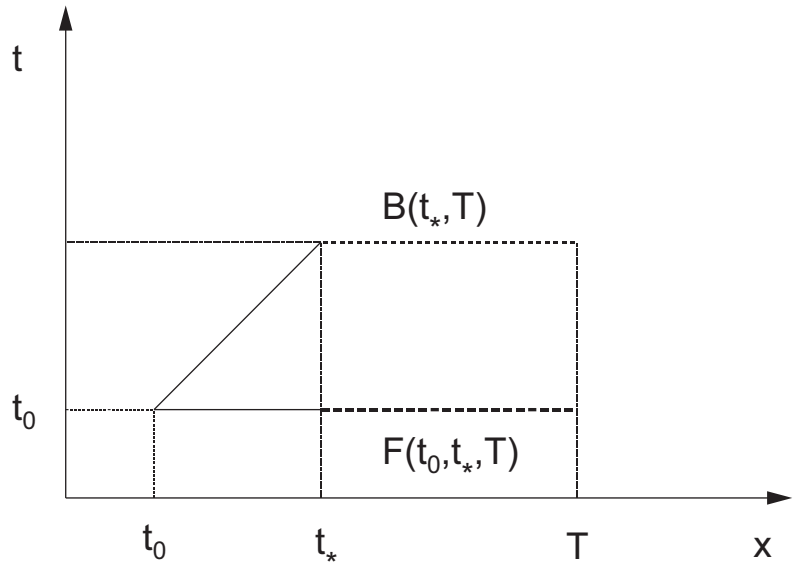

Figure 1.3: Bond price $B(t_*, T)$ and its forward price $F(t_0, t_*, T)$.

The London Interbank Offered Rate (**LIBOR**) is one of main interest instruments in the debt market. Libor is a daily quoted rate based on the interest rates at which banks are prepared to make a large deposit with other banks in the London wholesale money market (or interbank market). Libor was commenced officially by British Bankers' Association from 1 January 1986 and the minimum deposit is \$1000000. The duration of daily quoted Libor can be different, and overnight, 1-week, 2-weeks, 1-month, 3-month, 6-month and 12-month are often quoted by large commercial banks and financial institutions. Libor rates can have a duration of up to 30 years, and Libor with long duration can be obtained from the interest swap market.

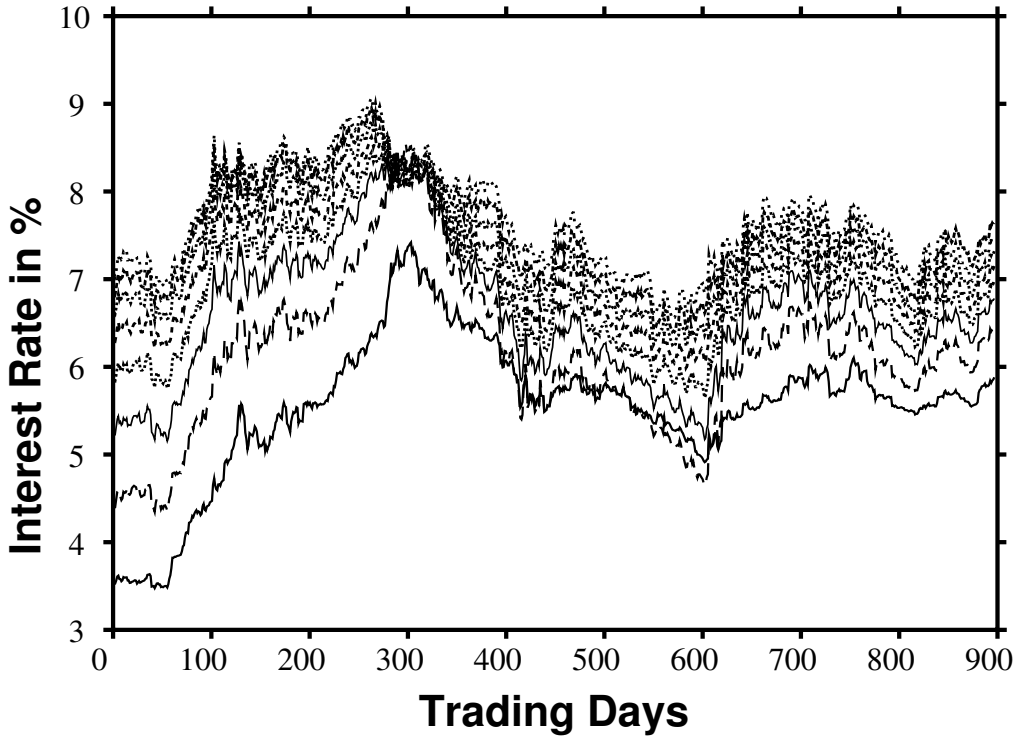

Figure 1.4: Daily Libor rate for $L(t, t + 7years)$, $L(t, t + 6years), \cdots L(t, t + 1years)$, and $L(t, t + 0.25years)$ with $t \in [1996, 1999]$

The 3-month Libor is the most quoted rate in the derivative market. All Libor caps, floors and swaps are based on 3-month Libor. The Libor rate $L(t, T_n)$ is a forward interest rate, fixed at time t, for a cash deposit from future time T_n to $T_n + \ell$. Libor time is defined as $T_n = n\ell$ and ℓ is called the tenor of Libor rates. Figure 1.5 shows the Libor rates on the Libor calendar and future time lattice.

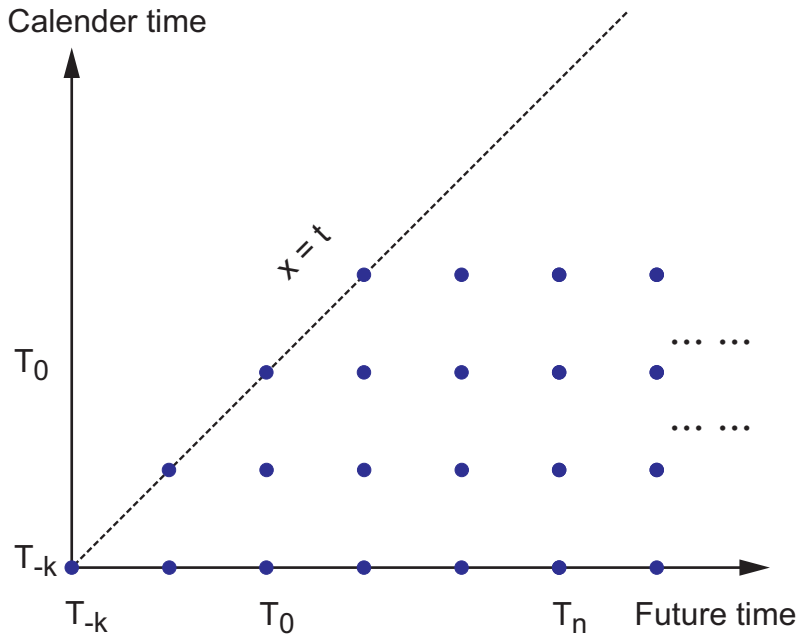

Figure 1.5: Libor rates defined on the time lattice with tenor ℓ.

The relationship between Libor $L(t,T)$ and its forward rates $f(t,x)$ is given by

$$L(t,T) = \frac{e^{\int_T^{T+\ell} dx f(t,x)} - 1}{\ell}$$

The zero coupon bond $B(t,T)$ in terms of Libor is

$$B(t,T) = \frac{1}{1+(T-t)L(t,T)}$$

Conversely Libor in terms of $B(t,T)$ is

$$L(t,T) = \frac{1}{\ell}\frac{B(t,T) - B(t,T+\ell)}{B(t,T+\ell)}$$

Then the bond and forward bonds in terms of Libor are

$$B(t,T_N) = \prod_{n=0}^{N-1} \frac{1}{1+\ell L(t,T_n)} \qquad (\S\,1.1.12)$$

$$F(t,T_1,T_2) = \prod_{T_1 \le T_n < T_2} \frac{1}{1+\ell L(t,T_n)} \qquad (\S\,1.1.13)$$

Sometimes the Libor are approximately equal to the forward interest rate for

$$L(t,T) = \frac{e^{\int_T^{T+\ell} dx f(t,x)} - 1}{\ell} \simeq f(t,T) + O(\ell)$$

§ 1.1.2 Martingale

In finance, *arbitrage* is the practice of taking advantage of a state of imbalance between two (or more) markets. When an arbitrage happens, the profit can be earned from the difference between the market prices. In principle, an arbitrage means risk-free. In academic use, an arbitrage is the possibility of a risk-free profit after transaction costs.

To avoid arbitrage, the *Rational pricing* with no arbitrage is assumed in pricing fixed income securities, particularly bonds, and is fundamental to the pricing of derivative instruments. Rational pricing is the assumption in financial economics that asset prices (and hence asset pricing models) will reflect the arbitrage-free price of the asset as any deviation from this price will be "arbitraged away".

In mathematical finance, the condition of no-arbitrage is equivalent to the existence of a risk-neutral measure. A risk-neutral measure, also called an equivalent martingale measure, is heavily used in the pricing of financial derivatives due to the fundamental theorem of asset pricing, which implies that in a complete market a derivative's price is the discounted expected value of the future payoff under the unique risk-neutral measure.

A martingale is a special kind of stochastic process in probability theory; a discrete-time *martingale* is a discrete-time stochastic process in which the conditional expected value of an observation at some time t is equal to the observation at that earlier time t_0. An arbitrary discrete stochastic process X_i, which is a martingale, satisfies the following

$$E[|x_n|] < \infty, \qquad (\S\,1.1.14)$$

$$E[X_{n+1}|x_1, x_2, , ..., x_n] = x_n. \qquad (\S\,1.1.15)$$

If the expectation value of random variables X_1, X_2,... X_n is already known to be x_1, x_2,...,x_n, the expectation value of the random variable X_{n+1} is simply x_n.

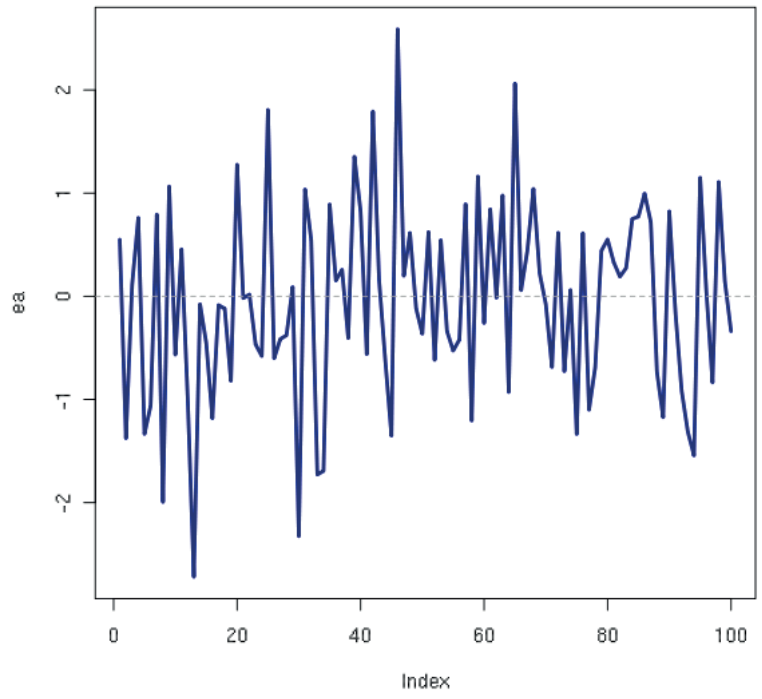

Figure 1.6: One random series of samples following Martingale process

A martingale is a model of a fair game where knowledge of past events never helps predict the mean of the future winnings. For example, x_n denotes the amount of money which the gambler has after nth game, and X_{n+1} represents the various possible outcome of the $n+1$th game. Under the martingale condition, the expectation value of the outcomes of the $n+1$th game is equal to the money which the gambler has at the end of the nth game, namely x_n. The expectation value of the outcomes of the $n+1$th game only depend on x_n and doesn't have any relation with the historical outcomes. $E[X_{n+1}] = E[X_n]$ can be proved by using Equation § 1.1.14, and is given by

$$\begin{aligned} E[X_{n+1}] &= \int dx_1 dx_2, ..., dx_n dx_{n+1} E[X_{n+1}|x_1, x_2, , ..., x_n] p(x_1, x_2, ..., x_{n+1}) \\ &= \int dx_1 dx_2, ..., dx_n dx_{n+1} x_n p(x_1, x_2, ..., x_{n+1}) \\ &= E[X_n] \\ \Rightarrow E[X_{n+1}] &= E[X_n] = E[X_{n-1}] = ... = E[X_1]. \end{aligned} \tag{§ 1.1.16}$$

§ 1.1.3 Numeraires

Numeraire is a basic standard by which values are computed; in other words, it is to measure the worth of different goods and services relative to one another. In a financial market, a particular numeraire is chosen to yield a martingale evolution for the forward bonds in the market. Money market numeraire, forward bond numeraire, forward numeraire and common Libor numeraire is introduced in this section.

Choose $M(t, t_*)$ as a numeraire for the money market, and $M(t, t_*)$ is given by

$$M(t, t_*) = e^{\int_t^{t_*} r(t')dt'}; \quad t : \text{fixed}, \tag{§ 1.1.17}$$

where $r(t)$ is the spot interest rate. The martingale condition is then given by

$$\begin{aligned} \frac{B(t,T)}{M(t,t)} &= E_t^M\big[\frac{B(t_*,T)}{M(t,t_*)}\big] \\ \Rightarrow B(t,T) &= E_t^M[e^{-\int_t^{t_*} r(t')dt'} B(t_*,T)], \end{aligned} \tag{§ 1.1.18}$$

where $E_M[...]$ denotes taking the expectation value with respect to the money market measure.

$B(t, T_I)$ is chosen for the forward bond numeraire, and the martingale condition for zero coupon bonds $B(t, T)$ is given by

$$\begin{aligned} \frac{B(t,T)}{B(t,T_I)} &= E_I\big[\frac{B(T_I,T)}{B(T_I,T_I)}\big] \\ \Rightarrow B(t,T) &= B(t,T_I)E_I[B(T_I,T)], \end{aligned} \tag{§ 1.1.19}$$

where $E_I[...]$ denotes taking the expectation value with respect to the forward neutral measure.

The forward numeraire is a collection of zero coupon bonds which is defined on Libor time. An collection of zero coupon bonds defined on Libor time from T_0 to T_{n+1} is given by

$$B(t, T_0), B(t, T_1), ..., B(t, T_n), B(t, T_{n+1}); \quad T_n = T_0 + \ell n. \tag{§ 1.1.20}$$

Suppose a zero coupon bond matures at future time T_{n+1}, the forward value of the bond at present time t_0 is given by

$$F(t_0, T_n, T_{n+1}) = e^{-\int_{T_n}^{T_{n+1}} dx f(t_0,x)} = \frac{B(t_0, T_{n+1})}{B(t_0, T_n)}. \tag{§ 1.1.21}$$

The martingale condition for the forward bond is given by

$$\begin{aligned} F(t_0, T_n, T_{n+1}) &= E_F[F(t_*, T_n, T_{n+1})] && (\S\,1.1.22)\\ \Rightarrow e^{-\int_{T_n}^{T_{n+1}} dx f(t_0,x)} &= E_F[e^{-\int_{T_n}^{T_{n+1}} dx f(t_*,x)}]. && (\S\,1.1.23) \end{aligned}$$

For modeling the Libor term structure, a common Libor numeraire is chosen for the the martingale evolution of all the Libor rates.

The Libor rate, which is defined on Libor time, can be expressed by using the Libor forward interest rate $f(t,x)$. Suppose $L(t,T_n)$ represents the Libor rate from T_n to $T_{n+\ell}$ and the tenor $\ell = T_{n+\ell} - T_n$, the Libor $L(t,T_n)$ is given by

$$L(t,T_n) = \frac{1}{\ell}(e^{\int_{T_n}^{T_{n+\ell}} dx f(t,x)} - 1). \qquad (\S\,1.1.24)$$

Because $e^{\int_{T_n}^{T_{n+\ell}} dx f(t,x)}$ can be expressed in terms of bond price, which is

$$e^{\int_{T_n}^{T_{n+\ell}} dx f(t,x)} = \frac{B(t,T_n)}{B(t,T_{n+\ell})}. \qquad (\S\,1.1.25)$$

Hence, the Libor can be rewritten in terms of bond, which is given by

$$\begin{aligned} L(t,T_n) &= \frac{1}{\ell}\Big(\frac{B(t,T_n)}{B(t,T_{n+\ell})} - 1\Big)\\ &= \frac{1}{\ell}\Big(\frac{B(t,T_n) - B(t,T_{n+\ell})}{B(t,T_{n+\ell})}\Big). && (\S\,1.1.26) \end{aligned}$$

From Equation § 1.1.26, the combination $L(t,T_n)B(t,T_{n+1})$ is equivalent to a portfolio of zero coupon bonds. Hence, $L(t,T_n)B(t,T_{n+1})$ is a traded asset and can be made into martingales by using an appropriate forward bond numeraire.

Choose the zero coupon bond $B(t,T_{I+1})$ as the numeraire, the martingale evolution of Libor rates is given by

$$\frac{L(t_0,T_n)B(t_0,T_{n+1})}{B(t_0,T_{I+1})} = E_L\Big[\frac{L(t,T_n)B(t,T_{n+1})}{B(t,T_{I+1})}\Big], \qquad (\S\,1.1.27)$$

where $E_L[...]$ denotes taking the expectation value with respect to the common Libor market measure. The time T_{I+1} can be freely chosen. It is found that different discounting bond $B(t,T_{I+1})$ can be used as the numeraire for Libor $L(t,T_n)$. The expectation value of $L(t,T_n)$ is invariant under different choices for the discounting bond $B(t,T_{I+1})$, this feature of Libor

Market Model is because in the LMM drift comes from the nontrivial property of Libor drift. This technique has many important applications in LIBOR and swap market models, as well as commodity markets.

§ 1.2 Introduction of Interest rate Derivatives

A derivative is an instrument whose value is dependent on the underlying securities. The underlying can be commodities, interest rates, exchange rates, index or equities, bonds and so on. The main types of derivatives are options, futures, forwards and swaps. An interest rate derivative is a derivative where the buyer has the right to pay or receive a notional amount of money at a given interest rate.

Figure 1.7 is the breakdown of the global derivatives markets for 2011 into the equity, foreign exchange and debt markets with a notional amount that is a staggering 647 trillion: almost ten times the global GDP for 2011 of 69.98 trillion. The equity options market was worth approximately US 103 trillion and accounted for about 16% of the total derivatives markets. The graph on the up-right gives the breakdown of the total number of contracts of the international derivatives markets in 2011, which was 25.21 billion. Equity has the major fraction of 84% of the total contracts. In the middle graph, about 70% of the global derivatives market, with a notional value of 473 trillion, is accounted by interest rate derivatives markets of which 80% is interest rate swaps.

§ 1.2.1 Options

Options are a type of financial instrument of derivatives. There are two basic types of options that are traded in the market, which are called call option and put option. A call option gives the holder the right but not the obligation to buy the underlying asset at a prefixed price, which is called strike price by a certain date. A put option gives the holder the right to sell the underlying asset at strike price. The exercise data is also called maturity of the contract. The options should be traded on or before options' expiration date. European options and American options are the two main different styles of options respectively. A European option can only be exercised at the expiration date, while an American option can be exercised at any time before expiration date.

From the definition of a call option, the value of an European call option at maturity T is

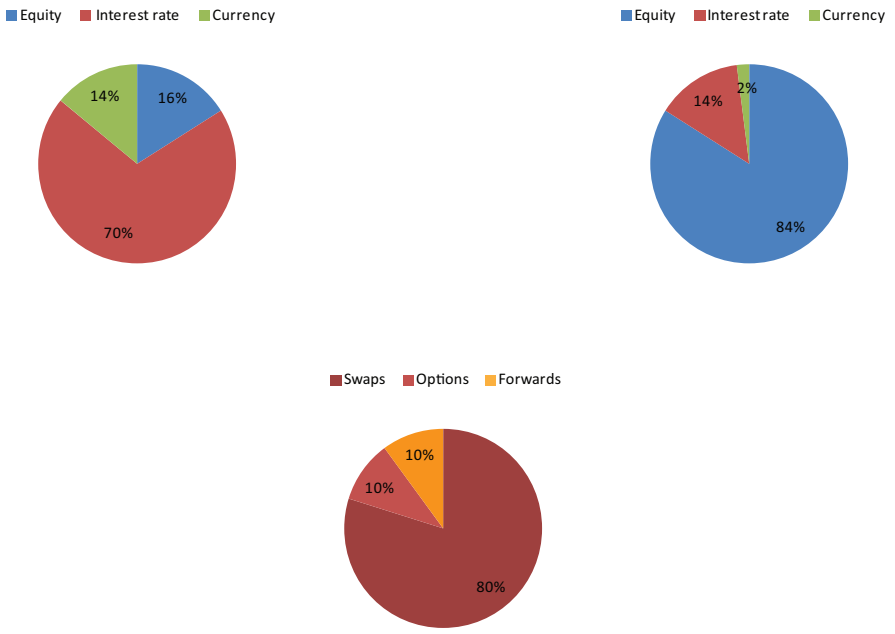

Figure 1.7: Global derivatives markets for 2011

given by

$$C(S,K,T) \quad = \quad (S-K)_+, \tag{§ 1.2.1}$$

where $(S-K)_+$ is called payoff function. This payoff function means that, at expiration date, the holder will earn the profit $S-K$ if the underlying price S is larger than strike price K. The holder will not earn any profit if the underlying price S is smaller than strike price K. The payoff function has the property

$$(a-b)_+ \quad = \quad (a-b)\Theta(a-b). \tag{§ 1.2.2}$$

Θ is the Heaviside function, which is given by

$$\Theta(x) = \begin{cases} 1 & x > 0 \\ \frac{1}{2} & x = 0 \\ 0 & x < 0. \end{cases}$$

Figure 1.8 shows the payoff function as a function of final $S(T)$ and the time evolution of call option from present time t to T. The fundamental problem in option theory is to find the

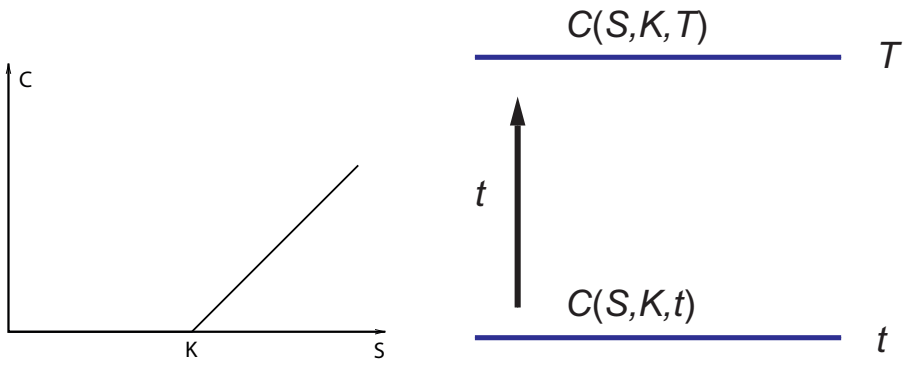

Figure 1.8: Payoff of call option and time evolution

present value of the option, namely $C(S, K, t)(t < T)$. Similarly, the payoff function of a put option is the reverse of a call option and is given by

$$P = (K - S)_+, \qquad (\S\, 1.2.3)$$

which means that, at expiration date, the holder will earn the profit $K - S$ if the underlying price S is smaller than strike price K. The holder will lose the underlying asset if the underlying price S is larger than strike price K.

The put-call parity hinges on the identify that

$$\Theta(x) + \Theta(-x) = 1 \qquad (\S\, 1.2.4)$$

Thus the difference in the call and put payoff function satisfies

$$(S - K)_+ - (K - S)_+ = S - K \qquad (\S\, 1.2.5)$$

§ 1.2.2 Volatility

To determine the price of the option $C(S, K, t)$, we need to know how the stock price $S(t)$ evolves in time.

In finance, volatility is a measure for variation of price of a financial instrument over time. Historic volatility is derived from time series of past market prices. An implied volatility is derived from the market price of a market traded derivative (in particular an option). The symbol σ is used for volatility, and corresponds to standard deviation, which should not be confused with the similarly named variance, which is instead the square, σ^2.

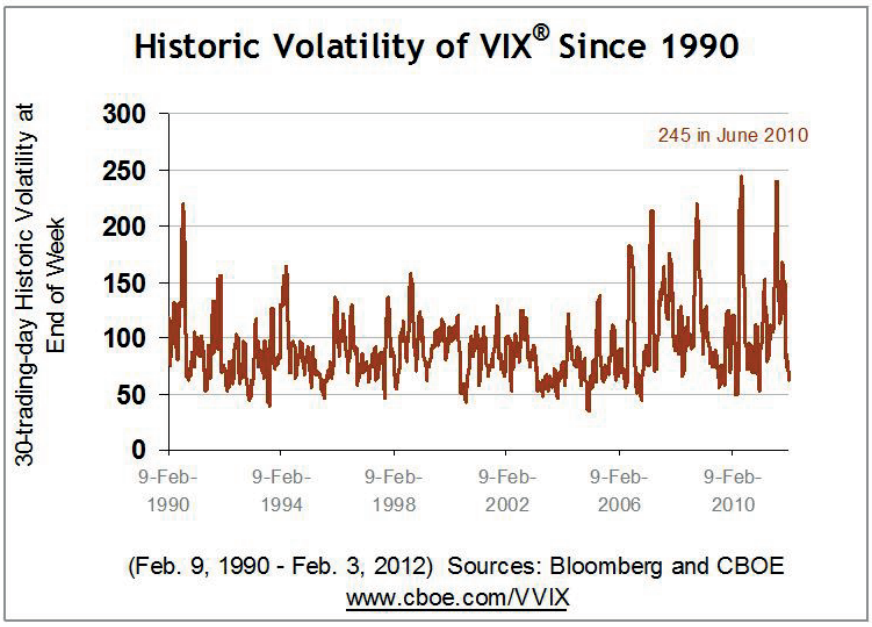

Figure 1.9: Historical Volatility of VIX since 1990

Starting from a constant volatility approach, assume that the derivative's underlying price follows a standard model for geometric brownian motion:

$$dS_t = \mu S_t dt + \sigma S_t dW_t$$

where μ is the constant drift (i.e. expected return) of the security price, σ is the constant volatility, and dW_t is a standard Wiener process with zero mean and unit rate of variance. The explicit solution of this stochastic differential equation is

$$S_t = S_0 e^{(\mu - \frac{1}{2}\sigma^2)t + \sigma W_t}$$

Historical volatility or statistical volatility is the realized volatility of a financial instrument over a given time period. Generally, this measure is calculated by determining the average deviation from the average price of a financial instrument in the given time period. Standard deviation is the most common but not the only way to calculate historical volatility. Stocks with a high historical volatility usually require a higher risk tolerance. Figure 1.9 is one example of Historical Volatility of VIX since 1990.

Implied volatility is the estimated volatility of a security's price. In general, implied volatility increases when the market is bearish and decreases when the market is bullish. This is due to the common belief that bearish markets are more risky than bullish markets. In

Historical Volatility	Implied Volatility
←	→
Looks back in time to show where volatility has been in the past.	Trader's view of expected future volatility based on current option prices.
**********	**********
Shows expected trading range of market	Indicator of the current sentiment of the market.

Figure 1.10: The comparison of Historical Volatility and Implied Volatility

addition to known factors such as market price, interest rate, expiration date, and strike price, implied volatility is used in calculating an option's premium. IV can be derived from a model such as the Black-Scholes Model which will be introduced in Chapter 2. Figure 1.10 shows the difference between Historical Volatility and Implied Volatility.

Stochastic volatility means the underlying security's volatility is a random process, governed by state variables such as the price level of the underlying security, the tendency of volatility to revert to some long-run mean value, and the variance of the volatility process itself, among others. One of the famous models is Heston model which assumes the following process

$$dS_t = \mu S_t dt + \sqrt{\nu_t} S_t dW_t$$

$$d\nu_t = \theta(\omega - \nu_t)dt + \xi\sqrt{\nu_t} dB_t$$

where ω is the mean long-term volatility, θ is the rate at which the volatility reverts toward its long-term mean, ξ is the volatility of the volatility process, and dB_t is, like dW_t , a gaussian with zero mean and $\sqrt{dt}$ standard deviation. However, dW_t and dB_t are correlated with a constant correlation value.

§ 1.2.3 Swap

An interest rate swap is contracted between two parties. Payments are made at fixed times T_n and are separated by time intervals ℓ, which is usually 90 or 180 days. The swap contract has a notional principal V , with a pre-fixed period of total duration and with the last payment

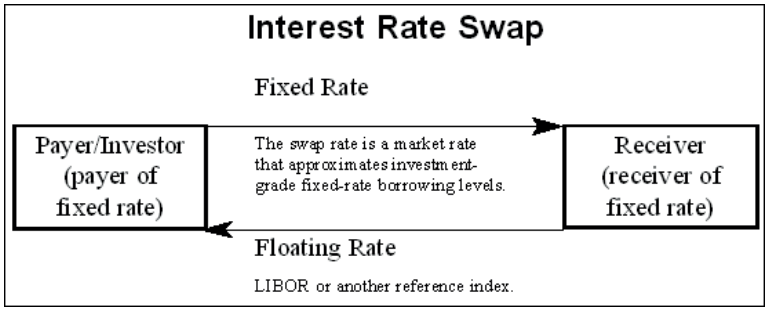

Figure 1.11: Diagram representing the interest rate swap

being made at time T_N. One party pays, on the notional principal V, a fixed interest rate denoted by R_S and the other party pays a floating interest rate based on the prevailing market rate, or vice versa. The floating interest rate is usually determined by the prevailing value of Libor at the time of the floating payment.

A floating rate receiver's swap, denoted by $swap_L$, means that the first party will receive the interest rate payments at the floating rate and pay at a fixed interest. Contrary to $swap_L$, a fixed rate receiver's swap, denoted by $swap_R$, means that the first party will receive the payments at a fixed interest rate and pay at the floating rate.

The simplest forward swap is called a forward *swaplet*. Suppose the contract of swaplet, entered at time t, has a notional principal of ℓV and the contract will be kept in a fixed time deposit from future time T_n to $T_n + \ell$. In this swaplet, the Libor rate $L(t, T_n)$ is chosen to be the floating interest rate and R_s denotes the fixed interest rate. The value of a forward floating rate receiver swaplet at present time t_0 is given by

$$swaplet_L(t_0, T_n) = \ell V B(t_0, T_n + \ell)[L(t_0, T_n) - R_s]. \qquad (\S\, 1.2.6)$$

The swap start at time T_0, with payments made at different Libor time T_n, $n = 1, 2, ...N$, has the first payment at time T_1 and final payment at time T_N. The present value of the floating rate receiver swap and fixed rate receiver swap is given by

$$swap_L(t_0, R_s) = \ell V \sum_{n=0}^{N-1} B(t_0, T_n + \ell)[L(t_0, T_n) - R_s], \qquad (\S\, 1.2.7)$$

$$swap_R(t_0, R_s) = \ell V \sum_{n=0}^{N-1} B(t_0, T_n + \ell)[R_s - L(t_0, T_n)]. \qquad (\S\, 1.2.8)$$

Hence, from above two equations, the following relation can be simply obtained

$$swap_L(t_0, R_s) + swap_R(t_0, R_s) \quad = \quad 0. \qquad (\S\, 1.2.9)$$

A swaption is an option which the holder has the right but not the obligation to enter into an underlying swap. Swaptions are simply the options on interest rate swaps. Hence, the swaption price of receiving floating rate payments and paying fixed rate is given by

$$\begin{aligned} C_L(t_0, T_0; R_s) &= E[swap_L(T_0, R_s)]_+ \\ &= \ell V E\Big[e^{\int_{t_0}^{T_0} dtr(t)} \sum_{n=0}^{N-1} B(T_0, T_n + \ell)[L(T_0, T_n) - R_s]\Big]_+. \end{aligned} \qquad (\S\, 1.2.10)$$

Chapter 2

Review of Quantum finance models

This chapter reviews some typical models in the framework of Quantum Finance. It is organized as follows: Section § 2.1 briefly reviews historical studies in the interest rate models. Section § 2.2 studies the Lagrangian model of Black-Scholes. Section § 2.3 introduces the Quantum field generalization of HJM model. Section § 2.4 reviews the Libor market model of quantum finance.

§ 2.1 Review of interest rate models

The short rate (short term interest, also means interest rate charged for short term loans) was firstly assumed normally distributed in Black-Scholes-Merton (1973) [7] model as $r_t = r_0 + at + \sigma W_t$, and this model gave a basic method to calculate the option price. However, this model is not able to capture the mean-reverting property of interest rates. This basic assumption proposed in Black-Scholes model was later used by Vasicek to develop the first one-factor short rate model to capture mean reversion. Vasicek (1977) [8] assumed that the short rate under the real-world measure evolves as a mean reverting-process with constant coefficients as $dr_t = (\theta - \alpha r_t)dt + \sigma dW_t$. However, a major drawback of this approach is that the short rate in Vasicek model can have negative values; but short rate cannot be negative values in the real market. Cox, Ingersoll and Ross (1985) [9] developed a general equilibrium model by introducing a square root term in the diffusion coefficient in Vasicek model as $dr_t = (\theta - \alpha r_t)dt + \sqrt{r_t}\sigma dW_t$. Their model provides a powerful tool for the study and analysis of interest rate because the instantaneous short rate in their model is always positive. However, all the models mentioned above are time-invariant models. The serious drawback of time-invariant

models is that these models endogenously produce the term structure of rates. This led Ho and Lee (1986) [10] to propose an exogenous term structure model, which is a different approach to short rate models as $dr_t = \theta_t dt + \sigma dW_t$. However, their model is still based on the assumption that the evolution of term structure follows a binomial tree process, and the method cannot give a better understanding of the interest rates. This model therefore cannot be regarded as a proper extension of the Vasicek model. Hull and White(1990) [11] proposed an extended model which is able to fit both term structure and volatilities by introducing one time-varying parameter and gives more flexibility for simulating the spot rate dynamics as $dr_t = (\theta_t - \alpha r_t)dt + \sigma_t dW_t$. However, such a model may be dangerous because it can generate negative interest rates with a positive probability. This shortcoming was solved by Black, Derman and Toy (BDT model) (1990) [12]. In their model, lognormal distribution is firstly combined with the mean reverting process of the short rate as $d\ln(r) = (\theta + \frac{\sigma_t'}{\sigma_t}\ln(r))dt + \sigma_t dW_t$. The major achievements of this model are the transparent calibration procedure of the yield curve and positive values generated in the calibration process. However, this model has mutually dependent mean-reversion and volatility terms. Later on, Black and Karasinski (1991) [13] modified this shortcoming of the BDT model in their celebrated lognormal short rate model by introducing independent parameters to avoid mutually dependent mean-reversion as $d\ln(r) = [\theta - \phi_t \ln(r)]dt + \sigma_t dW_t$.

All the models mentioned above are one-factor short rate models, there are also multi-factor models of the short rate, among them the best known are two, on is the Longstaff and Schwartz two factor model [14] as $dr_t = (\mu X + \theta Y)dt + \sigma_t\sqrt{Y}dW_t$ where X, Y are two independent stochastic process which follow Cox Ingersoll Ross model, the other is the Chen [15] three factor model (also called "stochastic mean and stochastic volatility model") as $dr_t = (\theta_t - \alpha_t)dt + \sigma_t\sqrt{r_t}dW_t$ where α_t, σ_t are two independent stochastic process which follow Cox Ingersoll Ross model. These one and multi-factor models model the interest rate evolution by means of the instantaneous short rate. The advantage of these models is that one can choose the related dynamics and coefficients in the related diffusion dynamics freely. However, these one and multi-factor models have one serious drawback. All of them are used to model short rate and a clear understanding of correlation structure of forward rates is difficult to achieve.

As mentioned before, Ho and Lee [10] proposed an alternative to short rate models based on a binomial tree process. Their basic idea led Heath, Jarrow and Morton (HJM)(1992) [16] to develop a general framework for modeling interest rate dynamics. Forward rates were chosen as basic fundamental quantities in HJM model and term structure was also translated to continuous time. The major achievement of HJM model is that forward rates are taken

as primary instrument directly because forward rates are directly traded in the debt market. HJM model is also the standard industry interest model nowadays. The great advantage of HJM models is that they give an analytical description of the entire yield curve, rather than just the short rate However, HJM model also has the limitation that it only allows a finite number of factors which determine the structure of the entire forward rate curve. This means that HJM model also cannot capture all the information of the structure of correlation of forward rates between different maturities. HJM model will be introduced detailed in Section § 2.3.

To overcome the restiction of HJM model, many models were proposed by Kennedy (1994) [17], Goldstein (2000) [18] and Baaquie (2001) [19]. Besides Baaquies quantum finance approach, all other models are based on a stochastic partial differential equation in infinite variables, and these models have a major limitation that all the processes are based on white noise. White noise is widely used in traditional finance, and short rate models and HJM models mentioned before also use white noise as the main calibration process (also called stochastic process or stochastic calculus). Compared to the stochastic process, the approach of quantum field theory, proposed by Baaquie [19], is a totally different mechanism which the expressions for all financial instruments are formally given as functional integral. One advantage of the approach based on quantum field theory is that it offers a different perspective on financial processes and a variety of computational algorithms, and nonlinearities in the forward rates as well as its stochastic volatility can be incorporated in a fairly straightforward manner. On the other hand, the field theory generalisation of the HJM model has been theoretically proven adequate for modelling the infinite degree of freedom with correlation since quantum field theory in physics has been developed exactly for cases including imperfect correlated infinite parameters.

§ 2.2 Lagrangian model of Black-Scholes

In 1973, Fisher Black, Myron Scholes, and Robert Merton made a revolutionary breakthrough in option pricing, which is known as Black-Sholes model. The Black-Scholes model gives the formula for a European option price. Myron Scholes and Robert Merton were awarded the 1997 Nobel prize for the Black-Scholes model. This model is used broadly in options pricing and has a significant impact on fundamental finance theory.

The assumptions of Black-Scholes model are:

- There is no arbitrage opportunity
- It is possible to borrow or lend money at risk-free rate
- Short selling is allowed
- There are no transaction fees
- The security does not pay dividends
- The log security follows a Gaussian distribution

In mathematical finance the underlying security $S(t)$ is assumed to follow stochastic differential equation that obeys the martingale condition, namely

$$\frac{dS_t}{S} = rdt + \sigma_0 dW_t \tag{§ 2.2.1}$$

where σ is the volatility of return, t is the dirft and W is white noise. European vanilla option price using Black Scholes model is

$$C(S, K, r, \sigma, (T - t_0)) = SN(d_+) - e^{-r(T-t_0)}KN(d_-) \tag{§ 2.2.2}$$

where

$$d_\pm = \frac{\ln(S/K) + r(T - t_0) \pm \sigma_0^2(T - t_0)/2}{\sigma_0\sqrt{(T - t_0)}}; \tag{§ 2.2.3}$$

and

$$N(x) = \frac{1}{\sqrt{2\pi}} \int_{-\infty}^{x} e^{-\frac{1}{2}z^2} dz \tag{§ 2.2.4}$$

The put option has the value

$$P(S, K, r, \sigma, T - t_0) = -SN(-d_+) + e^{-r(T-t_0)}KN(-d_-) \tag{§ 2.2.5}$$

The put-call parity is

$$C - P = S - e^{-r(T-t_0)}K \tag{§ 2.2.6}$$

Since $S(t) > 0$, the stock price is expressed by

$$S = e^x; \quad -\infty < x < +\infty.$$

In quantum finance, the underlying security and option price are both state vectors and, in

Dirac's notation, are denoted by

$$|x\rangle \quad ; \quad |C\rangle$$

In the state space notation, the payoff function and price for a call option are given by

$$\langle x|C(T;T)\rangle = (e^{x(T)} - K)_+ \quad ; \quad C(x,t;T) = \langle x|C(t;T)\rangle.$$

The present day value of an option is determined by the *conditional probability* $P(x,x';T,t)$ which is the probability that – given the value of the security $S(t) = e^x$ at time t– the security makes a transition to a final value of x' at future time T. The condition probability $P(x,x';T,t)$ has the required normalization, valid for all values of x, T, t

$$\int_{-\infty}^{+\infty} dx' \mathcal{P}(x,x';T,t) = 1 \qquad (\S\, 2.2.7)$$

The martingale condition for the underlying security, necessary for obtaining an option price that is free from arbitrage opportunities, requires that the discounted value of the future random value of the underlying security is equal to its present value. Hence the conditional probability must obey

$$e^x = e^{-r(T-t_0)} E[e^{x'}] = e^{-r\tau} \int_{-\infty}^{+\infty} dx' \mathcal{P}(x,x';T,t_0) e^{x'}, \qquad (\S\, 2.2.8)$$

Consequently, the price of the options is given, for remaining time $T - t_0$, the call option price $C(x,K,T,t_0)$ is given by

$$\begin{aligned} C(x,T,t_0) &= e^{-r(T-t_0)} E\Big[C(T,T)\Big] \\ &= e^{-r(T-t_0)} \int_{-\infty}^{+\infty} dx' \mathcal{P}(x,x';T,t_0) C(x',T,T) \end{aligned} \qquad (\S\, 2.2.9)$$

In particular, the price of the call option is given by

$$C(x,T,t_0) = e^{-r(T-t_0)} \int_{-\infty}^{+\infty} dx' \mathcal{P}(x,x';T,t_0) \Big(e^{x'} - K\Big)_+. \qquad (\S\, 2.2.10)$$

Baaquie [20] has shown that the Black-Scholes model can be obtained, using the framework

of quantum finance, from the following velocity Lagrangian $\mathcal{L}_{BS} = \mathcal{L}[x, \dot{x}]$ and action $\mathcal{S}$

$$\mathcal{L}[x, \dot{x}] = -\frac{1}{2\sigma_0^2}(\dot{x} + j)^2; \quad \mathcal{S} = \int_0^\tau dt \mathcal{L}[x, \dot{x}] \tag{§ 2.2.11}$$

The degree of freedom is written as $x = x_c + \epsilon$ with classical position x_c and stochastic piece ϵ. The transition amplitude is given by the following

$$\mathcal{K}(x_f|x_i) = \int_{-\infty}^{\infty} Dx e^{\mathcal{S}} = \int_{-\infty}^{\infty} D\epsilon e^{\mathcal{S}_\epsilon + \mathcal{S}_c} = N e^{\mathcal{S}_c}, \quad N = \int_{-\infty}^{\infty} D\epsilon e^{\mathcal{S}_\epsilon}$$

where $\mathcal{S}_c = S[x_c]$ is the classical action.

The classical solution of a system can be determined by requiring the classical action S to be stationary, which is equivalent to the Euler-Lagrangian equation

$$\left.\frac{\delta S}{\delta x(t)}\right|_{x(t)=x_c(t)} = \sum_{i=0}^{N} \left(-\frac{d}{dt}\right)^i \frac{\partial L}{\partial x^{(i)}} = 0, \tag{§ 2.2.12}$$

where $x^{(i)}$ represents the ith order time derivative of position x. The boundary condition $x(0) = x_f,\ x(\tau) = x_i,$ and $\epsilon(0) = \epsilon(\tau) = 0$. The classical solution for Black-Scholes model following equation of motion is $\ddot{x}_c = 0$, and the action is given by

$$\mathcal{S} \;=\; -\frac{1}{2\sigma_0^2}\int_0^\tau dt(\dot{x}_c + \dot{\epsilon} + j)^2 = \mathcal{S}_c + \mathcal{S}_\epsilon + R \tag{§ 2.2.13}$$

where the classical and stochastic action are

$$\mathcal{S}_c = -\frac{1}{2\sigma_0^2}\int_0^\tau dt(\dot{x}_c + j)^2,\ \mathcal{S}_\epsilon = -\frac{1}{2\sigma^2}\int_0^\tau dt(\dot{\epsilon}^2 + 2\dot{\epsilon}j) \tag{§ 2.2.14}$$

The residual term is zero since

$$R = -\frac{1}{\sigma_0^2}\int_0^\tau dt\dot{x}_c\dot{\epsilon} = -\frac{1}{\sigma_0^2}[-\dot{x}_c(0)\epsilon(0) + \dot{x}_c(\tau)\epsilon(\tau) - \int_0^\tau dt\ddot{x}_c\epsilon] = 0$$

The conditional probability $\mathcal{P}(x_f|x_i)$ is given by the transition amplitude

$$\mathcal{P}(x_f|x_i) = \frac{\mathcal{K}(x_f|x_i)}{\int_{-\infty}^{\infty} dx_f \mathcal{K}(x_f|x_i)} = \sqrt{\frac{1}{2\pi\sigma^2\tau}} e^{-\frac{1}{2\sigma^2\tau}(x_i - x_f + j\tau)^2} \tag{§ 2.2.15}$$

The drift is fixed by the martingale condition

$$e^{x_i} = e^{-r\tau}\int_{-\infty}^{+\infty} dx_f \mathcal{P}(x_f|x_i)e^{x_f} \quad \Rightarrow \quad j = r - \frac{\sigma_0^2}{2} \tag{§ 2.2.16}$$

The option price of equity is given by

$$\begin{aligned} C(S,K,r,\sigma,\tau) &= e^{-r\tau}\int_{-\infty}^{+\infty} dx_f \mathcal{P}(x_f|x_i)\Big(e^{x_f}-K\Big)_+ \\ &= \sqrt{\frac{1}{2\pi\sigma^2\tau}}e^{-r\tau}\int_{-\infty}^{+\infty} dx_f e^{-\frac{1}{2\sigma^2\tau}(x_i-x_f+j\tau)^2}\Big(e^{x_f}-K\Big)_+ \\ &= SN(d_+) - e^{-r\tau}KN(d_-). \end{aligned} \tag{§ 2.2.17}$$

The put option has the value

$$P(S,K,r,\sigma,\tau) = -SN(-d_+) + e^{-r\tau}KN(-d_-) \tag{§ 2.2.18}$$

The put call parity for the option [21] is given by

$$C + e^{-r\tau}K = P + S \tag{§ 2.2.19}$$

Δ is the dependence of S of the option price and is given by

$$\Delta = \frac{\partial V}{\partial S} = \begin{cases} N(d_+) & ; \quad V = C \\ -N(d_+) & ; \quad V = P \end{cases} \tag{§ 2.2.20}$$

In the Black-Scholes model, the option price depends on the underlying, strike price, interest rate, time to maturity and volatility. Volatility is not directly observable in the market, but instead, is implied by the option prices.

§ 2.3 Quantum field generalization of HJM model

The forward interest rate, denoted by $f(t,x)$, is the interest rate fixed at time t for an overnight loan at future time $x > t$. Both the bond market and interest paid on cash deposits are determined by $f(t,x)$. The standard industry bench mark is given by two models, namely the HJM model that is used to price bonds and the BGM-Jamshidian model that quantifies the interest rate paid on cash deposits.

To mathematically define the industry bench-mark models let $R(t)$ be Gaussian white noise with correlators given by

$$E[R(t)] = 0 \;\; ; \;\; E[R(t)R(t')] = \delta(t - t')$$

The HJM model is a linear model defined by

$$\frac{\partial f(t,x)}{\partial t} = \alpha(t,x) + \sigma(t,x)R(t) \qquad (\S\, 2.3.1)$$

where $\alpha(t,x), \sigma(t,x)$ are deterministic functions. A single white noise $R(t)$ is used to drive the entire evolution of forward interest rates and is not enough to describe the rich correlation of forward rates. It is natural to replace the one dimensional white noise with two dimensional quantum field $A(t,x)$, which is an random variable defined on both calendar and future time.

The quantum field theory of forward interest rates is a general framework for modelling the interest rates that provides a particularly transparent and computationally tractable formulation of interest rate instruments. Baaquie (2004) gives the quantum generalization of HJM model that Forward interest rates $f(t;x)$ are related to the two dimensional stochastic (random)field $A(t;x)$,

$$\begin{aligned} \frac{\partial f}{\partial t}(t,x) &= \alpha(t,x) + \sigma(t,x)A(t,x), & (\S\, 2.3.2) \\ f(t_*,x) &= f(t_0,x) + \int_{t_0}^{t_*} dt\alpha(t,x) + \int_{t_0}^{t_*} dt\sigma(t,x)A(t,x), & (\S\, 2.3.3) \end{aligned}$$

where the drift, under the measure of forward numeraire, is given by

$$\alpha_*(t,x) = \sigma(t,x)\int_{t_*}^{x} dx' D(x,x';t)\sigma(t,x'). \qquad (\S\, 2.3.4)$$

$A(t,x)$ is the quantum generalization of white noise $R(t)$ and it encodes the correlation (or information from data) of the forward rates $f(t,x)$ on future time x. Since $f(t,x)$ is a function of quantum field $A(t,x)$, the forward rate is also a two dimensional quantum field. From the view of Monte Carlo simulation, all financial instruments, such as coupon bond options, can be obtained by averaging the forward rates over all possible configurations.

The forward interest rate $f(t,x)$ is an independent random variable on both calendar and future time. Since the drift and volatility are deterministic, the random variable $A(t,x)$ is the most important factor in the evolution of $f(t,x)$. The dynamics of the quantum field

$A(t,x)$ were extensively studied in; the Lagrangian of $A(t,x)$, which can be used to describe the correlation of forward rates by using parameters μ and λ, is given by

$$\mathcal{L}[A] = -\frac{1}{2}\Big\{A^2(t,x)+\frac{1}{\mu^2}\Big\{\frac{\partial A(t,x)}{\partial x}\Big\}^2+\frac{1}{\lambda^4}\Big\{\frac{\partial^2 A(t,x)}{\partial^2 x}\Big\}^2\Big\}. \qquad (\S\,2.3.5)$$

The partition function, denoted by Z, is the functional integral over total configurations of $A(t,x)$ and is given by

$$Z = \int DAe^{S[A]}. \qquad (\S\,2.3.6)$$

$\int DA$ stands for integrating over all configurations of $A(t,x)$. The action $S[A]$ of the Lagrangian is given as follows

$$S[A] = \int_{t_0}^{\infty} dt \int_{t}^{\infty} dx\mathcal{L}[A]. \qquad (\S\,2.3.7)$$

A more general Gaussian Lagrangian, which is used for studying the empirical market data, is defined as

$$\mathcal{L}[A] = -\frac{1}{2}A(t,x)D^{-1}(x,x';t)A(t,x). \qquad (\S\,2.3.8)$$

As discussed before, the generating function is defined by

$$Z[h] = E\Big[\exp\Big\{\int_{t_0}^{\infty} dt\int_{t}^{\infty} dxh(t,x)A(t,x)\Big\}\Big]. \qquad (\S\,2.3.9)$$

This generating functional can be evaluated using Gaussian integration, which is shown as follows

$$\begin{aligned} Z[h] &= \frac{1}{Z}\int DAe^{S[A]+\int_{t_0}^{\infty} dt\int_{t}^{\infty} dxh(t,x)A(t,x)} \\ &= \exp\Big(\frac{1}{2}\int_{t_0}^{\infty} dt\int_{t}^{\infty} dxdx'h(t,x)D(x,x';t)h(t,x')\Big). \end{aligned} \qquad (\S\,2.3.10)$$

Hence, the propagator $D(x,x';t)$ is given by

$$\begin{aligned} E[A(t,x)A(t,x')] &= \frac{1}{Z}\int DAe^{S[A]}A(t,x)A(t',x') \\ &= \frac{\delta^2}{\delta h(t,x)\delta h(t',x')}Z[h]\big|_{h=0} = \delta(t-t')D(x,x';t). \end{aligned} \qquad (\S\,2.3.11)$$

Compared to the correlation function of HJM model, the propagator of quantum generalized model has full information of forward rates. Hence, the expectation value and correlation of $\partial f(t,x)/\partial t(t,x)$ is

$$E\big[\frac{\partial f}{\partial t}(t,x)\big] = E[\alpha(t,x)] = \alpha(t,x), \quad (\S\,2.3.12)$$

$$\begin{aligned} E\big[\frac{\partial f}{\partial t}(t,x)\frac{\partial f}{\partial t'}(t',x')\big] &= \sigma(t,x)\sigma(t',x')E[A(t,x)A(t',x')] \\ &= \delta(t-t')\sigma(t,x)D(x,x';t)\sigma(t,x'). \end{aligned} \quad (\S\,2.3.13)$$

The price of any interest rate instruments $F[A]$ can be evaluated by getting the expectation value $E[F[A]]$, which is equivalent to average $F[A]$ for all configurations of $f(t,x)$. Performing the Feynman path integral, the expectation value is given by

$$E\big[F[A]\big] = \frac{1}{Z}\int DAF[A]e^{S[A]}; \quad Z = \int DAe^{S[A]}. \quad (\S\,2.3.14)$$

The propagator used for the simulation is given in [22]

$$D(\theta,\theta') = \tfrac{\lambda}{2\sinh(2b)}[g(\theta+\theta') + g(\theta-\theta')] \quad (\S\,2.3.15)$$

$$g(\theta) = e^{-\lambda|\theta|\cosh(b)}\sinh\{b+\lambda|\theta|\cosh(b)\} \quad (\S\,2.3.16)$$

where $\theta = x-t; \theta' = x'-t$ and

$$e^{\pm b} = \frac{\lambda^2}{2\mu^2}[1 \pm \sqrt{1-4\frac{\mu^4}{\lambda}}]$$

In order to compare with empirical data, the normalized correlation function is given in [22] as

$$C(\theta,\theta') = \frac{D(\theta,\theta')}{\sqrt{D(\theta,\theta)D(\theta',\theta')}} \quad (\S\,2.3.17)$$

and shown in Figure 2.1.

Historical studies of swaption price in [23] show much advantages using the two-dimension field in quantum finance mode than the general HJM model in Figure 2.2.

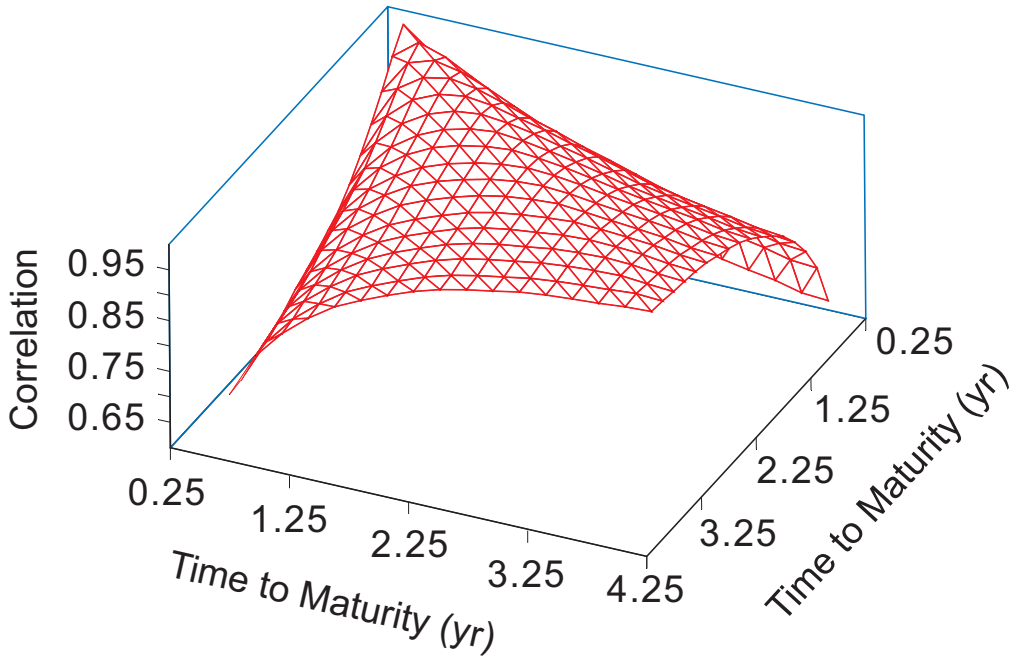

Figure 2.1: Normalized correlation from empirical studies of Libor

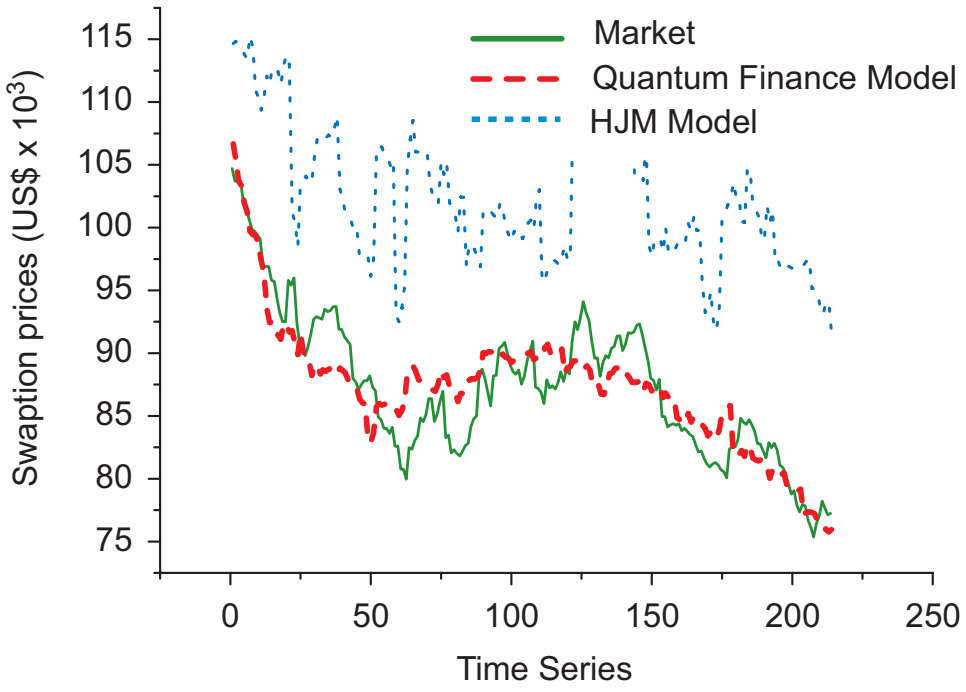

Figure 2.2: Swaption comparison between HJM model and quantum finance model

§ 2.4 Libor Hamiltonian Model

BGM-Jamshidian formulation of LMM is defined by

$$\frac{1}{L(t,T_n)}\frac{\partial L(t,T_n)}{\partial t} = \xi_n(t) + \gamma_n(t)R(t) \qquad (\S\,2.4.1)$$

where $\gamma_n(t)$ is a deterministic function; $\xi_n(t)$ is a function of Libor rates $L(t,T_n)$ and hence makes the model nonlinear.

The quantum finance formulation of the Libor Market Model (LMM) was first obtained by Baaquie [2] based on generalizing the one dimensional random noise $R(t)$ to a two dimensional classical stochastic field $A(t,x)$; from a mathematical point of view, $A(t,x)$ is a two dimensional Euclidean Gaussian quantum field. Libor forward interest rates $f_L(t,x)$, are in principle equal to $f(t,x)$ but written with a subscript L to differentiate it from the HJM forward interest rates, is defined for both calendar time t and future time x. The Libor forward rate in quantum finance approach is given by the following

$$\frac{\partial f_L(t,x)}{\partial t} = \mu(t,x) + \upsilon(t,x)A(t,x) \qquad (\S\,2.4.2)$$

where the drift $\mu(t,x)$ and volatility $\upsilon(t,x)$ both depend on the $f_L(t,x)$ making the model nonlinear. The correlation of the Gaussian field $A(t,x)$ is

$$E[A(t,x)A(t',x')] \;=\; \delta(t-t')D(x,x';t). \qquad (\S\,2.4.3)$$

where $D(x,x';t)$ is the propagator.

The quantum finance formulation of LMM $L(t,T_n)$ is given by

$$\frac{1}{L(t,T_n)}\frac{\partial L(t,T_n)}{\partial t} = \xi(t,x) + \int_{T_n}^{T_{n+1}} \gamma(t,x)A(t,x) \qquad (\S\,2.4.4)$$

where $\gamma(t,x)$ is the *deterministic volatility*. It is due to the deterministic volatility γ that the LMM is well defined.

Baaquie [2] defined the logarithmic field $\phi(t,x)$ that drives Libor interest rates as follows

$$\ell L(t,T_n) = e^{\int_{T_n}^{T_{n+1}} \phi(t,x)dx} \equiv e^{\phi_n(t)} \qquad (\S\,2.4.5)$$

$\phi(t,x)$ is mathematically equivalent to a two-dimensional Euclidean quantum field and has

dimensions of 1/time; the time evolution of $\phi(t,x)$ is given by

$$\frac{\partial\phi(t,x)}{\partial t} = -\frac{\Lambda_n(t,x)}{2} + \rho_n(t,x) + \gamma(t,x)A(t,x) \quad ; \quad T_n < x \le T_{n+1}$$
$$\Lambda_n(t,x) = \int_{T_n}^{T_{n+1}} dx'\gamma(t,x)D(x,x';t)\gamma(t,x')$$

The total drift has a deterministic piece $\Lambda_n(t,x)$ and a stochastic term $\rho_n(t,x)$.

LMM drift $\rho(t,x)$ above is derived based directly on the LMM Hamiltonian. We choose $B(t,T_{I+1})$ to be the forward bond numeraire; for all n, the drift is fixed so that

$$\chi_n(t) \equiv \frac{B(t,T_{n+1})}{B(t,T_{I+1})}$$

is a martingale. The drift $\rho(t,x)$ is determined in the Hamiltonian framework by the following condition [2]:

$$\mathcal{H}_\phi(t)\chi_n(t) = \mathcal{H}_\phi(t)\Big[\frac{B(t,T_{n+1})}{B(t,T_{I+1})}\Big] = 0: \quad \text{for all} \quad n \qquad (\S\,2.4.6)$$

Recall

$$\ell L(t,T_n) = \exp\{\int_{T_n}^{T_{n+1}} dx\phi(t,x)\} \equiv e^{\phi_n}.$$

The Hamiltonian of the Libor Market Model given by Baaquie [2],

$$\mathcal{H}_\phi(t) = -\frac{1}{2}\int_{x,x'} M_\gamma(x,x';t)\frac{\delta^2}{\delta\phi(x)\phi(x')} + \frac{1}{2}\int_x \Lambda(t,x)\frac{\delta}{\delta\phi(x)} - \int_x \rho(t,x)\frac{\delta}{\delta\phi(x)}$$

where

$$\rho(t,x) = \sum_{n=0}^{\infty}\theta_n(x)\rho_n(t,x); \quad \Lambda(t,x) = \sum_{n=0}^{\infty}\theta_n(x)\int_{T_n}^{T_{n+1}} dx' M_\gamma(x,x';t)$$

where $\theta_k(x)$ has the value 1 in the Libor range $T_k \le x < T_{k+1}$ and is equal to 0 when out of the range.

Functional differentiation by $\phi(x)$ yields

$$\frac{\delta L(t,T_k)}{\delta\phi(x)} = \theta_k(x)L(t,T_k).$$

The following are the three cases for the derivation.

$$\text{Case (i) } n > I,\ \chi_n(t) = \prod_{k=I+1}^{n} \frac{1}{1+\ell L(t,T_k)} = \exp\{-\sum_{k=I+1}^{n} \ln(1+\ell L(t,T_k))\}$$

$$\frac{\delta\chi_n(t)}{\delta\phi(x)} = -\sum_{k=I+1}^{n} \frac{e^{\phi_k}\theta_k(x)}{1+e^{\phi_k}} \qquad (\S\,2.4.7)$$

The summation term above is due to the discounting by the forward numeraire $B(t,T_{I+1})$. The second derivative yields

$$\frac{\delta^2\chi_n(t)}{\delta\phi(x)\delta\phi(x')} = -\sum_{k=I+1}^{n} (\frac{e^{\phi_k}}{1+e^{\phi_k}})^2\theta_k(x)\theta_k(x') - \sum_{k=I+1}^{n} \frac{e^{\phi_k}\theta_k(x)\theta_k(x')}{1+e^{\phi_k}} + \sum_{j,k=I+1}^{n} \frac{e^{\phi_j+\phi_k}\theta_k(x)\theta_k(x')}{(1+e^{\phi_j})(1+e^{\phi_k})}$$

Applying the log Libor Hamiltonian on $\chi_n(t)$

$$\mathcal{H}_\phi\chi_n(t) = \tfrac{1}{2}\int_{x,x'} M_\gamma[\sum_{k=I+1}^{n} (\frac{e^{\phi_k}}{1+e^{\phi_k}})^2\theta_k(x)\theta_k(x') - \sum_{j,k=I+1}^{n} \frac{e^{\phi_j+\phi_k}\theta_k(x)\theta_j(x')}{(1+e^{\phi_j})(1+e^{\phi_k})}$$
$$+ \sum_{k=I+1}^{n} \frac{e^{\phi_k}\theta_k(x)\theta_k(x')}{1+e^{\phi_k}}] - \frac{1}{2}\int_{x,x'} M_\gamma \sum_{n=0}^{\infty}\theta_n(x) \sum_{k=I+1}^{n} \frac{e^{\phi_k}\theta_k(x')}{1+e^{\phi_k}} + \int_x \rho(t,x) \sum_{k=I+1}^{n} \frac{e^{\phi_k}\theta_k(x)}{1+e^{\phi_k}}$$

Note the remarkable identity

$$\frac{1}{2}\sum_{j,k=I+1}^{n} A_{jk} = \sum_{j=I+1}^{n}\sum_{k=I+1}^{j} A_{jk} - \frac{1}{2}\sum_{k=I+1}^{n} A_{kk}$$

Taking

$$A_{jk} = \frac{e^{\phi_j+\phi_k}\theta_k(x)\theta_j(x')}{(1+e^{\phi_j})(1+e^{\phi_k})}$$

yields, after some cancelations

$$\mathcal{H}_\phi\chi_n(t) = \int_x \rho(t,x) \sum_{k=I+1}^{n} \frac{e^{\phi_k}\theta_k(x)}{1+e^{\phi_k}} - \int_{x,x'} M_\gamma \sum_{j=I+1}^{n}\sum_{k=I+1}^{j} \frac{e^{\phi_j+\phi_k}\theta_k(x)\theta_j(x')}{(1+e^{\phi_j})(1+e^{\phi_k})} \qquad (\S\,2.4.8)$$

and the Libor drift is given by

$$\begin{aligned}\rho_n(t,x) &= \sum_{j=I+1}^{n} \frac{e^{\phi_j}}{1+e^{\phi_j}} \int_{x'} M_\gamma(x,x';t) \\ &= \sum_{j=I+1}^{n} \frac{e^{\phi_j}}{1+e^{\phi_j}} \Lambda_j(x); \quad T_n \le x < T_{n+1}\end{aligned}$$

applied to Eq. § 3.9.3 leads to the cancelation of all the terms and yields the final result

$$\mathcal{H}_\phi \chi_n(t) = 0 \quad : \quad \text{martingale} \tag{§ 2.4.9}$$

Case (ii) $n < I$, the derivation similar to Case (i)

$$\chi_n(t) = \prod_{k=n+1}^{I} (1+\ell L(t,T_k)) = \exp\{\sum_{k=n+1}^{I} \ln(1+\ell L(t,T_k))\}$$

$$\Rightarrow \rho_n(t,x) = -\sum_{j=n+1}^{I} \frac{e^{\phi_j}}{1+e^{\phi_j}} \Lambda_j(x); \quad T_n \le x < T_{n+1}$$

Case(iii) $n = I, \chi_n(t) = 1$ yields

$$\mathcal{H}_\phi \chi_I(t) = 0 \Rightarrow \rho_I(t,x) = 0$$

.

So

$$\rho_n(t,x) = \left\{ \begin{array}{ll} \sum_{m=I+1}^{n} \frac{e^{\phi_m(t)}}{1+e^{\phi_m(t)}} \Lambda_m(t,x) & n > I \\ 0 & n = I \\ -\sum_{m=n+1}^{I} \frac{e^{\phi_m(t)}}{1+e^{\phi_m(t)}} \Lambda_m(t,x) & n < I \end{array} \right\} \quad : \quad T_n \le x < T_{n+1} \tag{§ 2.4.10}$$

§ 2.5 Correlation from a Gaussian propagator model

Our empirical analysis showed that the forward interest rate curve $f(t,x)$ could only be explained by including in the Lagrangian a term of order $\frac{\partial^2 f(t,x)}{\partial x^2}$, where x is future time.

The higher order of the future time derivative selects a set of random paths suitable for the evolution of the forward interest rates. Since the capital market is one entity, we model the evolution of equity to have a similar set of paths and this naturally leads to the Lagrangian discussed in this chapter.

We describe $\varphi_I(t)$ by a Gaussian model. Define a fourth order derivative Lagrangian by

$$\mathcal{L}[\varphi] = -\frac{1}{2}\sum_{I,J=1}^{N}\varphi_I\left[D^{-T}\left(1-\frac{1}{\mu^2}\frac{\partial^2}{\partial t^2}+\frac{1}{\lambda^4}\frac{\partial^4}{\partial t^4}\right)D^{-1}\right]_{IJ}\varphi_J \qquad (\S\,2.5.1)$$

where D, λ, μ are time independent $N \times N$ matrices. λ and μ are diagonal matrices.

The action functional is given by

$$S[\varphi] = \int_{-\infty}^{\infty}\mathcal{L}[\varphi]dt \qquad (\S\,2.5.2)$$

The joint probability distribution functional for the random variables $\varphi_I(t)$ is given by

$$P[\varphi] = \frac{1}{Z}\exp(S[\varphi]) \qquad (\S\,2.5.3)$$

where the partition function Z for the probability distribution is given by the Feynman path integral

$$Z = \int \mathcal{D}\varphi\exp(S[\varphi]), \quad \int\mathcal{D}\varphi \equiv \prod_I\prod_{t=-\infty}^{\infty}\int_{-\infty}^{\infty}d\varphi_I(t) \qquad (\S\,2.5.4)$$

The propagator is a quantity of fundamental importance since it governs the evolution of the stochastic variables. For the above Gaussian model, the propagator $G_{IJ}(t,t')$ is given by

$$\begin{aligned} G_{IJ}(t,t') &= E[\varphi_I(t)\varphi_J(t')] \\ &= \frac{1}{Z}\int\mathcal{D}\varphi\exp(S[\varphi])\varphi_I(t)\varphi_J(t') \end{aligned} \qquad (\S\,2.5.5)$$

According to [1], $G_{IJ}(t,t')$ yields

$$G^{-1}_{IJ}(t,t') = \left[D^{-T}\left(1-\frac{1}{\mu^2}\frac{\partial^2}{\partial t^2}+\frac{1}{\lambda^4}\frac{\partial^4}{\partial t^4}\right)D^{-1}\delta(t-t')\right]_{IJ} \qquad (\S\,2.5.6)$$

Considering $\delta(t,t') = \int_{-\infty}^{+\infty} \frac{d\omega}{2\pi} e^{i\omega(t-t')}$ yields,

$$G_{IJ}(t,t') = \left(D\Delta(t-t')D^T\right)_{IJ} \tag{§ 2.5.7}$$

The diagonal matrix $\Delta(t-t')$, when λ and μ are diagonal, is given by

$$\Delta_{II}(t-t') \equiv \lambda_I^4 \int_{-\infty}^{\infty} \frac{d\omega}{2\pi} \frac{e^{i\omega(t-t')}}{\lambda_I^4 + (\lambda_I^2/\mu_I)^2\omega^2 + \omega^4} \tag{§ 2.5.8}$$

Note that

$$\lambda_I^4 + (\lambda_I^2/\mu_I)^2\omega^2 + \omega^4 = (\omega^2 + a_I^+)(\omega^2 + a_I^-) \tag{§ 2.5.9}$$

$$\text{with} \quad a_I^\pm = \frac{\lambda_I^4}{2\mu_I^2}\left[1 \pm \sqrt{1 - 4\left(\frac{\mu_I}{\lambda_I}\right)^4}\right] \tag{§ 2.5.10}$$

Thus $\Delta_{II}(t-t')$ is given by [1]

$$\begin{aligned}\Delta_{II}(t-t') &= \frac{\lambda_I^4}{a_I^+ - a_I^-}\int_{-\infty}^{\infty}\frac{d\omega}{2\pi}\left[\frac{e^{i\omega(t-t')}}{\omega^2 + a_I^-} - \frac{e^{i\omega(t-t')}}{\omega^2 + a_I^+}\right] \\ &= \frac{\lambda_I^4}{2(a_I^+ - a_I^-)}\left(\frac{e^{-\sqrt{a_I^-}|t-t'|}}{\sqrt{a_I^-}} - \frac{e^{-\sqrt{a_I^+}|t-t'|}}{\sqrt{a_I^+}}\right)\end{aligned} \tag{§ 2.5.11}$$

Case I: $\sqrt{2}\mu_I < \lambda_I$; $a_I^\pm$ real

$$a_I^\pm = \lambda_I^2 e^{\pm 2b_I}; \quad e^{\pm 2b_I} = \frac{\lambda_I^2}{2\mu_I^2}\left[1 \pm \sqrt{1 - 4\left(\frac{\mu_I}{\lambda_I}\right)^4}\right]; \quad b_I \geq 0 \tag{§ 2.5.12}$$

$$\Delta_{II}(t-t') = \frac{\lambda_I e^{-\lambda_I|t-t'|\cosh(b_I)}}{2\sinh(2b_I)}\sinh[b_I + \lambda_I|t-t'|\sinh(b_I)] \tag{§ 2.5.13}$$

Case II: $\sqrt{2}\mu_I > \lambda_I$; $a_I^\pm$ complex

$$a_I^\pm = \lambda_I^2 e^{\pm i2\theta_I}; \quad e^{\pm i2\theta_I} = \frac{\lambda_I^2}{2\mu_I^2}\left[1 \pm i\sqrt{4\left(\frac{\mu_I}{\lambda_I}\right)^4 - 1}\right]; \quad 0 \leq \theta_I \leq \pi \tag{§ 2.5.14}$$

$$\Delta_{II}(t-t') = \frac{\lambda_I e^{-\lambda_I|t-t'|\cos(\theta_I)}}{2\sin(2\theta_I)}\sin[\theta_I + \lambda_I|t-t'|\sin(\theta_I)] \tag{§ 2.5.15}$$

We make a change of variable

$$z = t^{\eta}, \eta \in (0, 1] \tag{§ 2.5.16}$$

because the evolution of $\varphi_I(t) = \varphi_I(z)$ needs to be described in market time z instead of calendar time t. z reflects the future time anticipated by traders and investors [1].

From Eq. § 2.5.13 and § 2.5.15, $\Delta(z - z')$ yields

$$\Delta_{II}(z - z') = \begin{cases} \frac{\lambda_I \exp\{-\lambda_I|z-z'|\cosh(b_I)\}}{2\sinh(2b_I)} \sinh[b_I + \lambda_I|z - z'|\sinh(b_I)], \sqrt{2}\mu_I < \lambda_I \\ \frac{\lambda_I \exp\{-\lambda_I|z-z'|\cos(\theta_I)\}}{2\sin(2\theta_I)} \sin[\theta_I + \lambda_I|z - z'|\sin(\theta_I)], \sqrt{2}\mu_I > \lambda_I \end{cases} \tag{§ 2.5.17}$$

where b and θ are given in Eqs. § 2.5.12 and § 2.5.14.

$$\Delta_{II}(0) = \begin{cases} \frac{\lambda_I \sinh b_I}{2\sinh(2b_I)}, \text{ when } \sqrt{2}\mu_I < \lambda_I \\ \frac{\lambda_I \sin\theta_I}{2\sin(2\theta_I)}, \text{ when } \sqrt{2}\mu_I > \lambda_I \end{cases} \tag{§ 2.5.18}$$

Note that $\tau = t - t'$, μ_I in terms of angle is

$$\mu_I^2 = \begin{cases} \frac{1}{2}\lambda_I^2 \text{sech}(2b_I), \text{ when } \sqrt{2}\mu_I < \lambda_I \\ \frac{1}{2}\lambda_I^2 \sec(2\theta_I), \text{ when } \sqrt{2}\mu_I > \lambda_I \end{cases} \tag{§ 2.5.19}$$

And the normalized correlator $C(\tau)$ yields

$$h_{II}(\tau) = \frac{\Delta_{II}(\tau)}{\Delta_{II}(0)} = \begin{cases} \frac{\exp\{-\lambda_I\tau^{\eta}\cosh(b_I)\}}{\sinh(b_I)} \sinh[b_I + \lambda_I\tau^{\eta}\sinh(b_I)], \sqrt{2}\mu_I < \lambda_I \\ \frac{\exp\{-\lambda_I\tau^{\eta}\cos(\theta_I)\}}{\sin(\theta_I)} \sin[\theta_I + \lambda_I\tau^{\eta}\sin(\theta_I)], \sqrt{2}\mu_I > \lambda_I \end{cases} \tag{§ 2.5.20}$$

$h(\tau)$ in different domains are shown in Figure 2.3 for $\sqrt{2}\mu_I > \lambda_I$ and Figure 2.4 for $\sqrt{2}\mu_I < \lambda_I$. From Figure 2.3(c) and (d) the $h(z)$ does not converge for large τ. From Figure 2.4 does not has any oscillations for all τ. The domain we choose for correlation function is the complex domain $\sqrt{2}\mu_I > \lambda_I$ when $0 < \theta < \pi/2$.

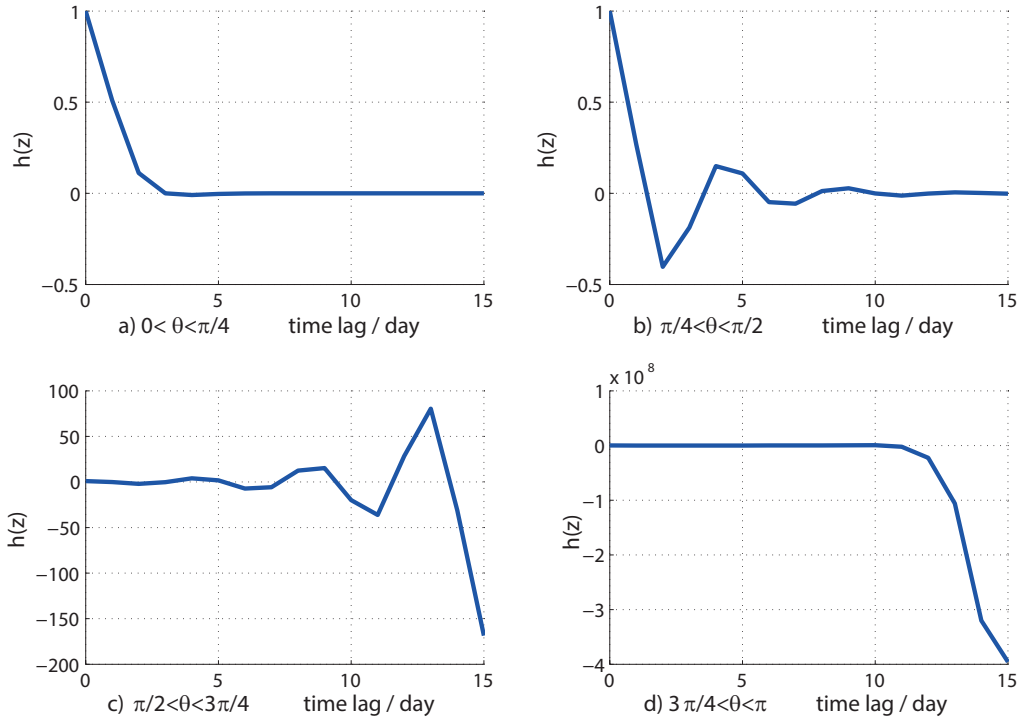

Figure 2.3: Theoretical $h(\tau)$ of four complex domains, $\sqrt{2}\mu_I > \lambda_I$.

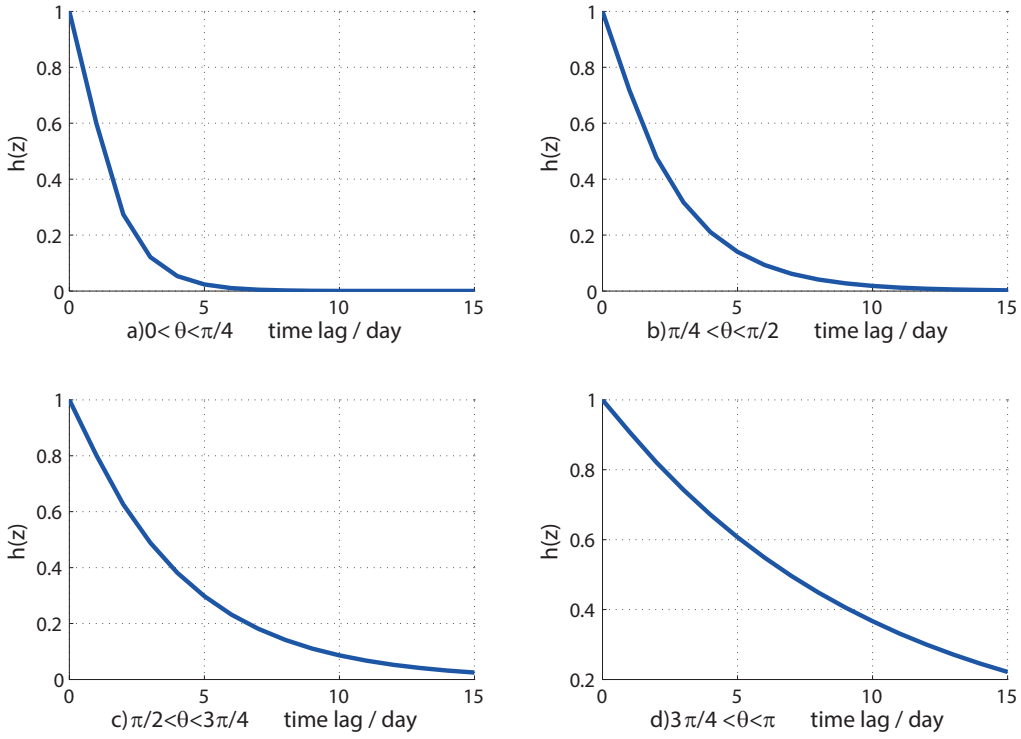

Figure 2.4: Theoretical $h(\tau)$ of real domains, $\sqrt{2}\mu_I < \lambda_I$.

Chapter 3

Pricing of Range Accrual Swap in Libor Market Model

We study the range accrual swap in the quantum finance formulation of the Libor Market Model (LMM). It is shown that the formulation can exactly price the path dependent instrument. An approximate price is obtained as an expansion in the volatility of Libor. The Monte Carlo simulation method is used to study the nonlinear domain of the model and determine the range of validity of the approximate formula. The price of accrual swap is analyzed by generating daily sample values by simulating of a two dimension Gaussian quantum field.

§ 3.1 Introduction

Range accrual swap is a type of a derivative product that is similar to normal interest rate swap. The investor may have a view that the market is or is not very volatile and that consequently some index will or will not stay within a predefined range. The range accrual index could be an interest rate, an FX rate or a commodity price. The investor makes an additional profit if the view taken is correct and loses money otherwise. The range accrual can also serve to hedge risks since the payments are based on daily observations and not on a pre-fixed rate.

The interest range accrual swap is one of the most popular non-vanilla interest rate derivatives; more than USD 160 billion of range accrual indexed on interest rates have been sold since 2004, and the total volumes have been increasing rapidly in the last few years. The present work investigates the range accrual swap based on the behavior of the 3-month Libor.

The range accrual for interest rates has been studied in many books and articles, such as Navatte and Quittard-Pinon [24], Nunes [25] using the Gaussian HJM (Heath−Jarrow−Morton) framework, Damiano Brigo and Fabio Mercurio using the BGM-Jamshidian formulation of LMM [26] and Yoon and Jang [27] with jump risk. The quantum finance formulation of the Libor Market Model has been studied in [2].

Quantum field theory has been applied to many *classical problems*; two famous examples are a) the solution of classical phase transitions by Wilson and which led to his physics Nobel Prize in 1982 [28] and b) the complete classification of knots and links in three dimensions by Witten, for which he was awarded the Fields Medal in 1989 [29]. These examples show that the mathematics of quantum mechanics extends far beyond not only quantum systems but instead can be applied to a wide variety of phenomena, including even the social sciences [30]. The formalism of quantum finance has been developed in this spirit and is based on the application of *quantum mathematics* to finance [31, 1]. In particular, interest rate models in quantum finance are based on the mathematics of a two-dimensional Euclidean quantum field.

This chapter is organized as follows. Section § 3.2 briefly reviews LMM in quantum finance. In Sections § 3.3 and § 3.4 the range accrual swap is defined in the mathematical framework of the quantum LMM. In Section § 3.5 we derive an analytical approximate formula for the price of the range accrual swap. In Sections § 3.6, § 3.7, we carry out a Monte Carlo simulation to evaluate the price of the range accrual swap. In particular, we compare the approximate analytical expression for the range accrual swap with simulation results. We draw some conclusions in the final Section § 5.7.

§ 3.2 Libor Market Model

The forward interest rate, denoted by $f(t,x)$, is the interest rate fixed at time t for an overnight loan at future time $x > t$. Both the bond market and interest paid on cash deposits are determined by $f(t,x)$. The standard industry bench mark is given by two models, namely the HJM model that is used to price bonds and the BGM-Jamshidian model that quantifies the interest rate paid on cash deposits.

To mathematically define the industry bench-mark models let $R(t)$ be Gaussian white noise with correlators given by

$$E[R(t)] = 0 \quad ; \quad E[R(t)R(t')] = \delta(t-t')$$

The HJM model is a linear model defined by

$$\frac{\partial f(t,x)}{\partial t} = \alpha(t,x) + \sigma(t,x)R(t) \qquad (\S\,3.2.1)$$

where $\alpha(t,x), \sigma(t,x)$ are deterministic functions.

The Libor interest rate $L(t,T_n)$ is a simple interest rate, fixed at time t, for making a cash deposit at future time T_n for a duration of time ℓ, called the tenor of the deposit. Simple interest Libor rates $L(t,T_n)$ are defined on the Libor future time lattice defined by $T_n = n\ell$, where ℓ is Libor tenor. The Libor lattice is shown in Figure 3.1; for fixed tenor ℓ Libor rates are only defined on the Libor interval $[T_n, T_{n+1}]$; the shaded portion in Figure 3.1 shows all the Libor rates that exist for the Libor lattice.

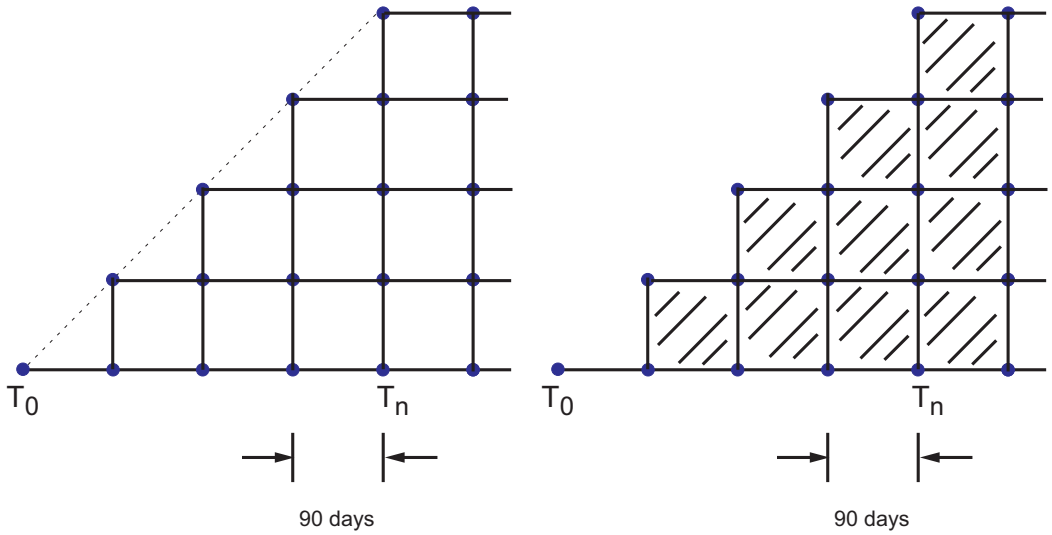

Figure 3.1: The Libor lattice defined by $L(T_n,T_m)$. The shaded portion shows the time dependence of the Libor rates for the Libor lattice.

In terms of Libor forward interest rates $L(t,T_n)$ is given by

$$1 + \ell L(t,T_n) = e^{\int_{T_n}^{T_{n+1}} dx f(t,x)} \qquad (\S\,3.2.2)$$

BGM-Jamshidian formulation of LMM is defined by

$$\frac{1}{L(t,T_n)}\frac{\partial L(t,T_n)}{\partial t} = \xi_n(t) + \gamma_n(t)R(t) \qquad (\S\,3.2.3)$$

where $\gamma_n(t)$ is a deterministic function; $\xi_n(t)$ is a function of Libor rates $L(t,T_n)$ and hence makes the model nonlinear.

The quantum finance formulation of the Libor Market Model (LMM) was first obtained by Baaquie [2] based on generalizing the one dimensional random noise $R(t)$ to a two dimensional classical stochastic field $A(t,x)$; from a mathematical point of view, $A(t,x)$ is a two dimensional Euclidean Gaussian quantum field. Libor forward interest rates $f_L(t,x)$, are in principle equal to $f(t,x)$ but written with a subscript L to differentiate it from the HJM forward interest rates, is defined for both calendar time t and future time x. The Libor forward rate in quantum finance approach is given by the following

$$\frac{\partial f_L(t,x)}{\partial t} = \mu(t,x) + \upsilon(t,x)A(t,x) \qquad (\S\, 3.2.4)$$

where the drift $\mu(t,x)$ and volatility $\upsilon(t,x)$ both depend on the $f_L(t,x)$ making the model nonlinear. The correlation of the Gaussian field $A(t,x)$ is

$$E[A(t,x)A(t',x')] \;\; = \;\; \delta(t-t')D(x,x';t). \qquad (\S\, 3.2.5)$$

where $D(x,x';t)$ is the propagator.

The quantum finance formulation of LMM $L(t,T_n)$ is given by

$$\frac{1}{L(t,T_n)}\frac{\partial L(t,T_n)}{\partial t} = \xi(t,x) + \int_{T_n}^{T_{n+1}} \gamma(t,x)A(t,x) \qquad (\S\, 3.2.6)$$

where $\gamma(t,x)$ is the *deterministic volatility*. It is due to the deterministic volatility γ that the LMM is well defined.

Baaquie [2] defined the logarithmic field $\phi(t,x)$ that drives Libor interest rates as follows

$$\ell L(t,T_n) = e^{\int_{T_n}^{T_{n+1}} \phi(t,x)dx} \equiv e^{\phi_n(t)} \qquad (\S\, 3.2.7)$$

$\phi(t,x)$ is mathematically equivalent to a two-dimensional Euclidean quantum field and has dimensions of 1/time; the time evolution of $\phi(t,x)$ is given by

$$\begin{aligned} \frac{\partial \phi(t,x)}{\partial t} &= -\frac{\Lambda_n(t,x)}{2} + \rho_n(t,x) + \gamma(t,x)A(t,x) \;\; ; \;\; T_n < x \leq T_{n+1} \\ \Lambda_n(t,x) &= \int_{T_n}^{T_{n+1}} dx'\gamma(t,x)D(x,x';t)\gamma(t,x') \end{aligned}$$

The total drift has a deterministic piece $\Lambda_n(t,x)$ and a stochastic term $\rho_n(t,x)$.

To find its present value, all future cash flows need to be discounted by a 'numeraire'–

based on the prevailing interest rates and encoding the time value of money. The forward bond numeraire is given by $B(t, T_{I+1})$; for any Libor based financial instrument $\mathcal{F}[L, t]$ the martingale condition states that

$$\frac{\mathcal{F}[L, T_0]}{B(T_0, T_{I+1})} = E_I \left[\frac{\mathcal{F}[L, T_n]}{B(T_n, T_{I+1})} \right] \tag{§ 3.2.8}$$

The subscript I is the symbol for the expectation value, namely $E_I[..]$, to indicate that the expectation value is being taken over a stochastic process that has a martingale evolution with respect to the numeraire $B(t, T_{I+1})$.

The drift $\rho_n(t, x)$ of the LMM is obtained by requiring that the time evolution of all Libor rates follow a martingale process with respect to the numeraire $B(t, T_{I+1})$; imposing the martingale condition derived in Appendix § 3.9 and yields the following drift [2]

$$\rho_n(t,x) = \left\{ \begin{array}{ll} \displaystyle\sum_{m=I+1}^{n} \frac{e^{\phi_m(t)}}{1+e^{\phi_m(t)}} \Lambda_m(t,x) & n > I \\ 0 & n = I \\ \displaystyle -\sum_{m=n+1}^{I} \frac{e^{\phi_m(t)}}{1+e^{\phi_m(t)}} \Lambda_m(t,x) & n < I \end{array} \right\} \quad : \quad T_n \leq x < T_{n+1} \tag{§ 3.2.9}$$

Note Eq. § 3.2.9 defines the drift $\rho_n(t, x)$ for x in the Libor lattice that $T_n < x \leq T_{n+1}$ for some n; as x takes values in different parts of the Libor lattice, the drift $\rho_n(t, x)$ also changes.

§ 3.2.1 Lagrangian and path integral for $\phi(t, x)$

The quantum field theory of the stochastic field driving the interest rates is defined by a functional integral over all configurations of $A(t, x)$. The partition function is given by

$$Z = \int DA e^{S[A]} \tag{§ 3.2.10}$$

The Lagrangian and action for the Gaussian quantum field $A(t, x)$ are given by the following

$$S[A] = \int_0^\infty dt \int_t^\infty dx \mathcal{L}[A] \; ; \; \mathcal{L}[A] = -\frac{1}{2} A(t,x) D^{-1}(x, x'; t) A(t, x') \tag{§ 3.2.11}$$

All financial instruments' prices are obtained by performing a path integral over the (fluctuating) two dimensional quantum field $A(t, x)$. The expectation value for an instrument, say

$Q[A]$, is denoted by $E[Q[A]]$ and is defined by the functional average over all values of $A(t,x)$, weighted by the probability measure e^S/Z, discussed in Baaquie[2]. Hence

$$E[Q[A]] = \frac{1}{Z}\int DAQ[A]e^{S[A]} \qquad (\S\,3.2.12)$$

The quantum field theory of the forward interest rates is given by

$$Z[h(t,x)] \;=\; E[e^{\int_{t_0}^{\infty}\int_0^{\infty} h(t,x)A(t,x)dx}]$$

For a quadratic Lagrangian, such as the one given in Eq. § 3.2.11, the generating function is obtained by performing the Gaussian integrations and yields

$$\begin{aligned} Z[h(t,x)] &= \frac{1}{Z}\int DAe^S e^{\int_{t_0}^{\infty} dt\int_0^{\infty} h(t,x)A(t,x)dx} \\ &= \exp\{\frac{1}{2}\int_{t_0}^{\infty} dt\int_0^{\infty} dxdx' h(t,x)D(x,x';t)h(t,x')\} \qquad (\S\,3.2.13) \end{aligned}$$

The correlators of the $A(t,x)$ quantum field are given by

$$E[A(t,x)] = 0 \qquad (\S\,3.2.14)$$

$$\begin{aligned} E[A(t,x)A(t',x')] &= \frac{1}{Z}\int DAe^{S[A]}A(t,x)A(t',x') \\ &= \delta(t-t')D(x,x';t). \qquad (\S\,3.2.15) \end{aligned}$$

The numerical simulation of $A(t,x)$ is discussed in Appendix § 3.10.

§ 3.2.2 Interest rate swaps

An interest rate swap is an agreement made today, to exchange two streams of cash flows at some future time. It is contracted between two parties in which one party A pays a fixed interest rate R_S and receives floating fixed by Libor (at the future date) whereas the other party B pays a floating Libor and receives fixed; Figure 3.2 schematically shows cash flows for a swap at some future time.

Consider a swaplet that receives a single floating payment and pays at a fixed rate R_S; the swaplet matures at time T_n and the floating rate is fixed by the value of the 90-day Libor, namely Libor $L(T_n,T_n)$; both the floating and fixed rates cash flows take place in *arrears*, at time T_{n+1}. For a sum of amount V, the value of the swaplet, at present time T_0, is equal to

the future cash flows – discounted by bond $B(T_0, T_{n+1})$ to present time and T_0 and is given by the following [2]:

$$Swaplet_L(T_0, R_s) = \ell V B(T_0, T_{n+1})\big[L(T_0, T_n) - R_s\big] \qquad (\S\, 3.2.16)$$

A swap consists of a portfolio of swaplets, starting at Libor time T_0; payments are made at fixed times $T_n = T_0 + n\ell$, with $n = 1, 2, ..., N-1$; the first payment is made at T_1 and the last payment at T_N. The value at time T_0 of the floating rate receiver $Swap_L$ and fixed rate receiver $Swap_R$ is

$$Swap_L(T_0, R_s) = \ell V \sum_{n=0}^{N-1} B(T_0, T_{n+1})[L(T_0, T_n) - R_s]$$
$$Swap_R(T_0, R_s) = \ell V \sum_{n=0}^{N-1} B(T_0, T_{n+1})[R_s - L(T_0, T_n)]$$
$$Swap_L(T_0, R_s) + Swap_R(T_0, R_s) = 0$$

The par value $R_p(T_0)$ is defined to make the initial values equal for floating rate receiver $Swap_L$ and fixed rate receiver $Swap_R$; hence

$$Swap_L(T_0, R_p(T_0)) = 0 = Swap_R(T_0, R_p(T_0))$$

§ 3.3 Range accrual swap

In a typical interest rate range accrual swap, the fixed rate R_S accrues *contingent* on a *pre-selected* Libor rate being within a *pre-fixed* range $[a, b]$ during a stipulated period preceding the payment. At payment date, the payment fraction is ξR_S where $\xi = \frac{\kappa}{M}$ and κ is the number of days that the pre-selected Libor was in the range for the payment period and M is the payment period of the individual swaplets. In this chapter, the payments are made every

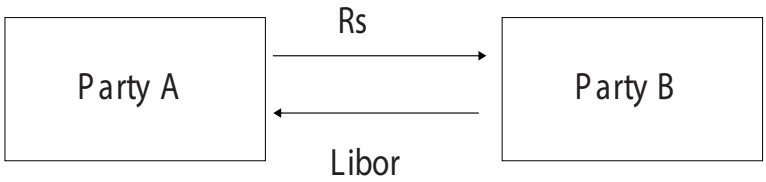

Figure 3.2: Diagram representing cash flows, at some future time, for a swap.

$M = 90$ days and the 90-day Libor rate is tracked during this period to see how many days it was within the pre-specified range $[a, b]$.

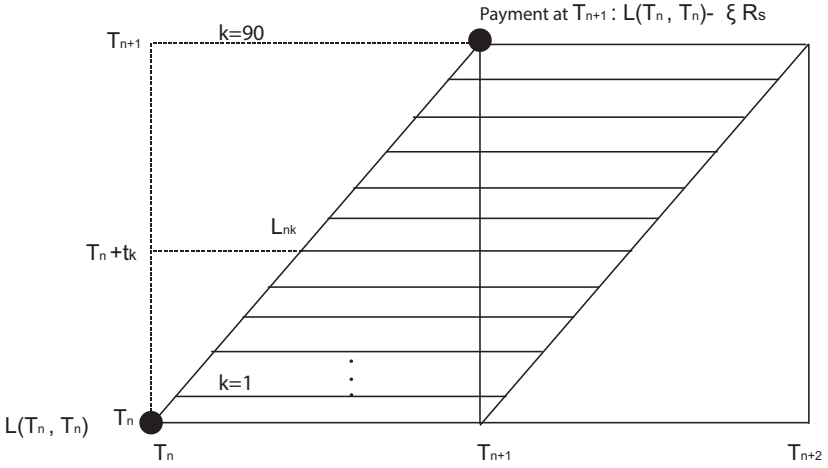

Figure 3.3: The 90-day Libor rates for one payment period.

Consider Figure 3.3, where a single 90-day payment period is shown – from calendar time T_n to the next payment time T_{n+1}. The Libor for the swaplet, namely $L(T_n, T_n)$ is fixed at time T_n; however, unlike a normal swap for which the fixed rates are always R_S, for the accrual case, it is only fixed at the payment date, namely at time T_{n+1}.

The 90-day Libor at calendar time $T_n + t_k$, namely L_{nk}, is defined by

$$1 + \ell L_{nk} \equiv \exp\left\{ \int_{T_n+t_k}^{T_{n+1}+t_k} dx \; f(T_n + t_k, x) \right\} \qquad (\S\, 3.3.1)$$

with the unit function given by

$$1_{a<z<b} = \begin{cases} 1 & z \in [a, b] \\ 0 & \text{otherwise} \end{cases}$$

The horizontal lines indicate the 90-day Libor L_{nk} for calendar time $T_n + t_k$. The value of the 90-day Libor is observed every day. In this way, it is determined for how many days κ was the 90-day Libor L_{nk} in the pre-fixed range. After 90 days, the rate for payment at time T_{n+1} is fixed to be $\xi R_S = \frac{\kappa}{M} \cdot R_S$ and the floating and 'fixed' cash flows are equal to $L(T_n, T_n) - \xi R_S$, as shown in Figure 3.3.

The stochastic cash-flow at calendar time T_{n+1} defines the range accrual swaplet as the

following:

$$Swaplet_A(T_n, T_n; a, b) = \ell V B(T_n, T_{n+1}) \Big[L(T_n, T_n) - \frac{R_s}{M} \sum_{k=1}^{M} 1_{a<L_{nk}<b} \Big], \qquad (\S\, 3.3.2)$$

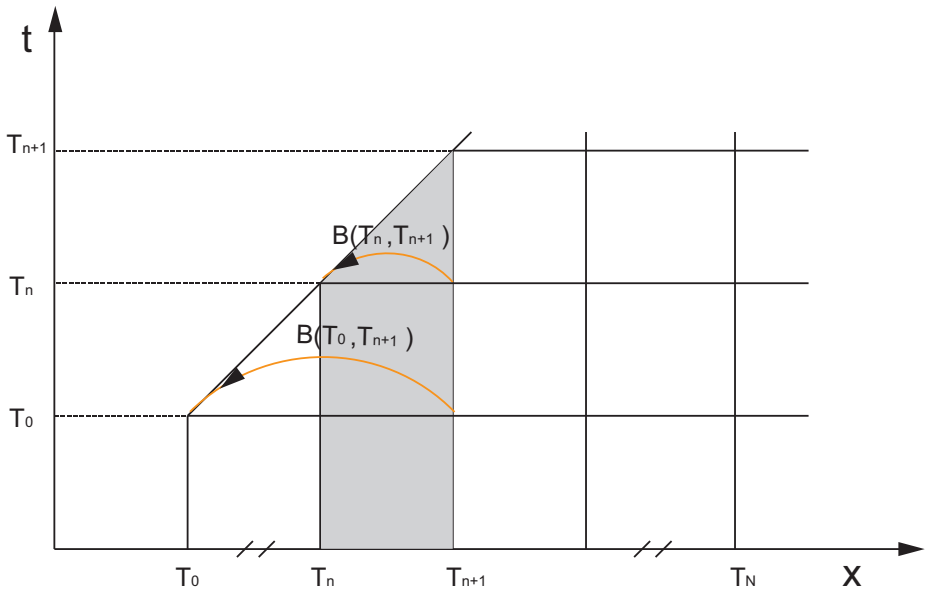

Figure 3.4: The bond numeraire $B(T_n, T_{n+1})$ used for discounting price. The shaded area is the time interval.

The accrual time is defined for the 90-day Libor by the following

$$\ell = 90\epsilon \quad ; \quad t_k = k\epsilon \quad ; \quad \epsilon = 1 \text{ day} \quad ; \quad k = 1, 2, ...90$$

The bond $B(T_0, T_{n+1})$ in Figure 3.4, expressed in terms of Libor rates, is given by

$$B(T_0, T_{n+1}) = \exp\{-\int_{T_0}^{T_{n+1}} dx f_L(T_0, x)\} = \prod_{i=0}^{n} \frac{1}{1 + \ell L(T_0, T_i)}. \qquad (\S\, 3.3.3)$$

For the swap accrual, the discounted value of each swaplet is evaluated separately; hence we can use a 'rolling' numeraire, choosing a numeraire tailored to simplify the calculation of each swaplet. The discounted price of a swaplet, using the numeraire $B(T_n, T_{I+1})$, is a martingale and yields, from Eqs. § 3.2.8 and § 3.3.2, that the swaplet price at present time T_0

is given by

$$\frac{Swaplet_A(T_0,T_n;a,b)}{B(T_0,T_{I+1})} = \ell V E_I\left[\frac{Swaplet_A(T_n,T_n;a,b)}{B(T_n,T_{I+1})}\right]$$
$$= \ell V E_I\left[\frac{B(T_n,T_{n+1})}{B(T_n,T_{I+1})}\{L(T_n,T_n) - \frac{R_s}{M}\sum_{k=1}^{M} 1_{a<L_{nk}<b}\}\right] \qquad (\S\,3.3.4)$$

Using the numeraire $B(T_n,T_{n+1})$ for discounting, namely taking $I=n$, yields the following accrual swaplet price

$$\frac{Swaplet_A(T_0,T_n;a,b)}{B(T_0,T_{n+1})} = \ell V E_n\Big[L(T_n,T_n) - \frac{R_s}{M}\sum_{k=1}^{M} 1_{a<L_{nk}<b}\Big] \qquad (\S\,3.3.5)$$

Since

$$E_n[L(T_n,T_n)] = E_n\Big[\frac{B(T_n,T_{n+1}) - B(T_n,T_n)}{\ell B(T_n,T_{n+1})}\Big] = L(T_0,T_n), \qquad (\S\,3.3.6)$$

the accrual swaplet, from Eqs. § 3.3.4 and § 3.3.6, is given by

$$Swaplet_A(T_0,T_n;a,b) = \ell V B(T_0,T_{n+1})\Big\{L(T_0,T_n) - \frac{R_s}{M}\sum_{k=1}^{M} E_n[1_{a<L_{nk}<b}]\Big\}$$

The main difference from a normal swaplet is the calculation of the accrual part $E_n[1_{a<L_{nk}<b}]$, which is expectation value of the 90-day Libor L_{nk} being in the range at kth day, with the expectation value being performed for the $B(t,T_{n+1})$ numeraire.

If the future fixed payments are deterministic, as is the case for the usual swaplet for which the fixed payment is R_S, we recover the result for the swaplet given in Eq. § 3.2.16, namely

$$Swaplet_L(T_0,R_s) = \ell V B(T_0,T_{n+1})\big[L(T_0,T_n) - R_s\big]$$

The Libor range accrual swap is given by the sum of swaplets for payments at different future calendar times T_n and yields

$$Swap_A(T_0,T_N;a,b) = \sum_{n=0}^{N-1} Swaplet_A(T_0,T_n;a,b) \qquad (\S\,3.3.7)$$

Note that unlike a normal $Swaplet(T_0,R_S)$, which has a deterministic value at time T_0

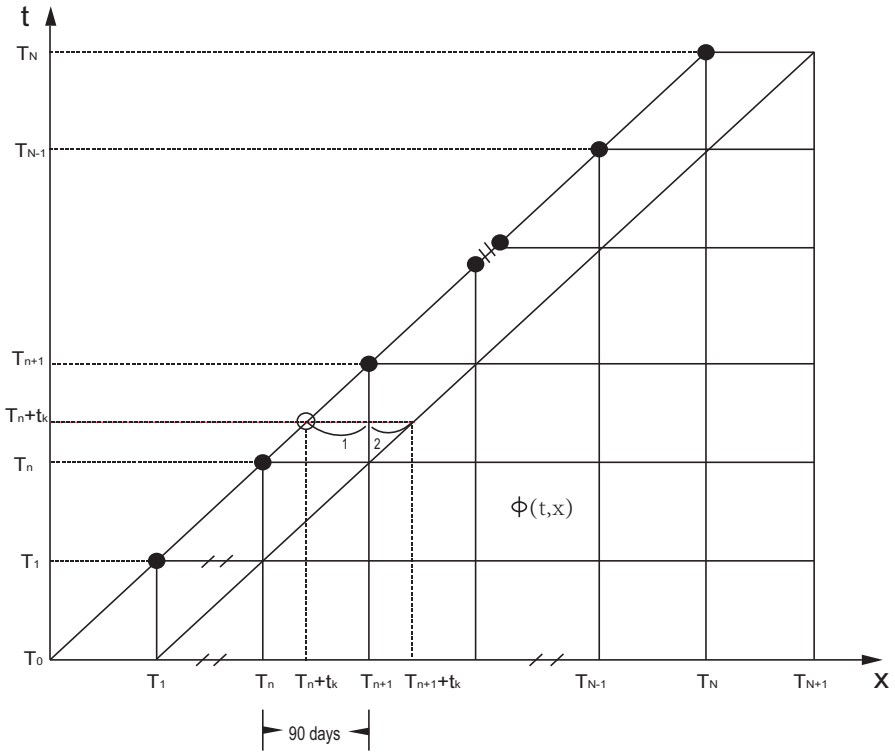

Figure 3.5: The payoff function of Libor rate accrual swap; the value for $\phi(t,x)$ is required for the entire trapezoid domain.

given by $\ell VB(T_0,T_{n+1})\big[L(T_0,T_n)-R_s\big]$, the range accrual $Swaplet_A(T_0,T_0;a,b)$ has a stochastic value, since the payment is only fixed at time T_1 and is given by $\ell VB(T_0,T_1)\big[L(T_0,T_1)-\xi R_s\big]$.

§ 3.3.1 Rang accrual swap payoff function

Figure 3.5 shows the *payoff function* of the range accrual swap $Swap_A(T_0,T_N;a,b)$. Each black dot in the figure represents a 90-day Libor $L(T_n,T_m)$; the diagonal on the edge is the line along which calendar time is equal to future time. All the payments for each swaplet is made at one of the black dots on the diagonal line.

The line parallel to the edge diagonal indicates the 90-day Libor that are observed daily to determine how many days the 90-day Libor was in the pre-specified range $[a,b]$. The payoff function has a closure at future calendar time T_N: the last accrual swaplet $Swaplet_A(T_0,T_{N-1};a,b)$ is exercised at time T_{N-1} with the final payments made at T_N.

The 90-day Libor L_{nk} being observed is indicated in Figure 3.5 by the horizontal line with

a circle; for time $T_n + t_k$, the figure shows that the 90-day Libor L_{nk} consists of a piece labeled 1 that starts at the diagonal edge, and then crosses the Libor lattice at Libor lattice at future time T_{n+1}, with the piece labeled 2 being the remaining part of the 90-day Libor.

For pricing the range accrual swap, the values of the log-Libor field $\phi(t, x)$ have to be determined for every point in the entire trapezoid. This will be more clear in Section § 3.6 where the simulation of the field $\phi(t, x)$ is carried out for pricing the accrual swap.

§ 3.4 Extension of Libor drift

In terms of the log-Libor field, Libor L_{nk} defined in Eq. § 3.3.1 is given as follows

$$\ell L_{nk} \equiv \ell L(T_n + t_k, T_n + t_k) = \exp\left\{ \int_{T_n + t_k}^{T_{n+1} + t_k} dx\ \phi(T_n + t_k, x) \right\} \qquad (\S\, 3.4.1)$$

Note that future time for L_{nk} does not lie in a Libor lattice , as given in Figure 3.1, since it crosses the Libor lattice at time T_{n+1} – as shown in Figure 3.5. At future time $T_n + t_k$, all the Libor rates for the full Libor lattice interval $[T_n, T_{n+1}]$ no longer exist since the Libor rates for $x < T_n + t_k$ have expired.

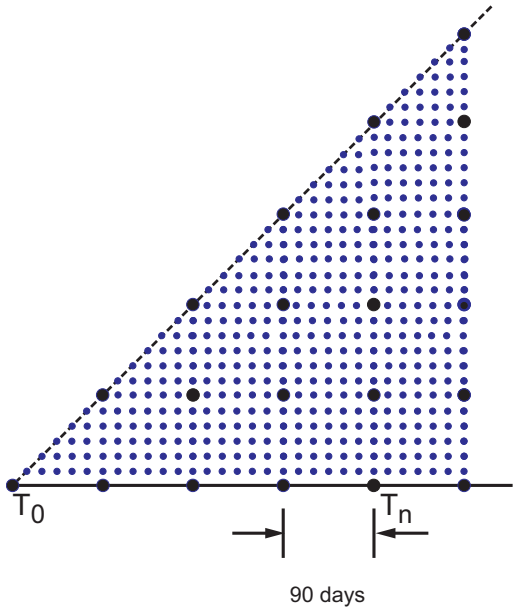

Figure 3.6: The domain for $\phi(t, x)$ required for pricing the range accrual swap.

As it stands, the Libor Market Model is only defined for future time x lying in a Libor lattice $[T_m, T_{m+1}]$, where time $T_m > t$ is in the future to calendar time t; in particular, the drift

in Libor Market Model is only defined for $\phi(t,x)$ with $T_n < x \leq T_{n+1}$. Comparing Figures 3.1 and 3.6 shows that the field $\phi(t,x)$ needs to be defined in the wedge on the diagonal that does not have any Libor rates on the Libor lattice.

Hence, the drift given in Eq. § 3.2.9 for the quantum formulation of LMM has to be extended for defining the evolution of $\phi(t,x)$ for x in the interval $[T_n + t_k, T_{n+1}]$. For the rolling numeraire, we take $I = n$ in the numeraire $B(t, T_{I+1})$; from Eq. § 3.2.9, the stochastic drift $\rho_n(t,x)$ of the Libor rate for $T_n \leq x < T_{n+1}$ is zero and is non-zero for $T_{n+1} \leq x < T_{n+2}$. Hence

$$\rho_n(t,x) = \begin{cases} 0 & x \in [T_n, T_{n+1}] \\ \neq 0 & x \in [T_{n+1}, T_{n+2}] \end{cases}$$

The stochastic drift for the range of $T_n \leq x < T_{n+2}$ is shown in Figure 3.7.

For the range of future time $T_n + t_k \leq x < T_{n+1}$, it follows from the discussion above that the stochastic drift $\rho_n(t,x)$ is zero. Hence, to extend the LMM so that it can price instruments such as the range accrual swap, we need to define the *deterministic drift* $\Lambda_n(t,x)$ for $T_n + t_k \leq x < T_{n+1}$.

Since $T_n + t_k$ does not lie on the Libor lattice, we extend the definition of deterministic drift $\Lambda_n(t,x)$ by cutting off the lower limit of the integration (that defines the deterministic drift) to a lower limit of $T_n + t_k$.

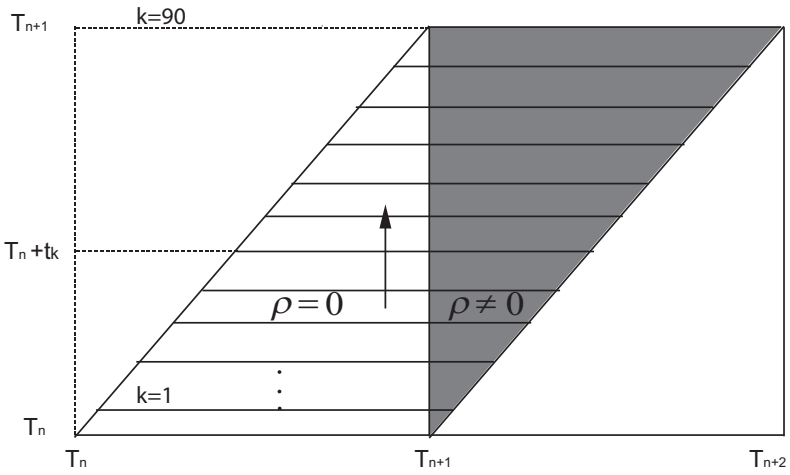

Figure 3.7: The stochastic drift for Libor L_{nk} that crosses the Libor lattice at time T_{n+1}.

We consequently obtain the evolution equation for $\phi(t,x)$ in the following two parts, and

which is shown in Figure 3.7.

$$
\begin{aligned}
&I: \quad T_n + t_k \le x < T_{n+1} \\
&\frac{\partial \phi(t,x)}{\partial t} = -\frac{\Lambda^{(1)}(t,x)}{2} + \rho_1(t,x) + \gamma(t,x)A(t,x) \\
&\Lambda^{(1)}(t,x) \equiv \int_{T_n+t_k}^{T_{n+1}} dx' \gamma(t,x) D(x,x';t) \gamma(t,x') \quad ; \quad \rho_1(t,x) = 0 \qquad (\S\,3.4.2) \\
&II: \quad T_{n+1} \le x < T_{n+1} + t_k \\
&\frac{\partial \phi(t,x)}{\partial t} = -\frac{\Lambda^{(2)}(t,x)}{2} + \rho_2(t,x) + \gamma(t,x)A(t,x) \qquad (\S\,3.4.3) \\
&\Lambda^{(2)}(t,x) = \Lambda_{n+1} = \int_{T_{n+1}}^{T_{n+2}} dx' \gamma(t,x) D(x,x';t) \gamma(t,x'); \\
&\rho_2(t,x) = \frac{e^{\phi_{n+1}(t)} \Lambda^{(2)}(t,x)}{1 + e^{\phi_{n+1}(t)}}
\end{aligned}
$$

Eq. § 3.4.2 represents the extension of LMM beyond the Libor lattice and Eq. § 3.4.3 follows from the definition of drift given afore-time in Eq. § 3.2.9. Figure 3.7 shows the shaded portion, for which the drift $\Lambda^{(2)}, \rho_2$ is fixed by the drift given by Eq. § 3.2.9; for the unshaded portion, the stochastic drift ρ_1 is zero but the deterministic drift $\Lambda^{(1)}$ is defined by extending the definition of drift beyond the Libor lattice.

The LMM has the initial condition specified at initial time T_0. The market fixes all $L(T_0, T_n)$ – and is shown in Figure 3.8 – from which one can extract all the logarithmic rates $\phi(T_0, x)$. To express L_{nk} in terms of the initial condition one needs to integrate logarithmic rates $\phi(t,x)$ using Eqs. § 3.4.2 and § 3.4.3, namely

$$
\begin{aligned}
&\int_{T_n+t_k}^{T_{n+1}+t_k} \phi(T_n + t_k, x) dx \\
= &\int_{T_n+t_k}^{T_{n+1}} dx \Big[\phi(T_0,x) + \int_{T_0}^{T_{n+}+t_k} dt (-\frac{\Lambda^{(1)}(t,x)}{2} + \rho_1(t,x) + \gamma(t,x)A(t,x)) \Big] \\
&+ \int_{T_{n+1}}^{T_{n+1}+t_k} dx \Big[\phi(T_0,x) + \int_{T_0}^{T_{n+}+t_k} dt (-\frac{\Lambda^{(2)}(t,x)}{2} + \rho_2(t,x) + \gamma(t,x)A(t,x)) \Big]
\end{aligned}
$$

Note that the drifts for the two time intervals combine to yield

$$
\begin{aligned}
\Lambda^{(1)}(t,x) + \Lambda^{(2)}(t,x) &= \int_{T_n+t_k}^{T_{n+2}} dx' \gamma(t,x) D(x,x';t) \gamma(t,x') \\
&\equiv \Lambda_{nk}(t,x)
\end{aligned}
$$

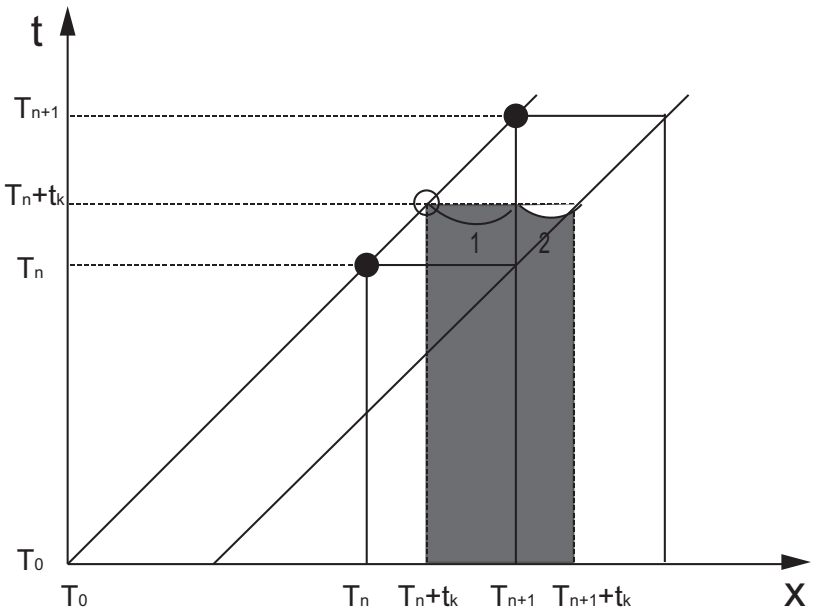

Figure 3.8: The dependence of L_{nk} on the initial Libor $L(T_0, T_m)$, fixed at time T_0 from market data.

Hence, in terms of the initial values, Libor L_{nk} is given by

$$\begin{aligned} \ell L_{nk} &= e^{\int_{T_n+t_k}^{T_{n+1}+t_k} \phi(T_n+t_k,x)dx} = e^{\int_{T_n+t_k}^{T_{n+1}+t_k} \phi(T_0,x)dx - \frac{1}{2}q_{nk}^2 + \varrho_{nk} + \omega_{nk}} \\ &= \ell L(T_0, T_n + t_k) \exp\{-\frac{1}{2}q_{nk}^2 + \varrho_{nk} + \omega_{nk}\} \end{aligned}$$

where

$$\begin{aligned} q_{nk}^2 &= \int_{T_0}^{T_{n+1}+t_k} dt \int_{T_n+t_k}^{T_{n+1}+t_k} dx \Lambda_{nk}(t,x) \\ w_{nk} &= \int_{T_0}^{T_{n+1}+t_k} dt \int_{T_n+t_k}^{T_{n+1}+t_k} dx \gamma(t,x) A(t,x) \qquad (\S\, 3.4.4) \\ \varrho_{nk} &= \int_{T_0}^{T_{n+1}+t_k} dt \int_{T_{n+1}}^{T_{n+1}+t_k} dx \rho_2(t,x); \quad \rho_2(t,x) = \frac{e^{\phi_{n+1}(t)}}{1+e^{\phi_{n+1}(t)}} \Lambda_{n+1}(t,x) \end{aligned}$$

§ 3.5 Approximate Price of Accrual Swap

The term $\rho_2(t,x)$ in Eq. § 3.4.3 makes L_{nk} depend nonlinearly on the quantum field $A(t,x)$. The volatility expansion for Libor drift was studied in [2]. One can expand L_{nk} as a power series in the volatility $\gamma(t,x)$, with the leading term yielding a linear theory for L_{nk}, and which in turn leads to an approximate analytic expression for the accrual swap.

The volatility approximation is based on the fact that $\rho_2(t,x) \approx \rho_2(T_0,x) + O(\gamma(t,x))$, and yields an expansion in $\phi(t) - \phi(T_0) = O(\gamma(t,x))$, which is a small quantity. Hence

$$\begin{aligned} \frac{e^{\phi(t)}}{1+e^{\phi(t)}} &= \frac{e^{\phi(T_0)}}{1+e^{\phi(T_0)}} + \frac{e^{\phi(t)} - e^{\phi(T_0)}}{(1+e^{\phi(t)})(1+e^{\phi(T_0)})} \\ &\simeq \frac{e^{\phi(T_0)}}{1+e^{\phi(T_0)}} + O(\gamma(t,x)) \end{aligned} \qquad (\S\, 3.5.1)$$

and this leads to the following linearization

$$\begin{aligned} \ell L_{nk} &= e^{\int_{T_n+t_k}^{T_{n+1}+t_k} \phi(T_0,x)dx - \frac{1}{2}q_{nk}^2 + \varrho_{nk} + \omega_{nk}} \\ &\simeq \ell L(T_0, T_n+t_k) e^{-\frac{1}{2}q_{nk}^2 + \varrho_{nk}^0 + \omega_{nk}} + O(\gamma(t,x)) \end{aligned}$$

Collecting the deterministic terms, we have

$$L_{nk} \simeq L_{nk}^0 e^{\omega_{nk}}, \qquad (\S\, 3.5.2)$$

where

$$\begin{aligned} L_{nk}^0 &= L(T_0, T_n+t_k) e^{-\frac{1}{2}q_{nk}^2 + \varrho_{nk}^0} \\ \varrho_{nk}^0 &= \int_{T_0}^{T_{n+1}+t_k} dt \int_{T_{n+1}}^{T_{n+1}+t_k} dx \rho_2(T_0,x) \\ \rho_2(T_0,x) &= \frac{e^{\phi_{n+1}(T_0)}}{1+e^{\phi_{n+1}(T_0)}} \Lambda_{n+1}(T_0,x), \end{aligned}$$

The range condition can be rewritten by taking the logarithm of the limits and yields, from Eq. § 3.5.2 the following

$$a < L_{nk} < b \quad \Rightarrow \quad A \leq \omega_{nk} \leq B$$

Hence, from Eq. § 3.4.4

$$A < \int_{T_0}^{T_n+t_k} dt \int_{T_n+t_k}^{T_n+t_k} dx\gamma(t,x)A(t,x) < B$$

where the logarithmic limits are given by

$$A = \ln(\frac{a}{L^0_{nk}}) = \ln(\frac{a}{L(T_0,T_n)}) - \int_{T_0}^{T_n+t_k} dt \int_{T_{n+1}}^{T_{n+1}+t_k} dx\rho_2(T_0,x) + \frac{1}{2}q^2_{nk};$$
$$B = \ln(\frac{b}{L^0_{nk}}) = \ln(\frac{b}{L(T_0,T_n)}) - \int_{T_0}^{T_n+t_k} dt \int_{T_{n+1}}^{T_{n+1}+t_k} dx\rho_2(T_0,x) + \frac{1}{2}q^2_{nk}$$

The range function can be written using a delta function as follows

$$1_{a<z<b} = \int_a^b \delta(\zeta - z)d\zeta = \frac{1}{2\pi}\int_a^b d\zeta \int e^{-i\xi(\zeta-z)}d\xi \qquad (\S\, 3.5.3)$$

The expectation value of $1_{a<L^n_k<b}$ can be obtained in the framework of the path integral. The linear approximation for the drift reduces computing the expectation value to the evaluation of the following Gaussian path integral that, using Eq. § 3.2.13, yields the following

$$\begin{aligned} E_n[1_{a<L_{nk}<b}] &= \int_A^B d\zeta \int \frac{d\xi}{2\pi} e^{-i\xi\zeta}\frac{1}{Z}\int DA e^{S[A]} e^{i\xi\int_{T_{n+1}+t_k}^{T_{n+1}+t_k} dx \int_{T_0}^{T_n+t_k} dt\gamma(t,x)A(t,x)} \\ &= \int_A^B d\zeta \int \frac{d\xi}{2\pi} e^{-i\xi\zeta} e^{-\frac{1}{2}\xi^2 q^2_{nk}} = \int_A^B d\zeta \frac{1}{\sqrt{2\pi q^2_{nk}}} e^{-\frac{1}{2q^2_{nk}}\zeta^2} \\ &= N(\frac{B}{q_{nk}}) - N(\frac{A}{q_{nk}}) \;\; ; \;\; N(x) = \frac{1}{\sqrt{2\pi}}\int_{-\infty}^{z} dz e^{-\frac{1}{2}z^2} \end{aligned}$$

The approximate price of the range accrual swaplet is given by

$$Swaplet_A(T_0,T_n;a,b) \simeq \ell V B(T_0,T_{n+1})\Big\{L(T_0,T_n) - \frac{R_s}{M}\sum_{k=1}^{M}\big[N(\frac{B}{q_{nk}}) - N(\frac{A}{q_{nk}})\big]\Big\} \qquad (\S\, 3.5.4)$$

The approximate price of the range accrual swap is given, from Eq. § 3.3.7, by summing over the approximate price of each range accrual swaplet given in Eq. § 3.5.4.

§ 3.6 Simulation of range accrual swap

To evaluate the price of the accrual swap, one needs to generate sample values of the Libor L_{nk}. To do so one needs to start with the initial values of Libor $L(T_0, T_n)$, given by the market, and extract from the market Libor the initial value of the log-Libor rates $\phi(T_0, x)$ for all $T_0 \leq x \leq T_{N+1}$. The numerical algorithm is then used to generate the sample values of L_{nk}, as shown in Figure 3.9, by simulating sample values of $\phi(t, x)$ with $t >_0$.

Suppose the present Libor interest rate is $\ell L(T_0, T_n) = \exp\{\int_{T_n}^{T_n+\ell} dx \phi_0(T_0, x)\}$. At time T, where $T > T_0$, the log-Libor is given by

$$\phi(T, x) = \phi(T_0, x) + \int_{T_0}^{T} dt \Big\{ -\frac{1}{2}\Lambda(t, x) + \rho(t, x) + \gamma(t, x) A(t, x) \Big\} \qquad (\S\, 3.6.1)$$

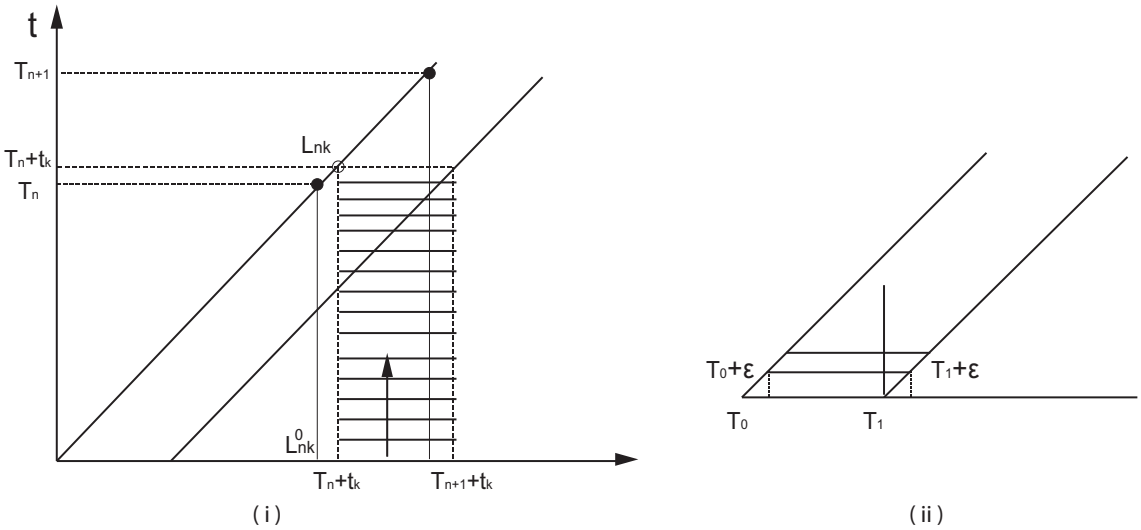

Figure 3.9: The updating algorithm for obtaining sample values of L_{nk}.

In the Monte Carlo simulation, the log-Libor rates $\phi(t, x)$ are updated on a discrete time lattice. Both calender time and future time are defined on a lattice with an interval of $\epsilon = 1$ day and yields

$$t \to t = T_0 + n\epsilon \quad ; \quad x \to x = T_0 + m\epsilon \qquad (\S\, 3.6.2)$$

The updating process for ϕ, from Eq. § 3.6.1, is given by

$$\phi(t + \epsilon, x) = \phi(t, x) + \epsilon \Big\{ -\frac{1}{2}\Lambda(t, x) + \rho(t, x) + \gamma(t, x) A(t, x) \Big\} \qquad (\S\, 3.6.3)$$

Hence the updating process for Libor is given by

$$\begin{aligned}
\ell L(t+\epsilon,x) &= \exp\Big\{\int_x^{x+\ell} dx'\phi(t+\epsilon,x')\Big\} \\
&= \exp\Big\{\int_x^{x+\ell} dx'[\phi(t,x')+\epsilon(-\frac{1}{2}\Lambda(t,x')+\rho(t,x')+\gamma(t,x')A(t,x'))]\Big\} \\
&= \ell L(t,x)\exp\Big\{\epsilon\int_x^{x+\ell} dx'[-\frac{1}{2}\Lambda(t,x')+\rho(t,x')+\gamma(t,x')A(t,x')]\Big\}
\end{aligned}$$

As shown in Figure 3.9 (i), the value of $\phi(t,x)$ is updated in steps of ϵ, indicated by horizontal lines, until one generates the values of $\phi(T_n+T_k,x)$ required for obtaining a sample value of L_{nk}.

Libor volatility $\gamma_m(\theta)$,where $\theta = x-t$ is the time to maturity in the unit of year, is taken as an (empirical) input in the simulation. It is obtained from the formula of Baaquie and Yang [22] and is given below

$$\gamma_m(\theta) = 0.051 - 0.038e^{-1.36*(\theta-0.25)} + 0.279(\theta-0.25)e^{-1.36*(\theta-0.25)} \qquad (\S\,3.6.4)$$

The volatility $\gamma_m(\theta)$ is plotted in Figure 3.10.

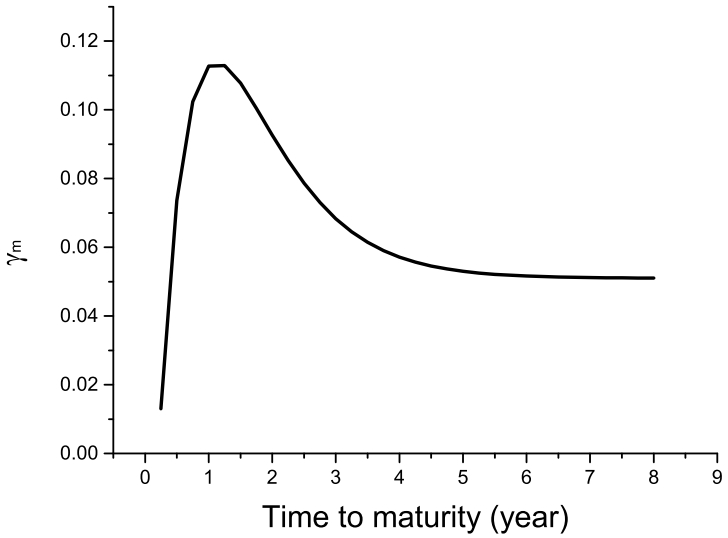

Figure 3.10: Volatility $\gamma(x-t)$ of log-Libor field $\phi(t,x)$

The first updating generates sample values of L_{01}, with $T_0+\epsilon = T_0+t_1$, that is is for

$n = 0, k = 1$ and is shown in Figure 3.9 (ii). The algorithm yields

$$\begin{aligned} L_{01} &= L(T_0 + \epsilon, T_0 + \epsilon) \\ &= L(T_0, T_0 + \epsilon) \exp\left\{\epsilon \int_{T_0+\epsilon}^{T_1+\epsilon} dx[-\frac{1}{2}\Lambda(T_0, x) + \rho(T_0, x) + \gamma(T_0, x)A(T_0, x)]\right\} \end{aligned}$$

The range of $T_0 + \epsilon \leq x < T_1 + \epsilon$ cuts across the Libor lattice at T_1, as shown in Figure 3.9 (ii). The drift, from Eqs. § 3.4.2 and § 3.4.3, has the following definition

$$\begin{aligned} &I: \quad T_0 + \epsilon \leq x < T_1 \quad ; \quad T \equiv T_0 + \epsilon \\ &\Lambda(T, x) = \Lambda^{(1)}(T, x) = \int_{T_0+\epsilon}^{T_1} dx' \gamma(T, x) D(x, x'; T) \gamma(T, x') \\ &\rho(T, x) = \rho_1(T, x) = 0 \\ &II: \quad T_1 \leq x < T_1 + \epsilon \\ &\Lambda(T, x) = \Lambda^{(2)}(T, x) = \int_{T_1}^{T_2} dx' \gamma(T, x) D(x, x'; t) \gamma(T, x'); \\ &\rho(T, x) = \rho_2(T, x) = \frac{e^{\phi_1(T_0)} \Lambda^{(2)}(T_0, x)}{1 + e^{\phi_1(T_0)}} \end{aligned}$$

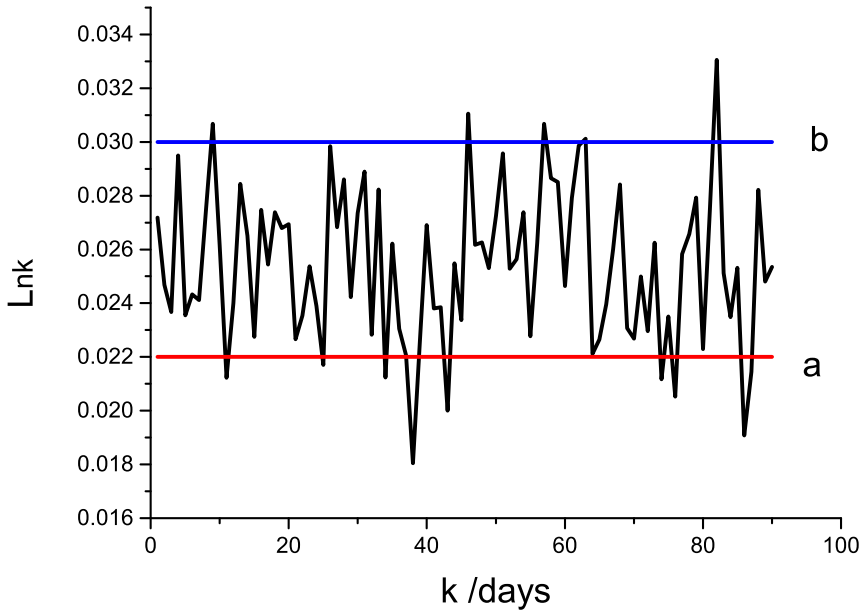

Figure 3.11: A sample configuration of Libor L_{nk} for volatility $\gamma = 50 * \gamma_m$

Figure 3.11 shows a typical configuration for Libor L_nk generated by our simulation. The value for volatility was taken to be $50 \times \gamma_m$ – where γ_m is the market volatility of Libor L_nk – to magnify the effect of the barrier crossings.

In the simulation, the price of the accrual swaplet is obtained by evaluating the average of the payoff for the sample configurations and yields

$$Swaplet_A(T_0, T_n; a, b) = \ell VB(T_0, T_{n+1})\Big\{L(T_0, T_n) - \frac{R_s}{M}\sum_{k=1}^{M}\frac{1}{\mathcal{N}}\sum_{l=1}^{\mathcal{N}}[1_{a\le L_{nk}^{(l)}\le b}]\Big\}$$

where $L_{nk}^{(l)}$ are the sample values of Libor and $\mathcal{N}$ is the total number of sample configurations.

§ 3.7 Result and discussion

The starting date T_0 is 0, and T_1 is set to be 90 days for the first settlement. The initial 90-day Libor at T_0 is $L(T_0, T_0) = 0.0269$ and the range we set is $(0.020, 0.030)$; In the simulation, $\epsilon = 1$ day.

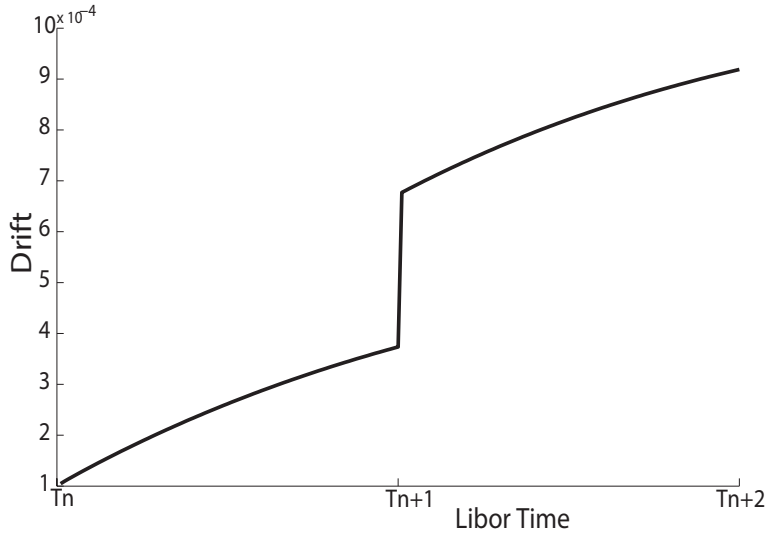

Figure 3.12: The discontinuity of drift across the Libor lattice at T_{n+1}.

Figure 3.12 shows the jump in the drift across a Libor lattice time. This is to be expected since on the diagonal edge, for a $swaplet(T_n, T_n; a, b)$, the drift for $x < T_{n+1}$ is deterministic whereas the drift for $x < T_{n+1}$ is a sum of deterministic and stochastic terms.

Define $I(k) = E_n[1_{a<L_{nk}<b}]$ to be the average value of Libor L_{nk} being in the range $[a, b]$

on kth day for numeraire $B(t, T_{n+1})$; we compute

$$\text{Approximate} : I_G(k) = N(\tfrac{B}{q_{nk}}) - N(\tfrac{A}{q_{nk}})$$
$$\text{Simulation} : I_S(k) = \tfrac{1}{\mathcal{N}} \sum_{l=1}^{\mathcal{N}} [1_{a \le L_{nk}^{(l)} \le b}]$$

The simulated value of $I(k)$ is compared with the approximation.

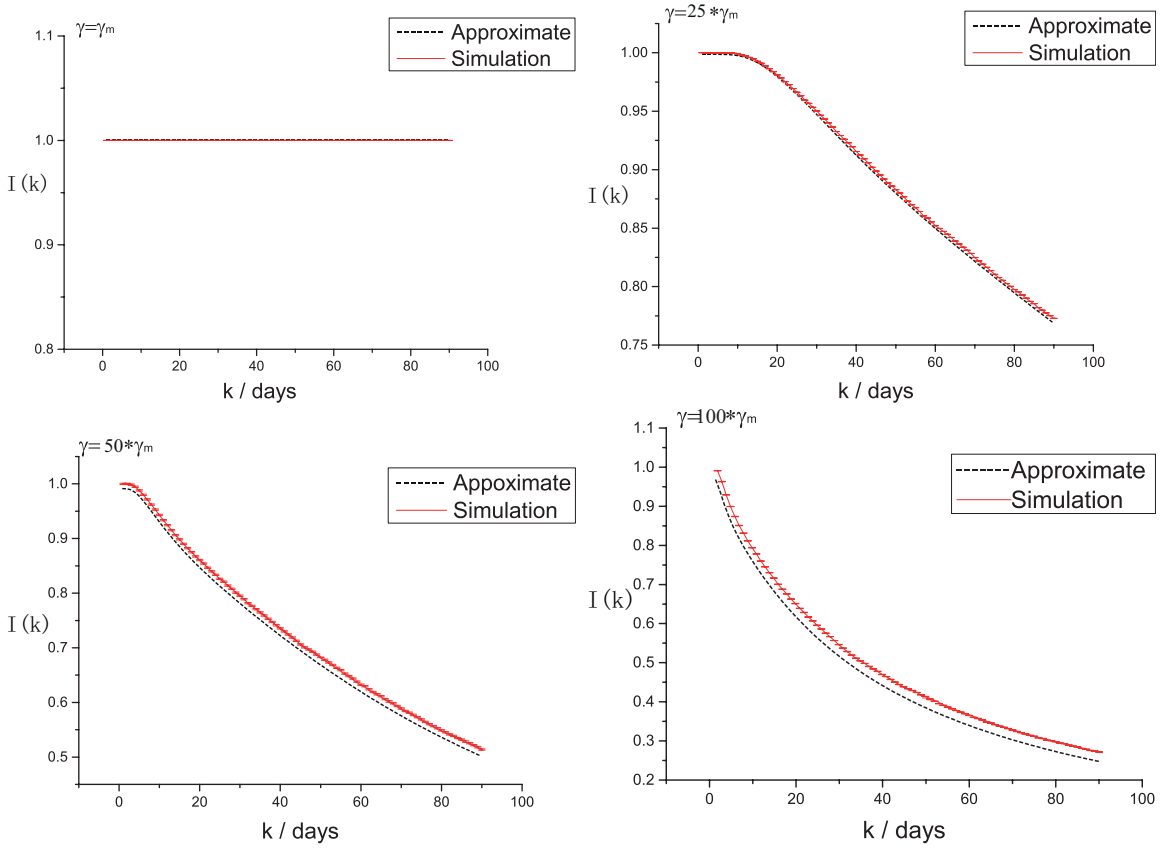

Figure 3.13: Comparison between simulation and approximate values of $I(k)$. The error bars are Monte Carlo errors of the simulation. The bound range is set $0.022 - 0.030$.

As shown in Figure 3.13, the approximate price is exactly the same with the simulation result when $\gamma = \gamma_m$. However it has a slight difference when $\gamma = 25 * \gamma_m$ but still can be acceptable in practice with the absolute error under 2%. The approximate result tends to have large errors with simulation when $\gamma = 50 * \gamma_m$ and $\gamma = 100 * \gamma_m$.

Define

$$\text{Absolute error} = \frac{1}{M} \sum_{k=1}^{M} \frac{|I_G(k) - I_S(k)|}{I_S(k)}$$

The absolute errors for different magnitudes of volatility are shown Figure 3.14. The approximation fails to give an accurate for volatility greater than $\gamma = 25 * \gamma_m$, as expected.

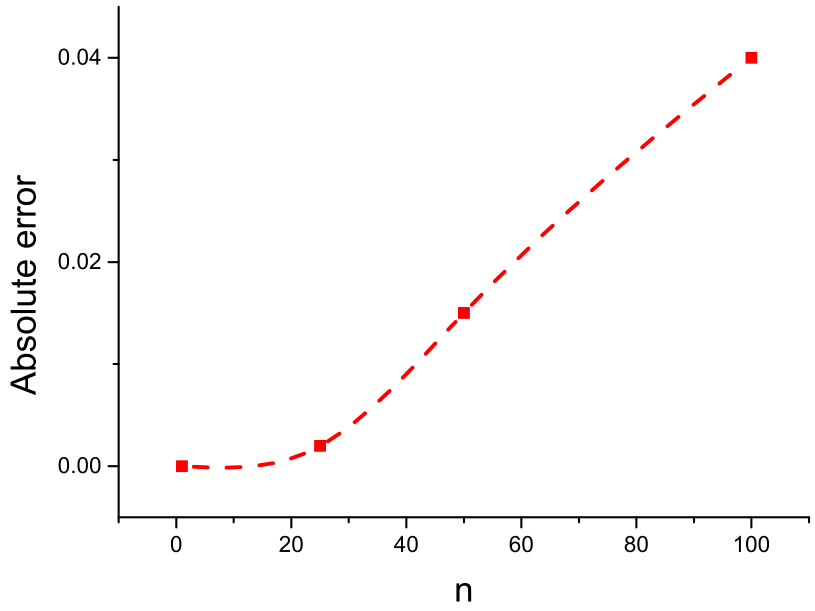

Figure 3.14: Absolute errors on times of volatilities $\gamma = n * \gamma_m$

The accrual swap price as a function of fixed leg R_S is plotted in Figure 3.15. The par value of accrual swap R'_P shows a larger value compared to the normal interest rate swap R_P . The par value shows the utility of the accrual swap, since one is effectively paying a much smaller value for the floating leg if the market becomes very volatile; and hence, in effect, one is receiving a higher fixed leg if the market is very volatile.

§ 3.8 Conclusion

The objective of this study was to price the interest rate range accrual swaps based on the formalism of quantum finance. The definition of the payoff function for the accrual swap required the employment of the logarithmic interest rates given by $\phi(t, x)$. The Libor Market Model defined for the Libor lattice was extended to accommodate the payoff of the accrual swap and this in turn was only possible because the pricing was obtained using the logarithmic field $\phi(t, x)$: unlike Libor $L(T, T_n)$, which is only defined for the Libor lattice, $\phi(t, x)$ is defined for the continuous domain defined by $t \geq T_0, x \geq t$.

An approximate formula was obtained by linearizing the nonlinear drift of the LMM. The Libor rates were studied numerically by using a simulation for updating daily Libor. The

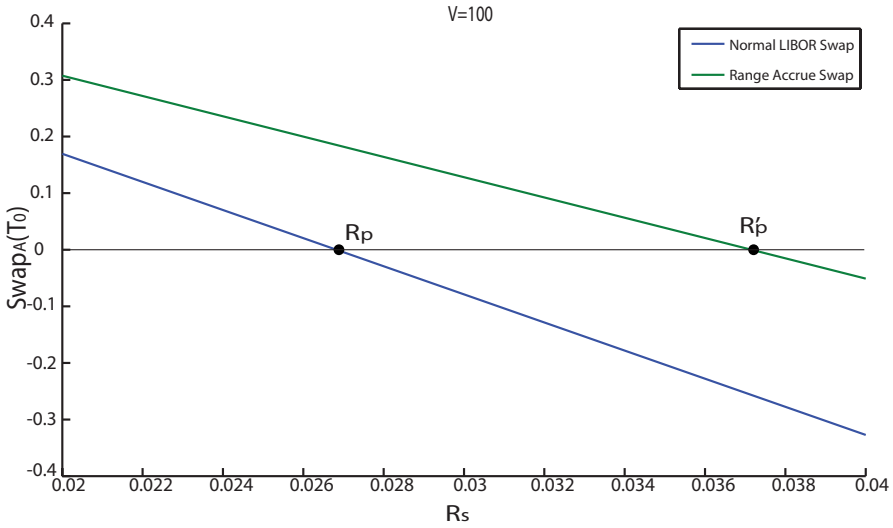

Figure 3.15: Par value of the normal and accrual swap, given by $Swap(R_p, T_0) = 0 = Swap_A(R'_p, T_0)$, respectively

simulation showed that the approximate price provides an excellent approximation when the Libor volatility γ_m is taken from the market. The simulation showed that the approximate accrual swap formula fails only for very high volatility that one does not expect for normal market conditions. The par value of the range accrual swap can be computed accurately using the approximate formula and opens the way for empirically studying the pricing of range accrual swaps.

§ 3.9 Appendix A. Derivation of the drift

LMM drift $\rho(t,x)$ above is derived based directly on the LMM Hamiltonian. We choose $B(t, T_{I+1})$ to be the forward bond numeraire; for all n, the drift is fixed so that $\chi_n(t) \equiv \frac{B(t,T_{n+1})}{B(t,T_{I+1})}$ is a martingale. The drift $\rho(t,x)$ is determined in the Hamiltonian framework by the following condition [2]:

$$\mathcal{H}_\phi(t)\chi_n(t) = \mathcal{H}_\phi(t)\Big[\frac{B(t,T_{n+1})}{B(t,T_{I+1})}\Big] = 0: \quad \text{for all} \quad n \tag{§ 3.9.1}$$

Recall $\ell L(t,T_n) = \exp\{\int_{T_n}^{T_{n+1}} dx\phi(t,x)\} \equiv e^{\phi_n}$. The Hamiltonian of the Libor Market Model given by Baaquie [2],

$$\mathcal{H}_\phi(t) = -\frac{1}{2}\int_{x,x'} M_\gamma(x,x';t)\frac{\delta^2}{\delta\phi(x)\phi(x')} + \frac{1}{2}\int_x \Lambda(t,x)\frac{\delta}{\delta\phi(x)} - \int_x \rho(t,x)\frac{\delta}{\delta\phi(x)}$$

$$\rho(t,x)=\sum_{n=0}^{\infty}\theta_n(x)\rho_n(t,x);\quad \Lambda(t,x)=\sum_{n=0}^{\infty}\theta_n(x)\int_{T_n}^{T_{n+1}}dx' M_\gamma(x,x';t)$$

where $\theta_k(x)$ has the value 1 in the Libor range $T_k\le x<T_{k+1}$ and is equal to 0 when out of the range.

Functional differentiation by $\phi(x)$ yields $\frac{\delta L(t,T_k)}{\delta\phi(x)}=\theta_k(x)L(t,T_k)$. The following are the three cases for the derivation.

Case (i) $n>I$, $\chi_n(t)=\prod_{k=I+1}^{n}\frac{1}{1+\ell L(t,T_k)}=\exp\{-\sum_{k=I+1}^{n}\ln(1+\ell L(t,T_k))\}$

$$\frac{\delta\chi_n(t)}{\delta\phi(x)}=-\sum_{k=I+1}^{n}\frac{e^{\phi_k}\theta_k(x)}{1+e^{\phi_k}} \qquad (\S\,3.9.2)$$

The summation term above is due to the discounting by the forward numeraire $B(t,T_{I+1})$. The second derivative yields

$$\frac{\delta^2\chi_n(t)}{\delta\phi(x)\delta\phi(x')}=-\sum_{k=I+1}^{n}(\frac{e^{\phi_k}}{1+e^{\phi_k}})^2\theta_k(x)\theta_k(x')-\sum_{k=I+1}^{n}\frac{e^{\phi_k}\theta_k(x)\theta_k(x')}{1+e^{\phi_k}}$$
$$+\sum_{j,k=I+1}^{n}\frac{e^{\phi_j+\phi_k}\theta_k(x)\theta_k(x')}{(1+e^{\phi_j})(1+e^{\phi_k})}$$

Applying the log Libor Hamiltonian on $\chi_n(t)$

$$\mathcal{H}_\phi\chi_n(t)=\tfrac{1}{2}\int_{x,x'}M_\gamma[\sum_{k=I+1}^{n}(\frac{e^{\phi_k}}{1+e^{\phi_k}})^2\theta_k(x)\theta_k(x')-\sum_{j,k=I+1}^{n}\frac{e^{\phi_j+\phi_k}\theta_k(x)\theta_j(x')}{(1+e^{\phi_j})(1+e^{\phi_k})}$$
$$+\sum_{k=I+1}^{n}\frac{e^{\phi_k}\theta_k(x)\theta_k(x')}{1+e^{\phi_k}}]-\frac{1}{2}\int_{x,x'}M_\gamma\sum_{n=0}^{\infty}\theta_n(x)\sum_{k=I+1}^{n}\frac{e^{\phi_k}\theta_k(x')}{1+e^{\phi_k}}+\int_x\rho(t,x)\sum_{k=I+1}^{n}\frac{e^{\phi_k}\theta_k(x)}{1+e^{\phi_k}}$$

Note the remarkable identity

$$\frac{1}{2}\sum_{j,k=I+1}^{n}A_{jk}=\sum_{j=I+1}^{n}\sum_{k=I+1}^{j}A_{jk}-\frac{1}{2}\sum_{k=I+1}^{n}A_{kk}$$

Taking

$$A_{jk}=\frac{e^{\phi_j+\phi_k}\theta_k(x)\theta_j(x')}{(1+e^{\phi_j})(1+e^{\phi_k})}$$

yields, after some cancelations

$$\mathcal{H}_\phi \chi_n(t) = \int_x \rho(t,x) \sum_{k=I+1}^{n} \frac{e^{\phi_k}\theta_k(x)}{1+e^{\phi_k}} - \int_{x,x'} M_\gamma \sum_{j=I+1}^{n}\sum_{k=I+1}^{j} \frac{e^{\phi_j+\phi_k}\theta_k(x)\theta_j(x')}{(1+e^{\phi_j})(1+e^{\phi_k})} \qquad (\S\,3.9.3)$$

and the Libor drift is given by

$$\begin{aligned} \rho_n(t,x) &= \sum_{j=I+1}^{n} \frac{e^{\phi_j}}{1+e^{\phi_j}} \int_{x'} M_\gamma(x,x';t) \\ &= \sum_{j=I+1}^{n} \frac{e^{\phi_j}}{1+e^{\phi_j}} \Lambda_j(x); \quad T_n \le x < T_{n+1} \end{aligned}$$

applied to Eq. § 3.9.3 leads to the cancelation of all the terms and yields the final result

$$\mathcal{H}_\phi \chi_n(t) = 0 \quad : \quad \text{martingale} \qquad (\S\,3.9.4)$$

Case (ii) $n < I$, the derivation similar to Case (i)

$$\chi_n(t) = \prod_{k=n+1}^{I} (1+\ell L(t,T_k)) = \exp\{\sum_{k=n+1}^{I} \ln(1+\ell L(t,T_k))\}$$

$$\Rightarrow \rho_n(t,x) = -\sum_{j=n+1}^{I} \frac{e^{\phi_j}}{1+e^{\phi_j}} \Lambda_j(x); \quad T_n \le x < T_{n+1}$$

Case(iii) $n = I, \chi_n(t) = 1$ yields $\mathcal{H}_\phi \chi_I(t) = 0 \Rightarrow \rho_I(t,x) = 0$.

§ 3.10 Appendix B. Simulation of the quantum field $A(t,x)$

Assume that $D(x,x';t) = D(\theta,\theta')$ for the remaining future time $\theta = x - t,\ \theta' = x' - t$. The propagator

$$E[A(t,x)A(t',x')] = \delta(t-t')D(\theta,\theta')$$

is the defining equation for simulating a Gaussian quantum field $A(t,x)$. Because the propagator (correlation function) D is always a positive and symmetric matrix, Cholesky decomposition can be used for decomposing D into the product of a lower triangular matrix and its

conjugate transpose.

The propagator used for the simulation is given in [22]

$$D(\theta,\theta') = \frac{\lambda}{2\sinh(2b)}[g(\theta+\theta') + g(\theta-\theta')] \qquad (\S\,3.10.1)$$

$$g(\theta) = e^{-\lambda|\theta|\cosh(b)}\sinh\{b+\lambda|\theta|\cosh(b)\} \qquad (\S\,3.10.2)$$

where $\lambda = \widetilde{\lambda}^{\eta}$, the calibration parameters are $\widetilde{\lambda} = 1.79,\ b = 0.85,\ \eta = 0.34$. The normalized propagator is plotted in Figure. 3.16.

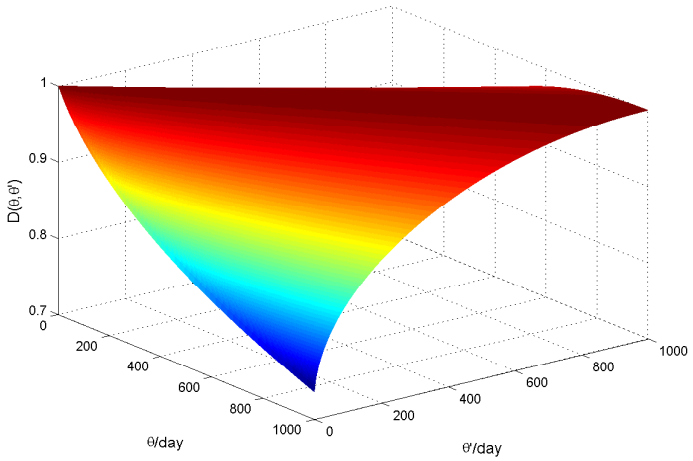

Figure 3.16: Propagator $D(\theta,\theta')$

Let $0 \le \theta \le \theta_M$, where $\theta_M = T - t$; the Cholesky decomposition for the propagator [32] yields

$$D(\theta,\theta') = \int_0^{\theta_M} Y(\theta,\zeta)Y^T(\zeta,\theta')d\zeta$$

For $\theta = T - t$, let

$$A(t,x) = \int d\zeta Y(\theta,\zeta)R(t,\zeta)$$

where $E[R(t,\zeta)R(t',\zeta')] = \delta(t-t')\delta(\zeta-\zeta')$. $R(t,\zeta)$is an independent Gaussian random variable for each calendar time t and future remaining time ζ. The simulation requires discrete calendar time and future time. For infinitesimals ϵ_t, ϵ_x we have

$$t, x \to m\epsilon_t, n\epsilon_x \quad ; \quad \theta \to p = m - n$$

The quantum field $A(t,x)$ and log-Libor rates $\phi(t,x)$ are expressed by

$$A(t,x) \to A_{m,n} \quad ; \quad \phi(t,x) \to \phi_{m,n}$$

For the process of updating $\phi_{m,n}$, the step size of calendar time t and the step size of future time x are also chosen to be equal $\epsilon = \epsilon_t = \epsilon_x = 1$ day,

$$\phi_{m+1,n} = \phi_{m,n} + \epsilon(\rho_{m,n} + \gamma_{m,n} A_{m,n})$$

The remaining future times $\theta = p$ and $\theta = p'$ in discrete time, are $p = n - m$ and $p' = n' - m'$ respectively.

$$E[A_{m,n} A_{m',n'}] = \frac{\delta_{m-m'}}{\epsilon} D[(n-m)\epsilon, (n'-m')\epsilon] = \frac{\delta_{m-m'}}{\epsilon} D_{p,p'}$$

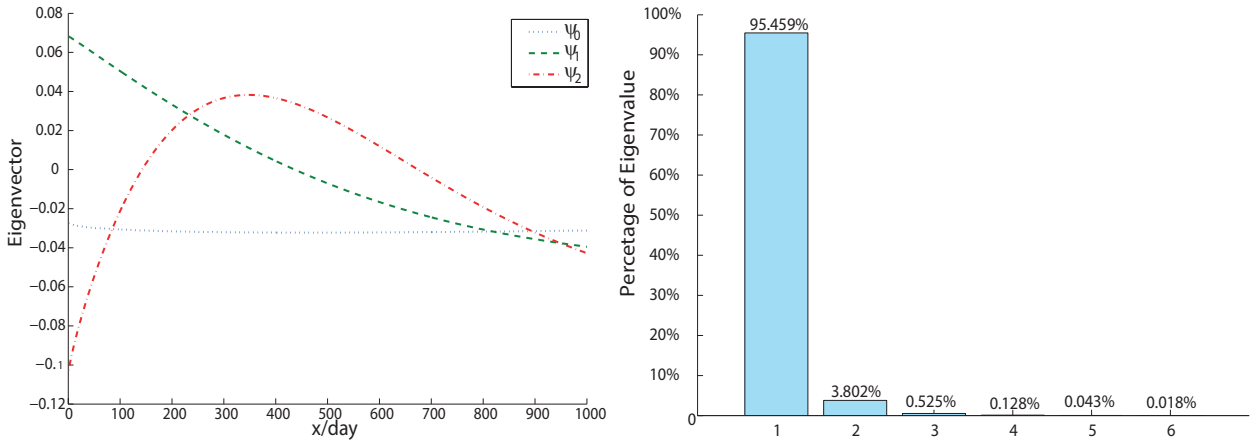

Figure 3.17: The Eigenvector and Eigenvalue for the ground state, first excited state and second excited state.(a)Eigenvector; (b)Eigenvalue.

Then

$$D_{p,p'} = \sum_{q=0}^{M-n} Y_{p,q} Y_{q,p'} \quad ; \quad A_{m,n} = \sum_{p'=0}^{M-n} Y_{p,p'} R_{m,p'}$$

where, for normal random variables R_{mn} are all identical and

$$R_{mn} = \frac{1}{\sqrt{\epsilon}} N(0,1). \qquad (\S\, 3.10.3)$$

The drift term $\rho_{m,n}$ in discrete time is given by

$$\rho_{m,n} = \epsilon\gamma_p \sum_{p=M_*-m}^{M-n} D_{p,p'}\gamma'_p$$

The eigenvalues and eigenvectors of the stiff propagator are

$$\sum_{p'=0}^{M-n} D_{p,p'}\psi_\iota(p') = \lambda_\iota\psi_\iota(p); \quad \iota = 0,1,2...M-n$$

where λ_ι is the eigenvalue of propagator D and ψ_ι its eigenvector. Note that

$$\sum_{\iota=0}^{M-n} \psi^*_\iota(p)\psi_\iota(p') = \delta_{p-p'}$$

Hence

$$A_{m,n} = \sum_{p'=0}^{M-n} Y_{p,p'}R_{m,p'} = \sum_{\iota=0}^{M-n} \sqrt{\lambda_\iota}\psi_\iota(p)Q_{m,l}$$

$$Y_{p,p'} = \sum_{\iota=0}^{M-n} \sqrt{\lambda_\iota}\psi^*_\iota(p)\psi_\iota(p') \quad ; \quad Q_{m,l} = \sum_{p'=0}^{M-n} \sqrt{\lambda_\iota}\psi_\iota(p')R_{m,p'}$$

The first eigenvalue is nearly 96% of the sum of eigenvalues, 3% and 0.4% are accounted for by the second and third eigenvalues, respectively. This fact suggests that three eigenvalues are enough for constructing the structure of the propagator as shown in Figure 3.17.

$$\begin{aligned}
\phi_{m+1,n} &= \phi_{m,n} + \epsilon(\rho_{m,n} + \gamma_{m,n}A_{m,n}) \\
&= \phi_{m,n} + \epsilon\rho_{m,n} + \epsilon\gamma_{m,n}\sum_{\iota=0}^{M-n} \sqrt{\lambda_\iota}\psi_\iota(p)Q_{m,l} \\
&= \phi_{m,n} + \epsilon\rho_{m,n} + \epsilon\sum_{\iota=0}^{M-n} \gamma^l_{m,n}\sqrt{\lambda_\iota}\psi_\iota(p)Q_{m,l}
\end{aligned}$$

$\gamma^l_{m,n} = \gamma_{m,n}\sqrt{\lambda_\iota}\psi_\iota(p)$ is the effective volatility.

Chapter 4

Linearized Hamiltonian of the LIBOR Market Model

The linearized Hamiltonian model is proposed to extend the LIBOR Market Model (LMM). Firstly, we studied the Hamiltonian of LIBOR Market Model in the framework of quantum finance, and the nontrivial upper triangle form of LIBOR drift is derived. The linearized Hamiltonian is derived to improve the explanatory capability of the model for market data. Our approach uses one more parameter to explain the initial condition and the model can be used to calibrate LIBORs with extremely high accuracy. Furthermore, the market time index is required for applying the model to multi-LIBOR, and the results imply that the LIBOR future time lattice becomes shorter as one goes from near future to distant future.

§ 4.1 Introduction

LIBOR Market Model is widely used in the interest rates modeling because of its theoretical and practical advantages. Built on the assumption that forward LIBOR rates follow a log-normal distribution, research on LIBOR market model has grown rapidly in the recent years. The LIBOR market model was introduced by Bruce-Gatarek-Musiela [33]. In Jamshidian's [34] work, the model was significantly developed and pricing swap rates were studied. The main advantage of the market model framework is that the Black's caplet formula can be exactly derived. However, identical with Black's formula, the LIBOR market model can only generate flat implied volatility structure. This main drawback contradicts the fact that the implied volatility observed in the market does have a complex structure known as volatility smile and skew.

There are two principal approaches for improving the LIBOR market model. One approach is to introduce stochastic volatility. Andersen et al. [35] and Joshi et al. [36] take into account the CEV (constant elasticity of variance) process and the displaced diffusion process respectively. Hagan et al. [37] and Rebonato [38] explain the complex stochastic volatility using SABAR model. Jump diffusion process is another research branch that the discontinuities of interest rates is modeled to get a better fit of market data. Glasserman et al. [39] [40] and Jarrow [41] studied this framework in great details.

However, these models are based on the assumption that the LIBOR market model can reflect all the information of a *complete market*. This assumption has strong restriction and hence is not practical. The real market can be an incomplete market and LIBOR market model may not be able to explain all the nontrivial properties of LIBORs. In this chapter, the LIBOR market model is examined to fit the LIBORs directly. Under the framework of quantum finance, the drift of the LIBOR market model is linearized, and multi-LIBORs are studied using the Hamiltonian approach.

§ 4.2 LIBOR Market Model

The 3-month LIBOR is the mainly quoted rate in the interest rate derivatives market. Let $T_0 < \cdots < T_n$ denote the discrete maturity time of LIBOR rates, the LIBOR rate $L(t, T_n)$ is the forward interest rate, fixed at time t, for a cash deposit from future time T_n to $T_n + \ell$ where ℓ is the discrete tenor. Figure 4.1 illustrates the 3-month LIBOR rates on the calendar and future time lattice. The 3-month LIBOR is used to calibrate our model here.

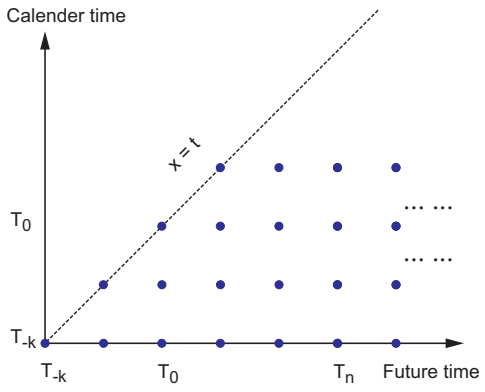

Figure 4.1: LIBOR rates defined on the time lattice with tenor ℓ.

Following the work of Gatarek et al. [33] and Jamshidian [34], each forward LIBOR rate $L(t, T_n)$ is modeled as a continuous time stochastic process. Under the respective T_n-Forward measure $\mathbb{P}_{T_n}$, the formulation of the single-factor BGM-Jamshidian model is given by

$$\frac{1}{L(t,T_n)}\frac{\partial L(t,T_n)}{\partial t} = \xi_n(t) + \gamma_n(t)R(t), \qquad (\S\,4.2.1)$$

$$E[R(t)R(t')] = \delta(t-t'), \qquad (\S\,4.2.2)$$

where $R(t)$ is Gaussian white noise and $\xi_n(t)$ is the stochastic drift. Because the evolution of LIBOR rate is driven by single stochastic process $R(t)$, the LIBOR rates of different maturity time are *perfectly correlated*. This main drawback of BGM model is not supported by the market data [42].

In order to overcome the limitation of BGM model, the quantum generalization of LIBOR Market Model (LMM) was firstly proposed by Baaquie (2009) [43] to incorporate the rich correlation between different forward LIBOR rates. The main innovation of the quantum finance approach is that the two dimensional stochastic field $A(t, x)$ is used to simulate the correlated stochastic process of each forward LIBOR rate. In essence, compared to one dimensional stochastic process $R(t)$, the stochastic field, also called *quantum field*, incorporates the correlation function naturally. In terms of the LIBOR rates $L(t, T_n)$, the quantum formulation of LMM is given by

$$\frac{1}{L(t,T_n)}\frac{\partial L(t,T_n)}{\partial t} = \xi(t,T_n) + \int_{T_n}^{T_n+\ell}\gamma(t,x)A(t,x), \qquad (\S\,4.2.3)$$

where $\gamma(t, x)$ is a deterministic volatility function and can be calibrated from the market data. In contrast to the BGM-Jamshidian framework, the correlation of the Gaussian quantum field $A(t, x)$ is given by

$$E[A(t,x)A(t',x')] = \delta(t-t')D(x,x';t). \qquad (\S\,4.2.4)$$

$D(x, x'; t)$, called *propagator* in terminology of quantum field theory, is the correlation function of the forward LIBOR rates of different maturities [42]. The quantum generalization of LIBOR Market Model gives the full description of correlation function and is enough to capture the complex structure of different LIBOR rates.

Some basic definitions are introduced in the following. From the definition of LIBOR rates,

LIBOR $L(t, T_n)$ can be expressed in terms of zero coupon bond as follows

$$L(t, T_n) = \frac{B(t, T_n) - B(t, T_{n+1})}{\ell B(t, T_{n+1})}. \quad (\S\, 4.2.5)$$

Numeraire is a fundamental concept for which the future cash flow of financial instruments is discounted. As defined in equation § 4.2.5, the combination $L(t, T_n)B(t, T_{n+1})$ can be expressed as a portfolio of zero coupon bonds. This unique feature of LIBORs leads to the unusual martingale condition of LIBORs given by

$$\chi_n(t) = \frac{L(t, T_n)B(t, T_{n+1})}{B(t, T_{k+1})}; \quad k : \text{fixed}, \quad (\S\, 4.2.6)$$

in which all instruments $\chi_n(t)$ are martingales for $n = 0, \pm 1, \pm 2, ..., \pm\infty$. Because of the unique martingale condition, the LIBOR drift can be derived using *common LIBOR numeraire* $B(t, T_{k+1})$. The nonlinear feature draws a distinction between the linear HJM model [44] and nonlinear BGM-Jamshidian model. Compared to HJM model, one another advantage of the LIBOR market model is that all LIBOR rates are defined to be positive, i.e., $L(t, T_n) \geq 0$ for all$0 \leq t \leq T_n$. Intuitively, a mathematical model should generate stochastic process or Gaussian fields spontaneously with any positive or negative values. Instead of the generalized LIBOR Market Model, the logarithmic LIBOR Market Model is proposed [42] to simulate the dynamic of logarithmic LIBOR $\phi_n(t)$. The transformation from LIBOR $L(t, T_n)$ to logarithmic LIBOR $\phi_n(t)$ is defined as

$$\ell L(t, T_n) = \exp \int_{T_n}^{T_{n+1}} dx \phi(t, x) \equiv e^{\phi_n(t)}. \quad (\S\, 4.2.7)$$

The two-dimensional Euclidean quantum field $\phi(t, x)$ certainly can take any value. The LIBOR market model can be formulated in terms of $\phi(t, x)$ as

$$\frac{\partial \phi(t, x)}{\partial t} = -\frac{1}{2}\Lambda_n + \rho_n(t, x) + \gamma(t, x)A(t, x) \quad (\S\, 4.2.8)$$

$$\Lambda_n(t, x) = \int_{T_n}^{T_{n+1}} dx' \gamma_{(t,x)} \mathcal{D}(x, x'; t) \gamma_{(t,x')}. \quad (\S\, 4.2.9)$$

The drift $\rho_n(t, x)$ is obtained by imposing the martingale condition $\chi_n(t)$ with respect to the numeraire $B(t, T_{k+1})$. Because the numeraire can be freely chosen and hence there are three

cases for different values of time T_k. The nontrival drift $\rho_n(t,x)$ is given in the following

$$\rho_n(t,x) = \begin{cases} \sum_{m=I+1}^{n} \frac{e^{\phi_{T_m}}}{1+e^{\phi_{T_m}}}\Lambda_{mn}(t), & T_n > T_k \\ 0, & T_n = T_k \\ -\sum_{m=n+1}^{I} \frac{e^{\phi_{T_m}}}{1+e^{\phi_{T_m}}}\Lambda_{mn}(t). & T_n < T_k \end{cases} \quad (\S\,4.2.10)$$

§ 4.3 Hamiltonian of LIBOR Market Model

The *Hamiltonian* is a differential operator corresponding to the time-evolution of a system and plays a central role in quantum theory. A Hamiltonian formulation of option theory has already been proved to be the generalization of Black-Scholes model [30]. Baaquie (2009) [43] proposed the Hamiltonian formulation of the martingale condition and show that the exact solution for the nonlinear drift can be derived using Hamiltonian approach. The Hamiltonian formulation is derived in terms of the logarithmic coordinates and is given by[43]

$$\begin{aligned} \mathcal{H}(t) &= -\frac{1}{2}\int_{x,x'} M_\gamma(x,x';t)\frac{\delta^2}{\delta\phi(x)\delta\phi(x')} + \frac{1}{2}\int_x \Lambda(t,x)\frac{\delta}{\delta\phi(x)} - \int_x \rho(t,x)\frac{\delta}{\delta\phi(x)} \quad (\S\,4.3.1) \\ \int_x &\equiv \int_t^\infty dx. \end{aligned}$$

For numeraire given by the zero coupon bond $B(t,T_{k+1})$, the LIBOR drift is the following [43]

$$\rho(t,x) = \sum_{n=0}^{\infty} H_n(x)\rho_n(t,x); \quad \rho_n(t,x) = \sum_{m=k+1}^{n} \frac{e^{\phi_m(t)}}{1+e^{\phi_m(t)}}\Lambda_m(t,x); \quad T_n > T_I. \quad (\S\,4.3.2)$$

$$\Lambda_n(t,x) = \sum_{n=0}^{\infty} H_n(x)\int_{T_n}^{T_{n+1}} dx' M_\gamma(x,x';t) \;\; ; \;\; M_\gamma(x,x';t) \equiv \gamma_{(t,x)}\mathcal{D}(x,x';t)\gamma_{(t,x')} \quad (\S\,4.3.3)$$

The characteristic function $H_n(x)$ for LIBOR time interval $[T_n, T_{n+1})$ is defined by

$$H_n(x) = \begin{cases} 1, & T_n \le x < T_{n+1} \\ 0. & x \notin [T_n, T_{n+1}) \end{cases} \quad (\S\,4.3.4)$$

Equation § 4.3.1 is the expression of Hamiltonian for continuous time labeled by t. The Hamiltonian is calibrated using daily LIBORs and hence the continuous time t needs to be

discretized. The discretized Hamiltonian density for future time x and x' is given by

$$\mathcal{H}_{x,x'}(t) = -\frac{1}{2}M_\gamma(x,x';t)\frac{\delta^2}{\delta\phi(x)\delta\phi(x')} + \frac{1}{2}\Lambda(t,x)\frac{\delta}{\delta\phi(x)} - \rho(t,x)\frac{\delta}{\delta\phi(x)}, \quad (\S\,4.3.5)$$
$$\mathcal{H}(t) = \int_{x,x'} \mathcal{H}_{x,x'}(t).$$

The calibration of the market model is invariant for different forward bond numerairea [45]. Here the numeraire $B(t,T_0)$, namely $k=-1$, is chosen and hence the summation over m in $\rho_n(t,x)$ starts from 0.

§ 4.3.1 Linear approximation of ρ

One of the most important advantage of the LIBOR market model is that the caplets price can be obtained simply using Black-Scholes model. However, because of the stochastic structure of nontrivial drift, the swaptions and other more complicated derivatives cannot be priced in closed form. Several approximation methods have been developed in the literature to simplify the drift term. The mostly used three approaches are frozen drift approximation [46, 47], log-normal approximations [48] and strong Taylor approximation [49]. In contrast to the mainly used methods, the linearization method is proposed. As can be seen in equation § 4.3.2, the drift $\rho(t,x)$ is nonlinear because the logarithmic LIBOR $\phi_m(t)$ is exponentiated. LIBOR varies slightly everyday and hence we can *linearize* the LIBOR drift. Define ϕ_n is equal to $\phi_n(t) - \phi_n(t_0)$, where ϕ_n is a small quantity. The expression of $\ell L(t,T_n)/[1+\ell L(t,T_n)]$ yields the following linearization

$$\frac{\ell L(t,T_n)}{1+\ell L(t,T_n)} = \frac{e^{\phi_n(t)}}{1+e^{\phi_n(t)}} \simeq \frac{e^{\phi_n(t_0)}(1+\phi_n)}{1+e^{\phi_n(t_0)}(1+\phi_n)}. \quad (\S\,4.3.6)$$

Since ϕ_n is around 10^{-4} for one day lag, equation § 4.3.6 yields an accurate approximation. Equation § 4.3.6 is further given by

$$\begin{aligned}\frac{e^{\phi_n(t_0)}(1+\phi_n)}{1+e^{\phi_n(t_0)}(1+\phi_n)} &= \frac{e^{\phi_n(t_0)}}{1+e^{\phi_n(t_0)}} + \frac{\phi_n e^{\phi_n(t_0)}}{(1+e^{\phi_n(t_0)})[1+e^{\phi_n(t_0)}(1+\phi_n)]} \\ &\simeq \rho_n^0 + \frac{\phi_n e^{\phi_n(t_0)}}{(1+e^{\phi_n(t_0)})(1+e^{\phi_n(t_0)})} \\ &= \rho_n^0 + \rho_n^0(1-\rho_n^0)\phi_n. \quad (\S\,4.3.7)\end{aligned}$$

Collecting the results, the expression of initial condition ρ_n^0 and the drift ρ_n are

$$\rho_n^0 = \frac{e^{\phi_n(t_0)}}{1+e^{\phi_n(t_0)}}; \quad \rho_n(t,x) = \sum_{i=0}^{n} \left[\rho_i^0 + \rho_i^0(1-\rho_i^0)\phi_i\right]\Lambda_i(t,x). \tag{§ 4.3.8}$$

The accuracy of linear approximation is examined for evaluating the value of martingale condition in appendix § 4.10. The results clearly show that the linear linearization can be used to approximate the drift with negligible errors. Equation § 4.3.8 can be used to linearize the Hamiltonian of the LIBOR market model given in Section § 4.3.2.

§ 4.3.2 Linearized Hamiltonian of the LIBOR market model

Since the approximate form of the drift is obtained, the discretized Hamiltonian $\mathcal{H}(t)$ can be defined directly. Firstly, we can transform $\phi(x)$ to $\phi_n(t)$ using the following chain rule for functional differentiation

$$\frac{\delta}{\delta\phi(x)} = \sum_{n=0}^{\infty} \frac{\delta\phi_n(t)}{\delta\phi(x)}\frac{\partial}{\partial\phi_n(t)} = \sum_{n=0}^{\infty} H_n(x)\frac{\partial}{\partial\phi_n(t)}; \quad \phi_n(t) = \int_{T_n}^{T_{n+1}} \phi(x)dx. \tag{§ 4.3.9}$$

Because $\phi_n(t_0)$ is a constant and $\phi_n = \phi_n(t) - \phi_n(t_0)$, we can replace $\phi_n(t)$ with ϕ_n in equation § 4.3.9. Discretizing continuous time, we have

$$\int_x \frac{\delta}{\delta\phi(x)} = \sum_{m=0}^{N} \frac{\partial}{\partial\phi_m}; \quad \int_{x,x'} M_\gamma(x,x';t)\frac{\delta^2}{\delta\phi(x)\delta\phi(x')} = \sum_{m=0}^{N}\sum_{n=0}^{N} M_{mn}\frac{\partial^2}{\partial\phi_m\partial\phi_n}$$

where

$$M_{mn} = \Lambda_{mn}(t) = \int_{T_m}^{T_{m+1}}\int_{T_n}^{T_{n+1}} M_\gamma(x,x';t)dxdx'. \tag{§ 4.3.10}$$

Substituting the approximate drift ρ_n into equation § 4.3.1, the linearized Hamiltonian can be obtained for LIBOR market model defined on discretized LIBOR lattice and is

$$\begin{aligned}\mathcal{H}(t) = &-\frac{1}{2}\sum_{m=0}^{N}\sum_{n=0}^{N} M_{mn}\frac{\partial^2}{\partial\phi_m\partial\phi_n} + \frac{1}{2}\sum_{m=0}^{N}\Lambda_{mm}(t)\frac{\partial}{\partial\phi_m} \\ &-\sum_{m=0}^{N}\sum_{i=0}^{m}\left[\rho_i^0 + \rho_i^0(1-\rho_i^0)\phi_i\right]\Lambda_{im}(t)\frac{\partial}{\partial\phi_m}.\end{aligned} \tag{§ 4.3.11}$$

Equation § 4.3.11 can be further simplified and written as follows

$$\mathcal{H} = -\frac{1}{2}\sum_{mn} M_{mn}\frac{\partial^2}{\partial\phi_m\partial\phi_n} + \sum_m \big[g_m - \frac{1}{2}\sum_{n=0}^{m}\phi_n f_{mn}\big]\frac{\partial}{\partial\phi_m}, \qquad (\S\,4.3.12)$$

$$g_m = \frac{1}{2}\Lambda_{mm}(t) - \sum_{n=0}^{m}[\rho_n^0\Lambda_{nm}(t)]; \quad f_{mn} = 2\big[\rho_n^0(1-\rho_n^0)\big]\Lambda_{nm}(t).$$

§ 4.4 LIBOR ground state

In quantum field theory, the *vacuum state* Ω, also called the ground state, is an eigenfunction of the LIBOR Hamiltonian with the lowest possible energy. The ground state of LIBOR describes the debt market when it is in equilibrium. Here, equilibrium refers to the stable sthchastic behavior of LIBORs. In particular, $|\Omega[\phi]|^2$ yields the probability distribution for LIBOR taking different possible values.

The LIBOR Hamiltonian vacuum state Ω obeys the following eigenfunction equation

$$\mathcal{H}\Omega = E\Omega. \qquad (\S\,4.4.1)$$

Since the LIBOR Hamiltonian has been linearized, the vacuum state Ω, in analogy with the simple harmonic oscillator, has the following form

$$\Omega = \mathcal{N}\exp\,(-\frac{1}{4}\sum_{mn} D_{mn}\phi_m\phi_n + \frac{1}{2}\sum_n j_n\phi_n),$$

where D_{mn} is a real and symmetric matrix and $\mathcal{N}$ is the normalization factor.

Before calculating the differential operator $\mathcal{H}$ acting on the vacuum state Ω, consider the following differentiations of Ω first

$$\frac{\partial}{\partial\phi_m}\Omega = (-\frac{1}{2}D_{mn}\phi_n + \frac{1}{2}j_n)\Omega, \qquad (\S\,4.4.2)$$

$$\frac{\partial^2}{\partial\phi_m\partial\phi_n}\Omega = \big[-\frac{1}{2}D_{mn} + (-\frac{1}{2}D_{nk}\phi_k + \frac{1}{2}j_n)(-\frac{1}{2}D_{ml}\phi_l + \frac{1}{2}j_m)\big]\Omega. \qquad (\S\,4.4.3)$$

D is a symmetric matrix and we have $D = D^T$; equations § 4.4.2 and § 4.4.3 yield

$$\begin{aligned}\mathcal{H}\Omega &= \frac{1}{2}\Big[\frac{1}{2}tr(MD) - \frac{1}{4}\phi(DMD)\phi + \frac{1}{2}\phi(DM)j - \frac{1}{4}jMj + gj - gD\phi + \frac{1}{2}\phi(fD)\phi - \frac{1}{2}\phi fj\Big]\Omega \\ &= E\Omega\end{aligned}$$

In principle, eigenvalue E should be a constant. All the ϕ and ϕ^2 dependent terms above have to be zero; hence we obtain the following equations

$$\phi DMj = 2\phi Dg + \phi fj, \tag{§ 4.4.4}$$

$$\phi(DMD)\phi = 2\phi(fD)\phi = \phi(fD + Df^T)\phi$$

$$\Rightarrow \quad DMD = (fD + Df^T). \tag{§ 4.4.5}$$

Denote $[\rho_i^0(1-\rho_i^0)]$ by P_i, the upper triangle matrix f is given by

$$2\begin{pmatrix} P_0\Lambda_{00} & P_0\Lambda_{01} & P_0\Lambda_{02} & ... & P_0\Lambda_{0N} \\ & P_1\Lambda_{11} & P_1\Lambda_{12} & ... & P_1\Lambda_{1N} \\ & & P_2\Lambda_{22} & ... & . \\ & & 0 & & \ddots \\ & & & & P_N\Lambda_{NN} \end{pmatrix}.$$

Matrix f is simply the LIBOR drift and can be rewritten as the multiplication of diagonal matrix $< P_0, P_1, \cdots, P_N >$ and an upper triangle matrix Λ^U, which is

$$f = 2\begin{pmatrix} P_0 & & & & \\ & P_1 & & & \\ & & P_2 & & \\ & & & \ddots & \\ & & & & P_N \end{pmatrix}\begin{pmatrix} \Lambda_{00} & \Lambda_{01} & \Lambda_{02} & ... & \Lambda_{0N} \\ & \Lambda_{11} & \Lambda_{12} & ... & \Lambda_{1N} \\ & & \Lambda_{22} & ... & . \\ & & 0 & & \ddots \\ & & & & \Lambda_{NN} \end{pmatrix}.$$

As defined in equation § 4.3.10, M_{mn} is equal to Λ_{mn}. Hence, the matrix Λ^U is simply equal to M^U, where M^U denotes the matrix with upper triangle elements of M_{mn}. The matrix f is

$$f = 2PM^U.$$

Because

$$Df^T = 2D(PM^U)^T = 2DM^LP$$

and D is a symmetric matrix, we have

$$fD + Df^T = 2(PM^U D + DM^L P)$$

Finally, we get the equation to obtain matrix D for the linearized LIBOR market model

$$DMD = fD + Df^T = 2(PM^U D + DM^L P). \quad (\S\,4.4.6)$$

Multiply D^{-1} on both sides, equation § 4.4.6 can be transformed as

$$D^{-1}PM^U + M^L PD^{-1} - \frac{1}{2}M = 0. \quad (\S\,4.4.7)$$

Equation § 4.4.7 is called the continuous Lyapunov equation that is widely used in control theory. In the calibration of the model, *lyap* package in Matlab is used to obtain the solution for matrix D. The results show that matrix D is symmetric and all eigenvalues are positive. From equation § 4.4.4, we have

$$DMj = 2Dg + fj.$$

Hence, the matrix j can be solved directly by

$$j = 2(DM - f)^{-1}Dg.$$

The ground state $\Omega[\phi]$ is a description of LIBOR in equilibrium. Because LIBOR data is irregular during and after the financial crisis, the data before the year 2008 is used in this calibration since it reflects more accurately the debt market being in equilibrium and hence can be used to study whether the ground state describes the debt market. We plan to study the financial meltdown of 2008 in using the excited states of the linearized Hamiltonian.

§ 4.5 Calibration of Single LIBOR

As discussed in Section § 4.3.2, the ground state is given by

$$\Omega = \mathcal{N} \exp\left(-\frac{1}{4}\sum_{mn} D_{mn}\phi_m\phi_n + \frac{1}{2}\sum_n j_n\phi_n\right) \quad (\S\,4.5.1)$$

Hence, the probability distribution for single LIBOR ϕ_I is simply

$$f(\phi_I) \quad = \quad |\Omega(\phi_I)|^2 = \mathcal{N} \exp\left(-\frac{1}{2} D_{II} \phi_I^2 + j_I \phi_I\right). \qquad (\S\, 4.5.2)$$

Intuitively, the ground state can be assumed time translation invariant for a single LIBOR of different calendar time. As can be seen in Figure 4.2(a), logarithmic LIBOR ϕ obviously has a trend and the drift of LIBOR rates cannot be simulated in this case. However, the data used for calibration is $\phi_n = \phi_n(t) - \phi_n(t_0)$ instead of $\phi_n(t)$. Hence, after removing the initial logarithmic LIBOR $\phi_n(t_0)$, the data can be de-trended. One day lag is used in this simulation which means that $t - t_0 = 1$. In order to get stable data for ϕ_n, the method of moving average is used to obtain the pure randomness of ϕ_n. After the calibration using different time length of moving average, we found that 10 previous days data points are the best choice for calculating the one day ϕ_n. In conclusion, the preceding method is the following

$$\text{De-trended Log LIBOR:} \quad \phi_n \quad = \quad \phi_i(t) - \frac{1}{L} \sum_{t'=t-L}^{t-1} \phi_i(t'); \quad L = 10. \qquad (\S\, 4.5.3)$$

Figure 4.2(b) is the result after subtracting the moving average and shows that the data doesn't have any trend and contains rich information on the randomness of LIBORs.

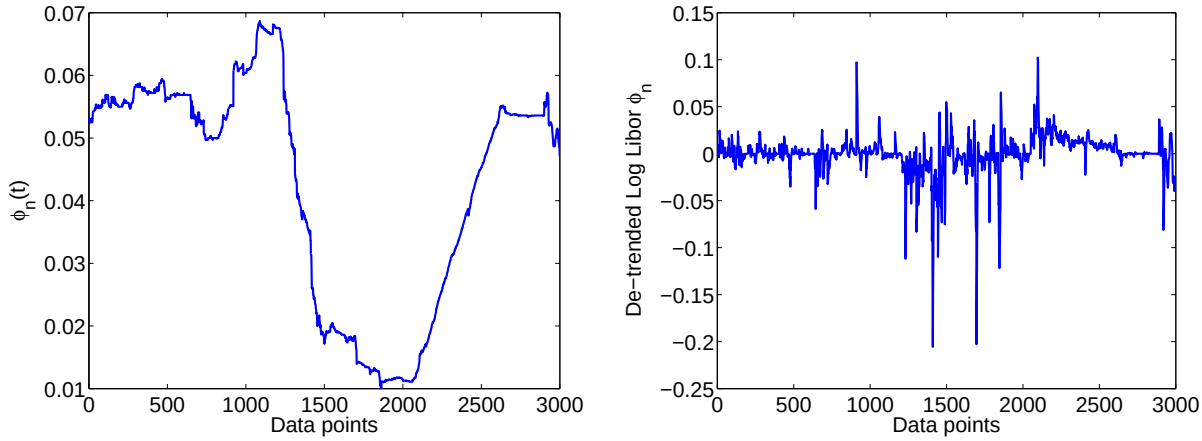

(a) (b)

Figure 4.2: Plots of logarithmic LIBOR. (a) Raw data $\phi_n(t)$. (b) De-trended Log LIBOR ϕ_n.

In equation § 4.4.7, the matrix D is the function of the matrix M and P. Matrix M is the covariance of ϕ_n and is obtained from LIBOR data directly. The diagonal matrix P has elements of $\rho_i^0(1-\rho_i^0)$ where ρ_i^0 refers to the initial condition.

Equation § 4.3.8 gives the expression of ρ_i^0 and hence ρ_i^0 can be calculated from LIBOR. According to data used in the calibration, the number of initial LIBOR is the same as the number of ϕ_n. The initial LIBOR is not unique because of the de-trending and no longer refer to the initial conditions; furthermore, the ground state makes no reference to the initial conditions of LIBOR; hence ρ_i^0 should be calibrated from data.

One of the main results is that, instead of considering ρ_i^0 to be the initial condition, the free parameters of the model that are fixed by the calibration.

3000 data points of LIBOR are used and the time period is from 1996-02-06 to 2007-12-31. Equation § 4.5.2 cannot be used to fit the data directly because the time scale of the matrix D is one year while ϕ_n is daily data. Hence, a rescaling needs to be incorporated into the model. Because we have the term $\phi D \phi$ in the ground state, D should be multiplied by the number of trading days in one year = 252 days squared to make sure both the model and data have same time scale. The probability distribution after rescaling is given by

$$f(\phi_I) \quad = \quad |\Omega(\phi_I)|^2 = \mathcal{N} \exp\left(-\frac{1}{2}\tilde{D}_{II}\phi_I^2 + j_I\phi_I\right) \quad ; \quad \tilde{D}_{II} = 252^2 \times D_{II}. \qquad (\S\, 4.5.4)$$

The fitting of probability distribution for single LIBOR is shown in Figure 4.3(a) in which R-square is also plotted on the graph. Our model fits the data with high accuracy, with the value of $\rho^0 = 0.065$ being obtained from the calibration.

The LIBOR market model is compared to our model and the initial condition $\rho^0 = 0.0105$ is calculated using the average value of initial LIBOR, and the fitting is shown in Figure 4.3(b). The initial condition for ρ^0 of data is too small and cannot fit the market data. Even the largest value of initial condition ρ^0 is 0.0169 which is much smaller than the ρ^0 obtained from the calibration. The calibration implies that the LIBOR market model mismatches with market data if the model is used directly without any modification. In conclusion, our interpretation of ρ^0 as a parameter of the model is supported by market data.

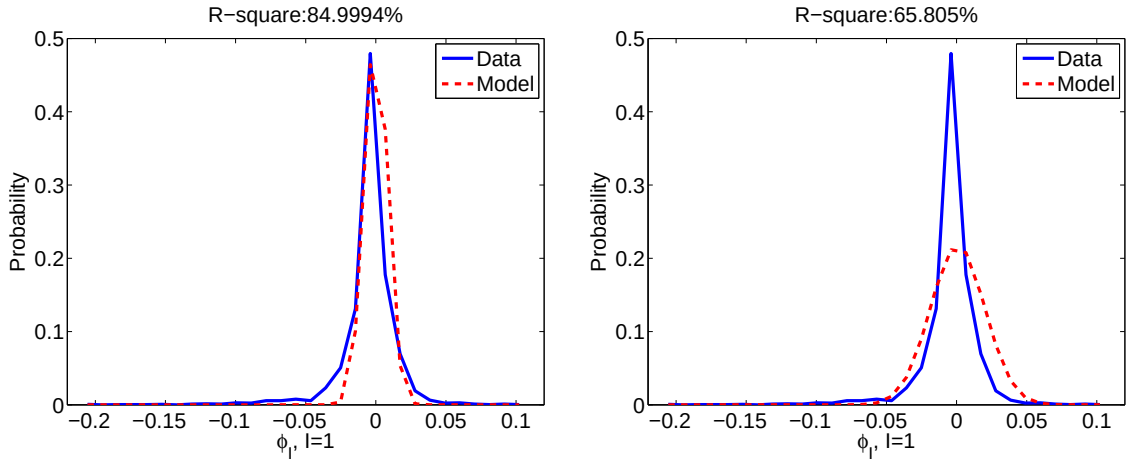

(a) (b)

Figure 4.3: The fitting of the probability distribution for single LIBOR. (a) ρ^0 is calibrated from data. (b) ρ^0 is calculated using the average value of initial LIBOR.

§ 4.6 Calibration of Multiple LIBOR

The results obtained in the section § 4.5 are the fitting of the model for single LIBOR. In this case, both the matrix D and vector j only have one element. As defined in equation § 4.4.7, matrix D contains both autocorrelation and cross correlation of LIBOR on different maturities time. In this section, the performance of the Hamiltonian model for multi-LIBOR is examined. The marginal probability density distribution function of the Ith LIBOR is

$$\begin{aligned} f(\zeta) &= |\Omega(\zeta)|^2 = \prod_{i=1}^{N} \int d\phi_i |\Omega(\phi_i)|^2 \delta(\zeta - \phi_I) \\ &= \mathcal{N} \int \frac{dh}{2\pi} \prod_{i=1}^{N} \int d\phi_i e^{ih(\zeta-\phi_I)} e^{S(\phi)}, \end{aligned} \tag{§ 4.6.1}$$

where the action S is given by

$$S(\phi) = -\frac{1}{2}\sum_{ij} \phi_i D_{ij} \phi_j + \sum_j j_j \phi_j = -\frac{1}{2}\phi D \phi + j\phi.$$

$f(\zeta)$ can be rewritten as

$$f(\zeta) = \mathcal{N}' \int e^{ih\zeta} \prod_{i=1}^{N} \int d\phi_i e^{S'(\phi)}, \quad S'(\phi) = -\frac{1}{2}\phi D\phi + j\phi - ih\phi_I.$$

The probability $f(\zeta)$ can be obtained by performing N-dimensional Gaussian integration directly

$$\begin{aligned} f(\zeta) &= \mathcal{N}'' \int_h \exp\{\frac{1}{2}(j_\alpha - ih\delta_{I\alpha})D^{-1}_{\alpha\beta}(j_\beta - ih\delta_{I\beta}) + ih\zeta\}dh \\ &= \mathcal{N}'' \int_h dh \exp\{-\frac{1}{2}h^2 D^{-1}_{II} + ih(\zeta - \sum_\alpha j_\alpha D^{-1}_{\alpha I}) + \frac{1}{2}jD^{-1}j\} \\ &= \tilde{\mathcal{N}} \exp\{-\frac{\left(\sum_\alpha j_\alpha D^{-1}_{\alpha I} - \zeta\right)^2}{2D^{-1}_{II}}\}. \end{aligned}$$

Finally, the probability distribution function for the Ith LIBOR is

$$f(\phi_I) = \tilde{\mathcal{N}} \exp\{-\frac{(b_I - \phi_I)^2}{2a_I}\}. \qquad (\S\,4.6.2)$$

The coefficients a_I and b_I are

$$a_I = D^{-1}_{II}; \quad b_I = \sum_\alpha j_\alpha D^{-1}_{\alpha I}, \qquad (\S\,4.6.3)$$

which are the functions of D_{mn} and j_n. As expected, a_I and b_I contain the information of nontrivial LIBOR drift. Here, matrix D is also replaced by $\tilde{D}$ to make sure $\tilde{D} = 252^2 \times D$ and ϕ_I have the same scale.

Equation § 4.6.2 [1] is used to fit the LIBOR of different maturity time, namely $L(t, 0, 3M)$, $L(t, 3M, 6M)$, $L(t, 6M, 9M)$ and $L(t, 9M, 12M)$. Two distinct methods are examined when calibrating the model. We firstly used four different ρ^0_I for each LIBOR $\phi_I, I = 1, 2, 3, 4$. The fitting results are plotted on Figure 4.4(a), and the four LIBOR $L(t, 0, 3M)$, $L(t, 3M, 6M)$, $L(t, 6M, 9M)$ and $L(t, 9M, 12M)$ are from right to left on the graph. It is obvious that our model can fit the first two LIBOR very well. However, values of four ρ^0_I obtained are 0.05, 0.004, 0.001 and 0.0007 respectively. These parameters differ by a factor of nearly 70. From the data, the differences between $L_I(t)$ are very small and less than 7%. Hence, one can

[1] The probability distribution of data is plotted by dividing [min max] of ϕ_I to 30 intervals. The number of ϕ_I is recorded in each interval. Here, we have four LIBOR and the axes of $\phi_I, I = 1, 2, 3, 4$ should be different. In the graph, the LIBOR $\phi_I, I = 1$ is used to be the axis. The other three axes of $\phi_I, I = 2, 3, 4$ have the similar value and are not plotted on the graph.

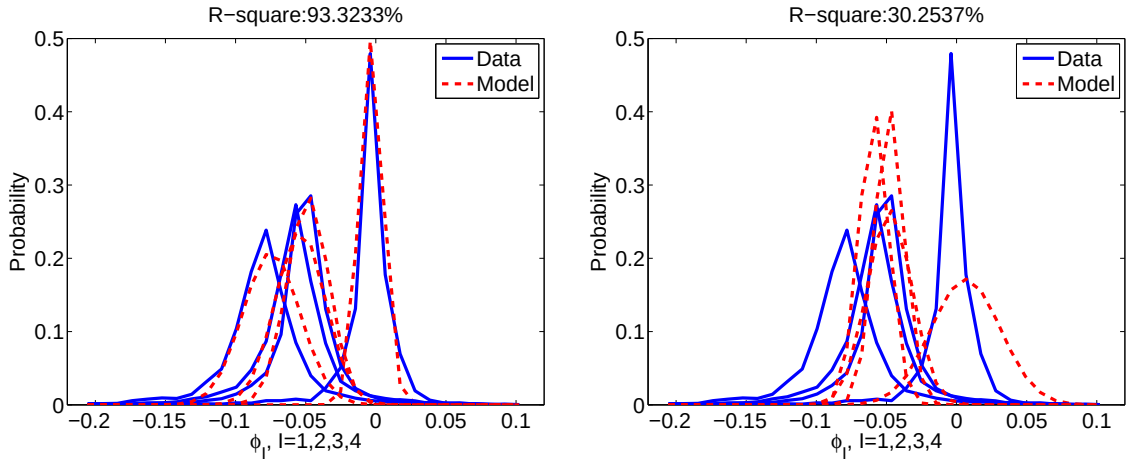

(a) (b)

Figure 4.4: The fitting of the probability distribution for multiple LIBOR. (a) Four different ρ_I^0 are used for the calibration. (b) One same ρ^0 is used for all LIBOR.

assume that all ρ_I^0 can be equal and the calibration results are presented in Figure 4.4(b).

The model cannot fit the market data with only one parameter ρ^0, and one more parameter $\eta(I)$ must be introduced into the model, which is discussed in section § 4.7.

§ 4.7 Market time index $\eta(I)$

Market time has been introduced in Baaquie [50] to quantitatively describe the subjective perceived of future time by traders, and which exists only in the minds of the traders. For the case of forward interest rates $f(t,x)$, it is assumed that future time x is to be replaced by market time z, where $z = (x-t)^\eta$ and η is a constant that for Eurodollars is approximately equal to 0.4; the forward rates are then described by $f(t,z)$.

The case of LIBOR is more complicated since LIBOR $L(t,T_n)$ is defined only for future time $T_n > t$ on the LIBOR future time lattice, as shown in Figure 4.5. Intuitively, market time should be different for the LIBOR of different maturity times. In contrast to market time index for forward interest rates $f(t,x)$, where η is a constant, the probability distribution function for LIBOR requires us to further generalize market time so that it depends on the LIBOR future time lattice defined by $T_I = \ell I, I = 0,1,2,....$

Recall LIBOR is defined for tenor ℓ that breaks up future time x into the following future

Figure 4.5: LIBOR $L(t, T_n)$ is defined for a given tenor ℓ for LIBOR lattice future time $T_n = \ell n$.

time LIBOR lattice

$$x(T_I) \;=\; I\ell + \tau; \quad 0 \le \tau < \ell \;\; ; \;\; I = 0, 1, 2, ... \qquad (\S\, 4.7.1)$$

The LIBOR lattice has a fixed tenor (lattice time interval) given by ℓ. In contrast, for nontrivial market time, the tenor ℓ for different maturity LIBOR varies as one moves forward into the future. Hence, the definition of the market time index for LIBOR is defined in such a manner so as to reflect the LIBOR future time lattice, namely one generalizes η to $\eta(T_I) \equiv \eta(I)$. The route for calibrating the LIBOR market time index $\eta(I)$ is to make equation § 4.6.2 consistent with market data.

Market time index on $\ell(I)$ yields the market time lattice, with varying tenor (future time lattice spacing), and is given as follows

$$z(T_I) \;=\; I\ell\lambda^{\eta(I)} + \tau'; \quad 0 \le \tau' < \ell\lambda^{\eta(I)} \;\; ; \;\; I = 0, 1, 2, ... \qquad (\S\, 4.7.2)$$

λ is a dimensionless factor and is used to make $x(T_I)$ and $z(T_I)$ both have the same dimension of time. The log LIBOR $\phi(t, x)$, defined on LIBOR lattice with fixed lattice spacing, is related to another rate $\xi(t, z)$ defined on the market time lattice, and is shown in Figure 4.6.

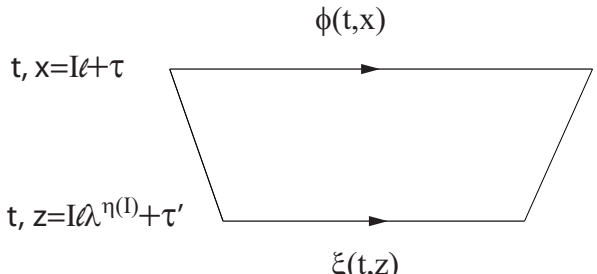

Figure 4.6: The fields $\xi(t, z)$ and $\phi(t, x)$; the tenor for market time is given by $I\ell\lambda^{\eta(I)} + \tau'$, where $0 \le \tau' < \ell\lambda^{\eta(I)}$.

The relation of $\phi(t, x)$ to $\xi(t, z)$ is obtained by requiring that the integration over log LIBOR $\phi(t, x)$ on future time must be equal to the integration over rate $\xi(t, z)$ on market

time; hence

$$\ell L(t,T_I) = \exp\int_{T_I}^{T_{I+1}} dx\phi(t,x) = \exp\int_{I\ell}^{(I+1)\ell} d\tau\phi(t,x) \approx \exp\{\ell\phi_I(t,x)\}, \quad (\S\,4.7.3)$$

$$\ell L(t,T_I) = \exp\int_{z(T_I)}^{z(T_{I+1})} dz\xi(t,z) = \exp\int_{I\ell\lambda^{\eta(I)}}^{(I+1)\ell\lambda^{\eta(I)}} d\tau'\xi(t,z) \approx \exp\{\ell\lambda^{\eta(I)}\xi_I(t,z)\}. \quad (\S\,4.7.4)$$

where $\phi_I(t,x)$ and $\xi_I(t,z)$ denote the logarithmic LIBOR in which future time is from T_I to T_{I+1} and $z(T_I)$ to $z(T_{I+1})$, respectively. Hence, the two fields are related by the following re-scaling

$$\phi_I(t,x) = \lambda^{\eta(I)}\xi_I(t,z) \quad (\S\,4.7.5)$$

From equation § 4.6.2, the marginal probability with market time $\eta(I)$ is computed using $\xi(t,z)$ and is then mapped to the market log LIBOR $\phi(t,x)$ and yields

$$f(\phi_I) = \tilde{\mathcal{N}}\exp\big[-\frac{\{b_I-\phi_I(t,x)\}^2}{2a_I}\big] = \tilde{\mathcal{N}}\exp\big[-\frac{\{b_I-\lambda^{\eta(I)}\xi_I(t,z)\}^2}{2a_I}\big] \quad (\S\,4.7.6)$$

Equation § 4.7.6 is used to fit the multi-LIBOR and we found that the value of λ is not unique and range from 0.1 to 0.3. The number of parameters used for calibration must be reduced to obtain stable results. Here λ is assumed to be ℓ/one year=0.25. This assumption is based on the fact that if one assumes the dimension is one year and $z(T_I)$ can be rewritten as $z(T_I) = I\ell^{\eta(I)+1} + \tau'$.

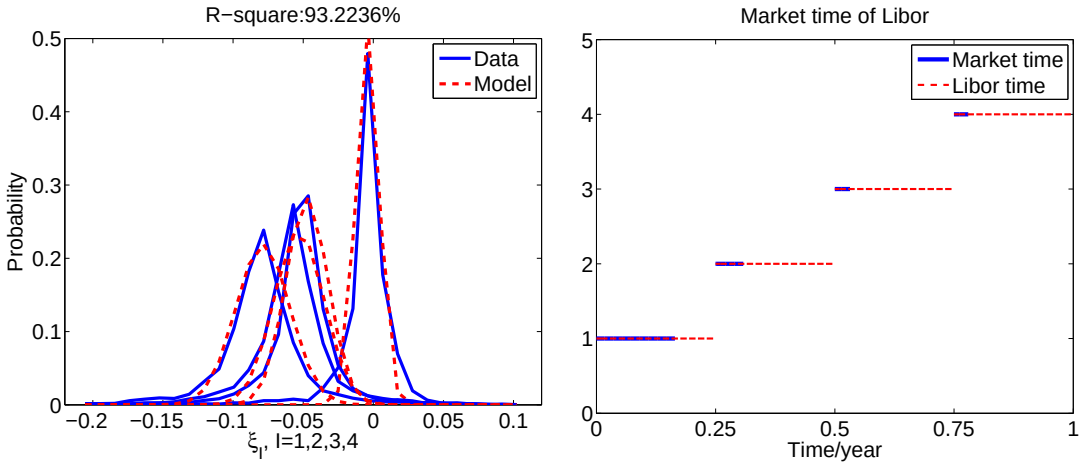

(a) (b)

Figure 4.7: (a) The fitting of the probability distribution for multiple LIBOR with one ρ_0 and $\eta(I), I = 1, 2, 3, 4$. (b) Comparison of LIBOR tenor between market time and LIBOR time.

The result of the fit for market time can be summarized as follows.

- As shown in Figure 4.7(a), our model matches the data with high accuracy. The values of $\eta(I)$ calibrated for LIBOR $L(t, 0, 3M)$, $L(t, 3M, 6M)$, $L(t, 6M, 9M)$ and $L(t, 9M, 12M)$ are 0.30, 1.05, 1.49 and 1.53 respectively.

- Using the values of $\eta(I)$, the interval of market time can be calculated; the comparison between market time and LIBOR time is given in figure 4.7(b). The tenor for $L(t, 0, 3M)$ is comparable to LIBOR time while the tenor is much shorter for $L(t, 9M, 12M)$. For $L(t, 0, 3M)$, market time is approximately equal to LIBOR time and we can conclude that the market is efficient.

- For $L(t, 9M, 12M)$, the LIBOR and LIBOR based derivatives are not traded frequently. The time interval between different trades is much higher compared to $L(t, 0, 3M)$. The frequency decrease when time goes to future and it seems the LIBOR time becomes short for the traders.

- Figure 4.7(b) shows that, when time goes from near future to distant future, the tenor for LIBOR changes to $\lambda^{\eta}(I)$; as $\eta(I)$ varies from 0.3 to 1.5, the tenor perceived by the traders becomes shorter and shorter.

- This remarkable result is what we expect since distant future seems shorter to the mind of the trader than near future for two reasons: one is that time in finance is perceived

in terms of rate of transactions and liquidity for distant future LIBOR is lower than for near future LIBOR; and secondly the subjective perception of future time by traders cannot capture distant future as accurately as near future. This is the identical result that is obtained for forward interest rates [50] and for equities [51].

§ 4.8 Matrix D of LIBOR market model

The matrix D_{market} of our model is shown in Figure 4.8(a) while the matrix D_{LM} of the LIBOR market model using the initial condition is plotted on Figure 4.8(c) where the initial condition is taken as the average value of initial LIBORs. Clearly, both D_{market} and D_{LM} have same structure. The only difference is the magnitude which comes from the values of ρ^0. As defined in equation § 4.4.7, the matrix D is the function of M and initial condition $P = \rho^0(1-\rho^0)$. The matrix M is calculated from market data and ρ^0 is a parameter that is calibrated from market data in the case of Figure 4.8(c). Hence, D_{market} and D_{LM} are differ by a rescaling factor which depends on the value of ρ^0; a single scaling by scaling factor $\mathcal{S}$ yields

$$D_{\text{market}} = \mathcal{S} D_{LM}; \quad \mathcal{S} \approx 8.3. \tag{§ 4.8.1}$$

However, the market time index $\eta(I)$ is introduced into the model and $\eta(I)$ carries the information of LIBOR tenor. From equations § 4.6.3 and § 4.7.6, one can incorporate $\eta(I)$ into D_{market} by constructing new matrix $D^{\eta(I)}_{\text{market}} = D_{\text{market}} \times \sqrt{\eta(I)\eta(J)}$. As shown in Figure 4.8(b), matrix $D^{\eta(I)}_{\text{market}}$ has a totally different structure compared to D_{LM}.

Due to our interpretation of ρ^0 and $\eta(I)$ as parameters to be calibrated that LIBOR market model can be applied to the state space of LIBOR. Here, we conclude that the generalization of the linearized Hamiltonian of the LIBOR market model is supported by data and incorporates the essential behavior of LIBOR.

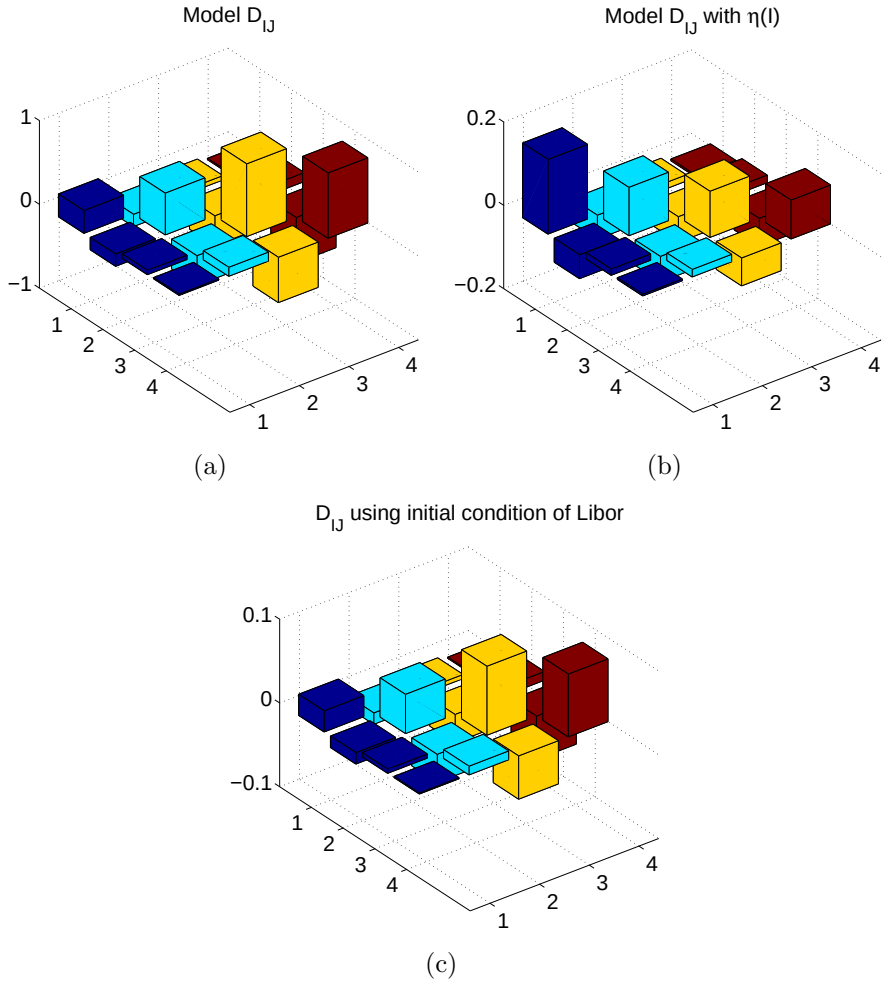

(a) (b) (c)

Figure 4.8: The matrix D. (a) D_{market} calibrated from data. (b) $D^{\eta(I)}_{\text{market}}$ calibrated from data. (c) D_{LM} calculated using initial condition which is the average value of LIBOR.

§ 4.9 Conclusions

We linearize the drift of the LIBOR market model for the Hamiltonian formulation and could then solve for its ground state. We re-interpreted the initial condition of the LIBOR market model as being free parameters of the Hamiltonian and calibrated these parameters from the data.

The probability distribution functions for a single LIBOR and multi-LIBOR were derived and the results showed that our model fits the data with high accuracy. The model could fit the data very well only by using the initial LIBOR as a parameter in conjunction with

the concept of market time. One of our main results is that the market time index can be generalized to the LIBOR case in a manner that respects the LIBOR lattice.

One can go further and find the excited states of the LIBOR Hamiltonian to describe the 2008 debt market that was far from equilibrium. Such a study, which we propose to undertake, would throw further light on the Hamiltonian formulation of the LIBOR market model.

§ 4.10 The quantification on the breaking of martingale

Equation § 4.3.12 gives the Hamiltonian of LIBOR market model in which the drift is linearized. One may contend that the linearization of drift will break the martingale condition and non-arbitrage condition may not be satisfied. The martingale condition is derived here using linearized Hamiltonian to examine whether the martingale condition still holds.

Choose the zero coupon bond $B(t, T_{k+1})$ to be the forward bond numeraire, and the martingale condition of LIBORs is given by

$$\chi_n(t) \;=\; \frac{B(t,T_n)B(t,T_{n+1})}{B(t,T_{k+1})}. \qquad (\S\, 4.10.1)$$

The drift $\rho(t,x)$ is derived in [50] by imposing the martingale condition on $\chi_n(t)$ which is

$$\mathcal{H}(t)\Big[\frac{B(t,T_n)B(t,T_{n+1})}{B(t,T_{k+1})}\Big] \;=\; 0. \qquad (\S\, 4.10.2)$$

Equation § 4.2.5 yields a recursion equation such that the bond $B(t,T_{n+1})$ can be expressed solely in terms of LIBOR rates as follows

$$B(t,T_{n+1}) \;=\; B(t,T_0)\prod_{i=0}^{n}\frac{1}{1+\ell L(t,T_i)} \qquad (\S\, 4.10.3)$$

in which $B(t,T_0)=1$ when $t=T_0$. There are three cases for $\chi_n(t)$, namely that $n=k$, $n>k$ and $n<k$, and all three cases yield same results. We only consider the case of $n>I$ and $\chi_n(t)$ can be expressed in terms of L_k

$$\chi_n(t) \;=\; L_n\prod_{i=k+1}^{n}(1+\ell L_i) = L_n\exp\Big\{-\sum_{i=k+1}^{n}\ln(1+\ell L_i)\Big\}. \qquad (\S\, 4.10.4)$$

In equation § 4.3.12, we have the term of $\sum_m \frac{\partial}{\partial\phi_m}$ which in turn have the following results by

acting this term on L_k

$$\sum_m \frac{\partial}{\partial \phi_m} L_i \quad = \quad H_i L_i. \tag{§ 4.10.5}$$

where H_i is the characteristic function given by equation § 4.3.4. In order to derive the martingale condition, one need to compute the first and second order derivatives of $\chi_n(t)$

$$\sum_{i=0}^{n} \frac{1}{\chi_n(t)} \frac{\delta \chi_n(t)}{\delta \phi_i} \quad = \quad H_n(x) - \sum_{i=0}^{n} \frac{L_i H_i(x)}{1+L_i}, \tag{§ 4.10.6}$$

$$\begin{aligned} \sum_{i=0}^{n}\sum_{j=0}^{n} \frac{1}{\chi_n(t)} \frac{\delta^2 \chi_n(t)}{\delta \phi_i \delta \phi_j} \quad &= \quad \Big[H_n(x) - \sum_{i=0}^{n} \frac{L_i H_i(x)}{1+L_i}\Big]\Big[H_n(x') - \sum_{j=0}^{n} \frac{L_j H_j(x')}{1+L_j}\Big]. \\ &\quad - \sum_{i=0}^{n} \frac{L_i H_i(x) H_i(x')}{1+L_i} + \sum_{i=0}^{n} \Big[\frac{L_i}{1+L_i}\Big]^2 H_i(x) H_i(x') \end{aligned} \tag{§ 4.10.7}$$

Compute the action of Hamiltonian § 4.3.12 using derivation § 4.10.6 and § 4.10.7, we have

$$\begin{aligned} \frac{1}{\chi_n(t)} \mathcal{H}(t) \chi_n(t) \quad &= \quad -\frac{1}{2} \sum_{i=0}^{n} \Big[\frac{L_i}{1+L_i}\Big]^2 \Lambda_{ii} + \sum_{i=0}^{n} \frac{L_i}{1+L_i} \Lambda_{in} \\ &\quad -\frac{1}{2} \sum_{i,j=0}^{n} \frac{L_i}{1+L_i} \frac{L_j}{1+L_j} \Lambda_{ij} - \zeta_n + \sum_{i=0}^{n} \frac{L_i}{1+L_i} \zeta_i. \end{aligned} \tag{§ 4.10.8}$$

where ζ_n and ζ_i are the linearized Libor drift. All the terms in equation § 4.10.8 are cancelled if the LIBOR drift is used without any manipulation. Form LMM in equation § 4.2.8, the Libor drift is

$$\text{LIBOR drift} \quad = \quad \sum_{i=0}^{n} \frac{L_i}{1+L_i} \Lambda_{in} \tag{§ 4.10.9}$$

The linearized Libor drift is

$$\zeta_n \quad = \quad \sum_{i=0}^{n} \big[\rho_i^0 + \rho_i^0 (1-\rho_i^0) \phi_i\big] \Lambda_{in} \tag{§ 4.10.10}$$

Using the following identity

$$\sum_{i=0}^{n} \sum_{j=0}^{i} A_{ij} \quad = \quad \frac{1}{2} \sum_{i,j=0}^{n} A_{ij} + \frac{1}{2} \sum_{i=0}^{n} A_{ii}, \tag{§ 4.10.11}$$

we can reinterpret equation § 4.10.8 as the summation of three different errors in the following

$$\begin{aligned}
\frac{1}{\chi_n(t)}\mathcal{H}(t)\chi_n(t) &= a_e + b_e + c_e \qquad (\S\,4.10.12)\\
a_e &= a - \tilde{a} = \sum_{i=0}^{n}\frac{L_i}{1+L_i}\Lambda_{in} - \sum_{i=0}^{n}\left[\rho_i^0 + \rho_i^0(1-\rho_i^0)\phi_i\right]\Lambda_{in}\\
b_e &= b - \tilde{b} = -\frac{1}{2}\sum_{i=0}^{n}\left[\frac{L_i}{1+L_i}\right]^2\Lambda_{ii} + \frac{1}{2}\sum_{i=0}^{n}\left[\frac{L_i}{1+L_i}\right]\left[\rho_i^0 + \rho_i^0(1-\rho_i^0)\phi_i\right]\Lambda_{ii}\\
c_e &= c - \tilde{c} = -\frac{1}{2}\sum_{i,j=0}^{n}\frac{L_i}{1+L_i}\frac{L_j}{1+L_j}\Lambda_{ij} + \frac{1}{2}\sum_{i,j=0}^{n}\frac{L_i}{1+L_i}\left[\rho_j^0 + \rho_j^0(1-\rho_j^0)\phi_j\right]\Lambda_{ij}
\end{aligned}$$

All the data points are used to calculate the value of martingale condition, and the mean value of equation § 4.10.12 is equal to 2.06×10^{-7}. In order to show the error is negligible, the ratio a_e/a, b_e/b and c_e/c are plotted on figure 4.9(a), 4.9(b) and 4.9(c) respectively. As can be seen, the value of martingale condition is almost zero, and the linearization of Hamiltonian doesn't break the martingale.

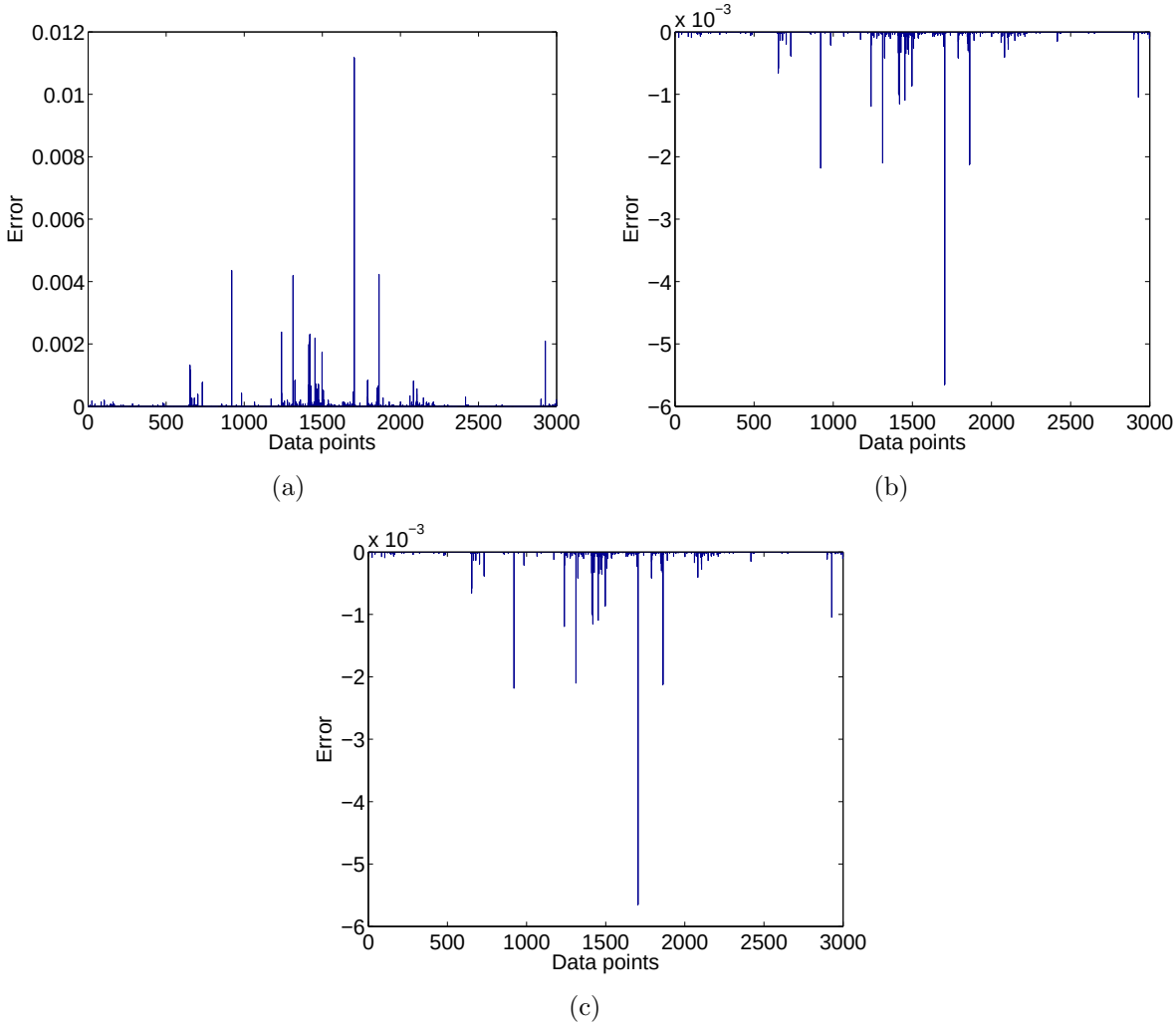

Figure 4.9: Three different source of errors. (a) a_e/a, (b) b_e/b, (c) c_e/c.

Chapter 5

Option Pricing and the Acceleration Lagrangian

The industry standard Black-Scholes option pricing formula is based on the current value of the underlying security and other fixed parameters of the model. The Black-Scholes formula, with a fixed volatility, cannot match the market's option price; instead, it has come to be used as a formula for generating the option price, once the so called *implied volatility* of the option is provided as additional input. The implied volatility not only is an entire surface, depending on the strike price and maturity of the option, but also depends on calendar time, changing from day to day. The point of view adopted in this chapter is that the instantaneous rate of return of the security carries part of the information that is provided by implied volatility, and with a few (time-independent) parameters required for a complete pricing formula.

An option pricing formula is developed that is based on knowing the value of *both* the current price and rate of return of the underlying security which in physics is called *velocity*. Using an acceleration Lagrangian model based on the formalism of quantum mathematics, we derive the pricing formula for European call options. The implied volatility of the market can be generated by our pricing formula. Our option price is applied to foreign exchange rates and equities and the accuracy is compared with Black-Scholes pricing formula and with the market price.

§ 5.1 Introduction

Options are part of a larger class of financial instruments. An option is a contract which gives the buyer or the seller the right, but not the obligation, to buy or sell an underlying asset or instrument at a specified strike price on or before a specified date. The right to buy is a call option while the right to sell is a put option. There are two style of options: European options that can only be exercised on maturity day and American options that can be exercised anytime before or on the date of expiration.

Options valuation is a topic of ongoing research in academic and practical finance. There are many pricing models in use based on the concept of risk neutral pricing and stochastic calculus. Black and Scholes produced a closed-form solution for a European option's theoretical price in 1973 [52]. The Black-Scholes model assumes a constant volatility and an underlying security that is following geometrical Brownian motion. It is observed that the market volatility is varying both with time and the price of the asset [21].

Implied volatility is derived from the market option price using the Black-Scholes model. The at-the-money (ATM) options are often used to calculate the implied volatility since they are the most traded contracts. It is now generally accepted that the implied volatility differ with strike prices and time to expiration as well as depending on calendar time. However, the volatility of the Black-Scholes model is a constant, which is inconsistent with market data.

Baaquie [20] obtained the Black-Scholes formula for a stock price with stochastic volatility based on the mathematical formalism of quantum mechanics applied to finance –called quantum finance in short. To contextualize the term 'quantum finance', note that Witten used the term 'quantum field theory', and that too in Euclidean time, in obtaining the Jones polynomial in his paper titled *Quantum Field Theory and the Jones Polynomial* [29]. The Jones polynomial is a mathematical description of distinct knots in three space dimensions; there is no $\hbar$ or any 'quantum process' in the Jones polynomial. Witten used the mathematics of quantum field theory to solve an entirely classical problem of knots and links – and for which he was awarded the Fields medal in 1989. The term 'quantum finance' is used in a similar spirit of addressing classical problems that arise in the stochastic description of finance using quantum mathematics.

The acceleration Lagrangian has been widely studied in quantum physics [53]; the fundamental problem with the acceleration and other higher time-derivative Lagrangians is that in Minkowski time, they all violate unitarity and give rise to a state space with a negative norm. Hence, to apply the acceleration Lagrangian to quantum mechanics needs a framework quite

different from the one used in standard quantum mechanics[54].

In quantum finance, one is analyzing the Lagrangian in Euclidean time. Classical random systems are not described by a state vector; hence, unlike quantum mechanics, the norm of the state vector is not directly related to the probabilistic aspects of the theory. In fact, in option theory, the option price has a divergent norm but is, nevertheless, an element of a state space.

In the chapter, option pricing is studied using the Euclidean acceleration Lagrangian, and which yields a pricing formula that can describe option market prices without requiring the recourse to implied volatility. The acceleration Lagrangian has been introduced in quantum finance models for studying the correlation of equities [55] and in [56] the acceleration model was studied to generate a maturity dependent formula for the volatility of European options.

This chapter is organized as follows: Section § 5.2, and § 5.3 reviews Black-Scholes model with implied volatility and its generalization to quantum finance model. In Section § 5.4, the acceleration Lagrangian is defined. The option price formula is derived and the martingale condition is analysed in Section § 5.5. Calibration results and comparison with the market are shown in Section § 5.6. In the last Section § 5.7 some conclusions are drawn.

§ 5.2 Black-Scholes model and implied volatility

An option is a derivative of an underlying security $S(t)$ and has a price $C(t)$; the derivative has a cash flow in the future $T > t$ that is determined by a payoff function. The option price $C(t_0, T)$ is the expectation value of the payoff, evolved from future time T to present time t_0 by the random evolution equation of the underlying security $S(t)$; the martingale condition is imposed on the evolution of the security to make the option price free from the possibility of arbitrage. The option price is given by discounting the future cash flow at the maturity of the option using the risk-free interest rate r and yields the option price. Hence

$$C(t,T) = e^{-r(T-t_0)} E\Big[C(T,T)\Big] \qquad (\S\, 5.2.1)$$

where $E[\cdots]$ stands for expectation value.

The payoff function of a call option is its value at maturity T, namely $C(T,T)$. The payoff has the following value: if the value of the underlying asset S is greater than the strike price K, on the option maturing the buyer makes the difference: $S - K$; if the value of the underlying asset S is less than the strike price K, the buyer does not exercise the option.

Hence the payoff for the call option is

$$C(T,T) = (S(T) - K)_+$$

The random evolution of $S(t)$ is shown in Figure 5.1.

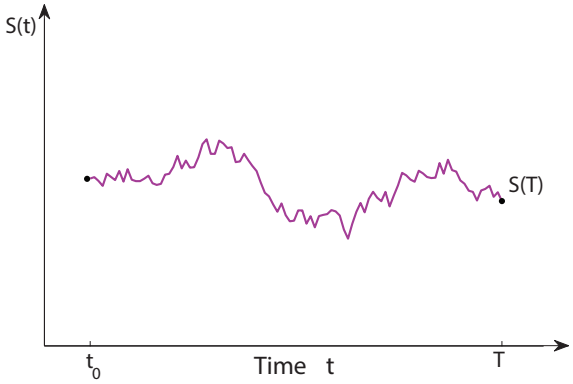

Figure 5.1: Some values $S(t)$.

In mathematical finance the underlying security $S(t)$ is assumed to follow a stochastic differential equation that obeys the martingale condition, namely

$$\frac{dS_t}{S} = rdt + \sigma_0 dW \qquad (\S\, 5.2.2)$$

where σ_0 is the volatility of return and W is white noise. The European option price, using the Black-Scholes model, is

$$C(S,K,r,\sigma,(T-t_0)) = SN(d_+) - e^{-r(T-t_0)}KN(d_-) \qquad (\S\, 5.2.3)$$

where

$$d_\pm = \frac{\ln(S/K) + r(T-t_0) \pm \sigma_0^2(T-t_0)/2}{\sigma_0\sqrt{(T-t_0)}}; \quad N(x) = \frac{1}{\sqrt{2\pi}}\int_{-\infty}^{x} e^{-\frac{1}{2}z^2}dz \qquad (\S\, 5.2.4)$$

The put option has the value

$$P(S,K,r,\sigma,T-t_0) = -SN(-d_+) + e^{-r(T-t_0)}KN(-d_-) \qquad (\S\, 5.2.5)$$

Implied volatility $\sigma_I = \sigma_I(K,T;t_0)$ is introduced as input into the Black-Scholes model and gives the current market price of the option. In other words, the value of σ_I is derived from

the market option price C_M using the Black-Scholes formula. Hence

$$C_M = C_{BS}(S, K, r, \sigma_I(K, T, t_0), T - t_0) \qquad (\S\, 5.2.6)$$

Generally, it is not possible to have a closed form of implied volatility. Historical data shows that σ_I depends on the strike price K and maturity $T - t_0$; furthermore, the implied volatility also depends on calendar time t_0, and hence is written as a surface for each instant t, namely $\sigma_I(K, T, t_0)$.

The Black-Scholes formula, based on the stochastic differential equation given in Eq. § 5.2.2 that has fixed σ_0, cannot yield the market price. In general, one cannot incorporate implied volatility $\sigma_I(K, T, t_0)$ in the stochastic differential equation given in Eq. § 5.2.2 since the strike price K is not part of the evolution of the underlying security but, instead, is determined by the payoff function. Moreover, it is not possible to obtain $\sigma_I(K, T, t)$ using any model since to price an option one needs to know the implied volatility in the future, namely for $t > t_0$. What this means in practice, is that the Black-Scholes formula is not very useful for pricing the options; instead, its main utility is in hedging the option price against the movements of the underlying security and the other parameters in the option price.

§ 5.3 Option pricing in Quantum Finance

Since $S(t) > 0$, the stock price is expressed by

$$S = e^x; \quad -\infty < x < +\infty.$$

In quantum finance, the underlying security and option price are both state vectors and, in Dirac's notation, are denoted by

$$|x\rangle \quad ; \quad |C\rangle$$

In the state space notation, the payoff function and price of a call option are given by

$$\langle x|C(T;T)\rangle = (e^x - K)_+ \quad ; \quad C(x, t; T) = \langle x|C(t;T)\rangle.$$

The initial position $x(t_0)$ at time t_0 randomly evolves to different values with final value of $x(T) = x'$, and is shown in Figure 5.2(a). In Figure 5.2(b) $x(t)$ evolves backward in calendar time, from remaining time $T - t_0$, to present time t_0. The random evolution equation of $x(t)$ is determined by either the Hamiltonian operator or by an appropriate Lagrangian, and is

discussed in detail in [20].

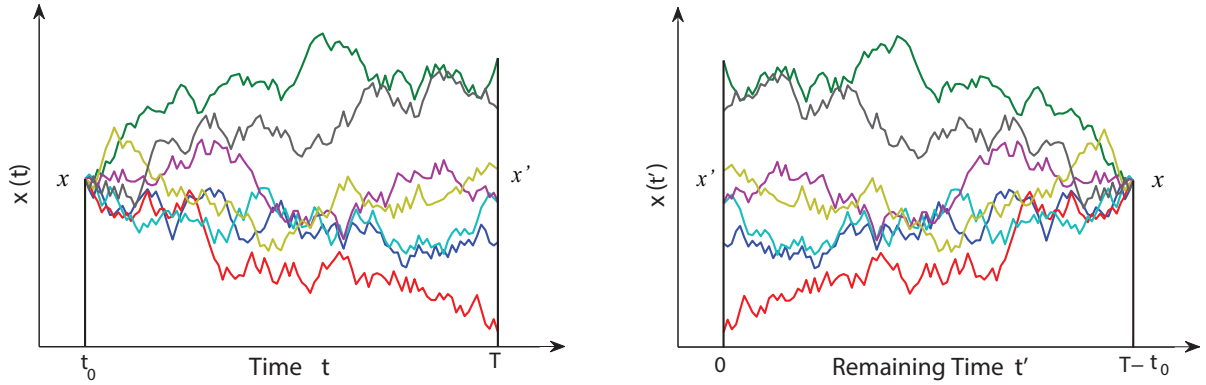

(a) Calendar time t

(b) Backward in remaining time $t' = T - t$

Figure 5.2: Random paths in calendar time and remaining calendar time. x is the initial position and x' is the final position.

The present day value of an option is determined by the *conditional probability* $\mathcal{P}(x, x'; T, t)$, which is the probability that – given the value of the security $S(t) = e^x$ at time t - the security makes a transition to a final value of x' at future time T. The conditional probability $\mathcal{P}(x, x'; T, t)$ has the required normalization, valid for all values of x, T, t, namely that

$$\int_{-\infty}^{+\infty} dx' \mathcal{P}(x, x'; T, t) = 1 \qquad (\S\, 5.3.1)$$

The martingale condition for the underlying security requires that the expected value of the future random discounted value of the underlying security is equal to its present value. Hence the conditional probability must obey

$$e^x = e^{-r(T-t_0)} E[e^{x'}] = e^{-r(T-t_0)} \int_{-\infty}^{+\infty} dx' \mathcal{P}(x, x'; T, t_0) e^{x'}, \qquad (\S\, 5.3.2)$$

Consequently, the martingale condition fixes one parameters in $\mathcal{P}(x, x'; T, t)$, for remaining time $T - t_0$, the option price $C(x, K, T, t_0)$ is given by

$$\begin{aligned} C(x, T, t_0) &= e^{-r(T-t_0)} E\Big[C(T, T)\Big] \\ &= e^{-r(T-t_0)} \int_{-\infty}^{+\infty} dx' \mathcal{P}(x, x'; T, t_0) C(x', T, T) \end{aligned} \qquad (\S\, 5.3.3)$$

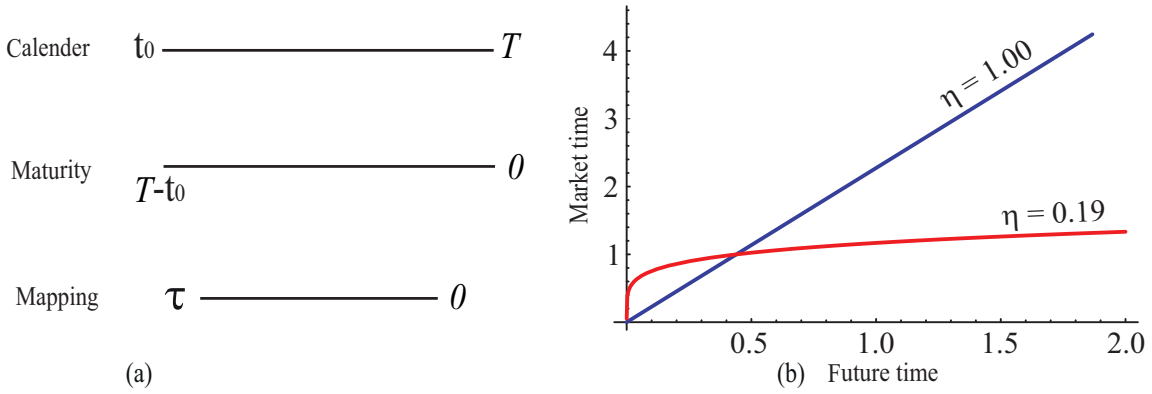

Figure 5.3: (a) Market time $\tau = \lambda[\lambda^{-1}(T-t_0)]^\eta$, where $T-t_0$ is real time in years. (b) Market time versus calendar time for $\lambda = 0.5$ year

In particular, the price of the call option is given by

$$C(x,T,t_0) = e^{-r(T-t_0)} \int_{-\infty}^{+\infty} dx' \mathcal{P}(x,x';T,t_0) \Big[e^{x'} - K\Big]_+ . \qquad (\S\, 5.3.4)$$

§ 5.3.1 Market time; remaining time

The time perceived by the option traders, called *market time*, is not the same as calendar time and needs to be incorporated into the option price. Market time is a measure of the number of financial transactions across the financial markets and reflects the degree of liquidity for financial instruments. The study of interest rates, equities and options [55, 56] shows that one can incorporate the effects of market time – in particular, into the pricing of options – by defining market time using a market index for time.

Let calendar time be denoted by $\tilde{t}$; define effective market time t and remaining market time τ to be

$$t = \lambda(\frac{\tilde{t}}{\lambda})^\eta \quad ; \quad \tau = \lambda(\frac{T-t_0}{\lambda})^\eta \qquad (\S\, 5.3.5)$$

where η is the dimensionless index of market time; λ is a constant that has the dimension of time. Figure 5.3 shows the relation of market time to calendar time. Both η, λ are determined from market option prices.

Market time has two important features, as shown in Figure 5.3(a):

- The empirical determination of η leads to the result that $0 \leq \eta \leq 1$.

- For $t < \lambda$, market time is larger than calendar time, effectively dilating time and hence slowing the rate of change as perceived by the market traders.
- For $t > \lambda$, market time is smaller than calendar time, shortening the perceived duration of instruments maturing at future calendar time T.

From now on, we will always use market time for modeling the random processes that drive the underlying securities and use calendar time only when discounting necessitates it.

§ 5.3.2 Stock price and velocity

To incorporate more information into the pricing of the option, one would like to make the option price depend on the present value of the security $x = \ln S$ as well as its present velocity v which in finance is the logarithmic rate of return

$$v = \frac{dx}{dt} = \frac{d\ln S}{dt} = \frac{1}{S}\frac{dS}{dt} : \text{ logarithmic rate of return} \tag{§ 5.3.6}$$

To compensate for the drawbacks of σ_0 in the Black-Scholes option price, we propose to model the option price using the historical data for a security together with its velocity in the following manner

$$C = C(x, v, K, r, \vec{a}, \tau) \tag{§ 5.3.7}$$

The option price is given by the acceleration Lagrangian, discussed in the next Section § 5.4; all the parameters $\vec{a} = (a, \alpha, \beta)$ are defined in the Lagrangian.

The conditional probability is given by $P(x, x'; v, v'; \tau)$ and the option price the generalization of Eq. § 5.3.4 and is given by

$$\begin{aligned} C(x, v; T - t_0) &= e^{-r(T-t_0)} E\Big[C(0)\Big] \\ &= e^{-r(T-t_0)} \int_{-\infty}^{+\infty} dx' dv' \mathcal{P}(x, x'; v, v'; \tau) C(x', v', 0) \end{aligned} \tag{§ 5.3.8}$$

The discounting of the future cash flow at calendar time T uses remaining calendar time $T - t_0$ since the discounting does not depend on how time is perceived by the traders. For the call option, the payoff is given by $t_0 = T$ and yields $\tau = 0$; hence

$$\langle x, v | C(0) \rangle = (e^x - K)_+$$

Note the payoff does not depend on the final velocity of the security v, as is the case for most of the traded instruments in the market; hence, one can integrate out the final velocity v' and the option price, from Eq. § 5.3.8 yields

$$\begin{aligned} C(x, v; T - t_0) &= e^{-r(T-t_0)} E\Big[C(0)\Big] \\ &= e^{-r(T-t_0)} \int_{-\infty}^{+\infty} dx' \mathcal{P}(x, x'; v; \tau) C(x', 0) \end{aligned} \tag{§ 5.3.9}$$

where

$$\mathcal{P}(x, x'; v; \tau) = \int_{-\infty}^{+\infty} dv' \mathcal{P}(x, x'; v, v'; \tau) \tag{§ 5.3.10}$$

The rest of the chapter analyzes the conditional probability for various derivative instruments.

In state space notation, the option price is given by

$$\langle x, v | C(K, r, \vec{a}, 0) \rangle = C(x, v, K, r, \vec{a}, \tau) \tag{§ 5.3.11}$$

The state space needs a basis consisting of two degrees of freedom, namely x, v and given by $|x, v\rangle = |x\rangle \bigotimes |v\rangle$.

- For a state space with state vector $|x\rangle$, Heisenberg's uncertainty principle, generalized to quantum finance in [20], implies that both x and $v = dx/dt$ cannot be degrees of freedom for the state space. Hence the state space is not suitable for our requirement.
- The properties of the state vector are encoded in the kinetic term of the Lagrangian and. Require $|x, v\rangle$ to be an allowed state vector entails a Lagrangian that needs two initial and two final boundary values. Hence, one has to go beyond the Lagrangians studied in quantum mechanics that have a kinetic term given by the square of the velocity $(dx/dt)^2$.
- Instead, to model an option price that depends on both the security and its derivative, we need a Lagrangian that has a kinetic term given by an *acceleration term*, namely $(d^2x/dt^2)^2$ and which can accommodate the state vector $|x, v\rangle$.

§ 5.4 The acceleration Lagrangian model

The conditional probability is now given by $P(x, x'; v, v'; T, t)$, we extend the Black-Scholes Lagrangian to an acceleration Hamiltonian and Lagrangian which needs *four* boundary conditions with initial and final values of the security and its velocity.

Consider the non-Hermitian acceleration Hamiltonian given by [57]

$$H = -\frac{1}{2a}\frac{\partial^2}{\partial v^2} - v\frac{\partial}{\partial x} + bv^2 + \frac{1}{2}cx^2 \tag{§ 5.4.1}$$

The Hamiltonian and its Hermitian conjugate both act on a state space $\mathcal{V}$ that has *two* degrees of freedom, namely position coordinate x and velocity degree of function v. The state function $|\Psi\rangle$ is given by

$$|\Psi\rangle \in \mathcal{V} \quad ; \quad \langle x, v|\Psi\rangle = \Psi(x, v) \tag{§ 5.4.2}$$

The completeness equation for the state space is given by

$$\int dxdv|x, v\rangle\langle x, v| = 1 \tag{§ 5.4.3}$$

The transition amplitude is given by the matrix element of the evolution operator, namely

$$\mathcal{K}(x, x'; v, v'; \tau) = \langle x, v|e^{-\tau H}|x', v'\rangle \tag{§ 5.4.4}$$

The conditional probability $\mathcal{P}(x, x'; v, v'; T, t)$ is given by appropriately normalizing the transition amplitude and yields

$$\begin{aligned}\mathcal{P}(x, x'; v, v'; \tau) &= \frac{\mathcal{K}(x, x'; v, v'; \tau)}{\int dx'dv'\mathcal{K}(x, x'; v, v'; \tau)} \\ \mathcal{P}(x, x'; v; \tau) &= \int dv'\mathcal{P}(x, x'; v, v'; \tau)\end{aligned} \tag{§ 5.4.5}$$

The conditional probability required to evaluate an option, as given in Eq. § 5.3.10, is obtained from Eq. § 5.4.5 above.

The Lagrangian and action for market time is obtained from the Hamiltonian and is given by [57]

$$\mathcal{L} = -\frac{1}{2}\Big(a\ddot{x}^2 + 2b(\dot{x} + j)^2 + cx^2\Big) \quad ; \quad \mathcal{S} = \int_0^\tau dt\mathcal{L} \tag{§ 5.4.6}$$

where

$$\dot{x} = \frac{dx}{dt} = v \quad ; \quad \ddot{x} = \frac{d^2x}{dt^2}.$$

A boundary term j has been added to the Lagrangian that is not in the Hamiltonian given in Eq. § 5.4.1; this boundary term, similar to the case of the Black-Scholes Lagrangian discussed in Appendix § 5.8, is required for fulfilling the martingale condition.

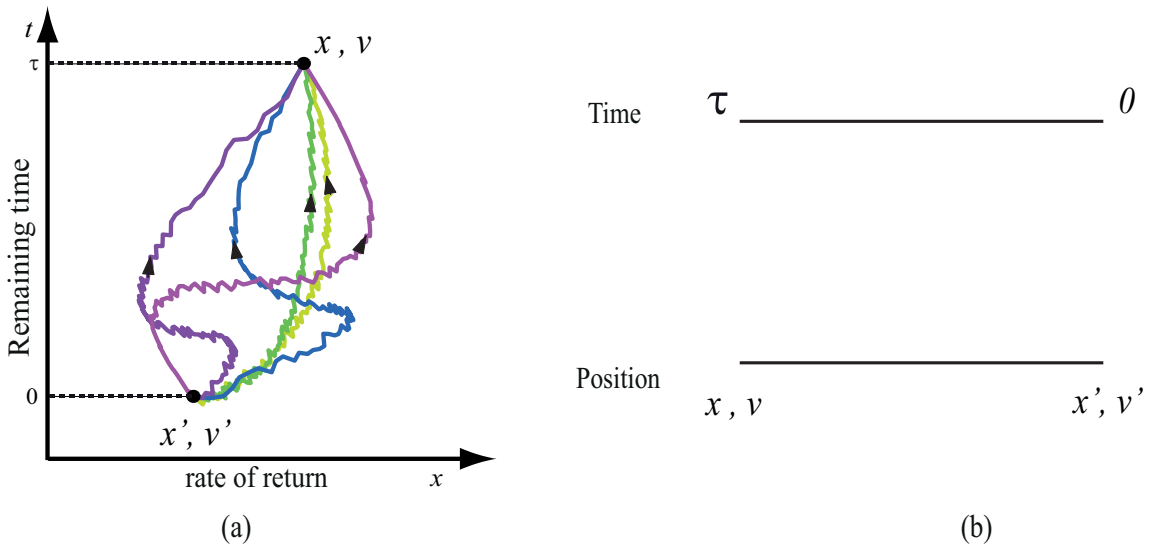

Figure 5.4: Evolution from x, v to x', v' in remaining time.

The transition amplitude $\mathcal{K}(x, x'; v, v'; T, t)$ given in Eq. § 5.4.7 has another representation defined by the (Euclidean) Feynman path integral over *all possible* paths $x(t)$ of the security from its initial value x, v at time t_0 to its final value of x', v' at time T. Figure 5.4 depicts the evolution from x, v to x', v' in remaining time $T - t_0$.

Hence, the transition amplitude in the Feynman path integral representation is given by

$$\mathcal{K}(x, x'; v, v'; \tau) = \int Dx e^{\mathcal{S}}$$
$$\text{B. C.'s}: \; x(0) = x', \; \dot{x}(0) = v'; \; x(\tau) = x, \; \dot{x}(\tau) = v \qquad (\S\, 5.4.7)$$

The transition amplitude has been studied in the Hamiltonian formalism in [57]. Since the acceleration Lagrangian is quadratic in the degrees of freedom, it is more efficient to analyze the transition amplitude starting from the path integral. For a classical solution x_c satisfying the boundary condition in Eq. § 5.4.7, consider the change of integration variables given by $x = x_c + \epsilon$, where ϵ is the new degree of freedom. The action yields $\mathcal{S}[x] = \mathcal{S}[x_c] + \mathcal{S}[\epsilon]$ and

the transition amplitude is given by

$$\mathcal{K} = \int_{-\infty}^{\infty} Dx e^{\mathcal{S}} = \int_{-\infty}^{\infty} D\epsilon e^{\mathcal{S}_\epsilon + \mathcal{S}_c} = N e^{\mathcal{S}_c}, \quad N = \int_{-\infty}^{\infty} D\epsilon e^{\mathcal{S}_\epsilon} \tag{§ 5.4.8}$$

where $Dx = D\epsilon$ since x_c is not stochastic. Hence

$$\mathcal{K} = N e^{\mathcal{S}_c(x,x';v,v';\tau)} \tag{§ 5.4.9}$$

where $\mathcal{S}_c = S[x_c]$ is the classical action and N is a normalization.

The acceleration Lagrangian, from Eq. § 5.4.6, is given by

$$\mathcal{L} = -\frac{1}{2}\Big(a\ddot{x}^2 + 2b(\dot{x}+j)^2 + cx^2\Big) \quad ; \quad \mathcal{S} = \int_0^\tau dt\mathcal{L}$$

and yields the Euler-Lagrangian Equation § 2.2.12, the classical solution $x_c(t)$ that satisfies following equation of motion. Using the notation, from Eq. § 5.5.5, for defining

$$a(\alpha^2 - \beta^2) = b, \quad a(\alpha^2+\beta^2)^2 = c$$

yields the classical solution

$$\ddddot{x}_c(t) - 2(\alpha^2-\beta^2)\ddot{x}_c(t) + (\alpha^2+\beta^2)^2 x_c(t) = 0. \tag{§ 5.4.10}$$

The complex root of the equation

$$y^4 - 2(\alpha^2-\beta^2)y^2 + (\alpha^2+\beta^2)^2 y = 0$$

is given by

$$y = \pm\alpha \pm i\beta$$

Hence, the classical solution $x_c(t)$ in Eq. § 5.4.10 has the general form

$$x_c(t) = e^{\alpha t}[a_1 \sin(\beta t) + a_2 \cos(\beta t)] + e^{-\alpha t}[a_3 \sin(\beta t) + a_4 \cos(\beta t)].$$

Imposing the boundary conditions given in Eq. § 5.4.7, namely

$$x(0) = x', \ \dot{x}(0) = v'; \ x(\tau) = x, \ \dot{x}(\tau) = v$$

yields the following values for $a_1,\ a_2,\ a_3,\ a_4$

$$
\begin{aligned}
a_1 &= \frac{\Lambda}{4}\Big[(\alpha\left(\beta(e^{-2\alpha\tau}-\cos(2\beta\tau))-\alpha\sin(2\beta\tau)\right))x' + (\beta(1-e^{-2\alpha\tau})-\alpha\sin(2\beta\tau))v' \\
&\quad + 2\left(\alpha e^{-\alpha\tau}\sin(\beta\tau)-\beta\sinh(\alpha\tau)\cos(\beta\tau)\right)v \\
&\quad + 2\left(\alpha^2 e^{-\alpha\tau}-\beta^2\sinh(\alpha\tau)\right)\sin(\beta\tau)+\alpha\beta\sinh(\alpha\tau)\cos(\beta\tau)x\Big] \\
a_2 &= \frac{\Lambda}{4}\Big[(2\alpha^2\sin^2(\beta\tau)+\beta^2(1-e^{-2\alpha\tau})+\alpha\beta\sin(2\beta\tau))x' + 2\alpha\sin^2(\beta\tau)v' \\
&\quad + 2\beta\sinh(\alpha\tau)\sin(\beta\tau)v + 2\beta(\beta\sinh(\alpha\tau)\cos(\beta\tau)+\alpha\cosh(\alpha\tau)\sin(\beta\tau))x\Big] \\
a_3 &= -\frac{\Lambda}{4}\Big[(\alpha\left(\beta(e^{2\alpha\tau}-\cos(2\beta\tau))+\alpha\sin(2\beta\tau)\right))x' + (\beta\left(e^{2\alpha\tau}-1\right)-\alpha\sin(2\beta\tau))v' \\
&\quad + 2(\alpha e^{\alpha\tau}\sin(\beta\tau)-\beta\sinh(\alpha\tau)\cos(\beta\tau))v \\
&\quad - 2\left(\alpha^2 e^{\alpha\tau}-\beta^2\sinh(\alpha\tau)\right)\sin(\beta\tau)+\alpha\beta\sinh(\alpha\tau)\cos(\beta\tau)x\Big] \\
a_4 &= -\frac{\Lambda}{4}\Big[(2\alpha^2\sin^2(\beta\tau)+\beta^2(1-e^{2\alpha\tau})-\alpha\beta\sin(2\beta\tau))x' - 2\alpha\sin^2(\beta\tau)v' \\
&\quad - 2\beta\sinh(\alpha\tau)\sin(\beta\tau)v - 2\beta(\beta\sinh(\alpha\tau)\cos(\beta\tau)+\alpha\cosh(\alpha\tau)\sin(\beta\tau))x\Big].
\end{aligned}
$$

In the above equations, Λ is

$$\Lambda = \frac{1}{\alpha^2\sin^2(\beta\tau)-\beta^2\sinh^2(\alpha\tau)}$$

Define the boundary condition of x, v and x', v' using the notion of x_1, x_2, x_3, x_4 for further use as following

$$
\begin{aligned}
x' = x_1,\ v' = x_2; \\
v = x_3,\ x = x_4.
\end{aligned}
\tag{§ 5.4.11}
$$

Figure 5.5 shows some typical classical solutions when varying the starting conditions of x_1 and x_2.

We obtain the action $\mathcal{S}$ using the same procedure as in Black-Scholes model but with the boundary conditions $\epsilon(0) = 0 = \epsilon(\tau),\ \ \dot{\epsilon}(0) = 0 = \dot{\epsilon}(\tau)$, we hence obtain

$$
\begin{aligned}
\mathcal{S} &= \mathcal{S}[x_c+\epsilon] = \mathcal{S}[x_c]+\mathcal{S}[\epsilon]+R \\
&= -\frac{a}{2}\int_0^\tau dt\ \Big((\ddot{x}_c+\ddot{\epsilon})^2 + 2(\alpha^2-\beta^2)(\dot{x}_c+\dot{\epsilon}+j)^2 + (\alpha^2+\beta^2)^2(x_c+\epsilon)^2\Big)
\end{aligned}
\tag{§ 5.4.12}
$$

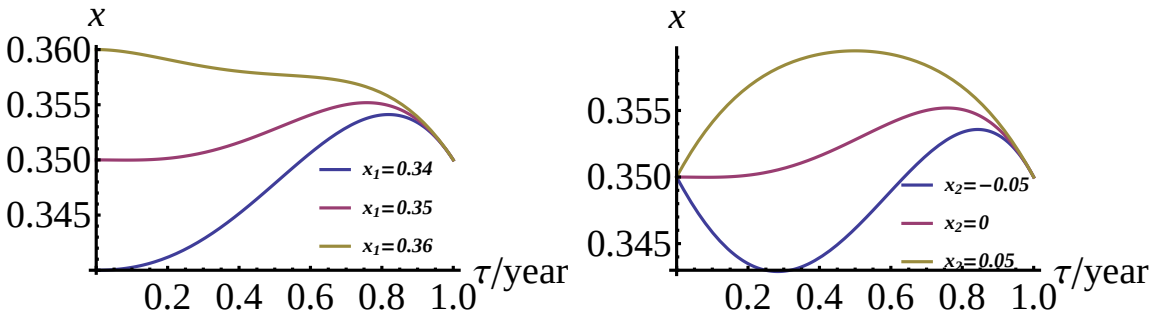

Figure 5.5: Some typical classical solutions with different starting values

where

$$\begin{aligned}
\mathcal{S}[x_c] &= -\frac{a}{2}\int_0^\tau dt\ \Big(\ddot{x}_c^2 + 2(\alpha^2-\beta^2)(\dot{x}_c+j)^2 + (\alpha^2+\beta^2)^2 x_c^2\Big),\\
\mathcal{S}[\epsilon] &= -\frac{a}{2}\int_0^\tau dt\ \Big(\ddot{\epsilon}_c^2 + 2(\alpha^2-\beta^2)\dot{\epsilon}^2 + (\alpha^2+\beta^2)^2\epsilon^2 + 2(\alpha^2-\beta^2)\cdot 2j\dot{\epsilon}\Big)\\
&= -\frac{a}{2}\int_0^\tau dt\ \Big(\ddot{\epsilon}_c^2 + 2(\alpha^2-\beta^2)\dot{\epsilon}^2 + (\alpha^2+\beta^2)^2\epsilon^2\Big)\\
R &= -a\int_0^\tau dt\ (\ddot{x}_c\ddot{\epsilon} + 2(\alpha^2-\beta^2)\dot{x}_c\dot{\epsilon} + (\alpha^2+\beta^2)^2 x_c\epsilon)\\
&= a(-\ddot{x}_c\dot{\epsilon} - 2(\alpha^2-\beta^2)\dot{x}_c\epsilon + \dddot{x}_c\epsilon)|_0^\tau - a\int_0^\tau dt\ \epsilon(\ddddot{x}_c - 2(\alpha^2-\beta^2)\ddot{x}_c + (\alpha^2+\beta^2)^2 x_c)\\
&= 0.
\end{aligned}$$

Integration $\mathcal{S}[x_c]$ by parts we can get

$$\begin{aligned}
\mathcal{S}[x_c] &= -\frac{a}{2}\int_0^\tau dt\ \Big(\ddot{x}_c^2 + 2(\alpha^2-\beta^2)(\dot{x}_c+j)^2 + (\alpha^2+\beta^2)^2 x_c^2\Big) \qquad (\S\,5.4.13)\\
&= -\frac{a}{2}\int_0^\tau dt\ \mathrm{d}(-\dddot{x}_c x_c + \ddot{x}_c\dot{x}_c + 2(\alpha^2-\beta^2)\dot{x}_c x_c + 4(\alpha^2-\beta^2)j x_c + (\alpha^2-\beta^2)j^2)\\
&+ a x_c(\ddddot{x}_c - 2(\alpha^2-\beta^2)\ddot{x}_c + (\alpha^2+\beta^2)^2 x_c)\\
&= -\frac{a}{2}\Big(-\dddot{x}_c x_c + \ddot{x}_c\dot{x}_c + 2(\alpha^2-\beta^2)\dot{x}_c x_c + 4(\alpha^2-\beta^2)j x_c + (\alpha^2-\beta^2)j^2\Big)\Big|_0^\tau\\
&= -\frac{1}{2}\sum_{I,J=1}^{4} x_I M_{IJ} x_J - 2a(\alpha^2-\beta^2)j x_4 + 2a(\alpha^2-\beta^2)j x_1 - a(\alpha^2-\beta^2)j^2\tau/2.
\end{aligned}$$

Note

$$M_{IJ} = -\frac{\partial^2\mathcal{S}_c}{\partial x_I \partial x_J}, \quad I,J = 1,2,3,4. \qquad (\S\,5.4.14)$$

The solution of M satisfies the following symmetry, discussed in [57]

$$\begin{aligned} M_{11} &= M_{44}, \qquad M_{22} = M_{33} \\ M_{12} &= -M_{34}, \quad M_{13} = -M_{24}. \end{aligned} \tag{§ 5.4.15}$$

Therefore, the action can be simplified using the symmetry that

$$\begin{aligned} \mathcal{S}_c &= -\frac{1}{2}M_{11}(x_1^2 + x_4^2) - \frac{1}{2}M_{22}(x_2^2 + x_3^2) - M_{23}x_2x_3 - M_{12}(x_1x_2 - x_3x_4) \\ &- M_{13}(x_1x_3 - x_2x_4) - M_{14}x_1x_4 + 2a(\alpha^2 - \beta^2)jx_1. \end{aligned} \tag{§ 5.4.16}$$

and the solution of M_{IJ} is given below:

$$\begin{aligned} M_{11} &= \Lambda a\Big[-\alpha\beta\left(\alpha^2 + \beta^2\right)\left(\alpha\sin\left(2\beta\tau\right) + \beta\sinh\left(2\alpha\tau\right)\right)\Big] \\ M_{12} &= \Lambda a\Big[-\left(\alpha^2 + \beta^2\right)\left(\alpha^2\sin^2\left(\beta\tau\right) + \beta^2\sinh^2\left(\alpha\tau\right)\right)\Big] \\ M_{13} &= \Lambda a\Big[-2\alpha\beta\left(\alpha^2 + \beta^2\right)\sin\left(\beta\tau\right)\sinh\left(\alpha\tau\right)\Big] \\ M_{14} &= \Lambda a\Big[2\alpha\beta\left(\alpha^2 + \beta^2\right)\left(\beta\cos\left(\beta\tau\right)\sinh\left(\alpha\tau\right) + \alpha\sin\left(\beta\tau\right)\cosh\left(\alpha\tau\right)\right)\Big] \\ M_{22} &= \Lambda a\Big[\alpha\beta\left(\alpha\sin\left(2\beta\tau\right) - \beta\sinh\left(2\alpha\tau\right)\right)\Big] \\ M_{23} &= \Lambda a\Big[2\alpha\beta\left(\beta\cos\left(\beta\tau\right)\sinh\left(\alpha\tau\right) - \alpha\sin\left(\beta\tau\right)\cosh\left(\alpha\tau\right)\right)\Big]. \end{aligned} \tag{§ 5.4.17}$$

§ 5.5 Option pricing

The classical action S_c is given in Appendix C. Using a matrix notation

$$X = \begin{pmatrix} x \\ v \end{pmatrix}, \; X' = \begin{pmatrix} x' \\ v' \end{pmatrix}$$

yields

$$\mathcal{S}_c(x, x'; v, v'; \tau) = -\frac{1}{2}X'^T M X' + G^T X'. \tag{§ 5.5.1}$$

where

$$M = \begin{pmatrix} M_{11} & M_{12} \\ M_{12} & M_{22} \end{pmatrix}; \; G = \begin{pmatrix} 2bj - M_{14}x + M_{24}v \\ M_{13}x - M_{23}v \end{pmatrix} \tag{§ 5.5.2}$$

The conditional probability, from Eqs. § 5.4.5 and § 5.4.9, is given by

$$\mathcal{P}(x,x';v,v';\tau)=\frac{e^{\mathcal{S}_c}}{\int_{-\infty}^{+\infty}dx'dv'e^{\mathcal{S}_c}}=\frac{2\pi}{\sqrt{\mathrm{Det}(M)}}e^{-\frac{(X'-QX-O)^T M(X'-QX-O)}{2}} \tag{§ 5.5.3}$$

where $\mathrm{Det}(M)=M_{11}M_{22}-M_{12}^2$, and

$$Q=\begin{pmatrix}\frac{M_{12}M_{24}-M_{22}M_{14}}{\mathrm{Det}(M)} & \frac{M_{12}M_{23}-M_{22}M_{13}}{\mathrm{Det}(M)}\\ \frac{M_{11}M_{13}+M_{12}M_{14}}{\mathrm{Det}(M)} & \frac{M_{12}M_{13}+M_{11}M_{23}}{\mathrm{Det}(M)}\end{pmatrix};\ O=\frac{2bj}{\mathrm{Det}(M)}\begin{pmatrix}M_{22}\\ -M_{12}\end{pmatrix}$$

The conditional probability $\mathcal{P}(x,x';v;\tau)$ of final position x' – given that we know the initial position x and velocity v – is given by using the classical action S_c given in Appendix C and yields

$$\mathcal{P}(x,x';v;\tau)\ =\int dv'\mathcal{P}(x,x';v,v';\tau)=\sqrt{\tfrac{1}{2\pi\nu^2}}e^{-\frac{1}{2\nu^2}(x'-\zeta x-\xi v-J)^2} \tag{§ 5.5.4}$$

For further simplifications, we define

$$a(\alpha^2-\beta^2)=b,\quad a(\alpha^2+\beta^2)^2=c \tag{§ 5.5.5}$$

The solution for the classical action S_c given in Appendix C yields the following

$$\begin{aligned}\nu^2 &= \frac{M_{22}}{\mathrm{Det}(M)}=\frac{2\Omega\alpha\beta[\beta\sinh(2\alpha\tau)-\alpha\sin(2\beta\tau)]}{a\left(\alpha^2+\beta^2\right)}\\ \zeta &= Q(1,1)=4\Omega\alpha\beta[\left(\alpha^2-\beta^2\right)\sinh(\alpha\tau)\sin(\beta\tau)+2\alpha\beta\cosh(\alpha\tau)\cos(\beta\tau)]\\ \xi &= Q(1,2)=-4\Omega\alpha\beta[\beta\sinh(\alpha\tau)\cos(\beta\tau)+\alpha\cosh(\alpha\tau)\sin(\beta\tau)]\end{aligned} \tag{§ 5.5.6}$$

where

$$\Omega=\frac{1}{\left(\alpha^2+\beta^2\right)^2-\alpha^2\left(\alpha^2-3\beta^2\right)\cos(2\beta\tau)-\beta^2\left(\beta^2-3\alpha^2\right)\cosh(2\alpha\tau)}$$

The following are the limiting cases for the results obtained above

$$\lim_{\tau\to0}\nu^2(\tau)=\frac{\tau^3}{3a}+O\left(\tau^4\right);\ \lim_{\tau\to\infty}\nu^2(\tau)=\frac{2\alpha}{a\left(3\alpha^2-\beta^2\right)\left(\alpha^2+\beta^2\right)} \tag{§ 5.5.7}$$

$$\lim_{\tau\to0}\zeta(\tau)=1+O\left(\tau^4\right);\quad \lim_{\tau\to\infty}\zeta(\tau)=0 \tag{§ 5.5.8}$$

$$\lim_{\tau\to0}\xi(\tau)=-\tau+O\left(\tau^4\right);\quad \lim_{\tau\to\infty}\xi(\tau)=0 \tag{§ 5.5.9}$$

In [56], the model was calibrated the model by postulating that ν^2 is the equal to the

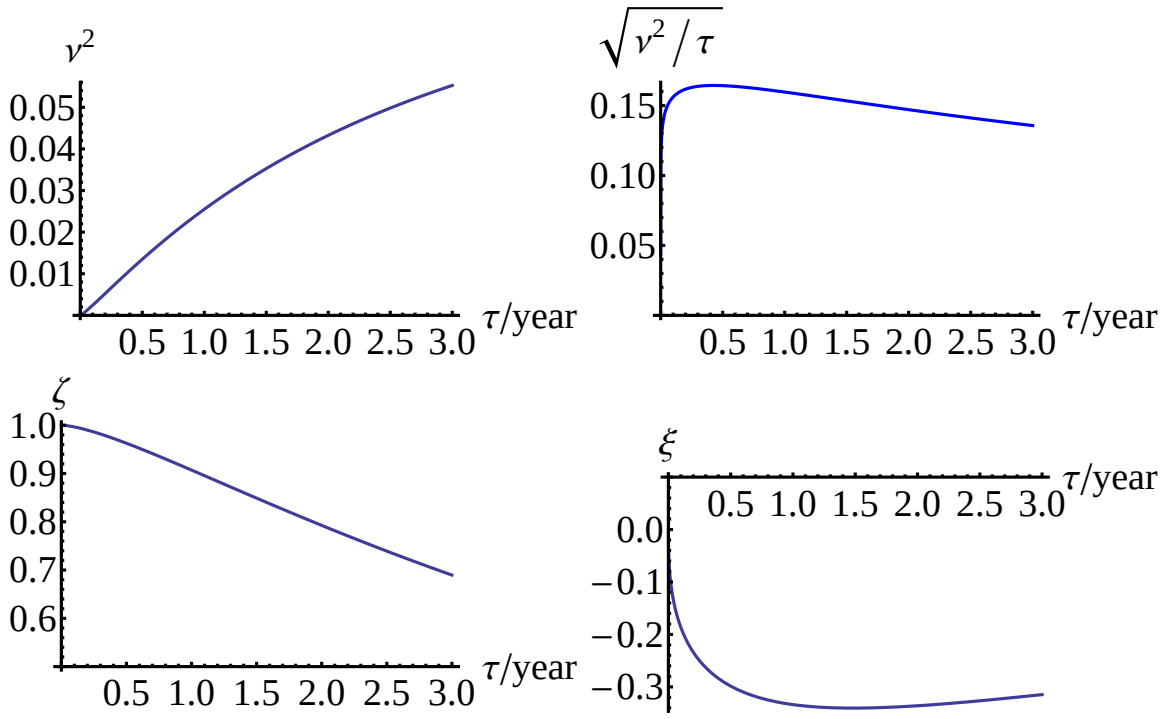

Figure 5.6: Function of the parameters $\nu^2,\ \sigma,\ \zeta,\ \xi$ on $a = 1, \alpha = 1.8566, \beta = 0.9853, \lambda = 0.3, \eta = 0.3941$.

implied market volatility for the strike price being ATM and yields

$$\nu^2(\tau) = (T - t_0)\sigma_I^2(S(t_0), T - t_0) \qquad (\S\, 5.5.10)$$

We do not follow the procedure adopted in [56], but instead, calibrate the model by matching the market option price with the model's price.

A typical set of fitting parameters are used to show the shapes of $\nu^2,\ \sigma,\ \zeta,\ \xi$ in Figure 5.6 for maturity from 0 to 3 years.

§ 5.5.1 Martingale condition

The value of J given in Eq. § 5.5.4 is fixed by the martingale condition. The conditional probability yields the following martingale condition

$$\begin{aligned} e^x &= e^{-r\tau}\int_{-\infty}^{+\infty} dx'\mathcal{P}(x,x';v;\tau)e^{x'} \\ &= \exp(-r\tau+\frac{\nu^2}{2}+\zeta x+\xi v+J). \end{aligned} \tag{§ 5.5.11}$$

J is fixed by the following equation

$$J = r\tau - \frac{\nu^2}{2}. \tag{§ 5.5.12}$$

The martingale condition for the acceleration model requires

$$\zeta_1 = 1; \quad \xi_1 = 0; \tag{§ 5.5.13}$$

As shown in Figure 5.6, the martingale is violated. From the limit of the parameters, we can see that ζ is limit to 1 which satisfy the martingale condition. And the ξ is negatively proportional to time τ which is related to the velocity. With all these parameters in conditional probability and the formula in Eq. § 5.3.4, the call option price strike K is

$$\begin{aligned} C(x,v;\tau) &= e^{-r\tau}\int_{-\infty}^{+\infty} dx'\mathcal{P}(x,x';v;\tau)\left[e^{x'}-K\right]_+ \\ &= e^{\zeta x+\xi v}N(d_+) - e^{-r\tau}KN(d_-) \\ \text{where } d_\pm &= \frac{\zeta x+\xi v-\ln(K)+r\tau\pm\frac{\nu^2}{2}}{\nu}. \end{aligned}$$

For stocks paying a annual continuous dividend q, the option price is

$$\begin{aligned} C(x,v;\tau) &= e^{-q\tau}e^{\zeta x+\xi v}N(d_+) - e^{-r\tau}KN(d_-) \\ \text{where } d_\pm &= \frac{\zeta x+\xi v-\ln(K)+(r-q)\tau\pm\frac{\nu^2}{2}}{\nu}. \end{aligned}$$

§ 5.5.2 FX Options

The most liquid European option is in foreign exchange market. FX call option is the right to buy foreign currency for a strike price in the domestic currency which we will take to be

the US dollar [58]. We use foreign exchange rate to examine our model. The exchange of the two currencies is shown in Figure 5.7. r_d is the domestic interest rate and r_f is the foreign interest rate.

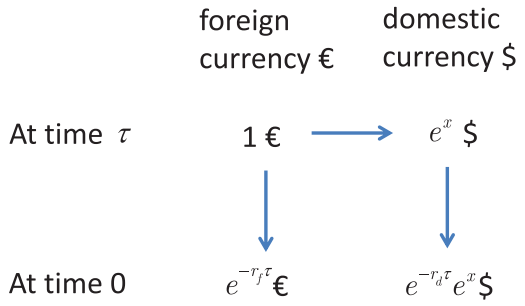

Figure 5.7: The exchange of two currencies .

The martingale condition for exchange rate $S = e^x$ yields from Figure 5.7, the following

$$e^x = e^{-(r_d - r_f)\tau} \int_{-\infty}^{+\infty} dx' \mathcal{P}(x, x'; v; \tau) e^{x'}, \tag{§ 5.5.14}$$

and the drift is given by

$$J = (r_d - r_f)\tau - \frac{\nu^2}{2} \tag{§ 5.5.15}$$

The FX call option price $C(K, \tau)$ is given by

$$\begin{aligned} C(x, v; \tau) &= e^{-r_d\tau} \int_{-\infty}^{+\infty} dx' \mathcal{P}(x, x'; v; \tau) \left[e^{x'} - K\right]_+ \\ &= e^{-r_f\tau} e^{\zeta x + \xi v} N(d_+) - e^{-r_d\tau} K N(d_-) \\ \text{where } d_\pm &= \frac{\zeta x + \xi v - \ln(K) + (r_d - r_f)\tau \pm \frac{\nu^2}{2}}{\nu}. \end{aligned}$$

The put option is

$$\begin{aligned} P(x, v; \tau) &= e^{-r_d\tau} \int_{-\infty}^{+\infty} dx' \mathcal{P}(x, x'; v; \tau) \left[K - e^{x'}\right]_+ \\ &= e^{-r_d\tau} \int_{-\infty}^{+\infty} dx' \mathcal{P}(x, x'; v; \tau) \left([e^{x'} - K]_+ + K - e^{x'}\right) \\ &= C(x, v; \tau) + e^{-r_d\tau} K - e^{-r_f\tau} e^x \end{aligned} \tag{§ 5.5.16}$$

The Put-Call parity is given by

$$C(x, v; \tau) - P(x, v; \tau) = e^{-r_f\tau} e^x - e^{-r_d\tau} K \tag{§ 5.5.17}$$

§ 5.6 Model's Calibration

The calibration for the market price C_M is done using formula

$$C_M = C_{BS}(S, K, r, \sigma_I(K, T, t_0), T - t_0) = C(x, v, K, r, \vec{a}, \tau) \qquad (\S\, 5.6.1)$$

The data we used is EURUSD exchange rate from 20131014 to 20140124. First we perform the vanilla calibration to fit the market price. To start the calibration, we need ATM implied volatility for all maturities (1m, 2m, 3m 6m, 1y, 18m, 2y and 3y) to get the price of ATM option.

The procedure is following:

- Get the implied volatility surface data from Bloomberg;
- Convert the implied volatility to prices for (K, τ) surface in Appendix B;
- The model is compared with ATM option price as well as with the prices for all K, τ, that is, with the surface prices;
- Fix the parameters matching the market prices for 20 days with the model's price;

R-square and RMS error are chosen to measure the goodness of fit. For each calendar date t, there is a fit of option price C_{data}, so the R-square R^2 is defined as

$$R^2 = 1 - \frac{\sum_n [C_M(n) - C_{\text{fit}}(n)]^2}{\sum_n [C_M(n) - \bar{C}_M(n)]^2} \qquad (\S\, 5.6.2)$$

where and $\bar{C}_{\text{data}}(n)$ is the mean of $C_{\text{data}}(n)$. Higher R^2 means better fit, and the exact fit has an R^2 value equal to 1.

RMS error is defined as

$$\text{RMS error} = \sqrt{\frac{1}{N}\sum_{n=1}^{N}\left[\frac{C_M(n) - C_{\text{fit}}(n)}{C_M(n)}\right]^2}. \qquad (\S\, 5.6.3)$$

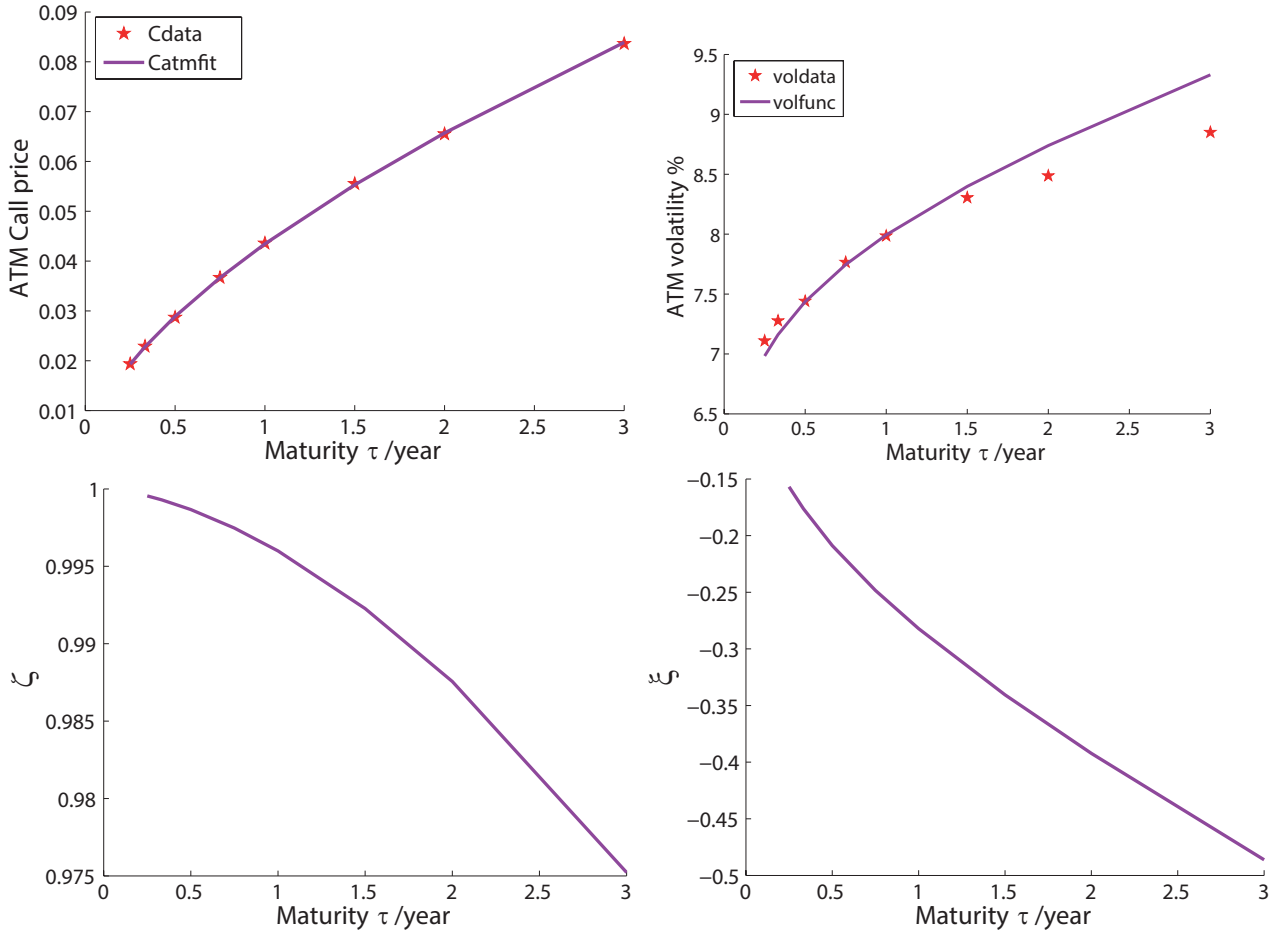

Figure 5.8: ATM fit

§ 5.6.1 Calibration using ATM option price

Figure 5.8 shows the typical fits with at the money strikes, the acceleration formula is exactly fitted with $R^2 = 1$ and RMS error $= 0.3\%$.

The fitting parameters on 2013-11-27 are listed in Table 5.1. $a = 1$ is positives that the Lagrangian converge. $\lambda = 0.11$ *year*, and for day unit fit $\lambda = 0.0032$ *day*. When maturity is longer than λ, the market time becomes shorter, while maturity is shorter than λ, the time becomes longer. η is around $\frac{1}{3}$; hence, for $T - t_0 \to 0$, we have from Eq. § 5.8.1, that

$$\nu^2 \sim \nu_0^2 (T - t_0)^{3\eta} = \sigma^2 (T - t_0).$$

We can fit the option price for whole surface using the parameters for the ATM fitting and obtain a error of $R^2 = 0.9993$ which is just slightly worse than fit for the whole surface and

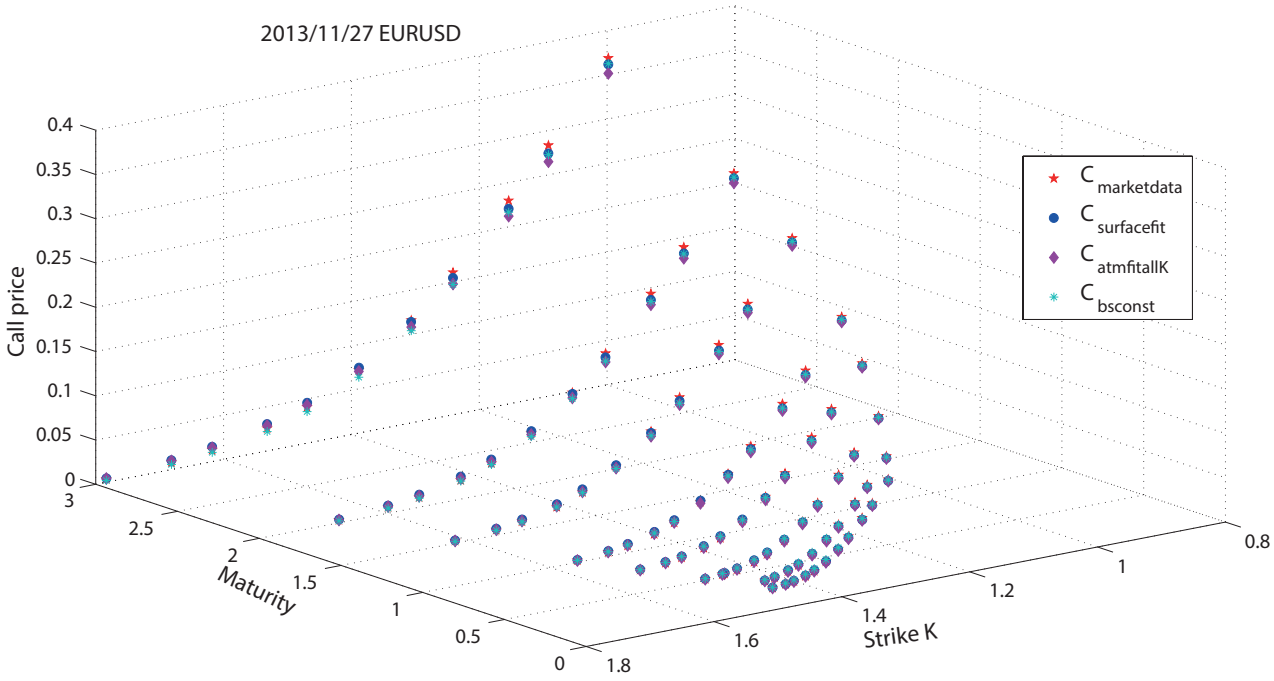

Figure 5.9: ATM fit applying to all K and τ, a direct fit for prices on the K, τ surface and Black-Scholes formula with constant volatility comparing the market price.

method	index	a	α	β	η	λ	R^2	RMS error
ATMfit	EURUSD	1.00	0.55	1.49	0.38	0.11	0.9993	6.5%
Surface	EURUSD	1.00	0.21	0.01	0.39	0.12	0.9995	13.4%

Table 5.1: ATM fit and surface fit parameters

shown in Figure 5.9. The parameters are given in Table 5.1. The Black-Scholes formula with constant volatility has the $R^2 = 0.9989$, but has higher RMS error = 17.9%.

§ 5.6.2 Market parameters

Base on the result of Ref. [56], we set $a = 1$. The fitting of parameters α, β, and η, λ are shown in Figure 5.10, which shows the ATM fitting parameters as a function of calender time.

Figure 5.11 shows the error for calender option price fit. The R-square is always greater than 0.999, which means when we can always fit ATM option exactly.

When we fix all the parameters, the error increases. The fit is still good but when we apply the fit to the surface (K, τ) the error increase faster and R-square is less than 0.995. We can fix the parameters for at most 10 days and the RMS error increases up to 10% in Figure 5.12.

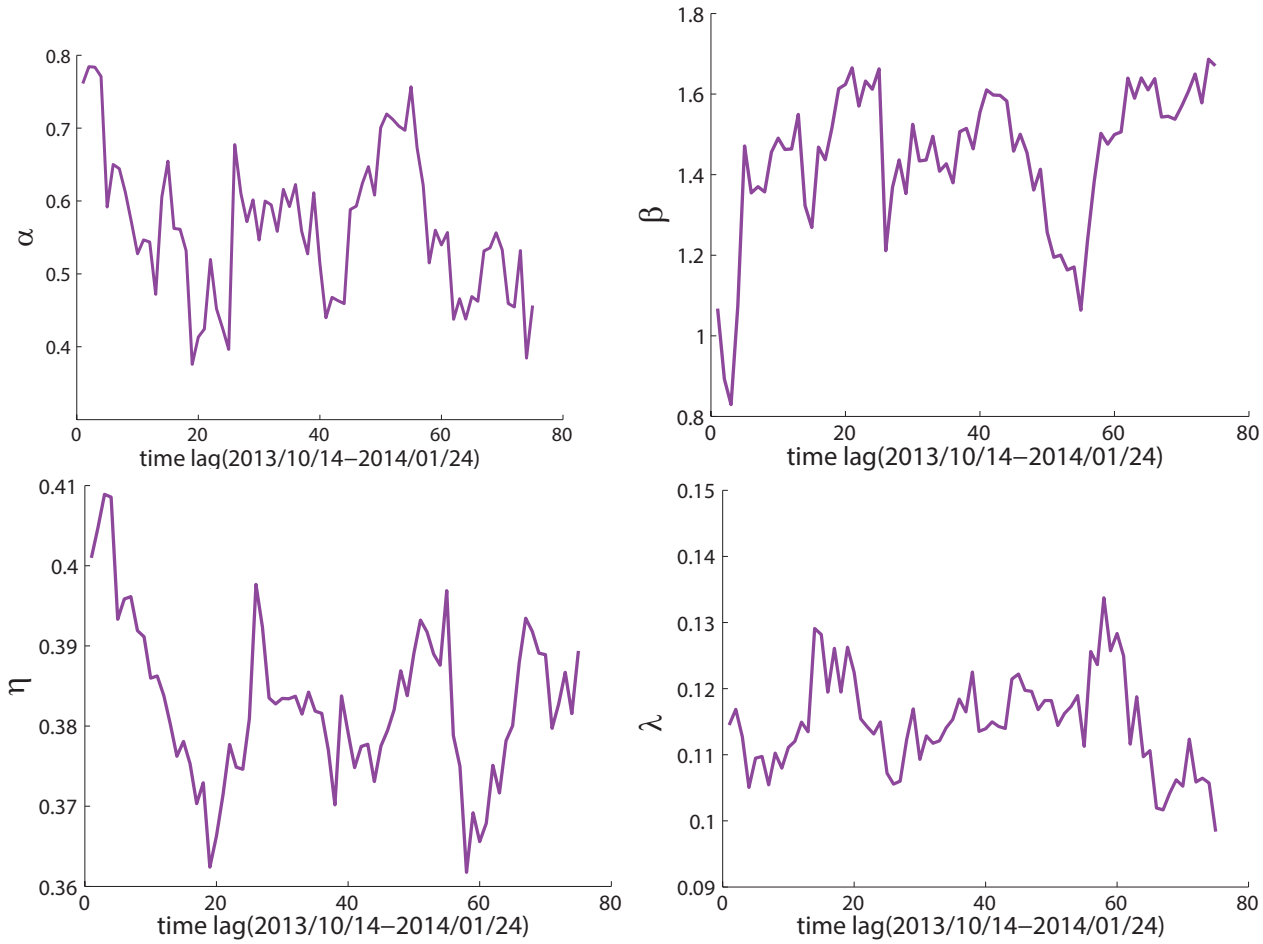

Figure 5.10: parameters

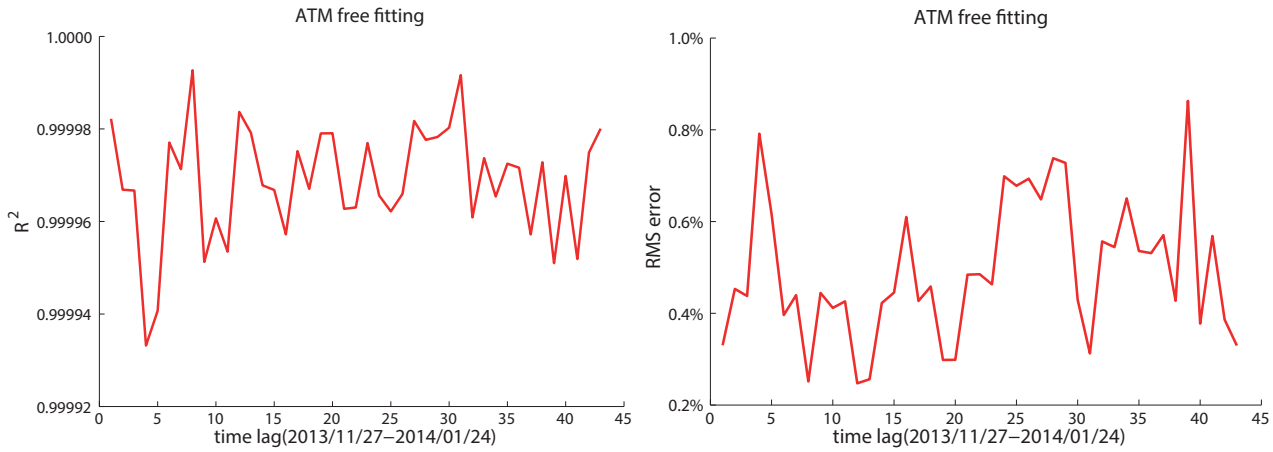

Figure 5.11: Rsq and RMS error for free fitting from 20131127-20140124

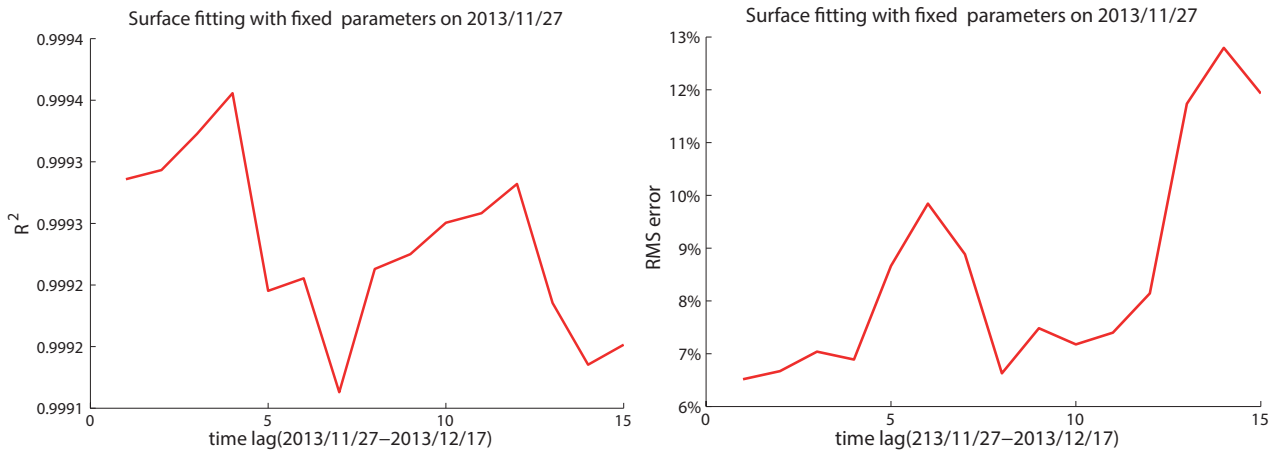

Figure 5.12: Rsq and RMS error for fix fitting from 20131127-20141217

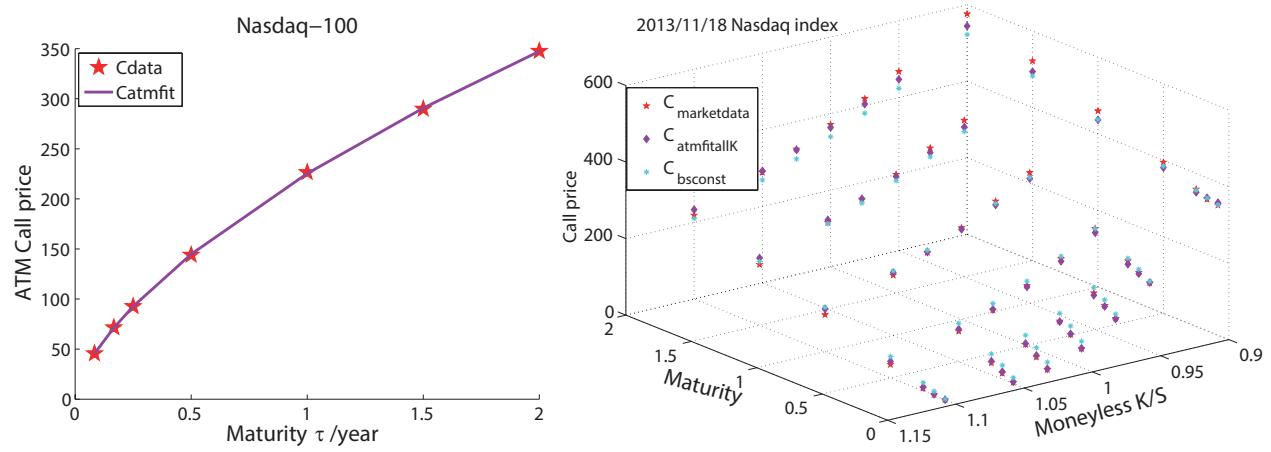

Figure 5.13: NASDAQ index fit on 20131118

§ 5.6.3 Equity fit

The model's price is applied to the Index of Nasdaq-100, which has higher volatility than FX options. In Figure 5.13, we have a good fit for both ATM fit, with $R^2 = 1$, and for the whole surface with $R^2 = 0.998$.

The typical values of the parameters for equity is given in Table 5.2. $\eta = 0.43$, $\lambda = 0.25$ *year* which are both higher than EURUSD with $\eta = 0.38$, $\lambda = 0.11$ *year*.

Unit	index	a	α	β	η	λ	R^2	RMSE
Year	NASDAQ	1.00	0.33	0.24	0.43	0.25 year	0.998	4.8%

Table 5.2: Fitting parameters of Nasdaq on 2013-11-18

§ 5.7 Conclusion

An option pricing formula has been developed that is based on the value of both the current price and velocity of the underlying security. Using an acceleration Lagrangian model based on the formalism of quantum finance, we derived the pricing formula for European call options. It was demonstrated that the implied volatility of the market can be generated by our pricing formula. The quantum finance option price was applied to both options on EURUSD foreign exchange rates and on an equity index; the accuracy of the model was seen to be better than the Black-Scholes pricing formula in matching the option's market price.

The general conclusion that one can draw from the analysis is that the Black-Scholes pricing formula has a short fall of information and implied volatility is introduced to offset this lacking. The acceleration model shows that incorporating the velocity of the security into the option price seems to compensate for the shortfall of information in the Black-Scholes pricing formula. The option price based on the value of the security and its velocity provides a mathematical framework for designing and pricing a whole new set of derivative instruments.

§ 5.8 Appendix A. Limits of the parameters

The infinite and zero limits of ν^2, ζ, ξ is the following

$$\lim_{\tau\to 0}\nu^2(\tau) = \frac{\tau^3}{3a} + O\left(\tau^4\right); \quad \lim_{\tau\to\infty}\nu^2(\tau) = \frac{2\alpha}{a\left(3\alpha^2-\beta^2\right)\left(\alpha^2+\beta^2\right)} \tag{§ 5.8.1}$$

$$\lim_{\tau\to 0}\zeta(\tau) = 1 + O\left(\tau^4\right); \quad \lim_{\tau\to\infty}\zeta(\tau) = 0 \tag{§ 5.8.2}$$

$$\lim_{\tau\to 0}\xi(\tau) = -\tau + O\left(\tau^4\right); \quad \lim_{\tau\to\infty}\xi(\tau) = 0 \tag{§ 5.8.3}$$

§ 5.9 Appendix B. FX market data

The moneyness m can be K, where K/S for equities and Δ for foreign exchange rates. Examples of implied volatility surface depending on moneyless m and maturity τ are as following for Nasdaq-100 in Table 5.3 and EURUSD in Table 5.4.

In the FX market implied volatilities are quoted in terms of delta, is given in Table 5.4. There are various definitions of delta. Hence, for the correct interpretation of the implied

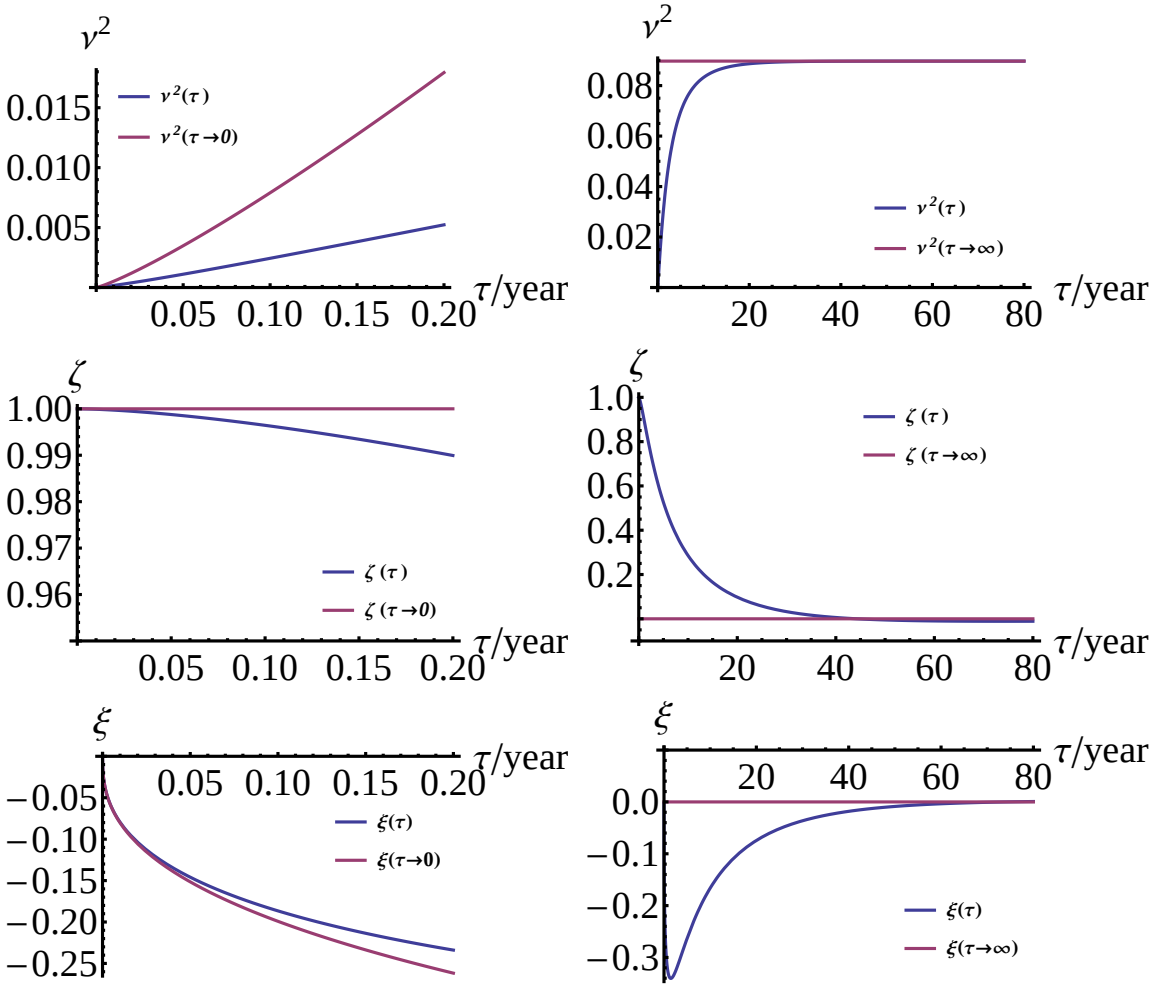

Figure 5.14: Zero and infinite τ limit of ν^2, ζ, ξ.

EXP	110%	105%	100%	95%	90%
1M	11.8027	11.5017	12.3024	15.6692	17.9884
2M	12.0794	11.9868	13.1772	15.4159	17.9348
3M	12.6619	12.8471	13.971	15.8271	18.2936
6M	13.5692	14.3777	15.5395	16.9749	18.6282
1Y	14.9828	15.7775	16.7385	17.8307	19.0408
18M	16.3875	17.1147	17.9268	18.8168	19.7856
2Y	17.2921	17.9285	18.631	19.4037	20.2431

Table 5.3: One day volatility surface data of NASDAQ-100 in terms of S/K

Exp	10D P	25D P	ATM	25D C	10D C
1M	8.844	8.008	7.308	7.123	7.271
2M	9.493	8.466	7.638	7.364	7.458
3M	10.07	8.903	7.913	7.543	7.605
6M	10.759	9.436	8.335	7.914	7.921
1Y	11.216	9.789	8.62	8.156	8.194
18M	11.654	10.158	8.948	8.468	8.476
2Y	11.782	10.345	9.14	8.605	8.547

Table 5.4: One day volatility surface data of EURUSD in terms of Δ

volatility quotes, it is important to know what definition is being used. Let us start with stating the Black-Scholes formula for FX European vanilla call options, given by

$$C(S, K, r_d, r_f, \tau) = e^{-r_f \tau} S N(d_+) - e^{-r_d \tau} K N(d_-)$$
$$\text{where } d_\pm = \frac{\ln(S/K) + (r_d - r_f)\tau \pm \sigma^2 \tau/2}{\sigma\sqrt{\tau}}.$$

The Black-Scholes delta of the option is equal to

$$\Delta_C = \frac{\partial C}{\partial S} = e^{-r_f \tau} N(d_+)$$

$$N^{-1}(e^{r_f \tau} \Delta_C) = \frac{\ln(S/K) + (r_d - r_f)\tau \pm \sigma^2 \tau/2}{\sigma\sqrt{\tau}}.$$

and the strike price K is given by

$$K = S \exp\{-N^{-1}(e^{r_f \tau} \Delta_C)\sigma\sqrt{\tau} + (r_d - r_f)\tau + \sigma^2 \tau/2\}.$$

In all currency markets except the Eurodollar market, the premium in the foreign currency is included in the delta. The premium-included delta is calculated as follow

$$\Delta_C^p = \Delta_C - \frac{C}{S} = \frac{K}{S} e^{-r_d \tau} N(d_-)$$

The logic of this premium-included delta can be illustrated with an example. Consider a bank that sells a call option on a foreign currency. This option can be delta hedged with an amount of delta of the foreign currency. However, the bank will only have to buy an amount equal to the premium-included delta when it receives the premium in the foreign currency. It can be observed from the above formula that the premium-included delta for a call is not strictly decreasing in strike like the Black-Scholes call delta. Therefore, a premium-included call delta

Market	ATM Delta	ATM Strike
$EUR/USD maturities < 2y$	$\Delta_C = e^{-r_f\tau}/2$	$S_0 e^{(r_d-r_f)\tau+\sigma^2_{ATM}\tau/2}$
$EUR/USD maturities \geq 2y$	$\Delta^F_C = 1/2$	$S_0 e^{(r_d-r_f)\tau+\sigma^2_{ATM}\tau/2}$
$maturities < 2y$	$\Delta^p_C = e^{-r_f\tau-\sigma^2_{ATM}\tau/2}/2$	$S_0 e^{(r_d-r_f)\tau-\sigma^2_{ATM}\tau/2}$
$maturities \geq 2y$	$\Delta^{Fp}_C = e^{-\sigma^2_{ATM}\tau/2}/2$	$S_0 e^{(r_d-r_f)\tau-\sigma^2_{ATM}\tau/2}$

Table 5.5: ATM convention formula for different FX

Exp		10D P	25D P	ATM	25D C	10D C
1M	Vol	8.844	8.008	7.308	7.123	7.271
	Strike	1.2778	1.3168	1.3534	1.3869	1.4193
2M	Vol	9.493	8.466	7.638	7.364	7.458
	Strike	1.2609	1.3094	1.3539	1.3941	1.4324
3M	Vol	10.07	8.903	7.913	7.543	7.605
	Strike	1.2378	1.2991	1.3549	1.4043	1.4515
6M	Vol	10.759	9.436	8.335	7.914	7.921
	Strike	1.2061	1.2849	1.3566	1.4204	1.4809
1Y	Vol	11.216	9.789	8.62	8.156	8.194
	Strike	1.1791	1.2728	1.3586	1.4352	1.5091
18M	Vol	11.654	10.158	8.948	8.468	8.476
	Strike	1.1395	1.2552	1.363	1.4611	1.5565
2Y	Vol	11.782	10.345	9.14	8.605	8.547
	Strike	1.1107	1.2423	1.3681	1.484	1.5962

Table 5.6: FX market convention form delta to strike

can correspond to two possible strike prices in Table 5.5. For emerging markets (EM) and for maturities of more than two years, it is usual for forward deltas to be quoted. These are defined as follows

$$\Delta^F_C = e^{r_f\tau}\Delta_C = N(d_+) \quad \text{and} \quad \Delta^{Fp}_C = \frac{K}{S}e^{(r_f-r_d)\tau}N(d_-)$$

The ATM strike refers to the strike of a zero delta straddle, i.e. the strike for which the call delta is equal to the put delta.This strike can be calculated analytically. The table below shows the ATM delta and the ATM strike for each market.

The FX volatility data converted to option strike price is in Table 5.6.

§ 5.10 Appendix C. Solution of Hamiltonian

The canonical Euclidean Hamiltonian for acceleration Langrangian is given by in Ref [59] as the following

$$\mathcal{H} = -\frac{1}{2\gamma}\frac{\partial^2}{\partial v^2} - v\frac{\partial}{\partial x} + \frac{\gamma}{2}(\omega_1^2+\omega_2^2)v^2 + \frac{\gamma}{2}(\omega_1^2\omega_2^2)x^2 \qquad (\S\,5.10.1)$$

The transformation is obtained to get a system of two decoupled harmonic oscillators H_0 using the operator $\mathcal{Q}$ in [59]

$$e^{-Q/2}He^{Q/2} = H_0; \quad \mathcal{Q} = axv - b\frac{\partial^2}{\partial x \partial v} \qquad (\S\,5.10.2)$$

where

$$\mathcal{H}_0 = -\frac{1}{2\gamma}\frac{\partial^2}{\partial v^2} - \frac{1}{2\gamma\omega_1^2}\frac{\partial^2}{\partial x^2} + \frac{\gamma}{2}\omega_1^2 v^2 + \frac{\gamma}{2}(\omega_1^2\omega_2^2)x^2 \qquad (\S\,5.10.3)$$

and the two decoupled harmonic oscillators, each for x, and v

$$\mathcal{H}_x = -\frac{1}{2\gamma\omega_1^2}\frac{\partial^2}{\partial x^2} + \frac{\gamma}{2}(\omega_1^2\omega_2^2)x^2; \quad \mathcal{H}_v = -\frac{1}{2\gamma}\frac{\partial^2}{\partial v^2} + \frac{\gamma}{2}\omega_1^2 v^2 \qquad (\S\,5.10.4)$$

The transition amplitude is given by the matrix elements of $\exp -\tau H$, namely

$$\mathcal{K} = < x_f, v_f|e^{-\tau H}|x_i, v_i > = < x_f, v_f|e^{-Q/2}e^{-\tau H_0}e^{Q/2}|x_i, v_i > \qquad (\S\,5.10.5)$$

To get $\mathcal{K}$ we have many ways, one of them is to integrating these three operators

$$\mathcal{K} = \int d\xi d\xi' d\eta d\eta' < x_f, v_f|e^{-Q/2}|\xi', \eta' >< \xi', \eta'|e^{-\tau H_0}|\xi, \eta >< \xi, \eta|e^{Q/2}|x_i, v_i > \qquad (\S\,5.10.6)$$

The results of the $\mathcal{Q}$ operator are given in the book by Baaquie Ref []that

$$\begin{aligned} < x_f, v_f|e^{-Q/2}|\xi', \eta' > &= N(\tfrac{1}{2})\exp(-\gamma\omega_1^2(x_f v_f + \xi'\eta') + \gamma\omega_1\sqrt{\omega_1^2-\omega_2^2}(x_f\eta' + \xi' v_f)) \\ < \xi, \eta|e^{Q/2}|x_i, v_i > &= N(\tfrac{1}{2})\exp(\gamma\omega_1^2(x_i v_i + \xi\eta) - \gamma\omega_1\sqrt{\omega_1^2-\omega_2^2}(x_i\eta + \xi v_i)) \end{aligned} \qquad (\S\,5.10.7)$$

And we can easily get the results of harmonic oscillators

$$< \xi', \eta'|e^{-\tau H_0}|\xi, \eta > = < \xi'|e^{-\tau H_x}|\xi >< \eta'|e^{-\tau H_v}|\eta > \qquad (\S\,5.10.8)$$

where

$$< \xi' | e^{-\tau H_x} | \xi >= \sqrt{\frac{\omega_2}{2\pi\gamma\omega_1^2 \sinh(\omega_2\tau)}} \exp\{-\frac{\omega_2}{2\gamma\omega_1^2 \sinh(\omega_2\tau)}[(\xi'^2 + \xi^2)\cosh(\omega_2\tau) - 2\xi'\xi]\}$$
$$< \eta' | e^{-\tau H_v} | \eta >= \sqrt{\frac{\omega_1}{2\pi\gamma \sinh(\omega_1\tau)}} \exp\{-\frac{\omega_1}{2\gamma \sinh(\omega_1\tau)}[(\eta'^2 + \eta^2)\cosh(\omega_1\tau) - 2\eta'\eta]\} (\S\, 5.10.9)$$

Summaries all these integration we get

$$\mathcal{K} = N \int d\xi' d\eta' d\xi d\eta e^{-\gamma\omega_1^2(x_f v_f + \xi'\eta') + \gamma\omega_1\sqrt{\omega_1^2-\omega_2^2}(x_f\eta' + \xi' v_f)} e^{\gamma\omega_1^2(x_i v_i + \xi\eta) - \gamma\omega_1\sqrt{\omega_1^2-\omega_2^2}(x_i\eta + \xi v_i)}$$
$$e^{-\frac{\omega_2}{2\gamma\omega_1^2 \sinh(\omega_2\tau)}[(\xi'^2+\xi^2)\cosh(\omega_2\tau) - 2\xi'\xi]} e^{-\frac{\omega_1}{2\gamma \sinh(\omega_1\tau)}[(\eta'^2+\eta^2)\cosh(\omega_1\tau) - 2\eta'\eta]}$$
$$= N \exp\{-\gamma\omega_1^2(x_f v_f - x_i v_i) - \frac{1}{2}XMX' + JX\} \quad (\S\, 5.10.10)$$

where the symmetric matrix is

$$M = \begin{pmatrix} \frac{\omega_2\cosh(\omega_2\tau)}{\gamma\omega_1^2\sinh(\omega_2\tau)} & \gamma\omega_1^2 & -\frac{\omega_2}{\gamma\omega_1^2\sinh(\omega_2\tau)} & 0 \\ \gamma\omega_1^2 & \frac{\omega_1\cosh(\omega_1\tau)}{\gamma\sinh(\omega_1\tau)} & 0 & -\frac{\omega_1}{\gamma\sinh(\omega_1\tau)} \\ -\frac{\omega_2}{\gamma\omega_1^2\sinh(\omega_2\tau)} & 0 & \frac{\omega_2\cosh(\omega_2\tau)}{\gamma\omega_1^2\sinh(\omega_2\tau)} & -\gamma\omega_1^2 \\ 0 & -\frac{\omega_1}{\gamma\sinh(\omega_1\tau)} & -\gamma\omega_1^2 & \frac{\omega_1\cosh(\omega_1\tau)}{\gamma\sinh(\omega_1\tau)} \end{pmatrix} \quad (\S\, 5.10.11)$$

and

$$J = \gamma\omega_1\sqrt{\omega_1^2 - \omega_2^2}(v_f, x_f, -v_i, -x_i)'; \quad X = (\xi', \eta', \xi, \eta) \quad (\S\, 5.10.12)$$

So

$$\int DX \exp(-\frac{1}{2}XMX' + JX) = \frac{4\pi^2}{\sqrt{Det[M]}} \exp(\frac{1}{2}JM^{-1}J) \quad (\S\, 5.10.13)$$

The final expression is

$$\mathcal{K} = \mathcal{N} \exp\{\frac{A}{2}(x_f^2 + x_i^2) + \frac{B}{2}(v_f^2 + v_i^2) + C(x_i v_f - x_f v_i) + D(x_i v_i - x_f v_f) + E x_i x_f + F v_i v_f\}$$

The coefficients are

$$
\begin{aligned}
A &= \Gamma\omega_2\left(\omega_2\sinh(\tau\omega_2)\cosh(\tau\omega_1)-\gamma^4\omega_1^5\sinh(\tau\omega_1)\cosh(\tau\omega_2)\right)\\
B &= \Gamma\omega_1^3\left(\omega_2\sinh(\tau\omega_1)\cosh(\tau\omega_2)-\gamma^4\omega_1^5\sinh(\tau\omega_2)\cosh(\tau\omega_1)\right)\\
C &= \Gamma\gamma^2\omega_1^4\omega_2\left(\cosh(\tau\omega_2)-\cosh(\tau\omega_1)\right)\\
D &= \frac{\Gamma}{\gamma^2(\omega_1^2-\omega_2^2)}[\omega_2^2\omega_1\left(\gamma^8\omega_1^8+1\right)\sinh(\tau\omega_1)\sinh(\tau\omega_2)\\
&\quad-\gamma^4\omega_1^4\omega_2\left(\omega_1^2+\omega_2^2\right)\left(\cosh(\tau\omega_1)\cosh(\tau\omega_2)-1\right)]\\
E &= \Gamma\omega_2\left(\gamma^4\omega_1^5\sinh(\tau\omega_1)-\omega_2\sinh(\tau\omega_2)\right)\\
F &= \Gamma\omega_1^3\left(\gamma^4\omega_1^5\sinh(\tau\omega_2)-\omega_2\sinh(\tau\omega_1)\right)
\end{aligned}
$$

$$
\mathcal{N} = \sqrt{\frac{(\omega_1^2-\omega_2^2)^2\gamma^4\omega_2\omega_1^3}{4\pi^2((\gamma^8\omega_1^{10}+\omega_2^2)\sinh(\tau\omega_1)\sinh(\tau\omega_2)-2\gamma^4\omega_2\omega_1^5(\cosh(\tau\omega_1)\cosh(\tau\omega_2)-1))}}
$$

where

$$
\Gamma = \frac{\gamma^3\omega_1(\omega_1^2-\omega_2^2)}{(\gamma^8\omega_1^{10}+\omega_2^2)\sinh(\tau\omega_1)\sinh(\tau\omega_2)-2\gamma^4\omega_2\omega_1^5(\cosh(\tau\omega_1)\cosh(\tau\omega_2)-1)}
$$

Chapter 6

Empirical Microeconomics Actions Functionals

A statistical generalization of microeconomics has been made in [60], where the market price of every traded commodity, at each instant of time, is considered to be an *independent random variable*. The dynamics of commodity market prices is modeled by an *action functional* – and the focus of this chapter is to empirically determine the action functionals for different commodities. The correlation functions of the model are defined using a Feynman path integral. The model is calibrated using the unequal time correlation of the market commodity prices and well as their cubic and quartic moments using a perturbation expansion. The consistency of the perturbation expansion is verified by a numerical evaluation of the path integral. Nine commodities drawn from the energy, metal and grain sectors are studied and their market behavior is described by the model to an accuracy of over 90% using only six parameters. The paper *empirically* establishes the existence of the action functional for commodity prices that was *postulated* to exist in [60].

§ 6.1 Introduction

Supply and demand are inseparable and the view taken in statistical microeconomics [60] is that supply and demand are two facets of a single entity, namely the microeconomics *potential function* $\mathcal{V}[\mathbf{p}]$. The potential is chosen to be the sum of supply and demand, namely [60]

$$\mathcal{V}[\mathbf{p}] = \mathcal{D}[\mathbf{p}] + \mathcal{S}[\mathbf{p}] \tag{§ 6.1.1}$$

The potential function $\mathcal{V}[\mathbf{p}]$, similar to mechanics, drives the evolution of market prices. For the special case when the prices are constant (time independent) – given by the constant prices $\mathbf{p}_0 = (p_{01}, p_{02}, .., p_{0N})$ – the prices *minimize the value* of the potential; namely that $\mathcal{V}[\mathbf{p}_0]$ is a minimum of $\mathcal{V}[\mathbf{p}]$.

The break up of the microeconomics potential into a supply and demand piece need not hold in general for all values of the price since the break up is essentially an *asymptotic property* of the microeconomics potential. One expects from the behavior of consumers and producers that the demand for a commodity increases with decreasing price and concomitantly, the production of a commodity increases with increasing price. Hence, the most general microeconomics potential is stipulated to have the following two limiting cases

$$\mathcal{V}[\mathbf{p}] \simeq \begin{cases} \mathcal{D}[\mathbf{p}] & : \quad p_i \to 0 \\ \mathcal{S}[\mathbf{p}] & : \quad p_i \to \infty \end{cases} \qquad (\S\, 6.1.2)$$

In the framework of statistical microeconomics, stationary prices are determined by the minimum value of the microeconomics potential, which replaces the standard microeconomics procedure of setting supply equal to demand.

The dynamics of market prices is determined by assigning a **joint probability distribution** for all possible evolutions of the stochastic market prices. The probability of the stochastic evolution of market prices is *postulated* to be proportional to the Boltzmann distribution, namely

$$\text{Joint probability distribution} \quad \propto \quad \exp\{-\mathcal{A}[\mathbf{p}]\} \qquad (\S\, 6.1.3)$$

where the action functional $\mathcal{A}[\mathbf{p}]$ determines the likelihood of the evolution of all the different values taken by all the prices.

In analogy with mechanics, the action functional is taken to be the sum of the potential term $\mathcal{V}[p]$ with a *kinetic term* $\mathcal{T}$, namely

$$\mathcal{A}[\mathbf{p}] = \int_{-\infty}^{+\infty} dt \mathcal{L}(t) = \int_{-\infty}^{+\infty} dt \Big(\mathcal{T}[\mathbf{p}(t)] + \mathcal{V}[\mathbf{p}(t)] \Big) \qquad (\S\, 6.1.4)$$

The action functional $\mathcal{A}[\mathbf{p}]$ depends on the *function* $\mathbf{p}(t),\ t \in [-\infty, +\infty]$: each possible function $p(t)$ gives one numerical value for $\mathcal{A}[\mathbf{p}]$. For this reason $\mathcal{A}[\mathbf{p}]$ is called a functional of the price function and is called the action functional, or action in brief.

The Lagrangian given by

$$\mathcal{L}(t) = \mathcal{T}[\mathbf{p}(t)] + \mathcal{V}[\mathbf{p}(t)] \qquad (\S\, 6.1.5)$$

The kinetic terms $\mathcal{T}[\mathbf{p}(t)]$ contains the time derivatives of the prices and together with the potential function, determines the time dependence of the stochastic prices; in particular, $\exp\{-\mathcal{A}[\mathbf{p}]\}$ determines the likelihood of the different random trajectories of the random prices.

§ 6.2 Model of the microeconomics potential

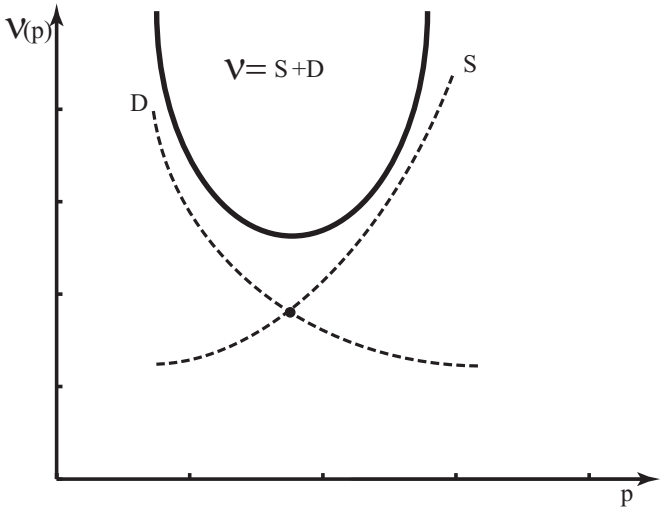

Figure 6.1: Potential $\mathcal{V}[\mathbf{p}]$ for the model.

The demand function is modeled to be [60]

$$\mathcal{D}[\mathbf{p}] = m \sum_{i=1}^{N} \frac{d_i}{p_i^{a_i}} \quad ; \quad a_i,\ d_i > 0 \qquad (\S\, 6.2.1)$$

and the supply function is modeled to be [60]

$$\mathcal{S}[\mathbf{p}] = m \sum_{i=1}^{N} s_i p_i^{b_i} \quad ; \quad b_i, s_i > 0 \qquad (\S\, 6.2.2)$$

The coefficients d_i, s_i, according to [61], are determined by macroeconomic factors such as

interest rates, unemployment, inflation and so on. In the statistical microeconomics model, the coefficients d_i, s_i are determined from the historical prices of a commodity. It is our view that all the macroeconomic information that affects a commodity is contained in its price. Hence it is a consistency check to see if the values of d_i, s_i given by a macroeconomic analysis of a commodity agree with the result obtained by studying solely the price of a commodity.

The sum of the demand and supply function yields the microeconomics potential

$$\begin{aligned} \mathcal{V}[\mathbf{p}] &= \mathcal{D}[\mathbf{p}] + \mathcal{S}[\mathbf{p}] \\ &= m\left[\sum_{i=1}^{N} \frac{d_i}{p_i^{a_i}} + \sum_{i=1}^{N} s_i p_i^{b_i}\right] \;\; ; \;\; d_i, s_i > 0 \; ; \;\; a, b > 0 \end{aligned} \qquad (\S\, 6.2.3)$$

The model microeconomics potential has the following expected asymptotic behavior of exhibiting a supply and demand function as expected from Eq. § 6.1.2

$$\mathcal{V}[\mathbf{p}] \simeq \begin{cases} \mathcal{D}[\mathbf{p}] = \displaystyle\sum_{i=1}^{N} \frac{d_i}{p_i^{a_i}} \;\; ; \;\; p_i \to 0 \\ \mathcal{S}[\mathbf{p}] = \displaystyle\sum_{i=1}^{N} s_i p_i^{b_i} \;\; ; \;\; p_i \to \infty \end{cases}$$

.

Figure 6.1 shows the shape of $\mathcal{V}[\mathbf{p}]$ for the model given in Eq. § 6.2.3; note the important feature of $\mathcal{V}[\mathbf{p}]$ that it has a (unique) global minimum at $\mathbf{p}_0$. The value of $\mathbf{p}_0$ is obtained by *minimizing* $\mathcal{V}[\mathbf{p}]$ and, from Eqs. § 6.2.3, yields the following

$$\begin{aligned} &\frac{\partial \mathcal{V}[\mathbf{p}]}{\partial p_i}\Big|_{\mathbf{p}=\mathbf{p}_0} = 0 \quad \Rightarrow \quad -a_i \frac{d_i}{p_{0i}^{a_i+1}} + b_i s_i p_{0i}^{b_i-1} = 0 \\ &p_{0i} = \left(\frac{a_i d_i}{b_i s_i}\right)^{1/(a_i+b_i)} \equiv p_0 \exp\{\hat{x}_i\} \end{aligned} \qquad (\S\, 6.2.4)$$

In standard microeconomics theory, the market prices $\mathbf{p}^*$ are fixed by equating demand to supply, shown graphically in Figure 6.1; for the model being considered, this yields the following

$$\mathcal{D}[\mathbf{p}^*] = \mathcal{S}[\mathbf{p}^*] \quad \Rightarrow \quad \frac{d_i}{(p_i^*)^{a_i}} = s_i (p_i^*)^{b_i} \quad \Rightarrow \quad p_i^* = \left(\frac{d_i}{s_i}\right)^{1/(a_i+b_i)}$$

The market price of a commodity obtained from standard microeconomics theory (by

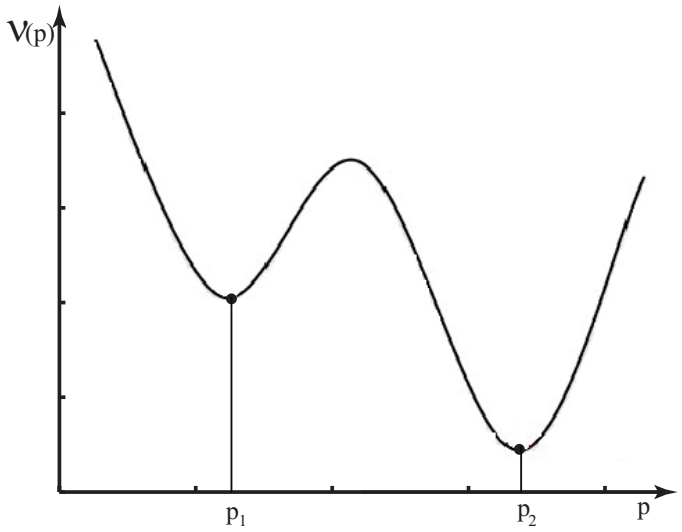

Figure 6.2: The shape of $\mathcal{V}[\mathbf{p}]$ with multiple minima. The market price is given by p_2.

equating supply to demand) gives a market price different from that obtained by minimizing the microeconomics potential. As one can see, except for the special case of $a_i = b_i$ – which is *not* the case for the result obtained from the empirical study of the commodities – the market price of the two approaches are quite different even for the same supply and demand functions.

The simple form of the microeconomics potential $\mathcal{V}[\mathbf{p}]$ given in Eq. § 6.2.3 allows one to write it as a sum of a demand and supply function for all values of the price. There can be complex cases of the microeconomics potential with multiple minima, as shown in Figure 6.2, where the concept of a demand and supply function are only asymptotic, according the general property of the microeconomics potential given in Eq. § 6.1.2; for this potential, the absolute minimum of the potential fixes the market price to be p_2, as shown in Figure 6.2 – a result that cannot be obtained using the concept of setting supply equal to demand. In summary the standard microeconomics theory of determining market prices by equating supply to demand is not valid in statistical microeconomics.

§ 6.3 Microeconomics Lagrangian and Action

The Lagrangian of a system determines the evolution of a dynamical system and for market prices represents all the factors determining its evolution. In particular, the interplay and competition of demand, supply with the 'kinetic energy' of market prices is encoded in the

Lagrangian.

The Lagrangian, from Eq. § 6.1.5, is given by the sum of the kinetic and potential factors and yields

$$\mathcal{L}(t) = \mathcal{T}[\mathbf{p}(t)] + \mathcal{V}[\mathbf{p}(t)]$$

The action functional determines the dynamics (time evolution) of market prices and, from Eq. § 6.1.4 is given by

$$\mathcal{A}[\mathbf{p}] = \int_{-\infty}^{+\infty} dt \mathcal{L}(t) = \int_{-\infty}^{+\infty} dt \Big(\mathcal{T}[\mathbf{p}(t)] + \mathcal{V}[\mathbf{p}(t)] \Big)$$

The model chosen for the potential and kinetic parts of the Lagrangian yields, from Eqs. § 6.2.3 and § 6.1.5 the following [60]

$$\mathcal{L}(t) = \frac{m}{2} \sum_{i,j=1}^{N} \left[L_{ij} \frac{\partial^2 x_i}{\partial t^2} \frac{\partial^2 x_j}{\partial t^2} + \tilde{L}_{ij} \frac{\partial x_i}{\partial t} \frac{\partial x_j}{\partial t} \right] + m \sum_{i=1}^{N} \frac{d_i}{p_i^{a_i}} + m \sum_{i=1}^{N} s_i p_i^{b_i} \qquad (\S\, 6.3.1)$$

The quantities $L_{ij}, \tilde{L}_{ij}, d_i, s_i, a_i, b_i$ are all real and independent parameters. Matrices L_{ij} is symmetric and positive definite.

The Lagrangian given in Eq. § 6.3.1 is nonlinear, since prices (and quantities) are always positive and hence represented by exponential variables as $p_i = p_{i0} e^{x_i}$.

For the case of a single commodity, let the price be $p = p_0 e^x$; the Lagrangian given in Eq. § 6.3.1 reduces to the following

$$\mathcal{L}(t) = \frac{1}{2} \left[L \left(\frac{\partial^2 x}{\partial t^2} \right)^2 + \tilde{L} \left(\frac{\partial x}{\partial t} \right)^2 \right] + \left[\frac{d}{p_0} e^{-ax} + s p_0 e^{bx} \right] \quad ; \quad p = p_0 e^x > 0 \qquad (\S\, 6.3.2)$$

§ 6.4 Market Prices

The market price of a commodity, at time t, is denoted by

$$p(t) = p_0 e^{x(t)}.$$

All commodity prices used here are the spot commodity prices from CBOT(Chicago Board of Trade).

The standard microeconomics theory [62] usually assumes that, at time t, there is one

unique market $p(t)$ for a given commodity. We take the view that there is no unique price for a given commodity. Instead, we assume that instead of having only one price at each instant, each price is assumed to simultaneously having an entire range of prices, from zero to infinity; in other words, the commodity price is undergoing a *continuous stochastic process*, with the price at any instant at a given location is inherently random [60].

The *general equilibrium theory* of microeconomics studies the interplay of supply in an economy with multiple markets, and shows that an equilibrium is reached such that all prices are in equilibrium and take their market value [62].

In statistical microeconomics, all the prices are fundamentally *dynamical* and changing, as expressed by the kinetic terms in the Lagrangian, namely

$$\mathcal{T}[x(t)] = \frac{1}{2}\left[L\left(\frac{\partial^2 x}{\partial t^2}\right)^2 + \tilde{L}\left(\frac{\partial x}{\partial t}\right)^2\right]$$

Hence, in contrast to the standard microeconomics theory, the dynamical nature of a stochastic price means that it is randomly changing and evolving in time. In particular, the prices are not the result of an equilibrium between supply and demand – as is expressed in the general equilibrium theory but, instead, market prices are determined by the form of the action functional $\mathcal{A}[x]$.

The fundamental assumption of statistical microeconomics is that the behavior of the price of a commodity is described by the microeconomic Lagrangian, a model of which is given in Eq.§ 6.3.2. The probability of the different prices being observed determined by a probability density functional that is, upto a proportionality constant Z, given by the action functional as follows

$$\text{Probability density functional} = \exp\{-\mathcal{A}[x]\}/Z.$$

Prices have a spatial variation since the price of a commodity varies for markets at different locations. The spatial variation in the price is not accounted for in the statistical microeconomics model [60] and the model needs to be generalized. One straight forward generalization is to consider prices to depend on both position and time; the positions on the globe can be specified by a two dimensional vector $\mathbf{r}$ and the price is then given by $p(t, \mathbf{r}) = p_0 \exp\{x(t, \mathbf{r})\}$. Assuming that prices are stochastic, the model Lagrangian then depends on $x(t, \mathbf{r})$ – which is mathematically described by a *three dimensional quantum field* ; this line of inquiry is left for the future.

Prices are taken to be inherently random and it is assumed that what one observes in the

market are *samples* of the prices considered as a random variable. The time series of prices is the result of sampling the random variations of the prices; the prices are taken to obey the ergodic process, namely that the ensemble average of a function of the prices is taken equal to the time average over the random outcomes of the prices.

Since prices follow a stochastic process, the appropriate description of prices is to determine the observed properties of the prices in terms of a statistical average over all possible values of the prices. The Feynman path integral is a mathematical formalism that provides an efficient procedure for evaluating these statistical averages. The mathematical aspects of the path integral are discussed in detail in [63].

§ 6.5 Microeconomics Feynman Path Integral

As discussed above in Section § 6.4, the observed market prices are taken to be a random sample of the random price. The appropriate description of prices considered as a stochastic process is to calculate its various expectation values. The correlation function is a measure of how the stochastic price varies over time. The correlation function of prices can be compared with the observed market value of these expectation values and hence provides a precise test of the accuracy of a model for the prices.

The correlation function of market prices is given by the expectation value of the product of prices, computed by summing over all possible histories of market prices using the path integral, and is given by the following

$$E[x(t_1)x(t_2)..x(t_N)] = \frac{1}{Z}\int Dx e^{-\mathcal{A}[x]}x(t_1)x(t_2)..x(t_N) \qquad (\S\, 6.5.1)$$

where

$$\mathcal{A}(x) = \int dt\mathcal{L}(t)dt;\ Z = \int Dx e^{-\mathcal{A}[x]}$$

The path integral consists of one integration – over all values of the price – for each instant of time; heuristically, this yields

$$\int Dx = \prod_{-\infty\leq t\leq+\infty}\int_{-\infty}^{+\infty} dx(t).$$

There are many techniques for giving a precise definition of $\int Dx$ [63].

One procedure is to discretize time into a lattice and consider only a finite number of lattice points; this truncation renders the path integral into an ordinary multiple dimensional integral – and is the basis of the numerical study of the path integral discussed in Section § 6.8. One has to take the limit of vanishing lattice spacing to obtain the path integral.

The path integral for commodity prices given in Eq. § 6.5.1 is nonlinear and nontrivial. The path integral can be studied perturbatively using Feynman diagrams and numerically using Monte Carlo and other well known methods. In many cases, the numerical approach is necessary for studying features that are inaccessible to a perturbation expansion.

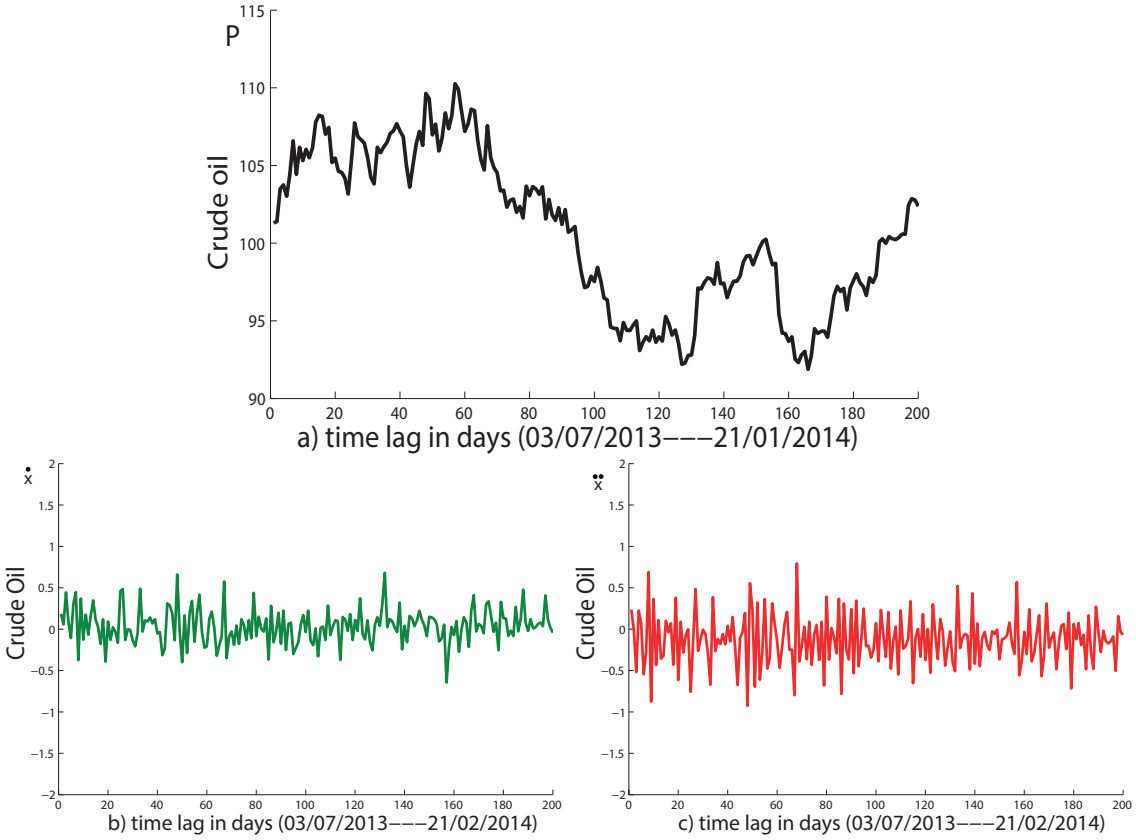

Figure 6.3: Example of commodity variables $p = e^x, \dot{x} = \frac{\partial x}{\partial t}$ and $\ddot{x} = \frac{\partial^2 x}{\partial t^2}$ of crude oil(Data source: http://www.investing.com/commodities/)

Figure 6.3 shows one sample value of the paths of the prices and the velocity and acceleration of these paths, namely $x, \partial x/\partial t$ and $\partial^2 x/\partial t^2$, over which the Feynman path integral is defined.

§ 6.5.1 Expansion of the microeconomics potential

Writing the potential in terms of variables defined in Eq. § 6.3.2 that are appropriate for studying the action functional near its maximum. The Lagrangian is given by

$$\mathcal{L}(x) = \mathcal{T}(x) + \mathcal{V}(x),$$

with

$$\mathcal{T}(x) = \frac{1}{2}L\ddot{x}^2 + \frac{1}{2}\widetilde{L}\dot{x}^2 \quad ; \quad \mathcal{V}(x) = de^{-ax} + se^{bx}$$

Note that the minimum of the potential Eq. § 6.2.3, which is given in Eq. § 6.2.4 and equal to $\hat{x}_i$, fixes the market price of all N commodities. Expanding the action functional about the minima of the potential $\hat{x}$ yields the following

$$\begin{aligned}\mathcal{A} &= \int_{-\infty}^{\infty} dt\mathcal{L}(x) = \int_{-\infty}^{\infty} dt[\frac{1}{2}L\ddot{x}^2 + \frac{1}{2}\widetilde{L}\dot{x}^2 + de^{-ax} + se^{bx}] \\ &= \int_{-\infty}^{\infty} dt[\frac{1}{2}L\ddot{x}^2 + \frac{1}{2}\widetilde{L}\dot{x}^2 + \mathcal{V}(\hat{x}) + \theta(x-\hat{x}) + \frac{\gamma}{2}(x-\hat{x})^2 + O(x-\hat{x})^3]\end{aligned}$$

where

$$\begin{aligned}\theta &= (-ade^{-a\hat{x}} + bse^{b\hat{x}}) = 0 \quad \Rightarrow \quad \exp\{\hat{x}\} = (\frac{ad}{bs})^{1/(a+b)} \\ \gamma &= (a^2de^{-a\hat{x}} + b^2se^{b\hat{x}}) = bs(b+a)e^{b\hat{x}}\end{aligned} \tag{§ 6.5.2}$$

§ 6.5.2 Gaussian propagator

The unequal time correlation function of the log of two prices, called the propagator in physics, is given by

$$G(t,t') = E[x_t x_{t'}] = \frac{1}{Z}\int Dx e^{-\mathcal{A}(x)} x_t x_{t'}$$

The Lagrangian has a form as $\mathcal{L}(x) = \frac{1}{2}\Big(L\ddot{x}^2 + \tilde{L}\dot{x}^2 + \gamma x^2\Big)$. We will show later that a more general quadractic term arises in Lagrangian due to nonlinearities and we hence parametrize the quadratic Lagrangian by the following

$$\mathcal{L}(x) = \frac{1}{2}\Big(L\ddot{x}^2 + \tilde{L}\dot{x}^2 + \Gamma x^2\Big)$$

The Lagrangian yields the following exact propagator [55]

$$\mathcal{A}[x] = \frac{1}{2}\int dt x(t)\frac{1}{2}[L\frac{\partial^4}{\partial t^4} - \tilde{L}\frac{\partial^2}{\partial t^2}]x(t') + \frac{\Gamma}{2}x^2(t) = \frac{1}{2}\int dt x(t)G^{-1}(t,t')x(t')$$

where

$$G^{-1}(t,t') = [L\frac{\partial^4}{\partial t^4} - \tilde{L}\frac{\partial^2}{\partial t^2} + \Gamma]\delta(t-t')$$

Using a Fourier transform to evaluate the propagator for the prices yields

$$G(t-t') \equiv \int_{-\infty}^{\infty}\frac{dk}{2\pi}\frac{e^{ik(t-t')}}{Lk^4 + \tilde{L}k^2 + \Gamma} = \frac{\frac{e^{-\sqrt{a^-}|t-t'|}}{\sqrt{a^-}} - \frac{e^{-\sqrt{a^+}|t-t'|}}{\sqrt{a^+}}}{2\Gamma(a^+ - a^-)};$$

$$\text{with } a^{\pm} = \frac{\tilde{L}}{2L}\left[1 \pm \sqrt{1 - 4\left(\frac{L\Gamma}{\tilde{L}^2}\right)}\right].$$

Case I: $4L\Gamma < \tilde{L}^2$; $a^{\pm}$ real, let $\omega = (\frac{\Gamma}{L})^{\frac{1}{4}}$, $a^{\pm} = \sqrt{\frac{\Gamma}{L}}e^{\pm 2\vartheta}$, $\cosh(2\vartheta) = \frac{\tilde{L}}{2\sqrt{L\Gamma}}$

$$G(t-t') = \frac{\omega e^{-\omega|t-t'|\cosh(\vartheta)}}{2\Gamma\sinh(2\vartheta)}\sinh[\vartheta + \omega|t-t'|\sinh(\vartheta)]$$

Case II: $4L\Gamma > \tilde{L}^2$; $a^{\pm}$ complex $a^{\pm} = \sqrt{\frac{\Gamma}{L}}e^{\pm i2\phi}$, $\cos(2\phi) = \frac{\tilde{L}}{2\sqrt{L\Gamma}}$

$$G(t-t') = \frac{\omega e^{-\omega|t-t'|\cos(\phi)}}{2\Gamma\sin(2\phi)}\sin[\phi + \omega|t-t'|\sin(\phi)]$$

In summary, the the complex branch yields the propagator

$$G(t-t') = Ne^{-\omega|t-t'|\cos(\phi)}\sin\{\phi + \omega|t-t'|\sin(\phi)\} \;\; ; \;\; N = \frac{\omega}{2\Gamma\sin\{2\phi\}} \qquad (\S\,6.5.3)$$

This behavior can only be modeled by the complex branch, hence our choice of domain and additional constraints as discussed above. In fact, in Chapter 4, we shall see that our model fits the market data excellently.

Note that the *market* correlation function additionally exhibits oscillations that do not vanish even for large $t-t'$, for which the model correlation function has decayed to zero. The value for $t-t'$ for which the model correlation function $G(t-t')$ is zero indicates the range of where our model is applicable, and which is a crucial component in fitting market data.

§ 6.6 Calibrating the propagator

The prices and volatility of different commodities vary over a wide range and the action should be written in terms of variables that factor out the scale of the prices and their volatilities. With this in mind we define a new set of variables $y(t)$ by the following change of variables from $x(t)$ to $y(t)$

$$y = \frac{x - \mu}{\sigma(x)} \qquad (\S\, 6.6.1)$$

where μ and $\sigma(x)$ are the mean and standard derivation of the log of prices $x(t)$, defined in Eq. § 6.12.1. For the scaled variable $y(t)$ that is of $O(1)$, an action functional can be written that has he same form for different commodities.

The parameters Γ, L and $\tilde{L}$ are fixed by empirically fitting the propagator $G(t - t')$.

We define the propagator as the connected auto-correlator defined by

$$G(t - t') = E[y(t)y(t')]_c \equiv E[y(t)y(t')] - E[y(t)]E[y(t')]$$

where the procedure for empirically obtaining the expectation value is discussed in Appendix § 6.12.

One needs to decide what is the minimum sample size N that accurately reflects the behavior of the time series. We found that for different groups of commodities, for example energy, metals and grains, there is a minimum sample size N. In Figure 6.12 the auto-correlation fit of $G(k)$ for different sample sizes N is shown; the auto-correlation for $N = 100$ shows spurious behavior since the data set is too small; we find that for crude oil a sample size of $N = 200$ days is the minimum size of the data for have a reliable estimate as it follows the same trend as a larger sample size of $N = 800$ days of data.

The goodness of fit of a set of points $y(x)$ when compared to its fitted value $y_{fit}(x)$ is given by

$$R^2 \quad = \quad 1 - \frac{\sum_x (y(x) - y_{fit}(x))^2}{\sum_x (y_x - E[y])^2}$$

where $E[y] = \dfrac{1}{N}\displaystyle\sum_{i=1}^{N} y_i$ is the mean of $y(x)$.

In general, we chooses a fixed size N for a given group of commodities. The auto-correlation

for crude oil and copper are illustrated in the Figures 6.4(a) and 6.4(b) respectively.

As shown in Figures 6.4(a) and 6.4(b), for crude oil and copper, the fit has $R^2 = 0.94$ and $R^2 = 0.96$, repectively. However, even for these cases, one cannot fit data for arbitrarily large time lag since once the propagator is zero, the applicability of the model ceases.

For crude oil, as shown in Figure 6.5 the fit depends on the period of the prices as well as how large a time lag one is modeling. For the case of Figure 6.5, the fit is good for 200 days.

We assume that the prices of commodities are stationary and obey

$$G(t - t') = G(|t - t'|) \qquad (\S\, 6.6.2)$$

where time lag is defined by

$$\text{time lag} = |t - t'|$$

Note that the fits are only valid for a *finite duration* of time, fixed by the *maximum* time lag – which is fixed by the value of the time lag $|t - t'|$ for which the propagator goes to zero. The range of validity depends on the commodity. For example, from Figure 6.5 we see that for crude oil, the propagator goes to zero for a time lag of about 200 days whereas for wheat it is 300 days and for copper it is 400 days, as shown in Figures 6.4(a) and 6.4(b).

If one tries to fit the model past the time lag for which the correlation function is zero, the fit fails since data may have large correlation out to very large lag time, as shown in Figure 6.5. One needs to break up a time interval into sub-intervals of about 200 days and then obtain a good fit – with $R^2 > .90$ – for each sub-interval by varying the parameters of the propagator.

Another possible limitation of the model is that for certain periods, when the market

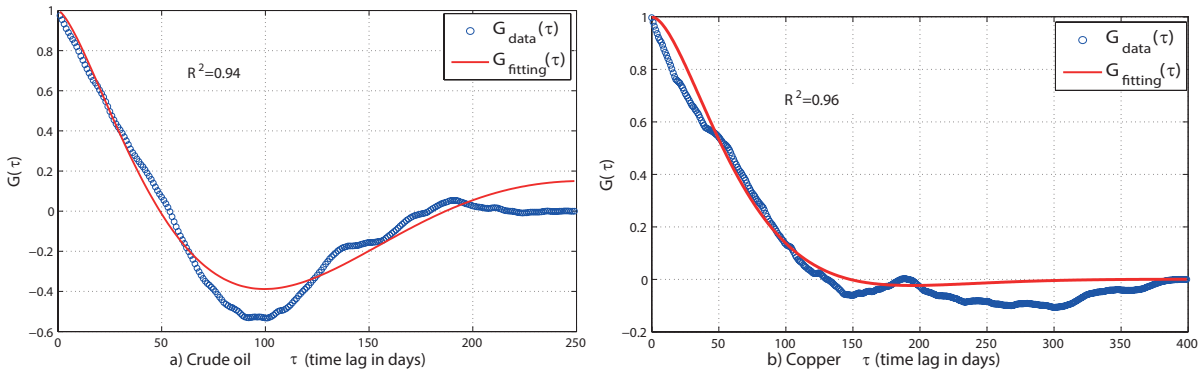

Figure 6.4: The correlation fit for crude oil and cooper.

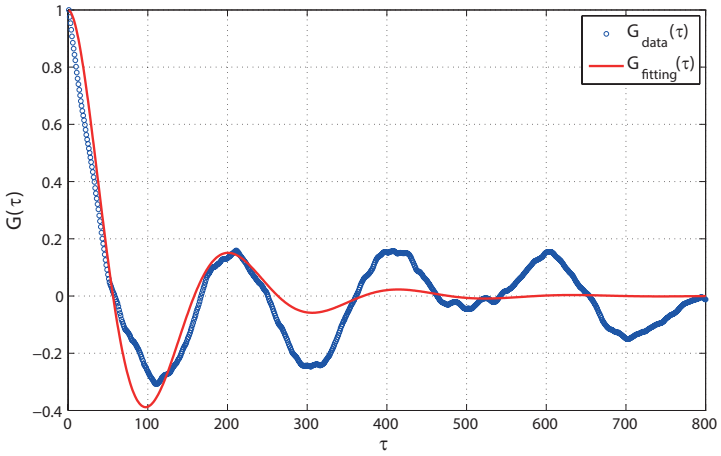

Figure 6.5: The correlation fit for crude Oil with different time lags.

Table 6.1: Propagator and parameters

Commodity	$\bar{x}$	$\sigma(x)$	Γ	L	$\tilde{L}$	range	R^2
Crude oil	4.600	0.0506	0.0418	296.08	-28.68	250	0.94
Brent oil	4.685	0.041	0.0556	2865.67	20.09	250	0.91
Heat oil	1.094	0.031	0.0527	9196.21	-12.92	250	0.90
Gold	7.287	0.123	0.0091	9181.46	69.22	400	0.94
Silver	3.175	0.185	0.0053	9135.72	121.9	400	0.93
Copper	1.2112	0.061	0.0137	9184.06	46.70	400	0.97
Corn	6.298	0.212	0.0103	9186.53	54.33	300	0.97
Wheat	6.618	0.152	0.0142	9246.48	40.41	300	0.99
Soybean	7.2842	0.101	0.0093	9181.37	71.60	300	0.97

undergoes a sudden change, the fit may not be good. So far, for the all commodities that we have studied, the propagator always yields a good fit out to the first 200 days or longer, depending on the commodity.

The parameters for the best fits are given in the Table 6.1 and are for recent data; the fits for the nine commodities are all good, with R^2 being greater than 0.91 for all of them.

§ 6.7 Nonlinear terms: Feynman diagrams

The Gaussian propagator can only yield three parameters, namely $L, \tilde{L}$ and Γ, whereas the action has six parameters. Hence, we need to use the higher nonlinear terms in the action to fully calibrate the model.

The calibration of the nonlinear terms of the model is absolutely indispensable. The reason being that it is only the nonlinear terms that go beyond the Gaussian model and provide a microeconomics potential that has a minimum that can match the average market price of a given commodity. In particular, in the absence of the nonlinear terms, the quadratic potential yields all average market price to be zero and is clearly quite useless for analyzing market prices.

We show below that the value of the nonlinear terms is ten times greater than the error term, clearly showing that the value of the nonlinear terms are a defining feature of market prices. To check the consistency of the evaluation of the nonlinear terms using Feynman diagrams, a numerical simulation is carried out in Section § 6.8 to confirm that the range of the nonlinear terms obtained from the market data can in fact be obtained using the Feynman perturbation expansion.

The action is written in terms of the scaled variable $y(t)$ and we obtain

$$\mathcal{A} = \int_{-\infty}^{\infty} dt[\frac{1}{2}L\ddot{y}^2 + \frac{1}{2}\widetilde{L}\dot{y}^2 + \frac{\gamma}{2}y^2 + \frac{\alpha}{3!}y^3 + \frac{\beta}{4!}y^4 + \cdots] + \text{const}$$

where

$$\begin{aligned} \alpha &= (-a^3 d e^{-a\bar{y}} + b^3 s e^{b\bar{y}}) = (b-a)\gamma \\ \beta &= (a^4 d e^{-a\bar{y}} + b^4 s e^{b\bar{y}}) = (a^2 - ab + b^2)\gamma \end{aligned}$$

Once we have obtained $\alpha, \beta, \gamma, \bar{y}$ from market data, the potential parameter of a, b, s, d are then given by the following

$$\begin{aligned} a &= \frac{\pm\sqrt{4\beta\gamma - 3\alpha^2} - \alpha}{2\gamma};\ b = a + \frac{\alpha}{\gamma} \\ s &= \frac{\gamma}{b(a+b)} e^{-b\bar{y}};\ d = \frac{\gamma}{a(a+b)} e^{a\bar{y}} \end{aligned}$$

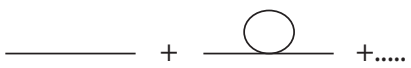

Figure 6.6: Feynman diagram for $E[y(t)y(t')]$.

Expanding the action functional yields the following expansion

$$e^{-\mathcal{A}} = e^{-(A_0+A_I)} = e^{-A_0}(1 - A_I - \frac{1}{2!}A_I^2 - \cdots)$$

where

$$A_0 = \frac{1}{2}\int dt[L\ddot{y}^2 + \widetilde{L}\dot{y}^2 + \gamma y^2] \;\; ; \;\; A_I = \int dt[\frac{\alpha}{6}y^3 + \frac{\beta}{24}y^4]$$

Hence

$$e^{-\mathcal{A}[\bar{x},y]} = e^{-\frac{1}{2}\int dt[L\ddot{y}^2+\widetilde{L}\dot{y}^2+\gamma y^2]}(1 - \int dt\frac{\alpha}{6}y^3 - \int dt\frac{\beta}{24}y^4) + O(y^5)$$

The correlation function to leading order in the nonlinear coupling is shown in Figure 6.6 and yields

$$E[y(t)y(t')]_c = G(t-t') - \frac{\beta}{2}G(0)\int dz G(z-t')G(z-t) + O(\beta^2)$$

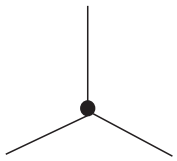

Figure 6.7: Feynman diagram for $E[y^3]$.

For equal time, since $G(t) = G(-t)$, we have

$$E[y(t)^2]_c = G(0) - \frac{\beta}{2}G(0)\int_{-\infty}^{\infty} dz G^2(z) = G(0) - \beta G(0)\int_0^{\infty} dz G^2(z)$$

The 'renormalized' coefficient for the quadratic term is given by

$$\Gamma = \gamma + \delta\gamma;\;\; \delta\gamma = \frac{\gamma}{2}\beta G(0)$$

To obtain the parameters α, β, we evaluate the expectation value of y^3, y^4. The equal time y^3 correlation is[1]

$$E[y(t)^3]_c = -2\alpha\int_0^{\infty} dz G^3(z) + O(\alpha\beta) \qquad (\S\, 6.7.1)$$

The Feynman diagram for $E[y^3]_c$ is shown in Figures 6.7.

The equal time y^4 correlation is given by[2]

$$E[y(t)^4]_c = 3G^2(0) - 2\beta\int_0^{\infty} dz G^4(z) + O(\beta^2) \qquad (\S\, 6.7.2)$$

The Feynman diagram for $E[y^4]$ is shown in Figures 6.8.

[1] $E[y^3(t)]_c = E[y(t)^3] - 2E[y(t)]E[y^2(t)]$.
[2] $E[y^4(t)]_c = E[y(t)^4] - 3E[y^2(t)]E[y^2(t)]$.

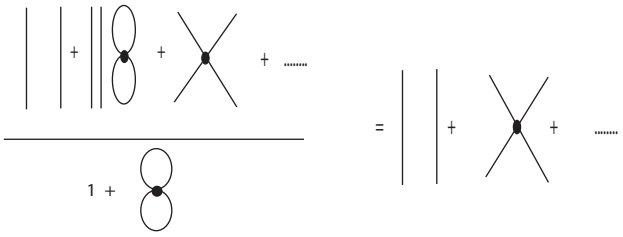

Figure 6.8: Feynman diagram $E[y^4]$.

Some integrations about that are useful for the Feynman diagrams are the following

$$\begin{aligned}
\int_0^\infty G(\tau)d\tau &= N\frac{\sin(2\phi)}{\omega},\ \int_0^\infty G^2(\tau)d\tau = N^2\frac{\sec(\phi)-\cos(3\phi)}{4\omega},\\
\int_0^\infty G^3(\tau)d\tau &= N^3\frac{2\sin^3(\phi)(11\cos(\phi)+2\cos(3\phi))}{3\omega(4\cos(2\phi)+5)},\\
\int_0^\infty G^4(\tau)d\tau &= N^4\frac{\sin^3(\phi)(50\cos(2\phi)+6\cos(4\phi)+47)\tan(\phi)}{16\omega(3\cos(2\phi)+5)}.
\end{aligned}$$

where $G(\tau)$, N is given in Eq. § 6.5.3.

§ 6.7.1 Calibration for crude oil

To illustrate the procedure followed for calibrating the action functional for the different commodities, we work out in detail the case of crude.

From the calibration of the propagator for crude oil, we have

$$\omega = 0.1091; \phi = 1.2781; N = 1.0444.$$

and hence

$$\begin{aligned}
\int_0^\infty d\tau G(\tau) = 2.2593;\ \int_0^\infty d\tau G^2(\tau) = 10.5957;\\
\int_0^\infty d\tau G^3(\tau) = 6.0011;\ \int_0^\infty d\tau G^4(\tau) = 6.0912
\end{aligned}$$

with $G^2(0) = 0.996$, which yields, from Eqs. § 6.7.1 and § 6.7.2

$$E[y(t)^3]_c = -12.0022\alpha \quad ; \quad E[y(t)^4]_c = 2.998 - 12.1824\beta \tag{§ 6.7.3}$$

The empirical value of the coefficients for crude oil are the following

$$E[y(t)^3]_c = 0.2881 \pm 0.0239 \quad ; \quad E[y(t)^4]_c = 1.7731 \pm 0.0072 \tag{§ 6.7.4}$$

Using Eqs. § 6.7.3 and § 6.7.4, we obtain the value of α, β as given below

$$\alpha = -0.024 \pm 0.002 \quad ; \quad \beta = 0.0997 \pm 0.0004 \tag{§ 6.7.5}$$

Note that the values obtained for both α, β are more than ten times the error, and hence are not a reflection of noise but rather reflect the nonlinearities in the evolution of the commodity price.

The values obtained for α, β are small and hence the Feynman expansion is justified. However, for other commodities, the value of α, β may be large so we need to find the range of α, β for which using the Feynman diagrams is in fact consistent. For this reason we do numerical calculation that does not assume α, β are small and find the range for which the Feynman expansion is valid. We will then evaluate these coefficients for the rest of the commodities following the same procedure as the one for crude oil.

§ 6.8 Monte Carlo simulation of the path integral

The Lagrangian for commodity prices is fundamentally nonlinear since the microeconomics potential has a power law dependence on the commodity prices. Since the theory is nonlinear, we need to determine the range of α, β for which the perturbation expansion using Feynman diagrams is valid.

We develop a Monte Carlo simulation for numerically evaluating the Feynman path integral for commodity prices that goes beyond Feynman perturbation theory [64]. The main purpose being to ascertain the range for the parameters of the Lagrangian for which perturbation theory is valid. This is of fundamental importance in the calibration of the model since empirical analysis is efficient and accurate if the correlation functions can be expressed as analytic functions of the model's parameters.

If the calibration leads to parameters outside the perturbative regime, then the calibration of the model would be immensely more difficult and with large systematic errors due to the necessity of evaluating the path integral numerically for each possible fit for the model's parameters with market data. Our Monte Carlo simulation of the path integral will show

that, in fact, the parameters required to match market data lies well within the perturbative domain of the path integral.

The simulation developed in this chapter builds on the work of Koo [65]. Although our work is largely similar to his, we shall describe in detail and often rederive the theoretical basis needed for the simulation to put it within the context of our application, and to clarify areas that we deem important.

The fundamental goal of the simulation is to numerically calculate the expectation value of an observable Q given by

$$E[Q(x)] = \frac{1}{Z}\int Dx e^{-\mathcal{A}(x)}Q(x), \quad \text{where} \quad Z = \int Dx e^{-\mathcal{A}(x)}.$$

The functional integration $\int Dx$ is over all the possible paths that $x(t)$ can take. The number of these possible paths is infinite and hence a straightforward calculation of the path integral is impractical. For simplicity, suppose time is *periodic* with a period τ, namely that

$$x(t) = x(t+\tau) \quad : \quad \text{Periodic}$$

For studying the correlation function for market prices, the limit of $\tau \to \infty$ will be taken. The correlation function for the periodic path integral is given by

$$C(t) = \frac{1}{Z}\int Dx \exp(-\mathcal{A}[x])x(0)x(t)$$

Note that most of the paths (functions) over which $C(t)$ is evaluated have negligible weight since the Boltzmann weighting factor $\exp\{-\mathcal{A}(x)\}$ is sharply peaked about a few paths. The most probable paths are only those close to the classical solution. Leveraging on this fact, Metropolis et al. [66] introduced a method of importance sampling, called the Monte Carlo method, for evaluating the Feynman path integral.

We start with the quadratic part of the Lagrangian given by

$$\mathcal{L}_0[x] = \frac{1}{2}L\ddot{x}^2 + \frac{1}{2}\tilde{L}\dot{x}^2 + \frac{\Gamma}{2}x^2$$

We start by choosing a number of discrete points to represent $x(t = n\epsilon) = x_n$, where $n = 0, \pm 1, \pm 2, .. \pm N$. For convenience (refer to Appendix 2), this is chosen to be an odd number equal to $2N + 1$. The range of time that is simulated in $0 \leq t \leq \tau$ and yields the

following time step between each point $\epsilon = \frac{\tau}{(2N+1)}$. The discretized quadratic action is then given by

$$\mathcal{A}_0[x] = \frac{1}{2}\epsilon \sum_{n=-N}^{+N} [L(\frac{x_{n-1} - 2x_n + x_{n+1}}{\epsilon})^2 + \tilde{L}(\frac{x_{n+1} - x_n}{\epsilon})^2 + \Gamma x_n^2]$$

The correlation functions for the quadratic action $\mathcal{A}_0[x]$ can be evaluated *exactly* even for the finite and discrete lattice with integration variables x_n; hence the accuracy of the numerical evaluation of the correlation functions can be checked against the exact result.

Since time has a periodic boundary condition, the discrete variables have the periodicity given by$x_n = x_{n+2N+1}$. The periodicity yields the following change of variable using Fourier transform

$$x_n = \sum_{k=-N}^{N} e^{\frac{i2\pi kn}{2N+1}} \varphi_k$$

The action is diagonal in the variables φ_k and is given by

$$\mathcal{A}_0[x] \quad = \quad \frac{1}{2}\epsilon \sum_{k,k'} \varphi_k \varphi_{k'} \delta_{k+k'} \{\Gamma + \frac{\tilde{L}}{\epsilon^2}\{2\sin(\frac{\pi k}{2N+1})\}^2 + \frac{L}{\epsilon^4}\{2\sin(\frac{\pi k}{2N+1})\}^4\}$$

Then discretized expression for the correlation function is

$$G_n = \frac{1}{Z_N} \prod_{m=-N}^{+N} \int_{-\infty}^{+\infty} dx_m \exp\{-\mathcal{A}_0[x]\} x_0 x_n$$

and where Z_N is the discretized partition function. Gaussian path integration yields the following exact result

$$G_n = \frac{1}{2\epsilon(2N+1)}[\sum_{k=-N}^{N} \frac{1}{B_k} \cos(\frac{nk\pi}{2N+1})]$$

where B_k is given by

$$B_k = [\Gamma + \frac{\tilde{L}}{\epsilon^2}\{2\sin(\frac{\pi k}{2N+1})\}^2 + \frac{L}{\epsilon^4}\{2\sin(\frac{\pi k}{2N+1})\}^4]$$

The correlation function is evaluated numerically using the Metropolis algorithm, and we plot the numerical values of the correlation function as well as the exact values in Figure 6.9. As the size of the lattice N increases, the correlation function of the simulated configurations converges to the expected theoretical values.

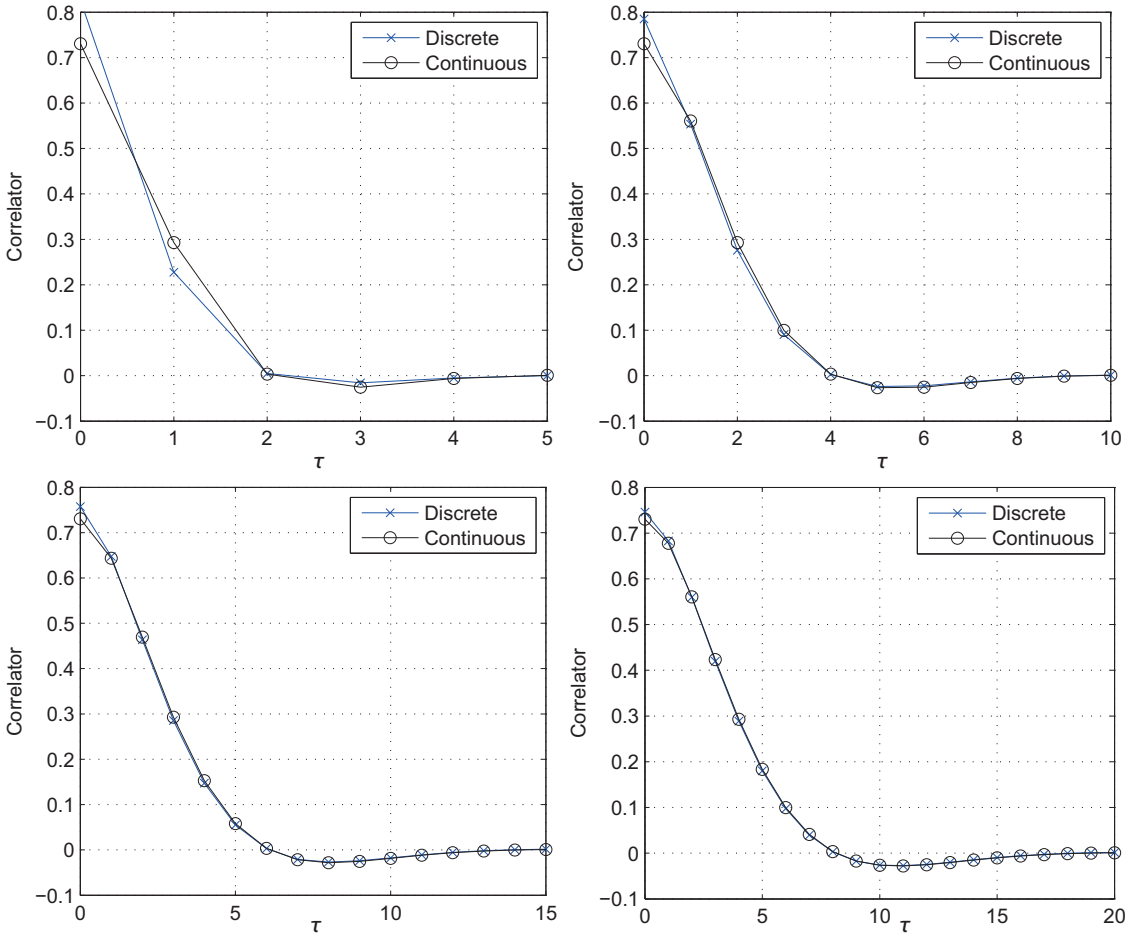

Figure 6.9: The correlation function obtained using discrete and continuous time, with $N = 5, 10, 15$, and 20.

All the simulations are run with the same number of configurations given by $\mathcal{M} = 100000$. We conclude that, as expected, systems with larger N have lower convergence rate. The amount of time needed to update the configurations increases linearly with N, and hence constitutes a limitation of the algorithm; for number of configurations $\mathcal{M}$, the error for the simulation is proportional to $1/\sqrt{\mathcal{M}}$.

From the results given in Figure 6.9, we conclude that expectation values obtained from the simulation converge to the expected theoretical values. We have also identified a major weakness of the algorithm, in that a significant amount of time would be necessary to simulate systems with larger N. In addition, simulating a Lagrangian with an acceleration term requires a significantly larger number of iterations.

We use the Monte Carlo simulation of the path integral to determine the range for per-

turbation theory. The parameters $L, \tilde{L}$ and Γ are first fixed using market data and then the value for $E[y^3]_c$ and $E[y^4]_c$ is numerically evaluated for a wide range of α, β. The numerical value is given by

$$E[y^3] = \frac{1}{Z_N} \prod_{n=-N}^{+N} \int_{-\infty}^{+\infty} dy_n \exp\{-\mathcal{A}[y]\} y_0^3$$

and a similar expression for $E[y^4]$. Note $\mathcal{A}[y]$ is the *full nonlinear* discretized microeconomics action

$$\mathcal{A}(y) = \mathcal{A}_0(y) + \frac{\alpha}{3!} y^3 + \frac{\beta}{4!} y^4$$

.

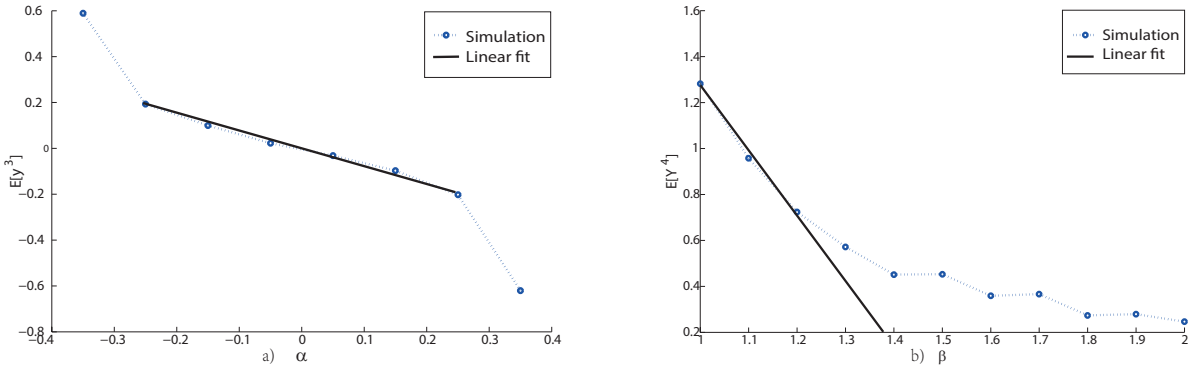

Figure 6.10: (a) Simulation $E[y^3]$ for the model. (b) Simulation $E[y^4]$ for the model.

The numerical values of $E[y^3]$ and $E[y^4]$, as a function of α, β is compared with the perturbative values, as given in Eqs. § 6.7.1 and § 6.7.2 respectively. The results are shown in Figure 6.10 and we conclude that the range for the validity of the Feynman perturbation expansion is given by

$$-0.25 \leq \alpha \leq 0.25 \quad ; \quad 0 < \beta \leq 1.2 \qquad (\S\, 6.8.1)$$

§ 6.9 The model's parameters for nine commodities

The empirical values of α, β will be seen to lie in the range given in Eq. § 6.8.1 and hence we can use the analytical results for $E[y^3]$ and $E[y^4]$ obtained using the Feynman diagram expansion. Hence we use the analytical expressions given in Eqs. § 6.7.1 and § 6.7.2 for $E[y^3]$ and $E[y^4]$ to fit the market data for nine commodities drawn from three different sectors.

We first fit the propagator, that does not depend on α, β except for a shift in the value of

Table 6.2: Complete calibration of all the model's parameters

Commodity	α	β	γ	a	b	s	d	RMSE
Crude oil	-0.024	0.0997	0.0917	1.411	0.625	0.072	0.0319	8.3%
Brent oil	0.0019	0.017	0.064	0.467	0.555	0.1125	0.1337	7.9%
Heat oil	0.0025	0.025	0.065	0.561	0.678	0.0776	0.094	9.4%
Gold	-0.0004	0.0315	0.025	1.148	1.105	0.0099	0.0096	8.2%
Silver	-0.0081	0.0213	0.016	1.828	0.307	0.0244	0.0041	9.4%
Copper	-0.0070	0.022	0.025	1.337	0.488	0.0277	0.0101	5.6%
Corn	-0.0025	0.0373	0.029	1.261	1.004	0.0128	0.0101	6.7%
Wheat	0.0014	0.0416	0.035	1.029	1.150	0.01398	0.0156	3.2%
Soybean	0.0021	0.0108	0.015	0.629	1.065	0.0081	0.0138	6.2%

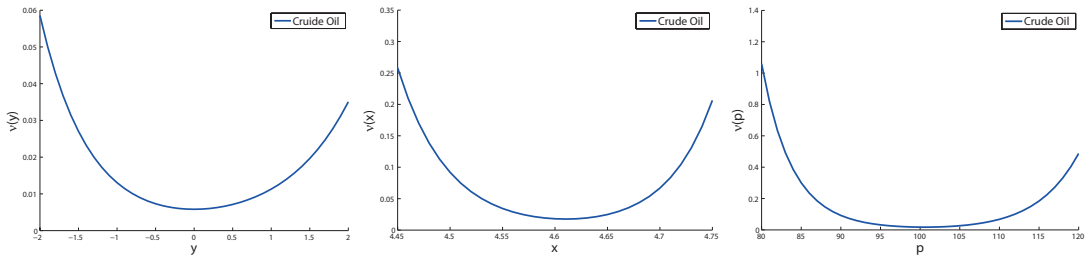

Figure 6.11: Microeconomics potential of crude oil in terms of $y = (x - \bar{x})/\sigma(x)$, $x = \log(p/p_0)$ and price p.

γ to Γ, and obtain the values of $L, \tilde{L}$ and Γ; Table 6.1 gives the parameters that reproduce the market correlation function. We then obtain the values of α and β reproduce the market y^3 and y^4 given in Table 6.2. The fact that the best fit for α, β lie within the perturbative range makes the calibration accurate and efficient.

§ 6.10 Microeconomics potential

The complete calibration of the microeconomics Lagrangian for the different commodities allows us to express the potentials directly in terms of the prices of the commodities. Figure 6.11 shows the microeconomics potential of crude oil. Note that the volatility of the commodity plays an important role in determining the range of important fluctuations for the commodities price. The microeconomics potentials for the other eight commodities is given in Appendix § 6.14.

The kinetic and potential terms for commodity prices shows the central role being played by the kinetic term; this term is absent in the standard treatments of microeconomics analysis

that are focused almost solely on supply and demand. Of course, whether the kinetic term in fact is important in the dynamics of commodity prices is an empirical question and needs to be further studied.

§ 6.11 Conclusion

A model for microeconomics based on the action functional and path integral proposed by Baaquie [60] has been studied empirically. A collection of nine commodities from three different sectors were analyzed to ascertain the validity and stability of the model when the commodities are varied.

The calibration and testing of the proposed statistical model of microeconomics are based on comparing the model's prediction with the empirical values of market prices as well as by comparing the model's propagator (unequal time correlation function) of market prices with the empirical propagator obtained from market data[60, 61, 55]. It was shown that the Feynman perturbation expansion yields a consistent and efficient method for calibrating the nonlinear model.

The procedure adopted for the calibration of the model, and in particular obtaining the supply and demand functions, are based on the assumption that all the information about the behavior of the commodities are contained in the observed market prices. This is quite unlike the procedure adopted in [61] where a large collection of macroeconomic data such as interest rates, unemployment, inflation and so on was required to estimate the supply and demand function. The approach adopted is also quite distinct from the Auto-regression Moving Average (ARMA) [67].

The most important result is that the *action functional* (as well as the Lagrangian) – consisting of the sum of a kinetic and a potential term – that was *postulated* in [60] has been empirically shown to *exist* in the market. The microeconomics Lagrangian provides a self-contained and comprehensive framework for the study of microeconomics. In particular, one can now investigate what are the underlying theoretical principles of microeconomics that would give rise to an action functional formulation of statistical microeconomics.

§ 6.12 Appendix A. Data analysis; sample size

The connection of the model with the market is based on the comparison of the expectation value of the log of the prices, for unequal time, with the same expectation value determined from the observed market prices. So it is imperative that a clear prescription be given on how to evaluate the expectation value of the prices from market data.

The time series of prices, as discussed in Section § 6.4, is viewed as the random samples of the stochastic price. All data used in the analysis of commodities is the closing daily commodity price.

A sample size N is the *total number of data points* being considered; for the data being considered, it is the value of observed market prices for the total number of N calendar days. The sample size N has to be fixed for obtaining the expectation values.

Consider a sample size N of the log of the stochastic price $x(t)$; time is discretized into daily values, namely $t = n\epsilon$, with $\epsilon = 1$ day. For daily prices, the time series gives a discrete set of values of $x(t) = x(n\epsilon) \equiv x_n$ and similarly for the scaled variable (defined in Eq. § 6.6.1) $y(t) = y(n\epsilon) \equiv y_n$.

The sample estimate of the mean and standard derivation is defined by[3]

$$\mu = \frac{1}{N}\sum_{i=1}^{N} x_i; \quad \sigma(x) = \sqrt{\frac{1}{N}\sum_{i=1}^{N}(x_i - \mu)^2} \tag{§ 6.12.1}$$

Recall the minimum of the macroeconomics potential, from Eq. § 6.5.2, is given by

$$\exp\{\hat{x}\} = (\frac{ad}{bs})^{1/(a+b)}$$

The market price of a commodity changes in time; for the purpose of calibration we take the market price that minimizes the potential, namely $\hat{x}$, to be equal to the average price

$$\hat{x} = \mu$$

The empirical correlation functions are generated using the averaging over the time series for prices of sample size N; the expectation value is defined, for values of $y(t)$ given at discrete

[3]The unbiased estimate of $\sigma(x)$ is defined by $\sigma^2(x) = \frac{1}{N-1}\sum_{i=1}^{N-1}(x_i - \mu)^2$, but we ignore this subtlety as it is irrelevant for our calculations.

times $n\epsilon$, as in Eq. § 6.12.3 by

$$G(k) \equiv E[y(t)y(t')] = \frac{1}{N}\sum_{n=1}^{N-k} y(t+\epsilon n)y(t'+\epsilon n) \quad ; \quad k\epsilon = |t-t'| \tag{§ 6.12.2}$$

The reason for using the denominator $1/N$ and not $1/(N-k)$ in Eq. § 6.12.2 is the following. The auto-correlation (covariance) between two observations x_n and x_{n+k} of a stationary stochastic process is defined as

$$r(k) = cov(x_n, x_{n+k}) = E[(x_n-\mu)(x_{n+k}-\mu)]; \quad r(0) = E[(x_n-\mu)^2] = \sigma(x)^2$$

The unbiased autocorrelation function is

$$\hat{r}_{unbiased}(k) = \frac{1}{N-k}\sum_{n=1}^{N-k}(x_n-\mu)(x_{n+k}-\mu)$$

An auto-correlation function needs to be positive-semidefiniteness for having a consistent Fourier transform and implies the condition [68]

$$|r(k)| >= |r(k')| \quad \text{for} \quad k > k'$$

It can be shown [68] that the following estimator is positive-semidefinite

$$r(k) = \frac{1}{N}\sum_{n=1}^{N-k}(x_n-\mu)(x_{n+k}-\mu)$$

and this definition for the auto-correlation that is used in all of our empirical analysis.

The normalized auto-correlation function is given by

$$\frac{r(k)}{r(0)} = \frac{1}{N}\sum_{n=1}^{N-k}(x_n-\mu)(x_{n+k}-\mu)\Big/\frac{1}{N}\sum_{n=1}^{N}(x_n-\mu)^2$$

and in terms of the scaled variable y, we have

$$G(k) = \frac{r(k)}{r(0)} = \frac{1}{N}\sum_{n=1}^{N-k} y_n y_{n+k} \tag{§ 6.12.3}$$

The sample size turns out to be an important factor is obtaining a stable result for the

auto-correlator $G(k)$. Since all empirical expectation values are obtained by using the method of a moving average, as expressed in the summation given in Eq. § 6.12.3, if the sample size is too small the number of terms used to evaluate $G(k)$ contain noise that is not canceled out by the sample size chosen.

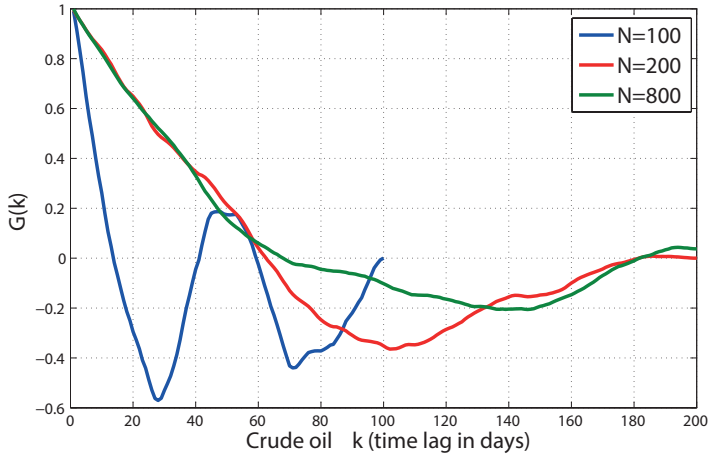

Figure 6.12: The auto-correlation fit for crude oil of $G(k)$ for different sample sizes N.

We evaluated $G(k)$ for varying sample sizes N. The result is shown in Figure 6.12. The result for $N = 100$ days is clearly incorrect since increasing the value of N shows a clear departure from the result obtained. We found that for N greater than 200 days, the auto-correlator converges to a value that remains relatively unchanged if we increase the sample size. For the sake of efficiency, we have used the smallest value of N for which the the result for $G(k)$; one is of course free to use a larger sample size.

Using the same data set, we did the fit for the model's propagator using the empirical result for real time and by a Fourier transform of the real time empirical result. Using the fact that the prices are supposed to be stationary, as given in Eq. § 6.6.2, the Fourier transform $\hat{G}(\omega)$ is defined by

$$\hat{G}_{data}(\omega) = 2\int_0^\infty dt\, \cos(\omega t) G_{data}(t)$$

The parameters $L, \tilde{L}, \Gamma$ of the model are given by fitting $G_{data}(\omega)$ with $G_{fitting}(\omega)$, where

$$G_{fitting}(\omega) = \frac{1}{L\omega^4 + \tilde{L}\omega^2 + \Gamma}$$

The Fourier transform of the auto-correlator $G(k)$ was empirically evaluated using Eq.§ 6.12.3 to confirm that the definition of the empirical expectation value gives the expected correct Fourier transform. As shown in Figure 6.13, the empirically value of the Fourier transform of

the auto-correlator $G(k)$ has an excellent fit with the theoretical value of $G(k)$.

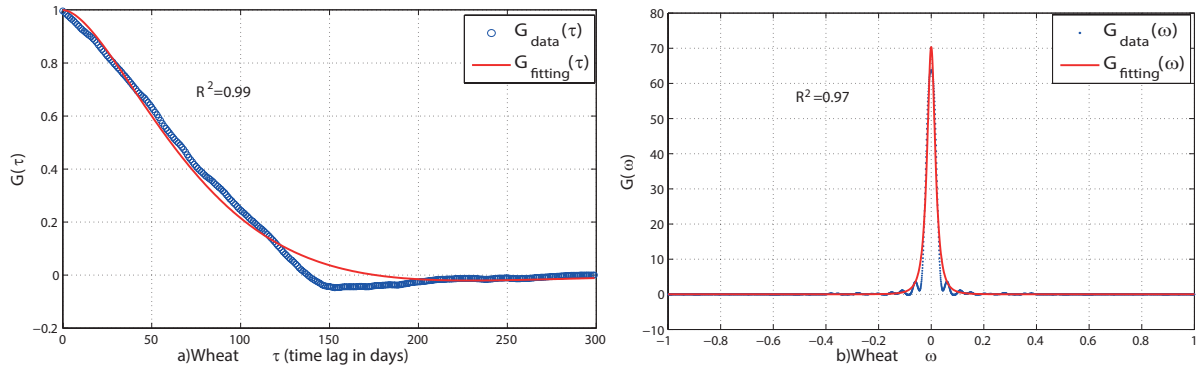

Figure 6.13: The correlation fit for wheat (a) Real time fit. (b) Fit of the Fourier transform.

The results are given in Figure 6.13(a) for the real time analysis and Figure 6.13(b) is the result given by the Fourier transform. Both fits give the same values for the parameters $L, \tilde{L}, \Gamma$ that are consistent with the accuracy of $R^2 = 0.99$ for the real time fit and $R^2 = 0.97$ for the fit in Fourier space. For multiple commodities, Fourier transforms provide an efficient way of calibrating the model and hence showing that both methods are consistent is the first step towards the analysis of the joint probability distribution of multiple commodities.

The error in the propagator for the fitting of the model to the market is very small, with R^2 being always larger than 0.90. This is discussed further in Section § 6.6.

§ 6.13 Appendix B. Monte Carlo simulation

In this method, we generate $M = 100,000$ configurations of $x(t)$, denoted $x^{(1)}(t), x^{(2)}(t), \ldots x^{(M)}(t)$ [65]. The only requirement is that, in the limit $M \to \infty$, the probability of occurrence of $x^{(i)}(t)$ is proportional to the weight of $x^{(i)}(t)$, namely

$$P(x^{(i)}(t)) = \frac{e^{-\mathcal{S}(x^{(i)}(t))}}{\sum_{k=1}^{M} e^{-\mathcal{S}(x'^{(k)}(t))}}$$

Furthermore, it simplifies the computation of $E[A]$ into

$$E[A] = \frac{1}{M} \sum_{i=1}^{M} A(x^{(i)}(t))$$

Consider a process where in one iteration, a configuration $x^{(i)}(t)$ evolves into a new one $x^{(j)}(t)$ according to the probability $W(x^{(i)}(t), x^{(j)}(t))$. By definition,

$$W(x^{(i)}(t), x^{(j)}(t)) \;\; \geq \;\; 0 \;\; ; \;\; \sum_{x^{(j)}} W(x^{(i)}(t), x^{(j)}(t)) = 1 \qquad (\S\, 6.13.1)$$

where the summation is over all possible paths of $x^{(j)}$. The probability that a configuration evolves from $x^{(i)}(t)$ to $x^{(j)}(t)$ in N iterations, denoted $W^{(n)}(x^{(i)}(t), x^{(j)}(t))$, is

$$W^{(n)}(x^{(i)}(t), x^{(j)}(t)) = \sum_{x} W^{(n-1)}(x^{(i)}(t), x) W^{(n)}(x, x^{(j)}(t))$$

The procedure above is importance sampling in that we are more likely to sample paths that have higher weight. In the limit $n \to \infty$, $W^{(n)}(x^{(i)}(t), x^{(j)}(t))$ converges to a value $p(x^{(j)})$ that is independent of the initial configuration. Thus, we can use this process to generate the configurations for the importance sampling; the only requirement is that

$$p(x^{(j)}) = P(x^{(j)}(t)) \qquad (\S\, 6.13.2)$$

Make time into lattice with $t = k\epsilon$ and we start by generating an arbitrary initial configuration $x_k^{(1)}$ for $k = 1, 2 \cdots 2N + 1$ Next, we attempt to update $x_{k=1}^{(1)}$ by proposing a new configuration $x'^{(1)}$ with

$$x_1'^{(1)} = x_1^{(1)} + u\Delta x \;\; ; \;\; x_k'^{(1)} = x_k^{(1)} \;\; \text{for} \;\; k \neq 1$$

where Δx is a pre-defined parameter and u is a random number drawn from a random variable uniformly distributed on the interval $[-1, 1]$, namely u is a sample value of the $U(-1, 1)$ random variable.

The probability for this change is computed. To determine whether we should accept or reject this change, a random number $z = U(0, 1)$ is generated. The change is accepted if $z < W(x^{(1)}, x'^{(1)})$ and rejected otherwise.

We then proceed to update $x_{k=2}^{(1)}$ following the same procedure as before. This step is repeated for all k in $x_k^{(1)}$. After the updating of the last $k = 2N + 1$ has been done, we have completed one iteration and the resulting $\{x_k^{(2)},\ k = 1, 2, ..2N + 1\}$ are saved as the second configuration $\{x_k^{(2)}\}$. The iteration is then repeated until we generate all the sample values of $\{x_k^{(n)}\}$.

The choice of initial configuration, although in principle arbitrary, plays an important role

in the simulation. The initial configuration in general is not an equilibrium configuration and so are the following iterations. As such, a certain number of initial iterations have to be discarded from the final output of program. This number depends on the choice of initial configuration; the further it is from equilibrium, the more are the iterations to be discarded. Hence, it is preferable to start with a configuration close to equilibrium.

The process of performing the initial iterations to bring the system to equilibrium described in the previous section is known as thermalization. Besides the choice of initial configuration, the number of necessary thermalization steps also determines the convergence of the simulation. In general, we find that systems with larger N have lower convergence, and hence require more thermalizations.

The value of Δx has to be chosen carefully. If the value is too small, the acceptance probability will be close to 1 and the new (likely to be accepted) configuration will not differ much from the previous configuration. This leads to high correlation between iterations, which in turn lower the convergence rate, as we will discuss below. On the other hand, if the value is too large, the acceptance probability will be small and the new configuration will most likely be rejected. This also lowers the convergence rate. Hence, Δx is chosen such that the acceptance rate is approximately 0.5, i.e.,

$$E[W(x^{(i)}, x'^{(i)})] \simeq 0.5$$

§ 6.13.1 Metropolis algorithm

We give a proof of Eq. § 6.13.2. Note that we are free to choose the explicit expression for $W(x^{(i)}, x^{(j)})$, as long as it satisfies Eq. § 6.13.1. For our purpose, we use

$$W(x^{(i)}, x^{(j)}) = min\{1, \exp[-(S(x^{(j)}) - S(x^{(i)}))]\}$$

which is known as the Metropolis algorithm. As it turns out, it suffices to impose

$$\frac{W(x^{(i)}, x^{(j)})}{W(x^{(j)}, x^{(i)})} = \frac{\exp(-S(x^{(j)}))}{\exp(-S(x^{(i)}))}$$

to achieve the desired outcome. We have

$$W(x^{(i)}, x^{(j)}) \exp(-S(x^{(i)})) = W(x^{(j)}, x^{(i)}) \exp(-S(x^{(j)}))$$

perform a summation over $x^{(j)}$ obtaining

$$\exp(-S(x^{(i)})) = \sum_{x_j} W(x^{(j)}, x^{(i)}) \exp(-S(x^{(j)}))$$

Iterating n times, we would then have

$$\exp(-S(x^{(i)})) = \sum_{x_k} W^n(x'^{(k)}, x^{(i)}) \exp(-S(x'^{(k)}))$$

In the limit $n \to \infty$,

$$\exp(-S(x^{(i)})) = p(x^{(i)}) \sum_{x_k} \exp(-S(x'^{(k)}))$$

so that we finally have

$$p(x^{(i)}) = \frac{\exp(-S(x^{(i)}))}{\sum_{x_k} \exp(-S(x^k))} = P(x^{(i)}(t))$$

§ 6.14 Appendix C. The microeconomics potentials

The microeconomics potential as a function of the price of the commodity $P = e^x$ – for the other eight commodities – are shown in Figure 6.14. The role of volatility in determining the degree of fluctuation and random variation should be noted.

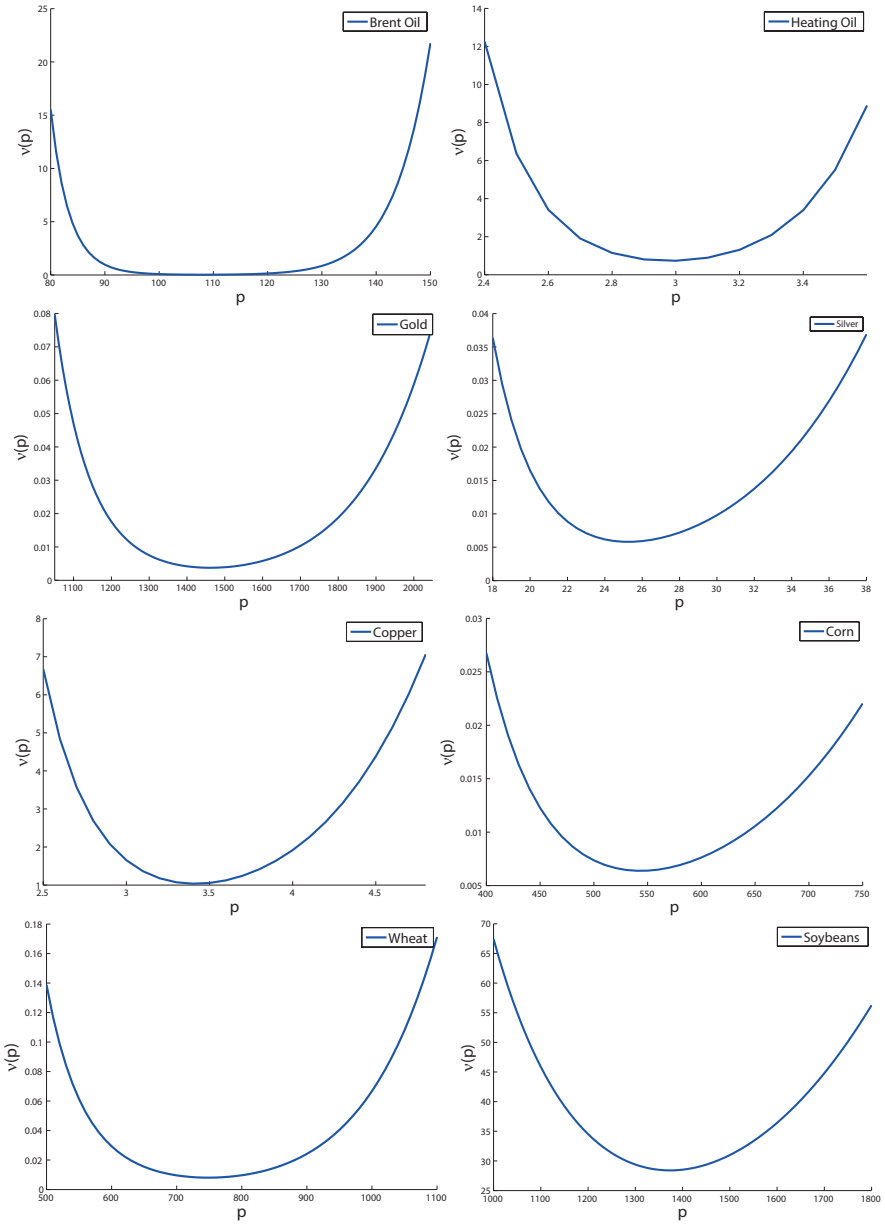

Figure 6.14: Microeconomics potential $\mathcal{V}$ vs $p = p_0 e^x$ for other main commodities.

Chapter 7
Conclusions

This dissertation investigated four models in quantum finance -Pricing of Range accrual swap, Hamiltonian of Libor Market Model, the acceleration Lagrangian model for option pricing and microeconomics potential. The four models display many non-trivial features of quantum mathematics and quantum finance. This chapter is organized as follows: the first four Sections review the purposes and significant results of these models. Section § 7.5 acknowledges the limitations and recommendations for future studies.

§ 7.1 Pricing of Range accrual swap

The Libor Market Model defined for the Libor lattice was extended to accommodate the payoff of the accrual swap and this in turn was only possible because the pricing was obtained using the logarithmic field $\phi(t,x)$: unlike Libor $L(T,T_n)$, which is only defined for the Libor lattice, $\phi(t,x)$ is defined for the continuous domain defined by $t \geq T_0, x \geq t$.

An approximate formula was obtained by linearizing the nonlinear drift of the LMM. The Libor rates were studied numerically by using a simulation for updating daily Libor. The simulation showed that the approximate price provides an excellent approximation when the Libor volatility γ_m is taken from the market. The simulation showed that the approximate accrual swap formula fails only for very high volatility that one does not expect for normal market conditions. The par value of the range accrual swap can be computed accurately using the approximate formula and opens the way for empirically studying the pricing of range accrual swaps.

§ 7.2 Hamiltonian of Libor Market Model

We linearize the drift of the LIBOR market model for the Hamiltonian formulation and could then solve for its ground state. We re-interpreted the initial condition of the LIBOR market model as being free parameters of the Hamiltonian and calibrated these parameters from the data.

The probability distribution functions for a single LIBOR and multi-LIBOR were derived and the results showed that our model fits the data with high accuracy. The model could fit the data very well only by using the initial LIBOR as a parameter in conjunction with the concept of market time. One of our main results is that the market time index can be generalized to the LIBOR case in a manner that respects the LIBOR lattice.

One can go further and find the excited states of the LIBOR Hamiltonian to describe the 2008 debt market that was far from equilibrium. Such a study, which we propose to undertake, would throw further light on the Hamiltonian formulation of the LIBOR market model.

§ 7.3 Acceleration Lagrangian for option pricing

An option pricing formula has been developed that is based on the value of both the current price and velocity of the underlying security. Using an acceleration Lagrangian model based on the formalism of quantum finance, we derived the pricing formula for European call options. It was demonstrated that the implied volatility of the market can be generated by our pricing formula. The quantum finance option price was applied to both options on EURUSD foreign exchange rates and on an equity index; the accuracy of the model was seen to be better than the Black-Scholes pricing formula in matching the option's market price.

The general conclusion that one can draw from the analysis is that the Black-Scholes pricing formula has a short fall of information and implied volatility is introduced to offset this lacking. The acceleration model shows that incorporating the velocity of the security into the option price seems to compensate for the shortfall of information in the Black-Scholes pricing formula. The option price based on the value of the security and its velocity provides a mathematical framework for designing and pricing a whole new set of derivative instruments.

§ 7.4 Empirical Microeconomics Actions Functionals

The statistical microeconomics model proposed by Baaquie has been studied empirically. Different commodities were analyzed to ascertain the validity and stability of the model when the commodities are varied. The procedure adopted for the calibration of the model, and in particular obtaining the supply and demand functions, are based on the assumption that all the information about the behaviour of the commodities are contained in the observed market prices.

The calibration and testing of the proposed statistical model of microeconomics are based on comparing the model's prediction with the empirical values of market prices as well as by comparing the model's propagator (unequal time correlation function) of market prices with the empirical propagator obtained from market data. It was shown that the Feynman perturbation expansion yields a consistent and efficient method for calibrating the nonlinear model. The microeconomics Lagrangian provides a self-contained and comprehensive framework for the study of microeconomics. In particular, one can now investigate what are the underlying theoretical principles of microeconomics that would give rise to an action functional formulation of statistical microeconomics.

§ 7.5 Future perspectives

To be a more comprehensive research, all of these models need further investigation in future work. More complicated derivatives should be examined using our path dependent models like Bermudan swaption, currency swaps etc. The correlation function of foreign exchange and multiple correlations of stocks are needed for examine the models in quantum finance. Besides, the non-trivial fit should provide an application in real markets, such as the hedging of equity, foreign exchange and commodities. The potentials of multiple commodities should be studied to enhance the concept of statistics microeconomics and the price theory in the Capital market could also be investigated to broaden the idea of macroeconomics.

Bibliography

[1] B. E. Baaquie. *Quantum Finance*. Cambridge University Press, UK, 1st edition, 2004.

[2] Belal E Baaquie. *Interest rates and coupon bonds in quantum finance*. Cambridge University Press, 2009.

[3] Belal E Baaquie, Xin Du, Pan Tang, and Yang Cao. Pricing of range accrual swap in the quantum finance libor market model. *Physica A: Statistical Mechanics and its Applications*, 401:182–200, 2014.

[4] Pan Tang, Belal E Baaquie, Xin Du, and Zhang Ying. Linearized hamiltonian of the libor market model:analytical and empirical results. *Submitted for publication*, 2014.

[5] Belal E Baaquie, Xin Du, and Jitendra Bhanap. Option pricing: Stock price, stock velocity and the acceleration lagrangian. *Physica A: Statistical Mechanics and its Applications*, 416:564–581, 2014.

[6] Belal E Baaquie, Xin Du, and Winson Tanputraman. Empirical microeconomics action functionals. *Physica A: Statistical Mechanics and its Applications*, 428:19–37, 2015.

[7] Robert C Merton. Option pricing when underlying stock returns are discontinuous. *Journal of financial economics*, 3(1):125–144, 1976.

[8] OA Vesicek. An equilibrium characterization of the term structures. *J. Financial Economics*, 5:177–188, 1977.

[9] John C Cox, Jonathan E Ingersoll Jr, and Stephen A Ross. A theory of the term structure of interest rates. *Econometrica: Journal of the Econometric Society*, pages 385–407, 1985.

[10] Thomas SY Ho and SANG-BIN LEE. Term structure movements and pricing interest rate contingent claims. *The Journal of Finance*, 41(5):1011–1029, 1986.

[11] John Hull and Alan White. Pricing interest-rate-derivative securities. *Review of financial studies*, 3(4):573–592, 1990.

[12] Fischer Black, Emanuel Derman, and William Toy. A one-factor model of interest rates and its application to treasury bond options. *Financial analysts journal*, pages 33–39, 1990.

[13] Fischer Black and Piotr Karasinski. Bond and option pricing when short rates are lognormal. *Financial Analysts Journal*, pages 52–59, 1991.

[14] Francis A Longstaff and Eduardo S Schwartz. Interest rate volatility and the term structure: A two-factor general equilibrium model. *The Journal of Finance*, 47(4):1259–1282, 1992.

[15] Lin Chen. *Stochastic Mean and Stochastic Volatility: A Three-factor Model of the Term Structure of Interest Rates and Its Applications in Derivatives Pricing and Risk Management*. Blackwell publishers, 1996.

[16] David Heath, Robert Jarrow, and Andrew Morton. Bond pricing and the term structure of interest rates: A new methodology for contingent claims valuation. *Econometrica: Journal of the Econometric Society*, pages 77–105, 1992.

[17] Douglas P Kennedy. The term structure of interest rates as a gaussian random field. *Mathematical Finance*, 4(3):247–258, 1994.

[18] Robert S Goldstein. The term structure of interest rates as a random field. *Review of Financial Studies*, 13(2):365–384, 2000.

[19] Belal E Baaquie. Quantum field theory of treasury bonds. *Physical Review E*, 64(1): 016121, 2001.

[20] Belal E Baaquie. *Quantum finance*. Cambridge University Press, 2004.

[21] John Hull and Alan White. The pricing of options on assets with stochastic volatilities. *The journal of finance*, 42(2):281–300, 1987.

[22] Belal E Baaquie and Cao Yang. Empirical analysis of quantum finance interest rates models. *Physica A: Statistical Mechanics and its Applications*, 388(13):2666–2681, 2009.

[23] Belal E Baaquie and Cui Liang. Feynman perturbation expansion for the price of coupon bond options and swaptions in quantum finance. ii. empirical. *PHYSICAL REVIEW-SERIES E-*, 75(1):016704, 2007.

[24] Patrick Navatte and François Quittard-Pinon. The valuation of interest rate digital options and range notes revisited. *European Financial Management*, 5(3):425–440, 1999.

[25] João Pedro Vidal Nunes. Multifactor valuation of floating range notes. *Mathematical Finance*, 14(1):79–97, 2004.

[26] Damiano Brigo and Fabio Mercurio. *Interest rate models-theory and practice: with smile, inflation and credit*. Springer, 2006.

[27] Bong-Gyu Jang and Ji Hee Yoon. Analytic valuation formulas for range notes and an affine term structure model with jump risks. *Journal of Banking & Finance*, 34(9): 2132–2145, 2010.

[28] L. P Kadanoff. Kenneth Geddes Wilson (1936−2013) Nobel-prize winning physicist who revolutionized theoretical science. *Nature 500 (7460)*, 30, 2013.

[29] Edward Witten. Quantum field theory and the jones polynomial. *Communications in Mathematical Physics*, 121(3):351–399, 1989.

[30] Haven E E. A discussion on embedding the blackscholes option pricing model in a quantum physics setting. *Physica A: Statistical Mechanics and its Applications*, 304: 507–524, 2002.

[31] B. E. Baaquie. Financial modeling and quantum mathematics. *Computers and Mathematics with Applications*, 65:1665–1673, 2013.

[32] Belal E Baaquie and Pan Tang. Simulation of nonlinear interest rates in quantum finance: Libor market model. *Physica A: Statistical Mechanics and its Applications*, 391(4):1287–1308, 2012.

[33] D Gatarek A. Brace and M. Musiela. The market model of interest rate dynamics. *Mathematical Finance*, 7:127–154, 1996.

[34] F. Jamshidian. Libor and swap market models and measures. *Finance and Stochastics*, 1(14):293–330, 1997.

[35] L. Anderson and J. Andresean. Volatility skews and extensions of the libor market model. *Applied Mathematical Finance*, 7(1):1–32, 2000.

[36] M. Joshi and R. Rebonata. A displaced-diffusion stochastic volatility libor market model: motivation, definition and implementation. *Quantitative Finance*, 3:458–469, 2003.

[37] Patrick Hagan, Andrew Lesniewski, and Diana Woodward. Probability distribution in the sabr model of stochastic volatility. *preprint*, 2005.

[38] Riccardo Rebonato and Richard White. Linking caplets and swaptions prices in the lmm-sabr model. *Journal of Computational Finance*, 13(2):19, 2009.

[39] Paul Glasserman and Nicolas Merener. Numerical solution of jump-diffusion libor market models. *Finance and Stochastics*, 7(1):1–27, 2003.

[40] Paul Glasserman and Steven G Kou. The term structure of simple forward rates with jump risk. *Mathematical finance*, 13(3):383–410, 2003.

[41] Robert Jarrow, Haitao Li, and Feng Zhao. Interest rate caps ??smile?? too! but can the libor market models capture the smile? *The Journal of Finance*, 62(1):345–382, 2007.

[42] B. E. Baaquie and Cao Yang. Empirical analysis of quantum finance interest rate models. *Physica A: Statistical Mechanics and its Applications*, 388(13):2666–2681, 1 July 2009.

[43] B. E. Baaquie. Interest rates in quantum finance: The Wilson expansion and Hamiltonian. *Physical Review E*, 80(4):046119, 2009.

[44] R. Jarrow D. Heath and A. Morton. Bond pricing and the term structure of interest rates: A new methodology for contingent claim valuation. *Econometrica*, 60:77–105, 1992.

[45] Belal E. Baaquie and Pan Tang. Simulation of nonlinear interest rates in quantum finance: Libor market model. *Physica A: Statistical Mechanics and its Applications*, 391: 12871308, 2012.

[46] Brace A and Musiela M. The market model of interest rate dynamics. *Mathematical finance*, 7:127–155, 1997.

[47] Eberlein E and zkan F. The lvy libor model. *Finance and Stochastics*, 9:327–348, 2005.

[48] Sabelfeld K Kurbanmuradov O and Schoenmakers J. Lognormal approximations to libor market models. *Journal of Computational Finance*, 6:69–100, 2002.

[49] Siopacha M and Teichmann J. Weak and strong taylor methods for numerical solutions of stochastic differential equations. *Quantitative Finance*, 11:517–528, 2011.

[50] B. E. Baaquie. *Interest Rates and Coupon Bonds in Quantum Finance.* Cambridge University Press, UK, 1st edition, 2009.

[51] B. E. Baaquie, Yang Cao, Ada Lau, and Pan Tang. Path integral for equities: Dynamic correlation and empirical analysis. *Physica A: Statistical Mechanics and its Applications*, 391(4):1408–1427, 2012.

[52] Fischer Black and Myron Scholes. The pricing of options and corporate liabilities. *The journal of political economy*, pages 637–654, 1973.

[53] Stephen William Hawking and Thomas Hertog. Living with ghosts. *Physical Review D*, 65(10):103515, 2002.

[54] Carl M Bender and Philip D Mannheim. No-ghost theorem for the fourth-order derivative pais-uhlenbeck oscillator model. *Physical review letters*, 100(11):110402, 2008.

[55] Belal E Baaquie, Yang Cao, Ada Lau, and Pan Tang. Path integral for equities: Dynamic correlation and empirical analysis. *Physica A: Statistical Mechanics and its Applications*, 391(4):1408–1427, 2012.

[56] Belal E Baaquie and Yang Cao. Option volatility and the acceleration lagrangian. *Physica A: Statistical Mechanics and its Applications*, 393:337–363, 2014.

[57] Belal E. Baaquie. Action with Acceleration I: Euclidean Hamiltonian and Path Integral. *International Journal of Modern Physics A*, 28, 2013.

[58] J Orlin Grabbe. The pricing of call and put options on foreign exchange. *Journal of International Money and Finance*, 2(3):239–253, 1983.

[59] Belal E Baaquie. Action with acceleration ii: Euclidean hamiltonian and jordan blocks. *International Journal of Modern Physics A*, 28(27), 2013.

[60] Belal E Baaquie. Statistical microeconomics. *Physica A: Statistical Mechanics and its Applications*, 392(19):4400–4416, 2013.

[61] David Coyle, Jason DeBacker, and Richard Prisinzano. Estimating the supply and demand of gasoline using tax data. *Energy Economics*, 34(1):195–200, 2012.

[62] Hal R Varian and WW Norton. *Microeconomic analysis*, volume 2. Norton New York, 1992.

[63] Belal E Baaquie. *Path Integrals and Hamiltonians: Principles and Methods*. Cambridge University Press, 2014.

[64] Winson Tanputraman. Modeling commodities in statistical microeconomics. *Honours thesis(National University of Singapore)*, 2014.

[65] Koo Wai Ming. Path integral quantum mechanics. *Honours thesis(National University of Singapore)*, 1988.

[66] Christian P Robert and George Casella. *Monte Carlo statistical methods*. Springer, 1999.

[67] John Johnston and John DiNardo. Econometric methods. *New York*, 19(7), 1972.

[68] Piet MT Broersen. *Automatic autocorrelation and spectral analysis*. Springer, 2006.